DECIPHERING THE EVOLUTIONARY HISTORY OF THE MONTANE NEW GUINEA AVIFAUNA: COMPARATIVE PHYLOGEOGRAPHY AND INSIGHTS FROM PALEODISTRIBUTIONAL MODELING IN A DYNAMIC LANDSCAPE

by

Brett W. Benz

Submitted to the Department of Ecology and Evolutionary Biology and the
Graduate Faculty of the University of Kansas
in partial fulfillment of the requirements for the degree of
Doctor of Philosophy

_____
A. Townsend Peterson (Chair)

_____
Robert G. Moyle

_____
Mark B. Robbins

_____
Robert M. Timm

_____
Stephen H. Benedict

Date Defended: 30 November, 2011

The Dissertation Committee for Brett W. Benz certifies
that this is the approved version of the following dissertation:

DECIPHERING THE EVOLUTIONARY HISTORY OF THE MONTANE NEW GUINEA AVIFAUNA: COMPARATIVE PHYLOGEOGRAPHY AND INSIGHTS FROM PALEODISTRIBUTIONAL MODELING IN A DYNAMIC LANDSCAPE

Committee:

_____
A. Townsend Peterson (Chair)

_____
Robert G. Moyle

_____
Mark B. Robbins

_____
Robert M. Timm

_____
Stephen H. Benedict

Date approved: 30 November, 2011

ABSTRACT

Integrating comparative phylogeographic methods with taxon-specific paleodistributional modeling provides a powerful approach for assessing historical environmental factors that have contributed to patterns of population genetic structure and species formation. Herein, I reconcile spatial analyses of genetic diversity with contemporary and paleoecological niche reconstructions in four co-distributed montane passerines to examine how Pleistocene climate change and topographic relief have influenced avian diversification across the New Guinea highlands. Phylogeographic analyses revealed substantial disparity in the distribution of genetic diversity among focal taxa, with *Peneothello cyanus* and *Crateroscelis robusta* exhibiting deep divergences along the Strickland River Valley, whereas *Rhipidura atra* and *Amblyornis macgregoriae* displayed evidence of gene flow and shallow genetic structure across this biogeographic boundary. Patterns of population genetic structure in *P. cyanus* and *C. robusta* were largely congruent with the distribution of contemporary sky-islands and historical population connectivity inferred from Last Glacial Maximum ecological niche reconstructions; however, Mantel tests indicate an isolation-by-distance effect has also impacted the distribution of genetic diversity in each of these taxa. By contrast, *R. atra* and *A. macgregoriae* exhibited weak geographic structure and indications of admixture or ancestral polymorphism among most sky-island populations, yet have maintained highly divergent lineages in the Vogelkop and Huon Peninsula, respectively. Signatures of demographic expansion were observed across each species complex, corroborating elevational shifts and range expansion predicted by Last Glacial Maximum ecological niche models. Although differences in dispersal capacity may have contributed to the discordant evolutionary histories among these taxa, limitations of the mtDNA data set preclude assessing the impact of stochastic or selective processes with confidence. This

investigation yields novel insight into the evolutionary dynamics that have shaped patterns of avian diversification and historical demography across the New Guinea highlands. Moreover, the phylogenetic relationships recovered within these geographically structured lineages have important implications for understanding the evolution of phenotypic traits, redefining species limits, and clarifying areas of endemism—knowledge critical to guiding future biodiversity investigation and developing informed conservation policies across the region.

ACKNOWLEDGMENTS

Numerous institutions and colleagues have been integral in helping me realize the completion of this dissertation. First and foremost, I thank my advisor A. Townsend Peterson, for his patient support and guidance during my time as a graduate student at KU. Conducting extensive collecting expeditions in Papua New Guinea has required substantial financial resources and proven extremely time consuming, yet Town and the KU Division of Ornithology have always come through in providing the means necessary to complete 4 major expeditions across the New Guinea highlands and sequence the large genetic data set that resulted from these trips. I am also indebted to the other members of my dissertation committee, Robert Moyle, Mark Robbins, Robert Timm, and Stephen Benedict, for their time and efforts in providing insightful discussions and advise throughout the course of my research.

My academic experience at KU has been enhanced by a number of fellow graduate students and staff in the department of ecology and evolutionary biology. Jennifer Pramuk and Mike Grose were extremely helpful in introducing me to molecular sequencing techniques and methods of phylogenetic analysis. I also benefited from discussions with the following students: Mike Anderson, Elisa Bonaccorso, Jake Esselstyn, Pete Hosner, Leo Legra, Charles Linkem, Yoshi Nakazawa, Árpi Nyári, Cameron Siler, and Jeet Sukumaran. I especially thank Andrés Lira-Noriega for his generous assistance in developing ecological niche reconstructions. Mark Robbins introduced me to specimen preparation techniques, and has been a continual source of guidance and academic inspiration throughout my time at KU. Thanks, Mark, for the many years of friendship and support.

I am grateful to the following institutions, curators, and collection managers who provided tissue loans for this research: Paul Sweet, Joel Cracraft, and George Barrowclough of

the American Museum of Natural History (AMNH), Kristof Zyskowski and Rick Prum of the Yale Peabody Museum (YPM), Jeremiah Trimble and Scott Edwards of the Harvard Museum of Comparative Zoology (MCZ), Nate Rice of the Philadelphia Academy of Natural Sciences (ANSP), Leo Joseph and Robert Palmer of the Australian National Wildlife Collection (ANWC), Ken Walker of the Victoria Museum (VM), and Town Peterson, Rob Moyle, and Mark Robbins of the University of Kansas Natural History Museum (KUNHM).

A number of people have been indispensable in helping me carryout fieldwork across Papua New Guinea. I owe special thanks to the former co-directors of the Wildlife Conservation Society PNG program Andrew Mack and Debra Wright, as they helped in countless ways with fieldwork logistics and provided me with a home away from home while in Goroka. The team of conservation biologists that Andy and Deb mentored within the PNG-WCS country program has recently established the Papua New Guinea Institute for Biodiversity Research, which has also been invaluable in helping with in-country logistics. In particular, I thank Banak Gamui, Miriam Supuma, Paul Igag, Katayo Sagata, Michael Kigl, Muse Opiang, Junior Novera, Anna Koki, Onika Okena, and Kamena Yoriene for their assistance in Goroka and support in the field over the last several years. I owe a great debt of gratitude to Ed Scholes who introduced me to the nuances of conducting fieldwork in Papua New Guinea and has provided many hours of stimulating discussions concerning Melanesian ornithology. It's been a real pleasure working with Ed over the years at various sites across the highlands of Papua New Guinea, and I look forward to further collaboration in the future. I thank Tim Laman for providing the opportunity to work in West Papua, Indonesia, in 2008, as well as helping to collect behavioral data on bowerbirds in the Foya Mountains. I acknowledge the Papua New Guinea Department of Environment and Conservation (DEC) for its continued support of this research, and providing

permits for specimen collection and exportation to KUNHM. I am indebted to James Robbins and the National Research Institute (NRI) staff who have been integral in arranging research visas and provincial approvals, and I also thank the Eastern Highlands, Madang, and Central province administrations for their support of this research through issuing provincial approvals. This research would not have been possible without the many kind Papua New Guinea landowners who assisted with fieldwork, and shared their homes, food, and extensive knowledge of regional bird diversity. Lastly, I thank my parents for their many years of support and encouragement throughout my academic endeavors.

Funding for this research was provided by the following sources: Wildlife Conservation Society Research Fellowship (BWB), KUNHM Panorama Fund grants (BWB), KUNHM Rudkin Fund (BWB), KU Department of Ecology and Evolutionary Biology (BWB), KU College of Liberal Arts and Sciences General Research Fund (A. T. Peterson), and a grant from the National Institutes of Health (A. T. Peterson).

TABLE OF CONTENTS

INTRODUCTION

New Guinea's extensive rainforest ecosystems harbor an exceptionally diverse biota of disparate biogeographic origins spanning Southeast Asia, Australia, and Oceania (Walker, 1972; Gressitt, 1982; Keast & Miller, 1996). The historical processes contributing to this biogeographic complexity and high species richness have long intrigued evolutionary biologists, yet few studies have addressed these issues with explicit tests of historical diversification (Wallace, 1869; 1876; Mayr, 1942; Darlington, 1957; 1965; Diamond, 1972; Simpson, 1977; Gressitt, 1982; Joseph et al., 2001; Joseph & Omland, 2009). Consequently, fundamental aspects of New Guinea's evolutionary history remain obscure for most taxonomic groups.

Owing to its relatively complete alpha taxonomy, New Guinea's avifauna has played a prominent role in the development of biogeographic hypotheses and speciation theory throughout the Papuan sub-region (Mayr, 1953; Schodde & Calaby, 1972; Diamond, 1972; 1973; MacArthur & Wilson, 1967; Mayr & Diamond, 2001). Early investigations typically inferred multiple waves of colonization via long-distance dispersal to explain the geographic origin and historical diversification of avian lineages across the island; however, recent progress in resolving phylogenetic relationships within the Australo-Papuan avifauna, coupled with advances in deciphering the region's dynamic tectonic history have shed new light on broad-scale patterns of colonization and speciation, revealing New Guinea's role as both source and filter of avian lineage diversity (Filardi & Moyle, 2005; Norman et al., 2007; Moyle et al., 2009; Nyari et al., 2009; Jønsson et al., 2010). By comparison, few molecular phylogenetic investigations have focused on the evolutionary processes driving in situ diversification within mainland New Guinea, owing largely to the paucity of modern avian systematic collections from key biogeographic regions across the island (Murphy et al., 2007; Joseph & Omland, 2009). The

evolutionary origin of New Guinea's montane avian species richness remains especially enigmatic, in that much of this diversity appears to stem from relictual Tumbunun lineages that have diversified across the vast interior highlands despite an apparent absence of major barriers to dispersal throughout these ranges for ~1800km (Diamond, 1972; Pratt, 1982). Likewise, the evolutionary mechanisms promoting patterns of fine-scale endemism and differentiation among montane populations have yet to be examined using modern population genetic analyses and GIS-based techniques to distinguish among alternative evolutionary hypotheses.

Herein, I use phylogeographic methods and paleodistributional modeling to explore the evolutionary dynamics driving spatial patterns of genetic diversity within New Guinea's montane avifauna. In Chapter 1, I reconcile analyses of population genetic structure and historical demography with paleoecological niche reconstructions in *Peneothello cyanus* (Petroicidae) to evaluate the role of Pleistocene climate change in shaping its phylogeographic history. A similar suite of methods is employed in Chapter 2 to assess phylogeographic relationships within the *Crateroscelis robusta* (Acanthizidae) species complex, and examine the evolutionary basis of its "leapfrog" distribution pattern across the interior highlands and outlying coastal sky-islands. In Chapter 3, I take a comparative phylogeographic approach by contrasting population genetic structure in four co-distributed taxa [*Rhipidura atra* (Rhipiduridae), *Amblyornis macgregoriae* (Ptilonorhynchidae), *P. cyanus*, and *C. robusta*] to evaluate how climate change, topography, and dispersal capacity have influenced avian diversification and historical demography in the New Guinea highlands. Below, I briefly review the orogenic history of New Guinea's contemporary montane topography, and introduce the principal evolutionary hypotheses that have been proposed to explain lineage formation and diversification within the island's montane avifauna.

Geological history and avian distributions in the New Guinea highlands

Approximately one-third of New Guinea's 580 resident bird species is endemic to its montane rainforest environments, which comprise a globally important center of avian diversity including several endemic families (Pratt, 1982; Stattersfield et al., 1998). Species richness is especially concentrated in the Central Dividing Ranges (CDRs), a rugged fold-and-thrust montane belt spanning ~1800 km with substantial land area at elevations >2000 m and remnant glaciers persisting on its highest peaks near 4800 m (Fig. 1). Orogenic formation of the CDRs was initiated in the mid-to-late Oligocene, as a consequence of tectonic rifting and collisional processes along the Australian and Pacific plate boundaries; however, the principal topographic features and elevational relief of these ranges have taken form more recently, in the late Miocene and early Pliocene (Dow, 1977; Pigram & Davies, 1987; Audley-Charles, 1991; Pigram & Symonds, 1991; Abbott et al., 1997; Hall, 2002). At least 32 distinct tectonostratigraphic terranes have been deposited along this collisional boundary, many of which are island-arc volcanic formations of oceanic affinity originating several thousand kilometers to the north (Pigram & Davies, 1987; Hall, 2002). This history of tectonic collision and terrane accretion also resulted in the docking and uplift of New Guinea's coastal ranges in the mid-to-late Pliocene, including fragments of the Tamrau and Arfak mountains in the Vogelkop Peninsula, and the North Coast Ranges, which include the Foya, Cyclops, Bewani, Torricelli, and Prince Alexander mountains (Pigram & Davies, 1987; Hall, 1998; 2002). The most recent of these collisions resulted in the formation of the Adelbert Range and Huon Peninsula as the Finisterre volcanic arc terranes docked with the New Guinea orogen 3.0–3.7 Myr ago (Pigram & Davies, 1987; Abbott et al., 1994; 1997). Despite its recent orogenic history, the Huon contains several peaks over 4000 m elevation, demonstrating the rapid orogenic uplift that may accompany these

collisional forces. Rates of uplift and lateral rifting remain less clear within the CDRs due to its geological complexity; however, an emerging consensus based on diverse lines of evidence indicates a recent and rapid orogenic history across much of the New Guinea highlands, which has important implications for understanding the assembly of its montane biota and evolution of biogeographic boundaries across this composite geological landscape (Dow, 1977; Löffler, 1977; Pigram & Davies, 1987; Audley-Charles, 1991; Pigram & Symonds, 1991; Abbott et al., 1997 Hall, 1998; 2001; 2002).

Peripherally isolated from the Central Highlands by narrow land bridges, lowland successor basins, and broad river valleys, species richness within New Guinea's outlying sky-island communities is depauperate by comparison to equivalent environments in the CDRs, whereas endemism and intraspecific variation among these coastal terranes is high, suggesting that gene flow between adjacent communities is limited. Within the largely contiguous Central Highlands and Papuan Peninsula, few potential geographic barriers to avian dispersal are evident, with the exception of several narrow intervening river valleys, among which headwaters of the Strickland and Watut–Tauri drainages correspond to traditionally recognized biogeographic boundaries (Pratt, 1982; Frith & Beehler, 1998; Heads, 2001a). The Watut–Tauri drainages also coincide with the northwestern limits of the Owen Stanley/Menyamya terranes, which share a distinct tectonic history from the adjacent Eastern Highlands (Pigram & Davies, 1987; Pigram & Symonds, 1991; Hall, 2002). Contemporary montane rainforest communities have become increasingly fragmented within the CDRs and outlying coastal ranges, although this trend is relatively recent, resulting from strong human population growth and rapid expansion of modern agricultural practices (Gressitt, 1982; Hope, 1996).

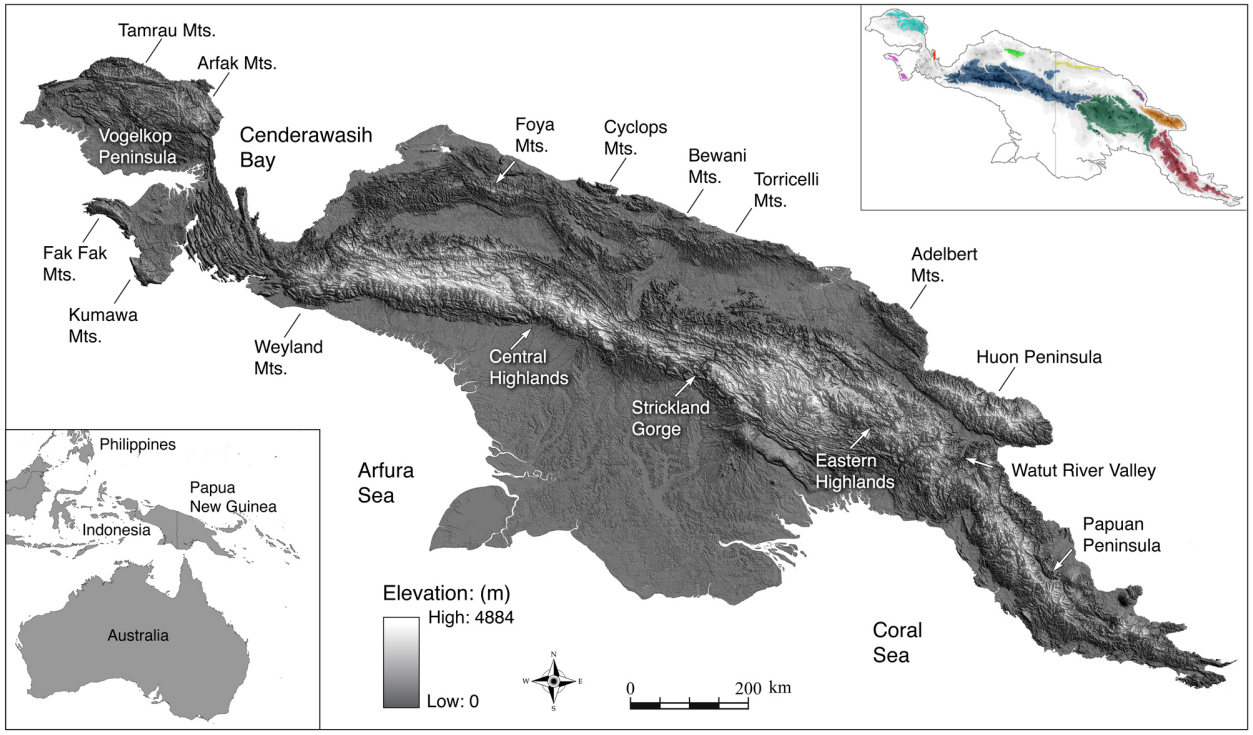

Figure. 1. Digital elevation model depicting New Guinea's extensive Central Dividing Ranges and outlying coastal sky-islands. Areas of montane avian endemism inferred from traditional taxonomic arrangements are indicated by the upper right colored inset.

Hypotheses of avian diversification in the New Guinea highlands

Early biogeographic assessments of New Guinea's highland avifauna generally invoked allopatric processes of diversification fueled by pervasive dispersal to explain spatial relationships among closely related lineages; however, these hypotheses provide few testable predictions within a spatiotemporal context, and have accordingly received criticism by several authors given the sedentary nature that characterizes much of New Guinea's montane avian diversity (Wallace, 1876; 1880; Mayr, 1953; Schodde & Calaby, 1972; Diamond, 1973; Heads, 2001a; Mayr & Diamond, 2001). Recent molecular phylogenetic studies have recovered limited support for two alternative hypotheses based on tectonic and climate driven vicariant speciation processes across New Guinea's highland landscape, which are discussed below (Heads, 2001a;

Norman et al., 2007; Irestedt, 2009). Nonetheless, these studies are limited to species-level relationships within broadly distributed genera that inhabit ecologically diverse habitats; thus, the environmental factors and demographic processes governing patterns of intraspecific diversification across the CDRs and coastal sky-islands have yet to be examined with modern phylogeographic methods for any taxon (Joseph & Omland, 2009).

Diamond (1972) proposed a "drop-out" hypothesis of New Guinea avian diversification centered on vicariant processes within the Eastern Highlands (Fig. 1), in which a continuous population differentiates across an east-west cline within the CDRs, subsequently undergoes localized extinction that further limits gene flow among clinal extremes, thereby permitting additional divergence and eventually the evolution of discrete lineages. As the two lineages reinvade their former distribution, Diamond invoked a competitive exclusion mechanism to promote elevational sorting that leads to the evolution of sharply delineated elevational sister taxa. Based on field observations throughout much of the Eastern Highlands, Diamond cited a suite of 9 species (e.g., *Climacteris leucophae*, *Macgregoria pulchra*, *Orthonyx temminckii*, *Amalocichla sclateriana*, among others) that appear to exhibit a ~ 400 km distributional gap, typically ranging from the Strickland Gorge east to the Watut–Tauri River valleys, as evidence of the localized "drop out" phase, whereas genera such as *Parotia*, *Melidectes*, and *Crateroscelis* have been cited as evidence of the competitive exclusion phase (Diamond, 1972; 1973; Pratt, 1982). Although an explicit mechanism for initiating these localized extinctions was not identified, Diamond suggested that climatic fluctuations and the associated elevational compression of montane vegetation zones may have been a dominant force, acting to restrict population connectivity during cooler periods (Diamond 1972; 1973).

Subsequent analyses of palynological spectra examined from multiple coring sites throughout the CDRs have shown that Pleistocene climate change impacted the distribution of New Guinea's montane floral communities dramatically (Nix & Kalma, 1972; Hope & Peterson, 1976; Walker & Hope, 1982; Haberle et al., 1990; Hope & Tulip, 1994; Hope, 1996). Summaries of pollen spectra from these independent study sites indicate a depression of present-day tree line from 3700 m (6ºC annual isotherm) to 2200 m during the Last Glacial Maximum (LGM); spanning 23,000–15,000 years before present (ybp), with ~2000 km^2 of glacial cover above 3500 m during this period. The elevational compression of montane floral communities was not commensurate, however, as alpine grasslands showed a significant down-slope expansion from the 3500 m snow line to 2200 m, whereas subalpine moss forests were constrained to a narrow elevational band limited to 200 m down-slope from the alpine grassland ecotone, or were lost altogether, depending on local topography (Hope, 1996). Upper to mid-montane *Nothofagus* forests experienced more moderate elevational displacement, ranging 900–2000 m, roughly a 1000 m drop from present-day distributions, while lower montane habitats were compressed to just 300 m down-slope of their present distribution before giving way to foothill and lowland forest environments. By contrast, New Guinea's coastal montane rainforest communities were affected less by cooler LGM climatic conditions, with floral distributions descending only a few hundred meters, as the biota of these terranes already exhibit considerable elevational compression, given their costal proximity and limited high altitude topography (Paijmans, 1976; Hope, 1996).

More recently, several researchers have embraced the regions complex tectonic history in explaining patterns of species richness and historical diversification within New Guinea's highland avifauna (Michaux, 1994; Heads, 2001b; 2002). In a series of studies examining

geographic distributions of the Paradisaeidae and other co-distributed avian groups, Heads (2001a, 2001b, 2002) proposed that New Guinea's terrane accretion history and rapid orogenic formation has uplifted elements of the island's lowland avifauna, providing opportunities for vicariant diversification across elevational gradients within the interior highlands. Heads (2001b, 2002) further surmised that west lateral rifting of these accreted terranes may explain broad-scale disjunctions among closely related avian lineages distributed across New Guinea's composite montane landscape (e.g. *Parotia*, *Paradisaea*, and *Astrapia*). Although similar biogeographic hypotheses have been suggested to explain the evolutionary history of other floral and faunal groups across the New Guinea orogen (Flanery, 1995; Polhemus & Polhemus, 1996; van Welzen, 1997), researchers have yet to explicitly test the spatiotemporal predictions of these tectonic-based hypotheses of diversification using modern phylogenetic techniques with robust geological and molecular calibrations (Heads, 2001a; 2001b; 2002; Norman, 2007; Irestedt, 2009).

CHAPTER ONE

PHYLOGEOGRAPHIC STRUCTURE AND PALEOECOLOGY REVEAL EFFECTS OF PLEISTOCENE CLIMATIC OSCILLATIONS IN A MONTANE NEW GUINEA PASSERINE (*PENEOTHELLO CYANUS*)

ABSTRACT

New Guinea's rugged montane landscape supports an avifauna of high species richness, strong elevational specialization, and fine-scale endemism among disjunct sky-island communities. The underlying evolutionary processes driving these patterns of diversification remain poorly understood, as lack of genetic sampling has precluded modern phylogeographic analyses for most taxonomic groups. Herein, I examine population genetic structure within a montane New Guinea passerine (*Peneothello cyanus*), and explore the role of Pleistocene climate fluctuations in shaping its evolutionary history. Mitochondrial sequence data (ND2, ND3, ATP6-8) and standard phylogeographic methods were used to examine the distribution of genetic diversity among 161 individuals of *P. cyanus* sampled across 28 localities. The resulting spatial assessments of genetic variation were reconciled with contemporary and paleoecological niche reconstructions to test hypotheses of climate-mediated diversification and historical demography in the New Guinea highlands. Phylogeographic analyses recovered three primary clades within *P. cyanus*, the distributions of which correspond to currently recognized subspecies and are consistent with prominent biogeographic boundaries including the Vogelkop Peninsula and Strickland River valley. Coalescent estimates of divergence times indicate that these lineages arose in the middle to lower Pleistocene, with ND2 pairwise sequence divergences ranging from 1.15–4.08% among regional lineages. Patterns of population genetic structure were largely

congruent with the distribution of contemporary sky-islands and montane rainforest connectivity inferred by ecological niche models projected to Last Glacial Maximum climatic conditions. Bayesian skyline plots exhibited signatures of demographic expansion in each subspecies over the most recent time interval, further corroborating the patterns of range expansion predicted by paleoecological niche reconstructions. These results suggest that Pleistocene climatic oscillations strongly influenced the demographic history of *P. cyanus*, yet statistically significant Mantel tests indicate that isolation-by-distance effects also contributed to phylogeographic structure among regional lineages. Shallow genetic divergences observed throughout the Eastern Highlands and Papuan Peninsula are consistent with low-level gene flow and recurrent population connectivity predicted by paleoecological niche reconstructions, whereas deeper genetic splits in the Bird's Neck region, Strickland Gorge, and North Coast Ranges indicate retention of genetic diversity across multiple climatic cycles.

INTRODUCTION

Pleistocene climatic oscillations have influenced profoundly the geographic distribution of species and the environments in which they inhabit, as evidenced by marine and terrestrial sedimentation, fossil records, paleoecological niche modeling, and spatial patterns of genetic variation (Graham et al., 1999; Avise, 2000; Jansson & Dynesius, 2002; Hewitt, 2004). The biotic consequences of these recurrent shifts in distribution have long been of interest to evolutionary biologists, with temperate ecosystems of the Northern Hemisphere playing a dominant role in advancing understanding of climate-mediated diversification in the Pleistocene (Hewitt, 1996; 2000; 2004).

By comparison, the influence of climatic cycling on patterns of population structure and speciation in tropical montane landscapes has received limited attention, despite their attributes of an ideal study system, including high species richness, strong elevational specialization, and acute sensitivity to climate change. Distributions of lineages that are isolated across high-elevation sky-islands during warm interglacial periods may experience significant elevational depression under cooler climates corresponding to periods of glacial maxima, such that disjunct populations are joined in low-elevation refugia, promoting gene flow or zones of hybridization (Hope 1996; Hewitt, 2004; Graham et al., 2006 Hooghiemstra et al., 2006). Alternatively, these distributional displacements may result in multiple low-elevation refugia or compressed patchy networks, the former maintaining genetic isolation whereas the latter may permit moderate to limited admixture between population isolates. The spatial dynamics of these alternative refugial models are dependent upon local topography, regional climate patterns, and species-specific responses to variation in ecological parameters (Graham et al, 1999; Moussalli et al., 2009; Lawson, 2010).

As each model carries distinct phylogeographic predictions with respect to demography, gene flow, and population genetic structure, emerging methods for deriving taxon-specific paleodistribution estimates from ecological niche modeling have become an integral component of the phylogeographic tool set, providing an explicit ecological and spatial context critical to examining the evolutionary processes driving lineage origin and diversification in the Pleistocene (Carstens & Richards, 2007; Richards et al., 2007; Carnaval et al., 2009; Moritz et al., 2009). In the present study, I integrate spatial analyses of genetic variation with ecological niche reconstructions to evaluate the role of Pleistocene climate change in shaping haplotype

diversity, historical demography, and paleodistributional patterns of the Slaty Robin (*Peneothello cyanus*), a forest-dwelling passerine endemic to the New Guinea highlands.

Study system

The Australo-Papuan Petroicidae includes ~45 species of small-bodied oscine passerine classified in 13 genera, among which *Peneothello* is comprised of four species endemic to New Guinea (Boles, 2007). The distribution of *P. cyanus* is particularly well suited for examining the biotic consequences of Pleistocene climatic fluctuations across New Guinea's highland landscape, as this species is broadly distributed but tightly linked to montane rainforest habitats owing to its elevational specialization, relatively weak dispersal capacity, and aversion to open environments. The elevational distribution of *P. cyanus* ranges 1600–2800 m in the Central Highlands, with peak densities in lower to mid-montane *Lithocarpus* and *Nothofagus* closed-canopy forest. On outlying coastal ranges, where montane habitats may be compressed by several hundred meters due to local climatic phenomena, *P. cyanus* regularly extends down to 1400 m in the Adelbert, Bewani, Torricelli, and Foya mountains (Diamond, 1969; Pratt, 1983). This species exhibits sharp elevational breaks between co-distributed congeners throughout much of its range, with congenerics *P. bimaculata* occupying foothill forest and *P. sigillata* inhabiting upper montane and subalpine forest/forest-edge environments. In the western half of its distribution, *P. cyanus* is restricted to lower montane forest habitats, and may occasionally extend below 1400 m, as *P. cryptoleuca* replaces it in middle to upper montane rainforest environments (Rand & Gilliard; 1959; Diamond, 1985). Three subspecies are currently recognized within the Slaty Robin, based on subtle variation in crown and body plumage

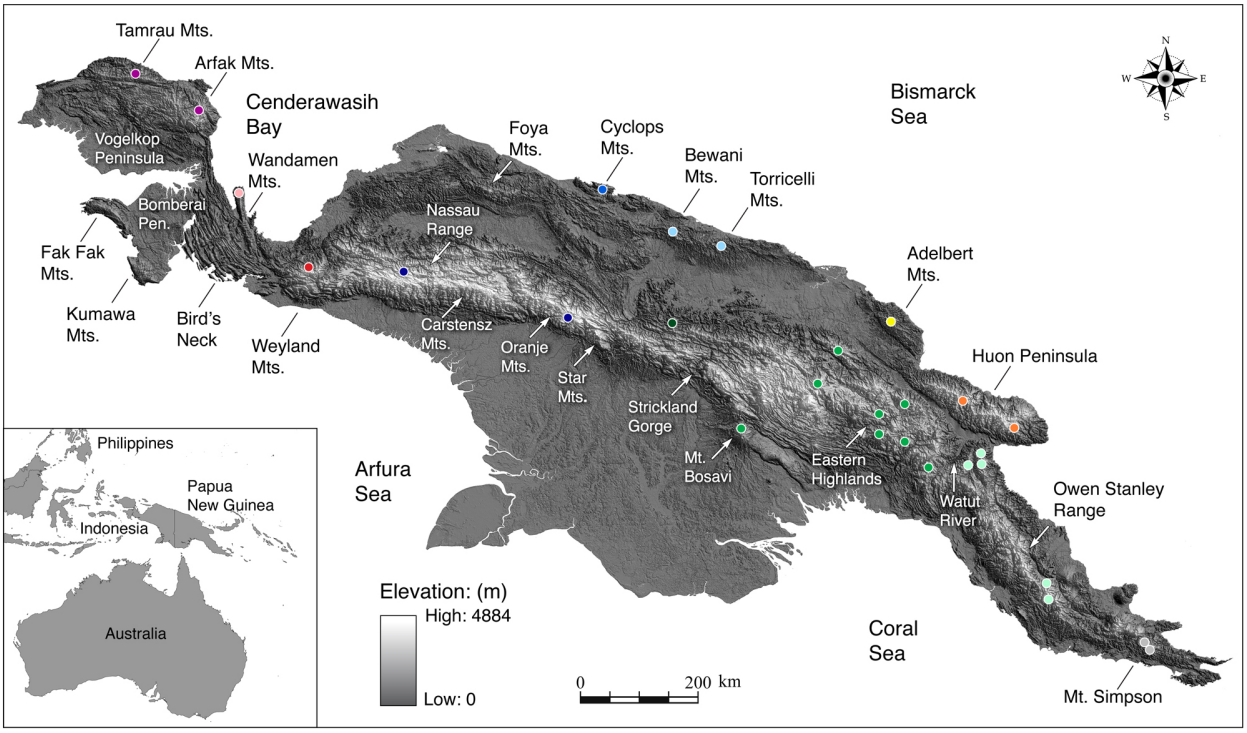

Figure. 1.1. Digital elevation model of New Guinea depicting the principal montane topographic features discussed in the present study. Collection localities of *Peneothello cyanus* are color coded by population and correspond to colors shown on the Bayesian inference topology and haplotype network.

coloration. Endemic to the Vogelkop Peninsula, nominate *P. c. cyanus* is overall lighter grey than *P. c. atricapilla,* which exhibits a subtly darker crown and ranges from the Wandamen mountains east to the Hindenburg Range, including peripherally isolated populations in the Foya, Cyclops, Bewani, and Torricelli Ranges (Fig. 1.1). The eastern taxon *P. c. subcyanea* is distinguished by a slightly lighter crown, and occupies the Central Highlands from the Strickland Gorge east throughout the Owen Stanley Ranges and Papuan Peninsula, as well as the outlying Mt. Bosavi, Adelbert Range, and Huon Peninsula populations.

In this contribution, I take a first look at the phylogeography of *P. cyanus*, evaluating haplotype diversity throughout its range to address a series of questions centered on the impact of Pleistocene climate change and diversification in the New Guinea highlands. (1) Is genetic

diversity structured geographically by contemporary montane rainforest sky-islands and traditionally recognized biogeographic boundaries within the Central Highlands, and to what extent is genetic variation concordant with distributions of morphologically defined taxonomic units? (2) Are genetic distances among populations consistent with patterns of environmental connectivity and isolation inferred by paleoecological niche reconstructions, or are estimates of population divergence times better explained by spatial relationships of sky-islands (i.e. isolation-by-distance) and/or deeper geological events within the Pliocene? (3) Do coastal sky-island populations represent independent colonization events from the Central Highlands, and has "upstream" dispersal (e.g. peripatric diversification) from costal sky-islands influenced population genetic structure within the CDRs? (4) Are trends of demographic expansion predicted by ecological niche models (LGM to present) congruent with genetic signatures of population demography, and how have isolated coastal populations responded to climate change in comparison to larger communities of the Central Highlands?

METHODS

Population sampling

I sampled 161 individuals of *P. cyanus* from 28 distinct localities, encompassing the full extent of the species' distribution apart from the Bomberai Peninsula and Foya Mountains (Fig. 1.1). Multiple field expeditions were conducted across key biogeographic regions in Papua New Guinea to assemble modern comparative voucher collections prepared as skin, skeletal, and fluid-preserved specimens. Associated tissue samples (muscle) were initially stored in 99% ethanol and later transferred to -70ºC storage at the University of Kansas Natural History Museum (KUNHM). When possible, specimens were collected along elevational transects

(1450–2800 m) comprising 2–3 camps per site to minimize sampling bias within demes and refine understanding of elevational limits in *P. cyanus* across New Guinea's ecologically diverse montane landscape.

In addition to the modern specimen series, ancient DNA tissues (toepad clippings) sampled from historical collections spanning 1928–1973 were utilized to include populations from Papua and West Papua, Indonesia, and to refine sampling resolution near suspected geographic breaks. Based on a recent phylogenetic analysis of the Petroicidae (Loynes et al., 2009), outgroup sampling included the three remaining congeneric species (*P. bimaculata*, *P. sigillata*, *P. cryptoleuca*), the closely related *Peneoenanthe pulverulenta* and *Melanodryas cucullata*, and four members of the confamilial *Poecilodryas*, including *P. placens*, *P. albispecularis*, *P. hypoleuca*, and *P. albonotata*. Specimen data including collection locality, latitude and longitude, institutional source, voucher number, and tissue type are detailed in Appendix 1.1.

Sequencing protocols

Whole genomic DNA was extracted from muscle tissue using proteinase K digestion under manufacturer's protocols (DNeasy Tissue Kit, QIAGEN), and a suite of four mtDNA genes including NADH dehydrogenase subunit-2 (ND2, 867 bp), ATP synthase subunits-6 and 8 (ATP6, 684bp; ATP8, 171bp), and NADH dehydrogenase subunit-3 (ND3, 351 bp) was amplified via 12µl polymerase chain reactions (PCR) using PureTaq RTG PCR beads (GE Healthcare). Thermocycle parameters for each external primer pair (Appendix 1.2) consisted of an initial 3 min denaturation at 94 ºC, followed by 35 cycles of 20 s at 94 ºC, 15 s at 53 ºC, and 60 s at 72 ºC, followed by a 7 min final extension at 72 ºC and 4 ºC soak. All PCR products

were cleaned of unincorporated DNTPs and primers with ExoSaP-IT purification (USB Corp.), visualized on a 1% agarose gel stained with ethidium bromide to assess amplification quality, and cycle-sequenced with ABI Prism BigDye v3.1 terminator chemistry under manufacture's thermocycling protocols using the same external PCR primer pairs. Cycle-sequencing products were desalted and cleaned of excess terminator dyes with Sephadex G-50 (medium) purification columns, and subsequently analyzed on an ABI 3730 Genetic Analyzer (Applied Biosystems).

Genomic extractions of ancient DNA samples were conducted outside of the main KUNHM molecular facility in a lab free of avian PCR and genomic procedures. Workstations and all equipment were cleaned with a 10% bleach solution prior to performing each set of extractions; to protect further against downstream contamination, filtered pipette tips were used throughout all ancient DNA sequencing procedures, as were multiple negative controls during extraction and amplification to enable detection of potential contamination. Samples were extracted using a DNeasy Tissue Kit (QIAGEN), extending the tissue lysis step overnight with the addition of 10 μl of 1M Dithiothreitol to facilitate complete digestion of the toepad sample, and all negative controls were tested for contamination using a NanoDrop spectrophotometer (Thermo Scientific). Complete ND3 sequences were obtained via the same external primer pair used for fresh tissues (Chesser, 1999), whereas a suite of internal primers were designed to sequence the entire ATP6–8 subunits using three ~350 bp amplicons with a minimal 15 bp overlap between fragments excluding primer sequences. The same three-amplicon approach was used to obtain 867 bp from the 5' end of the ND2 gene. Thermocycling protocols for all ancient DNA PCRs were modified to incorporate an annealing touch down of 10 cycles at 60 ºC, 10 cycles at 56 ºC, and 25 cycles at 52 ºC, followed by a 10 min extension at 72 ºC and 4 ºC soak. An additional 15 cycles were added to ABI's standard thermocycling protocols to maximize

signal strength of chromatograms. All other sequencing procedures followed standard protocols detailed above for fresh DNA samples.

Phylogenetic analysis

Chromatograms of complimentary strands were reconciled in SEQUENCHER v. 4.1 (Gencodes) and an initial sequence alignment was performed in CLUSTAL X (Thompson et al. 1997) under default settings. Subsequent gap adjustments were conducted by eye in MESQUITE v. 2.72 (Maddison & Maddison, 2009), followed by amino acid translation for comparison with *Gallus gallus* sequences (Dejardins & Morias, 1990) to confirm reading frames. I evaluated several partitioning strategies for the combined four-gene sequence alignment to optimize model specificity and assess the impact of parameterization on topology and node support. Partitions were selected *a priori* by gene and codon position, and best-fit models of evolution were determined for each partition in JMODELTEST v. 0.1.1 (Guindon & Gascuel, 2003; Posada, 2008) using the Bayesian Information Criterion (BIC), which offers advantages over other model selection criteria by minimizing overfitting of the data more effectively. Given the short read length of ATP8 sequences (171bp), ATP synthase subunits were combined, resulting in nine data partitions for the concatenated sequence alignment when subdivided by gene and codon position. Additional partitioning combinations run for comparison include by gene, by codon, and no partitioning.

I estimated phylogenetic relationships within *P. cyanus* from the concatenated four-gene data set using Bayesian inference (BI) implemented in MRBAYES v. 3.1.2 (Ronquist & Huelsenbeck, 2003; Altekar et al., 2004), with BIC selected models of nucleotide substitution applied to each respective partition. Analyses were conducted with a flat prior specified for

parameter estimation, and modified heating conditions of 0.15 were applied to four Markov chains run for $2x10^7$ generations sampled every 1000 generations resulting in 15,000 total trees after a conservative 25% initial burnin. Two or more analyses were conducted per partitioning scheme to guard against convergence on local optima, and stationarity of each run was assessed by monitoring average standard deviation of split frequencies, plotting –lnL against generation time, assessing model parameter posterior probability densities in TRACER v. 1.5 (Rambaut & Drummond, 2007), and examining clade posterior probabilities across runs using the compare and slide functions in AWTY (Nylander et al., 2008). Results of alternative partitioning strategies were evaluated by comparing the harmonic mean of the model likelihood $f(X|M_i)$ using Bayes Factors (BF) calculated in the program TRACER v. 1.5, to determine the optimal level of partitioning, with 2ln BF values >10 considered as strong evidence against an alternative partitioning model (Kass & Raftery, 1995; Suchard et al., 2001).

Topology and node support were also inferred via partitioned maximum likelihood (ML) analyses conducted in GARLI v. 2.0 (Zwickl, 2006), which implements a genetic algorithm and jointly estimates topology, branch lengths, and model parameters, yielding significant advances in computational efficacy for large data sets. Twenty independent runs were conducted under default parameters for the combined nine-partition data set to ensure that the optimal –lnL solution had been reached. Topologies were selected after 50,000 generations with no significant improvement in –lnL (improvement values set at 0.01 with a total improvement of < 0.05 compared to the last topology recovered). Node support was assessed using 1000 non-parametric bootstrap replicates using a reduced run termination criterion of 10,000 generations.

Population structure and demography

Minimum spanning networks of haplotype relationships were constructed for each gene using the Bandelt et al. (1999) algorithm implemented in NETWORK v. 4.5 (fluxus-engineering.com) to visualize spatial patterns of genetic variation. Analyses were performed using default parameters, with the MP optimization algorithm applied to minimize extraneous median vectors (Polzin & Daneschmand, 2003). Results of haplotype networks presented herein are limited to ND2 sequences, as this gene was representative of the other markers, which are part of the same mtDNA linkage group.

Genetic variation within populations was characterized using DNASP v. 5.0 (Librado & Rozas, 2009) to calculate summary statistics, including number of unique haplotypes (h), number of segregating sites (S), haplotype diversity (Hd), and the nucleotide diversity parameter π along with its 95% confidence interval. Pairwise F_{ST} statistics were used to estimate geographic structure of genetic diversity among sites and define population limits across the 28 collection localities. Three-way analyses of molecular variance (AMOVA) were conducted in ARLEQUIN v. 3.5 (Excoffier & Lischer, 2010) to examine further the geographic structure among populations and test the role of Pleistocene climate change in shaping genetic diversity across New Guinea's Central Highlands and outlying costal sky-islands. Samples were grouped by contemporary populations (table 2), Pleistocene sky-islands inferred from LGM ecological niche reconstructions (Fig. 8), and current taxonomy. Pleistocene sky-islands include the same suite of coastal populations defined in contemporary groupings, whereas populations of the CDRs and Papuan Peninsula were grouped into a single contiguous population based on extensive habitat connectivity. Mantel tests were implemented in IBDWS v. 3.16 (Isolation By Distance Web Service: http://ibdws.sdsu.edu/; Jensen et al., 2005) using 10,000 permutations to test for

correlations between genetic and geographic distances within regional lineages and the species as a whole. Geographic straight-line distances (km) between populations were estimated from geo-referenced collecting localities using ArcGIS (ESRI, Redlands, CA). Genetic distances were computed as $F_{ST}/1-F_{ST}$ as recommended in Rousset (1997), and given the stepping-stone pattern of distribution within *P. cyanus*, geographic distances were not log-transformed.

I evaluated the historical demography of populations in DNASP v. 5.0 using a suite of summary statistics based on the frequency spectrum of mutations including Tajima's *D*, Fu & Li's *D* (Fu & Li, 1993), and the R_2 statistic (Ramos-Onsins & Rozas, 2002). The latter statistic exhibits the greatest power in detecting demographic change in small sample sizes, as it measures the difference between the number of singleton mutations and the average number of nucleotide differences among sequences within a population. As such, the R_2 statistic should provide the best indication of population demographic history for this study based on relatively small sample sizes, whereas Fu & Li's *D* statistic has been shown to provide greater sensitivity to more recent bottleneck events (Soriano, 2008). Fu's *Fs* statistic (Fu, 1997), which is based on the haplotype distribution, was also calculated, as this statistic is among the most sensitive to recent population contractions (Ramos-Onsins & Rozas, 2002). The significance of each test statistic was assessed using 10,000 coalescent simulations conducted in DNASP v. 5.0. Lastly, the distribution of pairwise differences was used to infer demographic history by plotting mismatch distributions for each population and compared to a null hypothesis of demographic expansion, which exhibits a smooth, unimodal Poisson distribution (Harpending, 1994). The fit of observed data was assessed using the raggedness statistic (*r*) calculated in DNASP v. 5.0, with significance determined using 10,000 coalescent simulations. All population genetic summary statistics were derived from the full sequence alignment.

Bayesian skyline analyses were conducted for each clade using BEAST v1.5 (Drummond & Rambaut, 2006; 2007) to explore further the demographic history of *P. cyanus*, as this method takes into account the full compliment of historical phylogeographic information inherent to sequence variation, thereby offering advantages over traditional summary statistics that rely on the frequency spectrum of mutation or haplotype distribution (Drummond et al., 2005). Models of sequence evolution were determined for each clade and the combined data set using the BIC in JMODELTEST v. 0.1.1, and analyses were run for 10^7 generations under default parameters with sampling every 1000 generations. Multiple analyses were conducted per lineage to ensure that the run achieved stationarity as determined from posterior probability densities of model parameters examined in TRACER v. 1.5; a conservative 25% burnin was implemented for final analyses.

Gene flow and divergence times

Ongoing gene flow among adjacent populations in the eastern Central Highlands and Papuan Peninsula was estimated using IMA2 (Hey, 2010), which implements an isolation-with-migration coalescence model and Markov chain Monte Carlo (MCMC) search algorithm to sample genealogies from the data for comparison to driving values drawn from a specified prior distribution. These driving values are in turn used to assemble the posterior probability distribution of the effective population size ($2N_e\mu$), migration rate ($2N_f m$), and divergence time (t), with parameter values estimated from the distributional peak, whereas confidence intervals are calculated from the area under the curve. Pairwise analyses were conducted using the full ND2 sequence alignment to assess bidirectional migration between Mt. Stolle, Eastern Highlands, and Owen Stanley populations, each of which lacked reciprocal monophyly as

indicated by the BI topology and median-joining network. Pairwise analyses were run for 1 x 10^7 steps with 20 geometrically heated chains and an initial burnin period of 2 x 10^6 steps. Two runs were conducted with identical starting conditions for each pairwise analysis to confirm convergence was reached, while effective sample size values and parameter plots were examined to insure adequate mixing among chains was achieved. Small sample sizes precluded gene flow analyses between the Huon Peninsula and Adelbert Range; however, both populations exhibited evidence of low level migration in the BI topology and haplotype network.

Estimates of divergence times among populations were determined by calculating net nucleotide diversity between adjacent population pairs and applying a conservative range of divergence rates (2–5%) to account for uncertainty in ND2 mutation rate estimates (Lovette, 2004; Arbrogast et al., 2006). Net nucleotide diversity was determined from the equation $d = d_{xy} - 0.5 (d_x + d_y)$ where d_x and d_y represent average pairwise divergences within populations x and y, and d_{xy} is the average divergence among populations. The latter statistic was calculated in DNASP V. 5.0, whereas average pairwise divergences were calculated in PAUP v. 4.0b10 (Swofford, 2002). Coalescent estimates of divergence times between regional lineages were conducted in IMA2 with samples grouped by clade and a range of mutation scalars applied as above. Each run was conducted with 20 geometrically heated chains for 3 x10^7 steps and a 1 x 10^7 burnin. The migration parameter was set to zero, given the reciprocal monophyly among regional lineages.

Ecological niche modeling

I used the Genetic Algorithm for Rule-Set Prediction (GARP v 1.1.3; Stockwell & Peters, 1999) and Maxent v 3.3 (Phillips et al., 2006) software applications to generate ecological niche

models (ENMs) for *P. cyanus* under contemporary and paleoclimatic conditions. Both methods are evolutionary-computing approaches that use known occurrence points and raster GIS data layers summarizing relevant environmental dimensions to build ENMs based on relationships between the two data sets. The result of each approach is a map summarizing suitability of environmental conditions for the species in question. Optimization of model accuracy in GARP analyses is achieved via a genetic algorithm, with rule 'fitness' evaluated from independent subsets of available occurrence data (Stockwell & Peters, 1999). Predictive accuracy is further refined by developing 100 replicate models and identifying a 'best subset' based on omission and commission error statistics to produce a final consensus result (Anderson et al., 2003). I used a soft omission threshold of 20% and commission threshold of 50%, with all other parameters left at default settings. This procedure produced a best subset comprised of 10 models, which were in turn summarized to generate an estimate of the species potential distribution.

Maxent represents an alternative methodology based on the principle of maximum entropy, in which probabilities assigned to each pixel in the landscape are spread out maximally between 0 and 1, subject to the constraint of matching the environmental attributes of known occurrence data as closely as possible. As in GARP analyses, independent subsets of available occurrence data are used for model generation and training. All Maxent runs were conducted under default settings as recommended in Phillips (2006). Accuracy of Maxent models was assessed via the receiver operating characteristic (ROC) and AUC statistic.

Occurrence data for *P. cyanus* were drawn from GPS coordinates (spatial resolution ~5 m) recorded during PNG collecting expeditions, whereas distributional data from Papua and West Papua, Indonesia, were assembled from museum-specimen locality information and first-

hand sightings by BWB, with locality names georeferenced from published and online gazetteers when locality descriptors were sufficiently detailed and reliable.

A subset of the 19 bioclimatic coverages from the WorldClim dataset (1960-1990; Hijmans et al., 2005a) was used as the basis for ENMs, with dimensions including annual mean temperature, mean diurnal range, maximum temperature of the warmest month, minimum temperature of the coldest month, total annual precipitation, and precipitation of the wettest and driest months; this set is known to exhibit low correlation among ecological dimensions (pers. comm. A.T. Peterson). Last Glacial Maximum climates were analyzed at 2.5' spatial resolution based on a downscaling recently developed by R. Hijmans (Waltari et al., 2007). To achieve this downscaling, general circulation model simulation results from two climate models (Community Climate System Model, CCSM, http://www.ccsm.ucar.edu/, Kiehl & Gent 2004; Model for Interdisciplinary Research on Climate (MIROC), ver. 3.2; http://www.ccsr.utokyo.ac.jp/) were downloaded from the PMIP2 website (http://www.pmip2.cnrs-gif.fr/) at a 2.8° spatial resolution (~300 x ~300 km). The 2.5' spatial resolution surfaces were created by calculating the difference between LGM and contemporary conditions, and interpolating the differences to a 2.5' resolution grid using the spline function in ArcInfo (ESRI, Redlands, CA). Interpolated differences were then added to high-resolution WorldClim present-day climate data sets (Hijmans et al., 2005b) to create LGM bioclimatic coverages at resolutions relevant to the spatial scale of analysis while calibrating the simulated climate change data to the actual observed climate data. For spatial analyses of population expansion and contraction across climatic scenarios, GARP models were reclassified using the lowest presence thresholding approach described in Pearson et al., (2007), and area estimates calculated in ArcMap.

To provide a secondary measure of ecological niche displacement associated with LGM climatic conditions, palynological-based niche reconstructions were developed using published accounts of pollen spectra derived from multiple coring sites throughout the New Guinea highlands. Contemporary elevational limits of montane rainforest communities (1400–2800 m) were mapped based on general accounts of vegetation zonation (Paijmans, 1976; Johns, 1982) and distributional data collected first-hand during biodiversity surveys across PNG. A 'consensus map' of the elevational distribution of LGM montane rainforest communities (600–2000 m) was inferred from summaries of pollen cores detailed in Hope (1996) and references therein, which in turn was used to estimate patterns of connectivity and distributional shifts of *P. cyanus* populations, as the realized ecological niche of this taxon appears to be closely associated with the elevational limits of these montane floral communities.

Statistical tests of ecological niche divergence

New Guinea's montane climate patterns vary regionally both within the Central Highlands and among outlying coastal sky-islands. As such, I conducted "niche identity" and "background similarity" tests (Warren et al., 2008) for each primary clade (I-III) recovered in the BI analysis to test for niche conservatism among geographic lineages. Both tests consist of randomization procedures that rely on Schoener's *D* and Hellinger's *I* statistics to assess similarity of modeled ecological suitability values between two or more taxa. The niche identity test examines whether ENMs for a pair of taxa are significantly distinct by comparing observed *D* and *I* statistics to a null distribution that is generated by randomly partitioning the combined occurrence points of both taxa to create ENMs and similarity statistics based on pseudoreplicate data sets. Values of Schoener's *D* and Hellinger's *I* statistic range from 0 to 1 with values near 0 indicating a high

degree of divergence among ENMs and values approaching 1 indicating identical models. The background similarity test evaluates whether an ENM for one taxon predicts that of a second better than expected by chance alone. Rejection of the null hypothesis not only indicates statistical similarity among niche models, but also suggests that observed differences between models may be the consequence of taxon-specific habitat selection. Observed *D* and *I* similarity metrics are calculated from comparisons of ENMs for the taxa in question, which are in turn compared to a null distribution of similarity statistics generated by comparing the ENM of one taxon to ENMs produced by randomly drawing samples from the 'background' distribution of a second taxon. The background area was limited to mainland New Guinea and is theoretically equivalent to the "Mobility" region within the BAM framework (Soberon & Peterson, 2005), as recently confirmed in Barve et al., (2011).

Based on results of genetic sampling, the range of clade I was limited to the Vogelkop whereas clades II and III are assumed to meet along the Strickland River Valley. I used openModeller Desktop v. 1.0 to generate clade-specific ENMs using the same omission—commission thresholds implemented in the species-level models, with all other run parameters left at default settings. Niche identity and background similarity tests were conducted in the software package ENMTools v. 1.3 (Warren et al., 2008; 2010), with 100 pseudoreplicates generated for each test, resulting in statistical significance at the $P \leq 0.01$ level. Binary predictions were analyzed using the minimum training presence option for both tests (Pearson et al., 2007). Although results of these tests may be observed in either direction of the null distribution, I treated each statistical analysis as a one-tailed test, to focus the primary aim of these analyses on evaluating whether niche conservatism could be rejected among geographic lineages of *P. cyanus*.

RESULTS

Sequence attributes

The combined sequence alignment contained 2063 bp [ND2 (867 bp), ND3 (351 bp), ATP6 (684 bp) and ATP8 (171)] for 161 individuals of *P. cyanus* and 9 outgroup taxa, yielding 254 variable sites among ingroup samples, of which 190 were parsimony-informative (Table 1.1). Sequences appeared to be of mitochondrial origin rather than numts as no stop codons were present within open reading frames, base composition was homogenous across samples, and codon-specific substitution rates were consistent with known biases. A 3 bp insertion for the amino acid proline was observed at position 127 of all ingroup ATP8 sequences, but was absent from outgroup taxa with the exception of *P. placens*, which contained a threonine insertion at the same position. A 3 bp deletion was observed at position 130 in the ATP8 sequence of *P. sigillata*.

Ancient DNA samples resulted in clean chromatograms with no discrepancies among light and heavy strands due to degradation phenomena (deamination, etc) as has been reported in previous studies that examined numerous ancient DNA samples of similar age (Hofreiter et al., 2001; Sefc et al., 2006). Furthermore, overlapping amplicons aligned without conflict, and patterns of genetic variation were congruent across fresh and ancient DNA samples. Sequences of all unique haplotypes have been deposited in GenBank under accession numbers ##--##.

Phylogeographic relationships

Analysis of Bayes factors indicated that the more parameter-rich partitioning strategy was strongly favored over less complex models (BF > 739). As such, BIC selected models of sequence evolution were applied to each of nine partitions (by gene and codon) for the final BI and ML analyses, which resulted in near-identical topologies, differing only in terminal

Table 1.1 Attributes of sequence variation in 4 mtDNA genes within *Peneothello cyanus*.

Gene	Total sites	Informative sites (%)	Variable sites by codon (Informative) 1st	2nd	3rd	Nucleotide frequencies %A	%C	%G	%T	Best-fit model (BIC)
ND2	867	69 (7.9)	19 (15)	12 (8)	64 (46)	30.3	34.3	11.9	23.5	TrN+I
ND3	351	39 (11.1)	10 (6)	5 (4)	33 (29)	27.0	34.3	13.4	25.3	HKY+I
ATP-6	684	64 (9.3)	17 (13)	2 (0)	68 (51)	28.1	36.5	10.5	24.9	TrN+I
ATP-8	171	18 (10.5)	6 (2)	4 (3)	16 (13)	34.4	34.5	5.9	25.2	HKY
mtDNA	2063	190 (9.2)	52 (36)	23 (15)	181 (138)	30.0	34.9	10.4	24.7	TrN+I+Γ

rearrangements within clusters of genetically similar individuals. Given these minor differences, phylogenetic results presented herein are limited to the BI analysis for simplicity (Fig. 1.2). The monophyly of *Peneothello* was recovered with significant posterior probability support, yet species-level relationships within the genus were not fully resolved, given uncertainty surrounding the position of *P. bimaculata*. Strong support for a sister relationship between *P. sigillata* and *P. cryptoleuca* was unexpected considering the similarity in phenotype and ecological niche requirements between the latter taxon and *P. cyanus*. These results differ considerably from the findings of a previous phylogenetic study of the Petroicidae (Loynes et al., 2009), which placed *P. bimaculata* as sister to *Melanodryas* (ND2 parsimony analysis), and *Peneoenanthe pulverulenta* sister to *Peneothello cyanus*, rendering the genus paraphyletic (multi-locus Bayesian analysis). By contrast, the mitochondrial BI analysis herein recovered *P. pulverulenta* basal to a monophyletic *Peneothello*, supported by a posterior probability of 1.0 (Fig. 1.2). It is difficult to assess the nature of these discrepancies, given that node support values were not published for individual gene trees in the former study; however, lack of resolution among nuclear gene trees and short branch lengths suggests that insufficient character sampling combined with stochastic lineage sorting processes are the most plausible causes of topological differences among studies. While additional nuclear markers coupled with comprehensive taxon sampling will be required to resolve the evolutionary history of

Peneothello and closely related sister taxa, these uncertainties do not impact the phylogeographic results within *P. cyanus*, and are beyond the scope of the present study.

Strong support was recovered for monophyly of *P. cyanus*, which is composed of three primary clades that are largely concordant with the geographic distribution of morphologically defined subspecies (Rand & Gilliard, 1967; Boles, 2007). Samples from the Arfak and Tamrau mountains form a genetically distinctive Vogelkop lineage (clade I, *P. c. cyanus*), which is sister to a broadly distributed clade of geographically structured populations (clade II, *P. c. atricapilla*), including the Wandamen and Weyland mountains in the west, the Nassau and Oranje mountains of the Central Highlands, and the Cyclops and Bewani–Torricelli mountains along the north coast. These western clades are in turn sister to a weakly resolved cluster of populations from the eastern half of New Guinea, ranging from Mt. Stolle in West Sepik Province to the southeastern limit of the Papuan Peninsula, including outlying populations in the Adelbert Range and Huon Peninsula (clade III, *P. c. subcyanea*). Reciprocal monophyly was recovered among *P. c. cyanus* and *P. c. atricapilla* with significant posterior probability support, as was monophyly of populations within *P. c. atricapilla*. By contrast, few nodes within *P. c. subcyanea* received significant support and all populations within the clade except Mt. Simpson, exhibited evidence of potential admixture or ancestral polymorphism between adjacent populations. Average raw ND2 sequence divergence was relatively high within *P. c. atricapilla* (0.88%), whereas *P. c. cyanus* and *P. c. subcyanea* exhibited more moderate values of 0.31% and 0.45% respectively. Uncorrected ND2 pairwise sequence divergences among clades ranged from 2.5–3.8% between *P. c. cyanus* and *P. c. atricapilla*, while samples of *P. c. subcyanea* were 1.15%–4.08% divergent from western New Guinea clades (Appendix 1.3).

Figure 1.2. Bayesian inference topology of 122 unique *P. cyanus* haplotypes based on analysis of 2063 bp of mitochondrial sequence data. Significant posterior probability node support (≥ 0.95) is indicated by blacked circles, whereas nodes that received < 0.50 posterior probability support were collapsed.

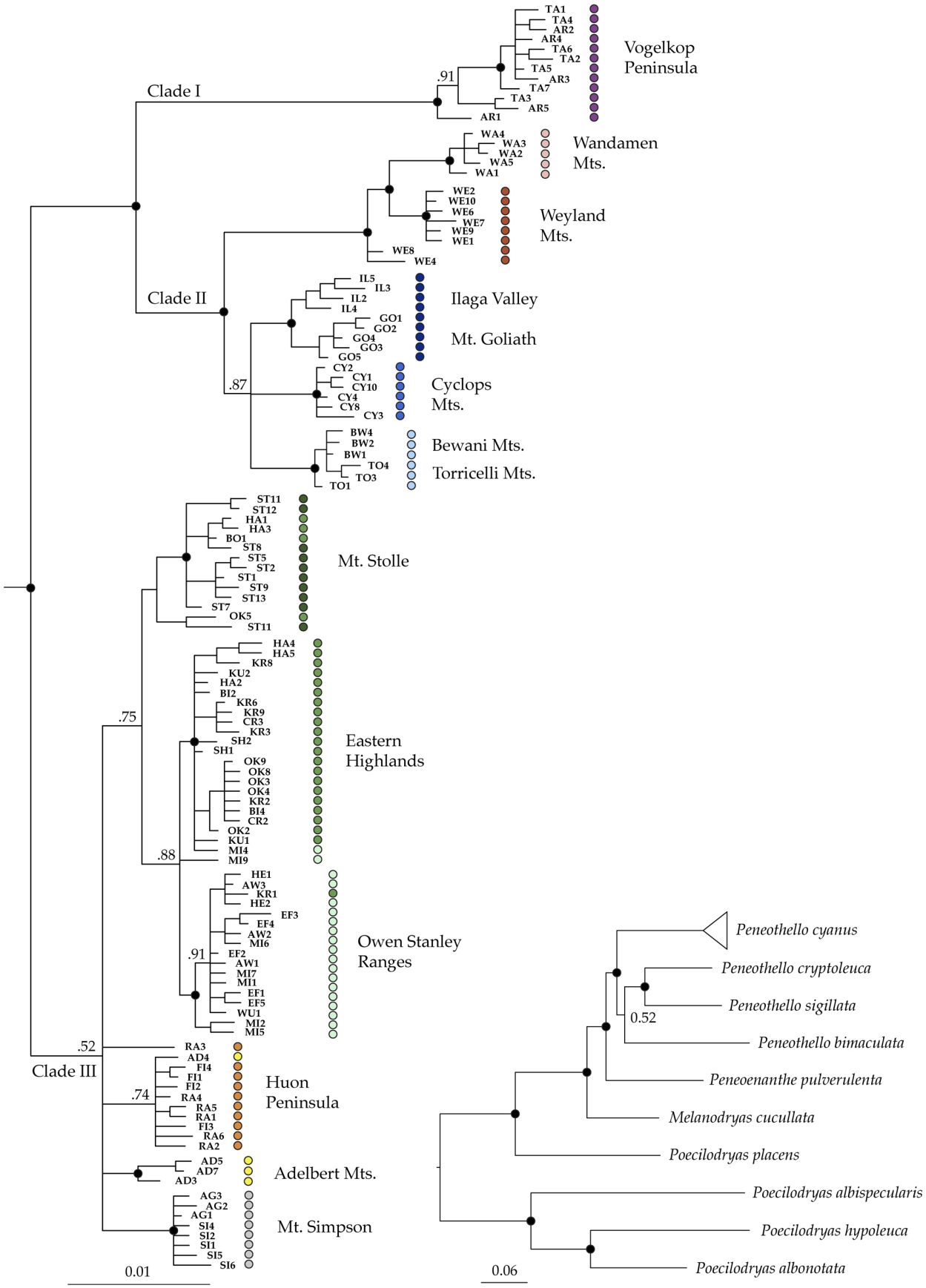
Clade I
Clade II
Clade III
.91
.87
.75
.88
.91
.52
.74
TA1
TA4
AR2
AR4
TA6
TA2
TA5
AR3
TA7
TA3
AR5
AR1
Vogelkop Peninsula
WA4
WA3
WA2
WA5
WA1
Wandamen Mts.
WE2
WE10
WE6
WE7
WE9
WE1
WE8
WE4
Weyland Mts.
IL5
IL3
IL2
IL4
GO1
GO2
GO4
GO3
GO5
Ilaga Valley
Mt. Goliath
CY2
CY1
CY10
CY4
CY8
CY3
Cyclops Mts.
BW4
BW2
BW1
TO4
TO3
TO1
Bewani Mts.
Torricelli Mts.
ST11
ST12
HA1
HA3
BO1
ST8
ST5
ST2
ST1
ST9
ST13
ST7
OK5
ST11
Mt. Stolle
HA4
HA5
KR8
KU2
HA2
BI2
KR6
KR9
CR3
KR3
SH2
SH1
OK9
OK8
OK3
OK4
KR2
BI4
CR2
OK2
KU1
MI4
MI9
Eastern Highlands
HE1
AW3
KR1
HE2
EF3
EF4
AW2
MI6
EF2
AW1
MI7
MI1
EF1
EF5
WU1
MI2
MI5
Owen Stanley Ranges
RA3
AD4
FI4
FI1
FI2
RA4
RA5
RA1
FI3
RA6
RA2
Huon Peninsula
AD5
AD7
AD3
Adelbert Mts.
AG3
AG2
AG1
SI4
SI2
SI1
SI5
SI6
Mt. Simpson
0.01
Peneothello cyanus
Peneothello cryptoleuca
Peneothello sigillata
0.52
Peneothello bimaculata
Peneoenanthe pulverulenta
Melanodryas cucullata
Poecilodryas placens
Poecilodryas albispecularis
Poecilodryas hypoleuca
Poecilodryas albonotata
0.06

Table 1.2. Summary of genetic diversity among twelve populations of *Peneothello cyanus* based on ND2 sequences. The number of unique haplotypes and segregating sites in parentheses are based on the four-gene mtDNA sequence alignment.

Population	*n*	Unique Haplotypes	Segregating Sites	Θ (site)	*k*	Haplotype Diversity	Nucleotide Diversity (π)	π 95% CI
Vogelkop Peninsula	13	8 (12)	11 (26)	0.00412	2.718	0.859	0.003135	0.001086
Wandamen Range	5	2 (5)	1 (5)	0.00055	0.600	0.600	0.000692	0.000664
Weyland Range	10	5 (8)	6 (17)	0.00246	1.867	0.756	0.002153	0.000940
Ilaga - Mt. Goliath	10	7 (9)	8 (17)	0.00328	2.267	0.933	0.002614	0.001097
Cyclops Range	10	3 (6)	3 (7)	0.00123	0.867	0.600	0.001000	0.000536
Torricelli Range	10	4 (6)	3 (7)	0.00123	1.200	0.711	0.001384	0.000344
Mt. Stolle	14	9 (11)	10 (29)	0.00365	2.604	0.912	0.003004	0.001004
Eastern Highlands	39	17 (26)	19 (50)	0.00525	2.705	0.928	0.003119	0.000590
Huon Peninsula	10	6 (9)	9 (28)	0.00369	1.800	0.778	0.002076	0.000914
Adelbert Range	8	3 (4)	6 (18)	0.00268	2.393	0.678	0.002760	0.001320
Owen Stanley	22	8 (18)	11 (29)	0.00351	1.459	0.601	0.001683	0.000494
Mt. Simpson	10	6 (8)	5 (12)	0.00205	1.000	0.778	0.001153	0.000592
Peneothello cyanus	161	78 (122)	95 (254)	0.01937	12.63	0.980	0.014576	0.001129

Population structure and demography

Population genetic analyses identified 78 unique ND2 haplotypes among 161 *P. cyanus* sequences, of which 49 were private haplotypes and 10 were shared by five or more individuals (Table 1.2; Fig. 1.3). Sequence variation was observed across 95 polymorphic sites distributed heterogeneously throughout the ND2 gene. Estimates of pairwise F_{ST} values revealed strong genetic structure across the Central Highlands and outlying coastal ranges, identifying 12 distinct populations among 28 collection localities (Table 1.2). Results of the ND2 median-joining network were congruent with BI analyses, confirming substantial genetic breaks among three primary clades that coincide with prominent biogeographic boundaries. Nominate *P. c. cyanus* haplotypes from the Vogelkop were linked to *P. c. atricapilla* samples from Ilaga Valley and Mt. Goliath by 21 mutational steps, whereas Weyland and Wandamen populations represent a distinct lineage separated from Mt. Goliath haplotypes by at least 6–9 mutational steps, respectively. Core haplotypes within populations of the eastern *P. c. subcyanea* clade were linked to one another by ≤ 3 substitutions, while samples from Mt. Stolle were separated from

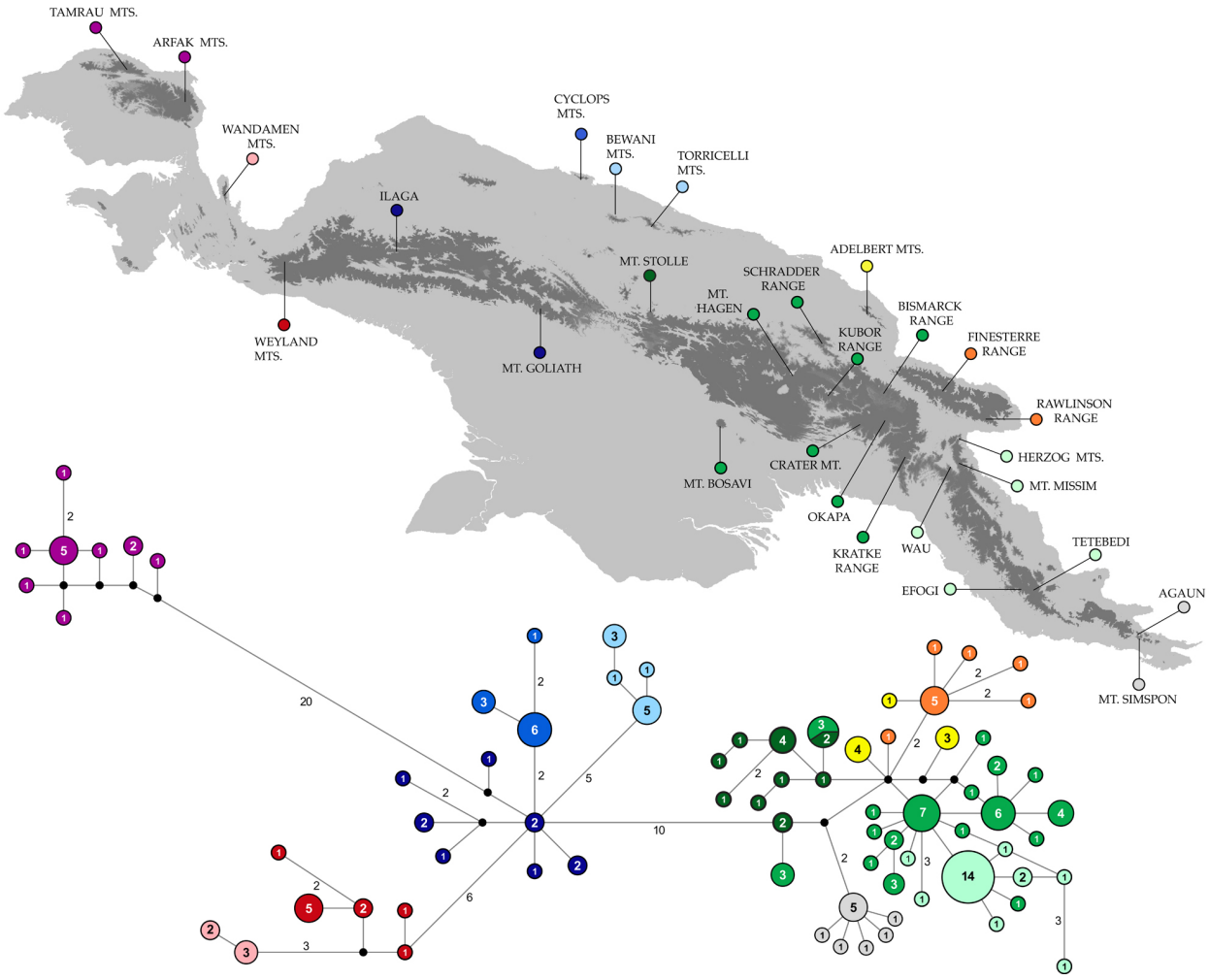

Figure 1.3. Minimum spanning network of ND2 haplotype relationships among 12 populations of *P. cyanus*. The number of individuals sharing a given haplotype are indicated within each ellipse, while values along network branches denote the number of mutational steps between haplotypes. Populations are color-coded and linked with collection localities depicted on the ecological niche model projection (dark grey shading) of *P. cyanus* inferred under contemporary climatic conditions.

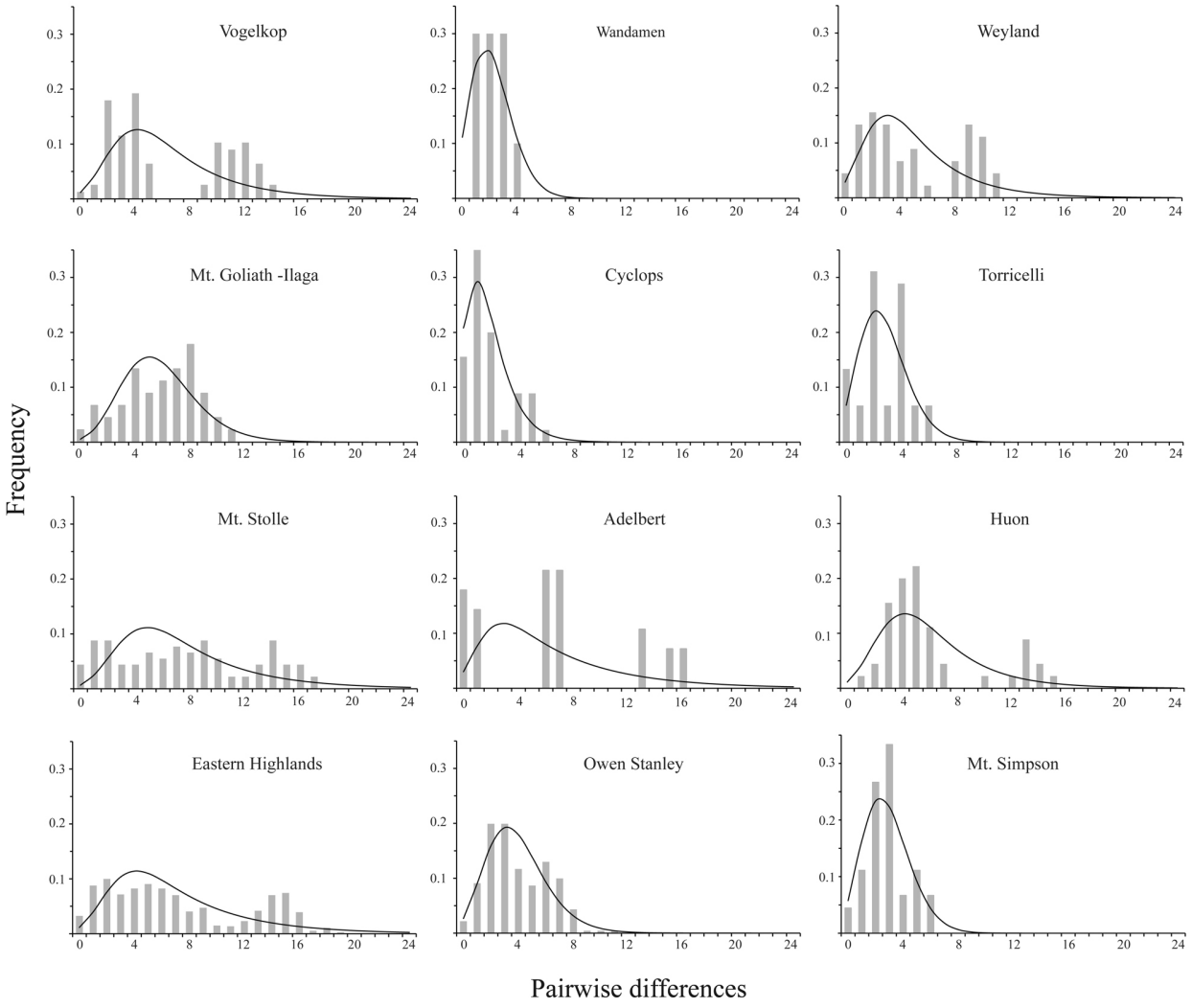

Figure 1.4. Mismatch distributions depicting observed frequencies of pairwise nucleotide differences within 12 populations of *P. cyanus* (gray bar graph). The distribution of expected frequencies under a model of demographic expansion are indicated by the black line graph.

Mt. Goliath haplotypes by ≥ 10 mutational steps. Indices of genetic variation were consistently higher among populations of the CDRs, which is to be expected given their large size in comparison with coastal sky-islands. Estimates of haplotype diversity (*h*), mean pairwise nucleotide differences (*k*), and nucleotide diversity (π) averaged 0.924, 2.53, and 0.003 respectively among populations of the CDRs (Eastern Highlands, Mt. Stolle, and Ilaga–Mt. Goliath), whereas smaller coastal populations of the Huon, Adelbert, Bewani–Torricelli, Cyclops, and Wandamen Ranges exhibited lower mean values of $h = 0.673$, $k = 1.3$, and $\pi = 0.0016$. Samples from the Vogelkop Peninsula also contained high levels of sequence variation ($h = 0.859$, $k = 2.7$, and $\pi = 0.003$) comparable to that of CDRs populations, while genetic diversity within the Papuan Peninsula was more moderate ($h = 0.66$, $k = 1.2$, and $\pi = 0.0013$), a pattern consistent with the ND2 haplotype network indicating that 14 of 22 individuals from the region shared the same haplotype.

Hierarchical three-way analyses of molecular variance confirmed that much of the genetic variation within *P. cyanus* was partitioned by subspecies (63.2%), whereas 26.3% was distributed among populations and 10.5% within populations (Fig. 1.7). When sequences were grouped by contemporary sky-islands, the distribution of genetic diversity was similar to the former AMOVA, with 49.7% of the sequence variation explained by sky-islands, 36.3% among populations, and 14.0% within populations. The distribution of LGM sky-island populations accounted for the least genetic diversity among the three partitioning schemes, with 34.3% distributed among LGM sky-islands, 53.12% among populations, and 12.6% within populations. All AMOVA results were significant at the $P < 0.001$ level. A Mantel test conducted on the full complement of *P. cyanus* samples recovered significant support for a positive correlation between geographic and genetic distances (r=0.5703, $P = 0.0002$), suggesting that an isolation-

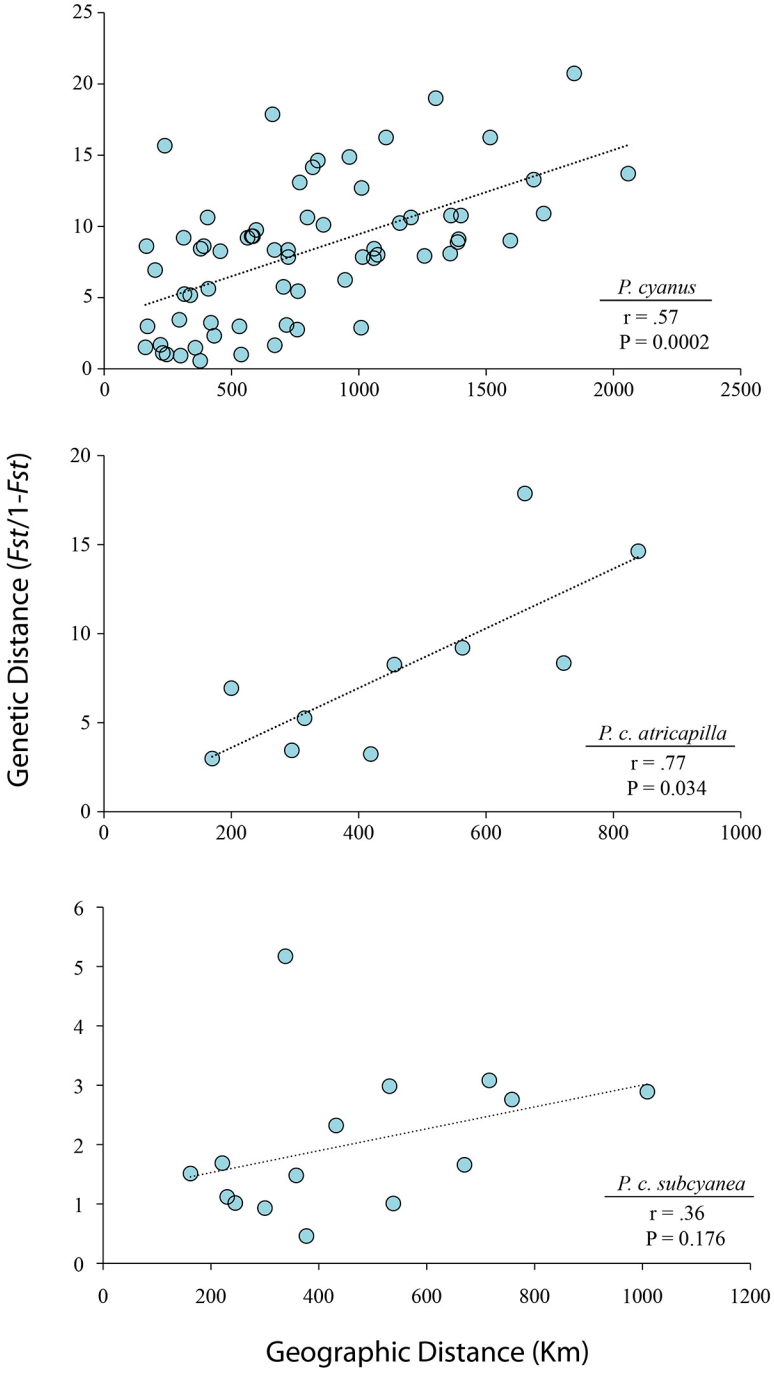

Figure 1.5. Results of Mantel tests conducted on the full data set and regional phylogroups corresponding to currently recognized subspecies. Statistically significant correlations in *P. cyanus* and *P. c. atricapilla* indicate an isolation-by-distance effect has shaped the distribution of genetic diversity among populations, whereas non significant results within *P. c. subcyanea* suggest that other factors are responsible for genetic structure east of the Strickland River Valley.

by-distance effect has contributed to the distribution of genetic diversity among populations (Fig. 1.5). The spatial patterns of genetic diversity within *P. c. atricapilla* also exhibited strong evidence of an isolation-by-distance effect (r=0.77, P = 0.034), whereas geographic and genetic distances among populations of *P. c. subcyanea* were not significantly correlated (r=0.36, P = 0.176).

Analysis of population genetic summary statistics, mismatch distributions, and Bayesian skyline plots revealed a broad trend of demographic expansion within populations and regional lineages of *P. cyanus*. Summary statistics based on the frequency of segregating sites including Tajima's *D*, Fu & Li's *D*, and Ramos-Onsin & Rozas R_2 each rejected the null hypothesis of constant population size for samples from the Huon Peninsula and Owen Stanley Ranges, indicating significant support for demographic expansion at the $P \leq 0.05$ level (Table 1.3).

The Ramos-Onsin & Rozas R_2 statistic recovered additional evidence of population expansion in the Vogelkop Peninsula, Wandamen Mountains, Eastern Highlands, and Mt. Simpson populations. Fu's F_S statistic was significantly ($P \leq 0.02$) negative for the same suite of populations, rejecting population stability and corroborating a pattern of demographic expansion. Mismatch distributions of populations from the Central Highlands were generally ragged or bimodal, while the Wandamen, Owen Stanley, and Mt. Simpson populations resembled the simulated distributions of population growth (Fig. 1.4). The null hypothesis of demographic expansion was rejected by significant raggedness index (r) statistics for the Mt. Stolle and Eastern Highlands populations; however, these results likely reflect low-level introgression and or shallow genetic structure among populations. A bimodal pattern in the distribution of pairwise differences was observed from samples of the Vogelkop Peninsula, Weyland Mountains, and Huon Peninsula, reflecting weak intrapopulation genetic structure, and in the

Table 1.3. Demographic summary statistics derived from the haplotype distribution, frequency spectrum of mutation, and distribution of pairwise sequence differences. All analyses were conducted on the pooled four-gene data set and statistically significant results (p-value ≤ 0.05) are indicated in bold. Number of unique haplotypes are indicated in parentheses.

Population	*n*	Tajima's *D*	Fu & Li 's *D*	Ramos-Onsin & Rozas R_2	FU's *Fs*	Raggedness Index (*r*)
Vogelkop Peninsula	13 (12)	-0.9823	-1.0300	**0.0957**	**-5.304**	0.064
Wandamen Range	5 (5)	-0.5619	-0.5348	**0.1612**	**-2.862**	0.140
Weyland Range	10 (8)	-0.7637	-0.5619	0.1189	-1.976	0.034
Ilaga - Mt. Goliath	10 (9)	-0.1275	-0.3046	0.1400	-3.087	0.023
Cyclops Range	10 (6)	-1.1163	-1.1314	0.1818	-2.082	0.161
Torricelli Range	10 (6)	0.5193	0.3767	0.1792	-1.002	0.227
Mt. Stolle	14 (11)	-0.6752	0.2974	0.1155	-2.247	**0.013**
Eastern Highlands	39 (26)	-1.4008	-1.2329	**0.0641**	**-11.106**	**0.010**
Huon Peninsula	10 (10)	**-1.8528**	**-2.0243**	**0.1019**	**-5.147**	0.043
Adelbert Range	8 (4)	-0.3030	-0.6094	0.2278	2.913	0.146
Owen Stanley	22 (18)	**-1.9335**	**-2.3323**	**0.0533**	**-13.134**	0.031
Mt. Simpson	10 (8)	-1.4628	-1.5531	**0.1110**	**-3.713**	0.112

later case, gene flow between adjacent sky-islands (Marjoram & Donnelly, 1994; Bertorelle & Slatkin, 1995).

Bayesian skyline plots demonstrated a clear signature of recent demographic expansion in each subspecies (Fig. 1.6), and a separate BSP analysis of the combined data set recovered a similar pattern of increasing N_e over the most recent time interval. Although confidence intervals were relatively large for BSP analyses given the reliance on a single mtDNA locus, the consistent trend of demographic expansion recovered by summary statistics and coalescent-based analyses presents a strong case for recent population growth throughout the species' distribution.

Gene flow and divergence times

Estimates of the migration parameter (*m*) from coalescent analyses in IMa2 (Fig. 1.8) indicated low-level gene flow from the Eastern Highlands to Mt. Stolle, with a non-zero posterior probability peak of 1.65 females per generation (95% HPD 0.0 –10.2), whereas migration from the Eastern Highlands to the Owen Stanley Ranges was slightly lower, at 1.15 females per

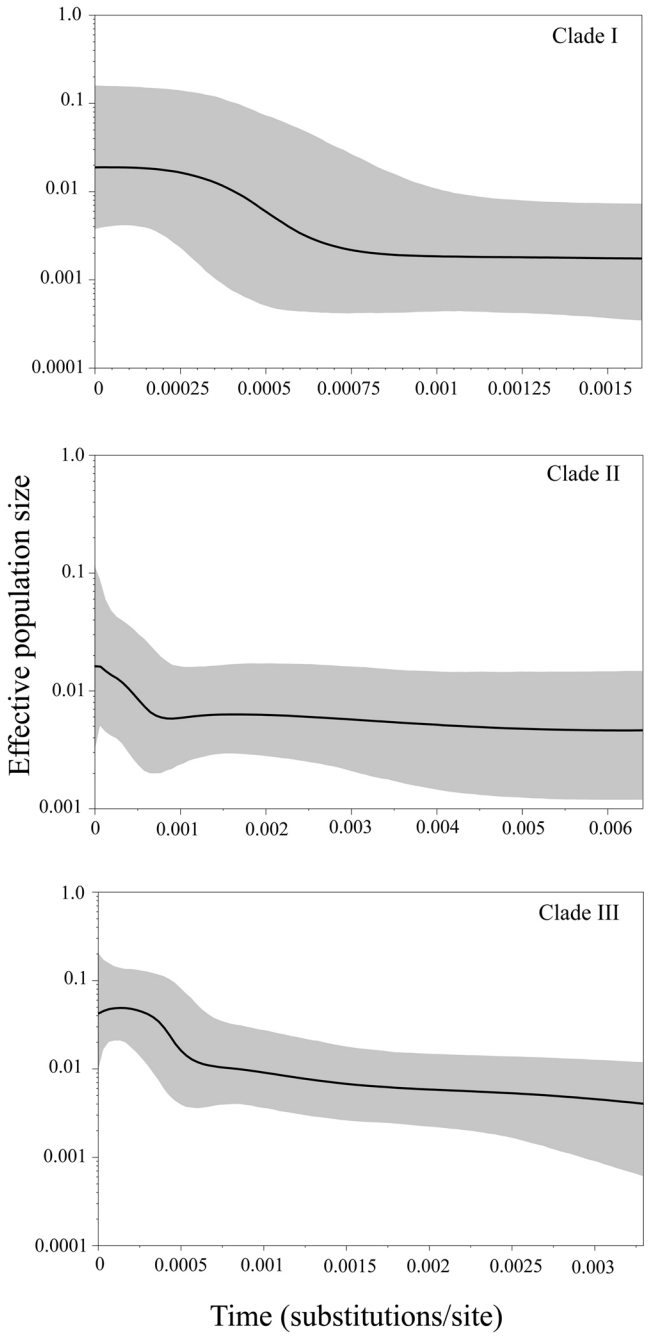

Figure 1.6. Bayesian skyline plots depicting the demographic history of three primary lineages within *P. cyanus*. The central black line represents the median effective population size as a function of time, N_e*t ($\log_{10}$) and the grey shaded interval depicts the 95% highest posterior probability density.

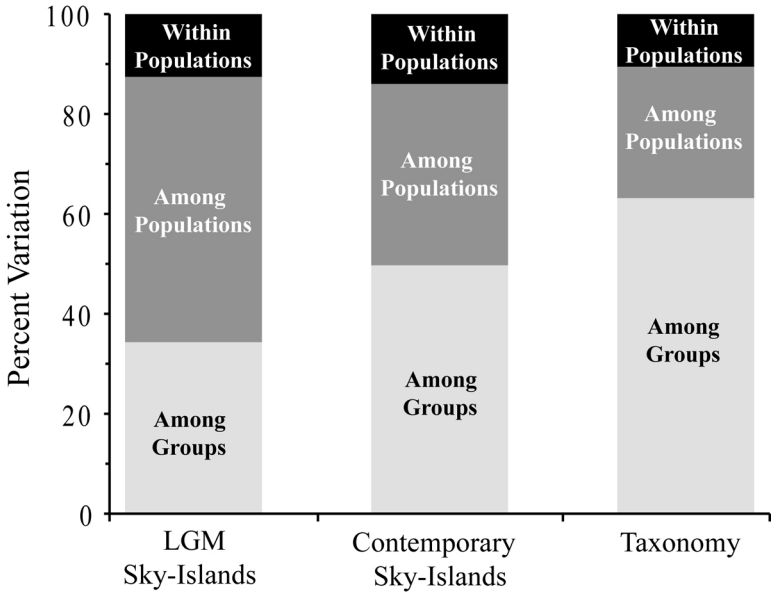

Figure 1.7. Results of three-way analyses of molecular variance in which genetic diversity was partitioned by Last Glacial Maximum sky-islands, contemporary sky-islands, and taxonomy (i.e., clades I, II, and III). Each level of comparison recovered significant genetic partitioning at the $P < 0.001$ level.

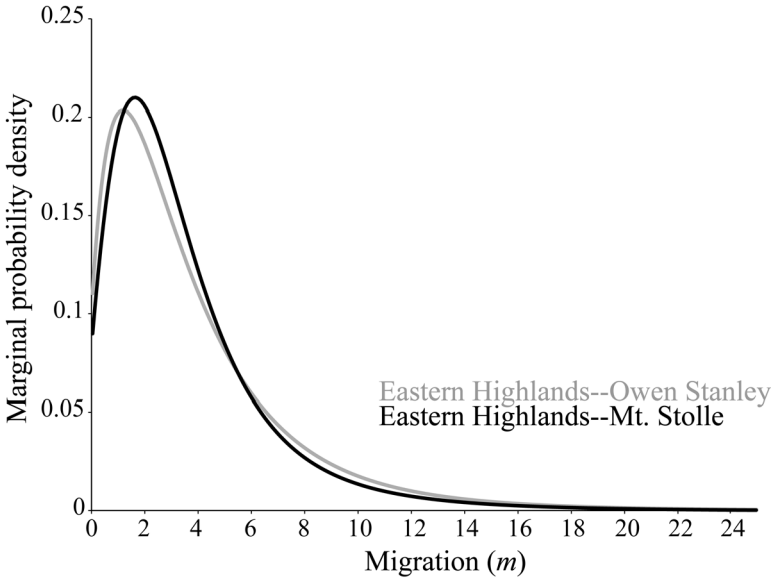

Figure 1.8. Estimates of the migration parameter *m* between populations of the Owen Stanley Range, Eastern Highlands, and Mt. Stolle in number of females per generation.

Table 1.4. Estimates of population divergence times based on corrected genetic distances of ND2 sequences.

Population	Time (5%/Myr)	Time (2%/Myr)
Vogelkop – Ilaga / Mt. Goliath	538,360	1,320,590
Weyland – Ilaga / Mt. Goliath	148,460	387,115
Ilaga / Mt. Goliath – Cyclops	52,260	130,650
Ilaga / Mt. Goliath – Torricelli	121,000	303,050
Ilaga / Mt. Goliath – Mt. Stolle	284,420	711,050
Mt. Stolle – Eastern Highlands	36,770	91,925
Eastern Highlands – Adelbert	30,210	75,525
Eastern Highlands – Huon	57,850	144,625
Eastern Highland – Owen Stanley	23,900	59,995
Huon – Adelbert	36,364	90,910
Owen Stanley – Huon	79,410	198,525
Owen Stanley – Simpson	111,640	279,100
Simspon – Eastern Highlands	84,700	211,750
Simpson – Mt. Stolle	82,600	206,500

generation (95%HPD 0.0–9.09). Gene flow estimates in the opposite direction for both pairwise analyses were below 0.05, with marginal posterior probability densities peaking at zero, suggesting a pattern of directional gene flow from the Eastern Highlands, although this result may be a consequence of small sample sizes and geographically biased collecting efforts. Multiple runs conducted for each pairwise analysis converged on similar results and ESS values were high for all parameters across each run, indicating that adequate mixing was achieved.

Coalescent estimates of divergence times among subspecies conducted in IMa2 revealed that the split between *P. c. cyanus* and *P. c. atricapilla* ranged from 343,000–924,00 ybp (95% HPD 136,100 – 618,828 to 345,000 –1,535,200 ybp) using mutation scalars of 2–5%, while the divergence time between the former clades and *P. c. subcyanea* was estimated at 515,500–1,242,000 ybp (95% HPD 279,200 –742,500 to 691000 –1,844,300 ybp). These results are consistent with population divergence times estimated from corrected genetic distances which indicate diversification within *P. cyanus* has taken place across a broad time interval ranging

from 60,000 –1,320,000 ybp assuming a diversification rate of 2%/Myr, whereas a rate of 5%/Myr yields a time span of 23,900–538,400 ybp. With exception of the shallow split between the Eastern Highlands and Owen Stanley Ranges (23,900–59,995), all divergence time estimates predate the onset of LGM climatic conditions; however, divergence time estimates between the Eastern Highlands and Adelbert Range, Eastern Highlands and Mt. Stolle, and the Huon Peninsula and Adelbert Range also approach the LGM time interval assuming a 5%/Myr mutation rate (Table 1.4).

Ecological niche modeling

Results of GARP and Maxent ecological niche reconstructions were largely congruent within each time period; however, Maxent models consistently overpredicted environmental suitability across high-elevation biomes that are well above tree line in all modeling runs. As such, I focus on the GARP results herein, which yielded contemporary ENMs with sharp elevational limits that closely approximate the known distribution of *P. cyanus*. Narrow breaks in ecological suitability were predicted across river valleys of the CDRs and Papuan Peninsula, including the Strickland, Watut, Tauri, and Adau River drainages (Fig. 1.9). The Sepik, Idenburg, and Ramu–Markham River valleys represent substantial biogeographic barriers between the CDRs and outlying coastal sky-islands, whereas the Vogelkop, Bird's Neck, and Bomberai populations are isolated by expanses of unsuitable environmental conditions associated with low-elevation rainforest and narrow land bridges. An unexpected disruption in the species' potential distribution predicted in the vicinity of Oksibil, along the southern slopes of the Star mountains, appears to be the consequence of a localized artifact in the BIO12 (mean annual precipitation) environmental data layer, likely owing to the lack of data collection stations in the region.

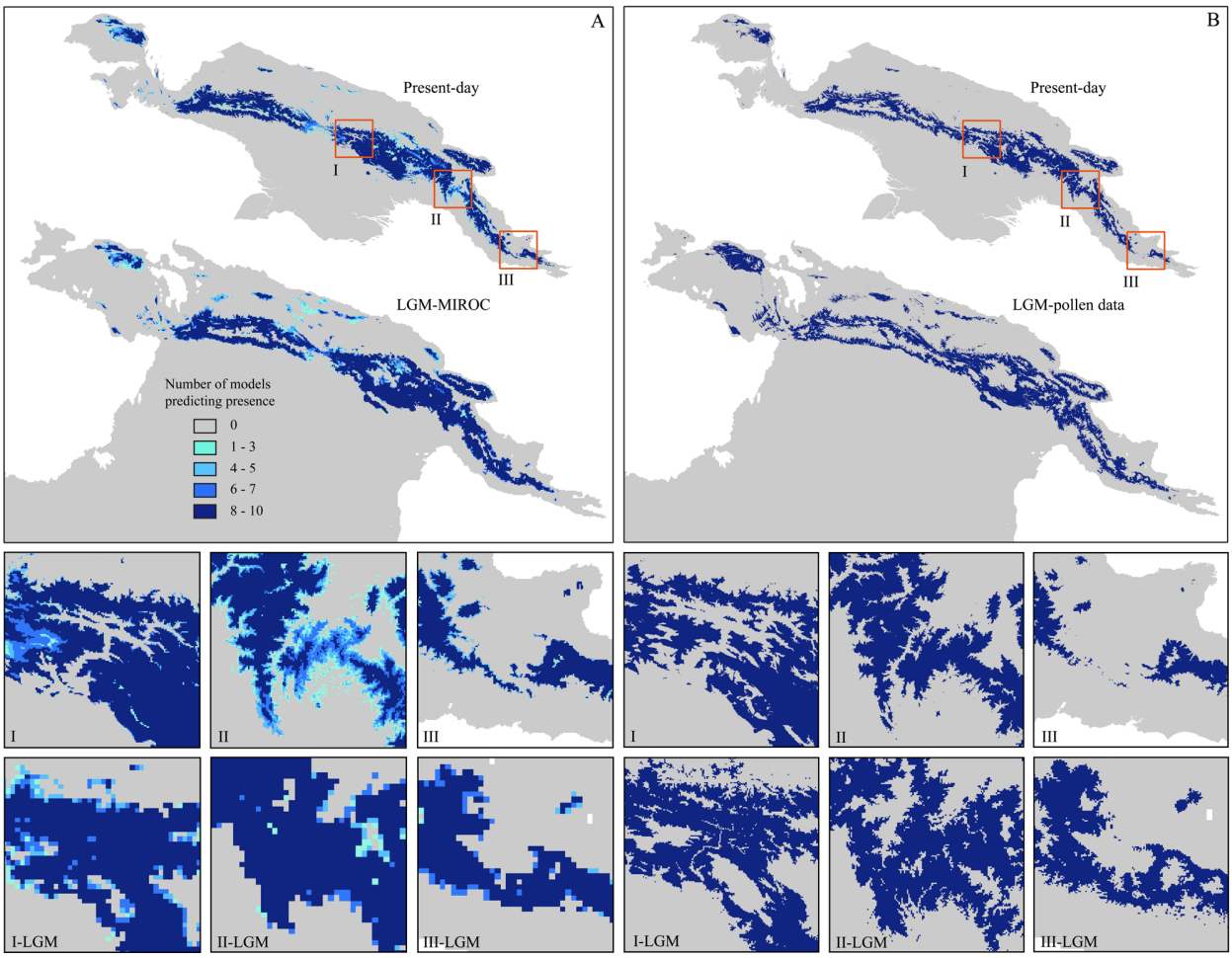

Figure 1.9. (A) Ecological niche reconstructions depicting the potential distribution of *P. cyanus* under contemporary and Last Glacial Maximum climatic conditions. (B) Visualizations of the species' potential elevational range under contemporary and Last Glacial Maximum climatic conditions inferred from specimen locality information and summaries of palynological data.

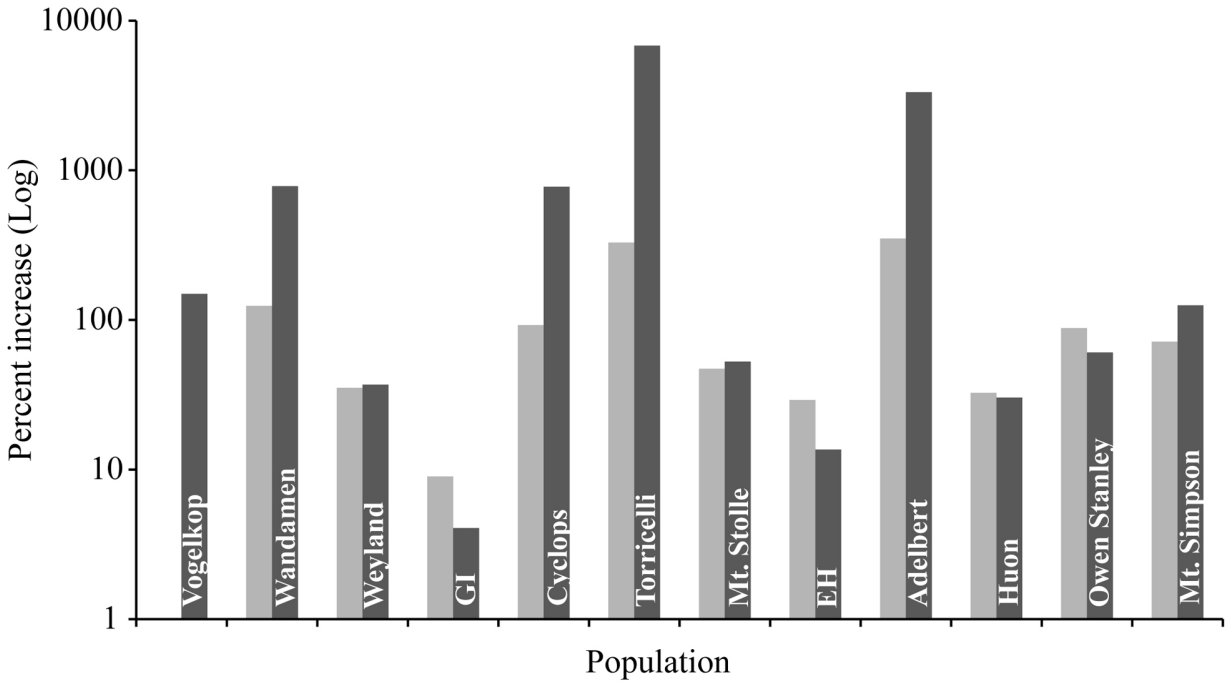

Figure 1.10. Estimates of population expansion inferred from ecological niche models (light grey) and palynologically-based (dark grey) distribution estimates under Last Glacial Maximum climatic conditions.

Moreover, SPOT 4-Vegatation imagery taken from 1998–2000 confirms that montane rainforest environments are largely contiguous along the southern and northern slopes of the Star Mountains (Stibig et al., 2003).

Paleodistribution reconstructions based on the CCSM and MIROC general circulation models exhibited clear patterns of elevational depression across all *P. cyanus* populations under LGM climatic conditions; however, the distribution of environmental suitability differed substantially among these models, particularly in the CDRs, Papuan Peninsula, and Vogelkop. The MIROC projections revealed a pattern of increased population connectivity throughout the CDRs, including fully contiguous corridors of environmental suitability across the Eastern Highlands and Papuan Peninsula, as well as a narrow corridor linking Mt. Bosavi to the Muller Range (Fig. 1.9). By contrast, the CCSM projections exhibited extensive breaks in

environmental suitability across the southern slopes of the Snow Mountains and northern limits of the Owen Stanley Ranges, contradicting what is currently known in terms of the paleoecology of the region (Appendix 1.4). Consequently, the MIROC paleoecological niche reconstructions were used to form the basis of LGM spatial distribution analyses, which revealed that 11 of the 12 populations identified by genetic analyses exhibited patterns of geographic expansion under LGM climatic conditions, with the largest fluctuations taking place in coastal populations of the Cyclops, Torricelli, and Adelbert Ranges (Figs. 1.9 & 1.10.)

Estimates of the species' potential distribution inferred from palynological data were similar to MIROC reconstructions, with increased population connectivity indicated across the CDRs during the LGM, as well as spatial expansion in all 12 populations (Fig. 1.10). Pollen summaries throughout the Central Highlands suggest that LGM elevational depression of montane floral communities was likely more severe than predicted by ENMs, as treeline shifted to ~2200 m, whereas lower montane rainforest communities extended as low as 600 m, resulting in strong geographic isolation between northern and southern slopes of the CDRs (Fig. 1.9B). While this method of retrodicting potential distributions is rudimentary and contains a number of caveats, it provides a valuable alternative perspective on regional paleoecological trends, and is well suited to New Guinea's montane landscape, given its narrow latitudinal range and minimal variance in adiabatic lapse rates. Coincidently, 84% of the predictive power in Maxent distribution models was derived from annual mean temperature surfaces.

Statistical tests of ecological niche divergence

Both Schoener's *D* and Hellinger's *I* statistics reject the null hypothesis of niche equivalency among *P. cyanus* geographic lineages (Appendix 1.5), which is consistent with the compressed

elevational distributions observed in nominate *cyanus* and *P. c. atricapilla* due to competitive exclusion interactions with *P. cryptoleuca* in the Vogelkop, western CDRss, and adjacent coastal sky-islands. However, caution is warranted in interpretation of these results, as niche equivalency may be rejected among taxa that exhibit identical ecological requirements, due to effects of regional habitat heterogeneity and sampling bias (Godsoe, 2010; Peterson, 2011).

Background similarity tests confirm that ENMs of primary geographic lineages are more similar than expected by chance alone, with observed *D* and *I* statistics approaching 1 for each comparison (Appendix 1.6). These results indicate clade specific ENMs have significant power in predicting the distribution of conspecific lineages, which is also evidenced by predicted suitability of unsampled sky-island populations in the Bird's Neck region and northern coastal ranges. Although results of *D* and *I* similarity metrics were congruent among niche identity and background similarity tests, the behavior of Hellinger's *I* statistic was typically more robust, perhaps due to the limited occurrence data for clades I and II, or the implicit biological assumptions associated with the *px,i* variable in Schoener's *D* statistic (Warren et al., 2008). Consequently, I refer to the *I* statistic hereafter as the basis of discussion regarding diversification of ecological niches.

DISCUSSION

Assessing patterns of population connectivity and the paleoenvironmental factors responsible in disrupting or promoting introgression among closely related genealogical lineages are central foci in modern phylogeography; however, until recently, the capacity to ecologically characterize the spatiotemporal distribution of these environmental features was often limited to vague or speculative narratives with little power to distinguish among alternative hypotheses (Avise,

2000; Richards et al., 2007; Waltari et al., 2007; Peterson, 2009). By reconciling contemporary and paleoecological niche reconstructions with spatial analyses of genetic diversity, this study provides an explicit ecological framework for evaluating the mechanisms driving diversification in a montane New Guinea passerine. Molecular phylogeographic analyses reveal a complex evolutionary history in *P. cyanus*, characterized by recent demographic expansion and substantial genetic structure across the Central Highlands, Papuan Peninsula, and outlying coastal sky-islands. These results are largely congruent with elevational shifts of montane rainforest and geographic patterns of population connectivity inferred from paleodistribution models, indicating that Pleistocene climatic oscillations likely played an important role in shaping genetic diversity within the Slaty Robin. Given the uncertainty surrounding mtDNA mutation rates and shortcomings of single locus analyses in assessing timing of diversification, I do not attempt to date specific coalescent events with precision; nonetheless, divergence time estimates (23,900–1,320,590 ybp) based on a conservative range of mutation rates fall entirely within the Pleistocene. The significant disparity among population age estimates suggests that diversification in *P. cyanus* spans multiple climate cycles; a pattern consistent with long-distance dispersal and retention of genetic diversity among continually isolated populations. As such, several facets of genetic structure may also be explained by an isolation-by-distance effect across the central highlands and outlying coastal sky-islands. Herein, the spatial relationships among genetic and ecological data sets are discussed by geographic region, highlighting potential discord between analyses while exploring alternative environmental factors and natural history attributes that may provide insight on the species recent evolutionary history.

Population genetic structure and paleoecology

Phylogeographic analyses identified three primary clades within *P. cyanus*, the distributions of which correspond to geographic patterns of subtle variation in plumage characteristics among subspecies, and are consistent with prominent biogeographic boundaries shared by a diversity of avian taxa (Rand & Gilliard, 1959; Diamond, 1969; Pratt, 1982; Frith & Beehler, 1998). Given the largely linear distribution of New Guinea's montane topography, significant positive correlations between genetic and geographic distances revealed by Mantel tests were not unexpected, as AMOVA results indicated that 63% of the genetic diversity within *P. cyanus* is distributed among subspecies, which exhibit an east-west linear arrangement. Although long-distance dispersal from the CDRs to peripherally isolated sky-islands has enabled the Slaty Robin to colonize all of New Guinea's montane communities, these events are evidently rare, thereby permitting the evolution and retention of genetic diversity across multiple climate cycles, despite reduced dispersal distances required for successful colonization during periods of glacial maxima.

Nominate *P. c. cyanus* appears to be restricted to the Vogelkop Peninsula, with substantial populations in the Arfak and Tamrau Mountains; however, additional sampling is required to clarify the status of isolated Fak Fak and Kumuwa Mountain populations, as these communities share several endemic taxa with the Vogelkop (Diamond, 1985; Gibbs, 1992). Surprisingly, nominate *cyanus* does not share a direct or exclusive relationship with adjacent Wandamen or Weyland populations, but rather is genetically most similar to populations in the Central Highlands including Ilaga Valley and Mt. Goliath (Fig. 1.3). This unexpected phylogeographic pattern may be explained by long-distance dispersal across Cenderawasih Bay via a narrow land bridge linking Yapen island with the Vogelkop during periods of glacial

maxima, or more likely, a series of colonization events through the Bird's Neck region, facilitated by patchy networks of montane rainforest that were present during cooler climates associated with glacial cycling (Fig. 1.9). Although ENMs indicate significant disjunctions of environmental suitability between these regions during LGM climatic conditions, the narrow montane ridges that would support such networks are approaching the resolving limits of the underlying climate data layers used to construct these paleodistribution models, limiting their capacity to depict fine-scale environmental features. Moreover, these models do not take into account congeneric interactions with *P. cryptoleuca*, which replaces *P. cyanus* in mid-to-upper montane habitats, thereby compressing the latter species' upper elevational limits by several hundred meters in the western half of the CDRs and peripherally isolated coastal ranges (Diamond, 1985). Palynologically-based LGM distribution estimates predict a more extensive sky-island network across the Bird's Neck region; nonetheless, these montane communities have remained isolated from the Vogelkop by multiple breaks in ecological suitability spanning 10 km or more, which is consistent with the distribution of genetic diversity across the region, and high levels of avian endemism present in the Arfak and Tamrau mountains. Given the limited differences in phenotype, vocalizations, and ecology that separate nominate *cyanus* from adjacent populations in the Bird's Neck and Central Highlands, the presence of a substantial genetic split between these geographic lineages suggests further cryptic genetic diversity may be present within the Vogelkop avifauna.

Strong geographic structure was recovered among *P. c. atricapilla* haplotypes, revealing five reciprocally monophyletic populations with divergence time estimates that predate the most recent glacial maximum. In the clade's western distributional limits, a sister relationship between Wandamen and Weyland populations is in agreement with expanded sky-island

networks predicted by paleodistribution projections of niche models; however, the geographic origin of this lineage is unclear, given that LGM and contemporary projections also indicate extensive population connectivity between the Weyland and Nassau Ranges. An apparent absence of geographic or ecological barriers across the southern slopes of these ranges suggests that the lineage may have originated as a peripheral isolate within the Bird's Neck region and subsequently recolonized the Weyland Mountains. While evidence for peripatric diversification and "upstream" dispersal from outlying sky-island populations into the CDRs remains tenuous within New Guinea's highland avifauna, the dearth of molecular phylogeographic studies in this system has precluded rigorous assessment of traditional allopatric dogma and alternative hypotheses of diversification among the island's montane communities. Comprehensive genetic sampling via modern ornithological surveys in the Bird's Neck and adjacent terranes will be imperative to advancing phylogeographic understanding of the region.

Based on results from the ND2 median-joining network, north coast *P. c. atricapilla* populations in the Cyclops and Bewani–Torricelli ranges represent independent dispersal events from the Star Mountains. A shared biogeographic history between these distant montane communities has been inferred in other avian taxa based on phenotypic similarities (Diamond, 1969), indicating a potential corridor for dispersal between the Idenburg and Sepik headwaters via the Border Mountains. Although paleodistribution projections predict several intermediate sky-islands within the Border and Nimboran Ranges, the extensive Idenburg and Sepik river basins have undoubtedly limited dispersal between the Central Highlands and north coast populations, as evidenced by persistence of genetic diversity in the Cyclops and Bewani–Torricelli Ranges across multiple glacial cycles. Paleodistribution models also indicate breaks of suitable habitat between the Prince Alexander, Torricelli, and Bewani Ranges during periods of

glacial maxima, which is consistent with distinct haplotype groups observed from the latter two sites (Figs. 1.2, 1.3). Given this species' limited capacity for dispersal and aversion to open environments, direct "jump dispersal" between adjacent sky-islands or from the CDRs to outlying populations seems an unlikely mode of colonization in *P. cyanus* and indeed for much of New Guinea's montane passerine diversity. A more plausible mechanism of sky-island colonization from the Central Highlands entails dispersal through foothill or lowland closed canopy rainforest, most likely by immature or juvenile individuals, which tend to wander into substandard habitats more so than other age classes (BWB, pers. obs). This may explain the absence of Eastern Highlands haplotypes in the Bewani–Torricelli Ranges, as the broad Sepik swamplands would pose a formidable barrier to dispersal of this nature for a montane species adapted to closed forest environments.

Haplotypes from Mt. Goliath and Ilaga Valley were grouped into a single population based on sampling limitations, genetic distances, and marginal F_{ST} values, yet these sites likely represent distinct populations, considering the lack of apparent gene flow and strong geographic isolation during cooler glacial-maximum climates. Although the precise contact zone between *P. c. atricapilla* and *P. c. subcyanea* remains unclear, plumage characteristics indicate potential introgression near the Strickland River valley (Rand & Gilliard, 1967; Coates, 1990), which forms a substantial break in the distribution of montane rainforest across the CDRs during interglacial climates (Fig. 1.9). Genetic sampling confirms that *subcyanea* extends at least 75 km northwest of the Strickland headwaters, with no evidence of admixture in specimens collected from Mt. Stolle; however, this result is not unexpected given that niche models predict population connectivity between the Eastern Highlands and Mt. Stolle across each climate scenario, whereas the Hindenburg and Victor Emmanuel Ranges to the south are largely isolated

from Mt. Stolle and the northern slopes of the Central Ranges by steep headwater valleys of the Sepik and Ok Om river drainages. In a montane avifauna with few clear cut biogeographic boundaries across nearly 800 km of the Central Highlands, the Strickland River valley and headwater tributaries have clearly played an influential role in maintaining regional patterns of genetic structure, as evidenced by the diverse suite of taxa that exhibit population and species-level breaks across this drainage system (*Amblyornis*, *Astrapia*, *Crateroscelis*, *Melanocharis*, *Pachycephala*, *Peneothello*, among others). However, these patterns are difficult to reconcile with paleoecological niche reconstructions, which indicate montane rainforest habitat was likely continuous across the Strickland River valley during cooler climates associated with periods of glacial maxima. While this result may be a consequence of the coarse resolution in paleoclimatic data layers, palynological-based reconstructions were largely consistent with ecological niche reconstructions, revealing an extremely narrow break across the Strickland Gorge region, with substantial environmental suitability throughout the Sepik and Ok Om headwaters (Fig. 1.9B). As such, it remains unclear whether the Strickland River has promoted in situ diversification within *P. cyanus* or is simply acting as a secondary contact zone whereby reduced gene flow during interglacial climates serves to maintain genealogical lineages that originated elsewhere in the central highlands.

Patterns of genetic structure within *P. c. subcyanea* reflect a more recent phylogeographic history influenced by low-level gene flow and recurrent periods of population connectivity across the Central Highlands and Papuan Peninsula. Paleoecological niche projections depict broad corridors of montane rainforest across the Watut and Tauri River Valleys during LGM climatic conditions, corroborating the shallow genetic split observed between Eastern Highlands and Owen Stanley populations, but also raising questions as to why a number of montane

lineages exhibit biogeographic breaks in this region or have failed to colonize the Papuan Peninsula all together (e.g. *Archboldia*, *Pteridophera*, *Paradigalla*, among others). These results also cast doubt on the role of Pleistocene climate change as a catalyst in Diamond's (1972) "drop-out" hypothesis, in which he argued that elevational compression of montane rainforest due to climatic oscillations may have caused widespread extinction across regions of the Central Highlands thereby driving vicariant diversification processes in montane lineages (e.g., *Parotia*). Although "dropout" patterns across the Central Highlands remain a biogeographic conundrum given what is currently known in terms of paleoecological trends in the Pleistocene and orogenic history of the CDRs and Papuan Peninsula, comparative analyses across a broad diversity of taxonomic groups including mid-montane taxa such as *Climacteris leucophae* and *Erythrura papuana* as well as high-elevation specialists such as *Archboldia* and *Macgregoria* will be essential to assessing the evolutionary history and mechanisms governing patterns of distribution and diversification in these complex montane ecosystems.

The phylogeographic history of *P. c. subcyanea* in the southeastern tip of the Papuan Peninsula is also puzzling, considering that specimens from Mt. Simpson are genetically most similar to haplotypes from Mt. Stolle and the Eastern Highlands (Fig. 1.3), despite a narrow corridor of montane rainforest predicted across the Keveri Hills during LGM climatic conditions. This scenario suggests an absence of gene flow between Mt. Simpson and the Owen Stanley Ranges, which is consistent with the presence of distinctive lineages among other taxa in the region. Outlying *P. c. subcyanea* populations in the Adelbert Mountains and Huon Peninsula have clearly remained geographically isolated from the Eastern Highlands and Owen Stanley Ranges by the extensive Ramu–Markham River valley; nonetheless, genetic distances between these populations are quite shallow, indicating recent colonization and/or substantial influence

from gene flow. Lastly, a single specimen from Mt. Bosavi was genetically identical to samples from Mt. Hagen and Mt. Stolle, as revealed by the ND2 haplotype network, suggesting recent colonization and/or substantial gene flow most likely from Mt. Sisa, which paleodistribution models predict was contiguous with Mt. Bosavi during the LGM.

Historical demography and niche conservatism

Palynological spectra sampled throughout the Central Highlands leave little doubt that Pleistocene climate oscillations dramatically influenced the distribution of New Guinea's highland biodiversity (Hope, 1996). Montane rainforest habitats underwent elevational shifts in distribution by as much as 1800 m between climatic extremes, resulting in recurrent episodes of sky-island expansion and contraction as taxa tracked ecological niche requirements along elevational gradients. The demographic impact of these climatic fluctuations among lineages of *P. cyanus* has been most pronounced in range-restricted coastal sky-islands, with population area estimates inferred by LGM distribution models indicating a two-fold or greater increase in area across five of six peripherally isolated populations (Fig. 1.9). By comparison, populations in the Central Highlands and Papuan Peninsula have experienced more moderate fluctuations in the extent of their potential distributions, which is primarily a consequence of their broad geographic range and local topographic aspect. Area estimates inferred from ecological niche model projections and palynological scenarios exhibit moderate discord among coastal sky-islands, as niche model estimates were based on a conservative thresholding approach (Pearson et. al., 2007), and perhaps more importantly, pollen-based estimates were largely derived from coring sites within the CDRs that do not reflect regional climatic variation characteristic of coastal montane communities.

Coalescent-based Bayesian skyline plots corroborate the species-wide demographic response predicted by ecological niche models, indicating simultaneous population growth in each subspecies over the most recent time interval. Indices of genetic variation were also consistent with a pattern of spatial expansion, evidenced by high levels of nucleotide diversity across the CDRs and Papuan Peninsula, whereas outlying sky-islands exhibited only moderate reductions in genetic diversity despite their substantially smaller ranges (Table 1.2). By contrast, mismatch distributions depicted a more complex picture of historical demography characterized by signatures of large, historically stable populations from the Eastern Highlands and Mt. Stolle; however, these results appear to be influenced by sample size limitations, weak intrapopulation genetic structure, and low-level gene flow. Moreover, significant Fu's F_s and Ramos-Onsin & Rozas R_2 statistics reject stability in the Eastern Highlands and suggest a pattern of population expansion. The discord between these alternative measures of demography likely reflect the greater power that R_2 and F_s statistics exhibit when sample sizes are relatively small as is the case here (Ramos-Onsins & Rozas, 2002), while shallow genetic structure associated with the patchy distribution of montane rainforest communities across the Eastern Highlands coupled with introgressed haplotypes from the west may account for the ragged mismatch distributions from these regions. Bimodal mismatch distributions in the Vogelkop, Weyland, and Huon populations also appear to reflect shallow genetic structure, and in the latter case, gene flow from the Adelbert Range (Marjoram & Donnelly, 1994; Bertorelle & Slatkin, 1995).

Retention of similar ecophysiological tolerances among closely related lineages has been observed in a wide array of taxonomic groups over varying evolutionary time frames, and is of particular interest in topographically complex landscapes given the potential for niche conservatism to drive allopatric speciation processes in the face of environmental fluctuations

(Peterson et al., 1999; Wiens & Graham, 2005; Kozak & Wiens, 2007; Peterson & Nyari, 2007). Although the ecological niche reconstructions developed herein fail to explain genetic breaks observed in the Weyland Mountains and Strickland River valley, these models generally exhibit strong spatial congruence with the molecular phylogeographic data set. Statistical tests of ecological niche divergence corroborate a pattern of niche conservatism across *P. cyanus* phylogroups derived in the mid-to-early Pleistocene. Values of Hellinger's *I* statistic approached 1.0 in niche equivalency and background similarity tests, and are consistent with the hypothesis that niche conservatism has played a significant role in shaping the demography and phylogeographic history of the Slaty Robin. Nonetheless, broad-scale comparative analyses will be required to assess the extent to which niche conservatism has impacted the evolution of New Guinea's montane avifauna, as the emerging biogeographic history of the region is complex with a number perplexing distributional patterns that have yet to be explained.

Methodological limitations

Several caveats accompany the methods used herein for reconstructing paleoecological niche distributions, which require careful consideration in drawing conclusions from these results, especially in complex tropical landscapes like the New Guinea highlands. Limitations in spatial resolution of bioclimatic coverages constrain the ability of ENMs to resolve fine-scale environmental variation associated with narrow montane ridges or steep river valleys, features that have likely played a crucial role in shaping distribution and phylogeographic structure across New Guinea's highland topography. These limitations may be especially acute within the coarser LGM environmental data layers, which were interpolated from 2.8° spatial resolution down to 2.5' bioclimatic surfaces (~4.6 x ~4.6 km). A further source of potential error in

"retrodicting" ecological niche models within tropical montane environments stems from spatiotemporal variation of lapse rates and cloud lie, which may accompany the subtle thermal fluctuations of Equatorial ocean currents and glacio-eustatic cycling associated with Pleistocene climate change (Hope, 1996). As demonstrated by New Guinea's dramatic elevational shifts in treeline across LGM and interglacial climatic extremes, extrapolating distributional shifts of environmental variables based on contemporary climatic analogues may produce inaccurate estimates of elevational zonation (Hope, 1996). This consideration may explain the minor discord between ENMs and palynological estimates of LGM distributional limits in *P. cyanus*, and makes a strong case for incorporating alternative data sources in paleoecological modeling techniques. Lastly, the contemporary distributional limits of *P. cyanus* may not represent the species' fundamental ecological niche (i.e. ecophysiological limitations), but rather a subset of its potential distribution, constrained by congeneric competition that likely varies across time and space, thereby introducing substantial uncertainty into the process of accurately predicting paleodistributions within *Peneothello*.

A suite of fast-evolving mtDNA markers were selected to form the basis of this investigation, as an initial screening of two nuclear introns including the fifth intron of the transforming growth factor (TGFb2) and the eleventh intron of the glyceraldehyde-3-phospahte dehydrogenase gene lacked informative variation across most populations. Consequently, these results represent a single estimate from the coalescent and require caution in their interpretation, as individual gene trees may fail to capture the species true population history due to stochastic variation in lineage sorting processes (Brito & Edwards, 2008; Galtier et al., 2009). Moreover, reliance on single-locus data sets precludes acquiring accurate estimates of the coalescent variance surrounding population parameters of gene flow, divergence time, and effective

population size. While emerging next generation pyrosequencing methods coupled with more efficient SNP discovery techniques will enable multilocus approaches capable of resolving these deficiencies (Lerner & Fleischer, 2010), the mtDNA-based results herein shed new light on the impact of Pleistocene climate change in the New Guinea highlands, providing novel phylogeographic hypotheses to guide future comparative investigations within the island's diverse montane biota.

APPENDIX

Appendix 1.1. Summary of specimens included in this study.

Topology Code	Taxon	Locality	Latitude	Longitude	Source	Voucher Number
Ingroup	*Peneothello cyanus*	PNG: Central Province				
SI1	*P. c. subcyanea*	Mt. Simpson	-9.99982	149.50718	KUNHM	114154
SI2	*P. c. subcyanea*	Mt. Simpson	-9.99982	149.50718	KUNHM	114155
SI3	*P. c. subcyanea*	Mt. Simpson	-9.99982	149.50718	KUNHM	114156
SI4	*P. c. subcyanea*	Mt. Simpson	-9.98955	149.48674	KUNHM	114902
SI5	*P. c. subcyanea*	Mt. Simpson	-9.99982	149.50718	KUNHM	114091
SI6	*P. c. subcyanea*	Mt. Simpson	-9.99982	149.50718	KUNHM	T14586
SI7	*P. c. subcyanea*	Mt. Simpson	-9.98955	149.48674	KUNHM	T14629
EF1	*P. c. subcyanea*	Owen Stanley Range: Efogi	-9.15	147.66667	ANWC	26578
EF2	*P. c. subcyanea*	Owen Stanley Range: Efogi	-9.15	147.66667	ANWC	24506
EF3	*P. c. subcyanea*	Owen Stanley Range: Efogi	-9.15	147.66667	ANWC	24505
EF4	*P. c. subcyanea*	Owen Stanley Range: Efogi	-9.15	147.66667	ANWC	24504
EF5	*P. c. subcyanea*	Owen Stanley Range: Efogi	-9.15	147.66667	ANWC	26524
		PNG: Milne Bay Province				
AG1	*P. c. subcyanea*	Agaun	-9.92917	149.38333	ANWC	8078*
AG2	*P. c. subcyanea*	Agaun	-9.92917	149.38333	ANWC	8079*
AG3	*P. c. subcyanea*	Agaun	-9.92917	149.38333	ANWC	8111*
		PNG: Oro Province				
AW1	*P. c. subcyanea*	Owen Stanley Range: Awoma	-9.18333	148.13333	ANWC	E199
AW2	*P. c. subcyanea*	Owen Stanley Range: Awoma	-9.18333	148.13333	ANWC	E187
AW3	*P. c. subcyanea*	Owen Stanley Range: Awoma	-9.18333	148.13333	ANWC	26830
AW4	*P. c. subcyanea*	Owen Stanley Range: Awoma	-9.18333	148.13333	ANWC	26847
		PNG: Morobe Province				
HE1	*P. c. subcyanea*	Herzog Mts: Wagu	-6.8	146.8	ANWC	25196*
HE2	*P. c. subcyanea*	Herzog Mts: Wagu	-6.8	146.8	ANWC	25256*
HE3	*P. c. subcyanea*	Herzog Mts: Wagu	-6.8	146.8	ANWC	25319*
MI1	*P. c. subcyanea*	Owen Stanley Range: Mt. Missim	-7.21991	146.81598	MCZ	167492*
MI2	*P. c. subcyanea*	Owen Stanley Range: Mt. Missim	-7.21991	146.81598	MCZ	167493*
MI3	*P. c. subcyanea*	Owen Stanley Range: Mt. Missim	-7.21991	146.81598	MCZ	167494*
MI4	*P. c. subcyanea*	Owen Stanley Range: Mt. Missim	-7.21991	146.81598	MCZ	167495*
MI5	*P. c. subcyanea*	Owen Stanley Range: Mt. Missim	-7.21991	146.81598	MCZ	167496*
MI6	*P. c. subcyanea*	Owen Stanley Range: Mt. Missim	-7.21991	146.81598	MCZ	167497*
MI7	*P. c. subcyanea*	Owen Stanley Range: Mt. Missim	-7.21991	146.81598	MCZ	167498*
MI8	*P. c. subcyanea*	Owen Stanley Range: Mt. Missim	-7.21991	146.81598	MCZ	167499*
MI9	*P. c. subcyanea*	Owen Stanley Range: Mt. Missim	-7.21991	146.81598	MCZ	167500*
WU1	*P. c. subcyanea*	Owen Stanley Range: Wau	-7.34099	146.68141	PNGNM	23523*
FI1	*P. c. subcyanea*	Huon Peninsula: Finisterre Range	-6.08165	146.57224	KUNHM	95794
FI2	*P. c. subcyanea*	Huon Peninsula: Finisterre Range	-6.08165	146.57224	KUNHM	92365
FI3	*P. c. subcyanea*	Huon Peninsula: Finisterre Range	-6.08165	146.57224	KUNHM	93567
FI4	*P. c. subcyanea*	Huon Peninsula: Finisterre Range	-6.08165	146.57224	KUNHM	T4584
RA1	*P. c. subcyanea*	Huon Peninsula: Rawlinson Mts.	-6.45833	147.4333	AMNH	823638*
RA2	*P. c. subcyanea*	Huon Peninsula: Rawlinson Mts.	-6.45833	147.4333	AMNH	823635*
RA3	*P. c. subcyanea*	Huon Peninsula: Rawlinson Mts.	-6.45833	147.4333	ANWC	25690*
RA4	*P. c. subcyanea*	Huon Peninsula: Rawlinson Mts.	-6.45833	147.4333	ANWC	25691*
RA5	*P. c. subcyanea*	Huon Peninsula: Rawlinson Mts.	-6.45833	147.4333	ANWC	25761*
RA6	*P. c. subcyanea*	Huon Peninsula: Rawlinson Mts.	-6.45833	147.4333	ANWC	25762*
		PNG: Madang Province				
AD1	*P. c. subcyanea*	Adelbert Range	-4.71727	145.27482	KUNHM	111475
AD2	*P. c. subcyanea*	Adelbert Range	-4.71727	145.27482	KUNHM	114781
AD3	*P. c. subcyanea*	Adelbert Range	-4.71727	145.27482	KUNHM	114787

Topology Code	Taxon	Locality	Latitude	Longitude	Source	Voucher Number
AD4	*P. c. subcyanea*	Adelbert Range	-4.71727	145.27482	KUNHM	111570
AD5	*P. c. subcyanea*	Adelbert Range	-4.71727	145.27482	KUNHM	111571
AD6	*P. c. subcyanea*	Adelbert Range	-4.71727	145.27482	KUNHM	111572
AD7	*P. c. subcyanea*	Adelbert Range.	-4.71727	145.27482	KUNHM	111573
AD8	*P. c. subcyanea*	Adelbert Range.	-4.71727	145.27482	KUNHM	111574
SH1	*P. c. subcyanea*	Schradder Range	-5.22057	144.48821	KUNHM	114747
SH2	*P. c. subcyanea*	Schradder Range	-5.22057	144.48821	KUNHM	114809
		PNG: Eastern Highlands Province				
KR1	*P. c. subcyanea*	Kratke Range	-7.061	145.82433	KUNHM	113283
KR2	*P. c. subcyanea*	Kratke Range	-7.061	145.82433	KUNHM	113284
KR3	*P. c. subcyanea*	Kratke Range	-7.061	145.82433	KUNHM	113285
KR4	*P. c. subcyanea*	Kratke Range	-7.061	145.82433	KUNHM	113286
KR5	*P. c. subcyanea*	Kratke Range	-7.061	145.82433	KUNHM	114184
KR6	*P. c. subcyanea*	Kratke Range	-7.061	145.82433	KUNHM	114293
KR7	*P. c. subcyanea*	Kratke Range	-7.061	145.82433	KUNHM	114294
KR8	*P. c. subcyanea*	Kratke Range	-7.061	145.82433	KUNHM	T16485
KR9	*P. c. subcyanea*	Kratke Range	-7.061	145.82433	KUNHM	T16487
OK1	*P. c. subcyanea*	Okapa District: Kimigomo	-6.42718	145.58016	KUNHM	113254
OK2	*P. c. subcyanea*	Okapa District: Kimigomo	-6.42718	145.58016	KUNHM	113255
OK3	*P. c. subcyanea*	Okapa District: Kimigomo	-6.42718	145.58016	KUNHM	114828
OK4	*P. c. subcyanea*	Okapa District: Kimigomo	-6.42718	145.58016	KUNHM	111557
OK5	*P. c. subcyanea*	Okapa District: Kimigomo	-6.42718	145.58016	KUNHM	T16176
OK6	*P. c. subcyanea*	Okapa District: Kimigomo	-6.42718	145.58016	KUNHM	T16184
OK7	*P. c. subcyanea*	Okapa District: Kimigomo	-6.42718	145.58016	KUNHM	T16186
OK8	*P. c. subcyanea*	Okapa District: Kimigomo	-6.42718	145.58016	KUNHM	T16187
OK9	*P. c. subcyanea*	Okapa District: Kimigomo	-6.42718	145.58016	KUNHM	T16201
CR1	*P. c. subcyanea*	Crater Mountain	-6.69444	145.10666	KUNHM	95984
CR2	*P. c. subcyanea*	Crater Mountain	-6.69444	145.10666	KUNHM	95985
CR3	*P. c. subcyanea*	Crater Mountain	-6.65045	145.17143	KUNHM	T12291
BI1	*P. c. subcyanea*	Bismarck Range	-5.95166	145.4	KUNHM	113263
BI2	*P. c. subcyanea*	Bismarck Range	-5.95166	145.4	KUNHM	113264
BI3	*P. c. subcyanea*	Bismarck Range	-5.95166	145.4	KUNHM	114850
BI4	*P. c. subcyanea*	Bismarck Range	-5.95166	145.4	KUNHM	114863
BI5	*P. c. subcyanea*	Bismarck Range	-5.95166	145.4	KUNHM	114869
BI6	*P. c. subcyanea*	Bismarck Range	-5.95166	145.4	KUNHM	114244
BI7	*P. c. subcyanea*	Bismarck Range	-5.95166	145.4	KUNHM	114245
BI8	*P. c. subcyanea*	Bismarck Range	-5.95166	145.4	KUNHM	T16290
		PNG: Chimbu Province				
KU1	*P. c. subcyanea*	Kubor Range	-6.04883	144.52266	AMNH	705338
KU2	*P. c. subcyanea*	Kubor Range	-6.04883	144.52266	AMNH	802635
		PNG: Western Highlands Province				
HA1	*P. c. subcyanea*	Mt. Hagen	-5.79419	143.99600	AMNH	802633*
HA2	*P. c. subcyanea*	Mt. Hagen	-5.79419	143.99600	AMNH	705341*
HA3	*P. c. subcyanea*	Mt. Hagen	-5.79419	143.99600	AMNH	705344*
HA4	*P. c. subcyanea*	Mt. Hagen	-5.79419	143.99600	AMNH	705342*
HA5	*P. c. subcyanea*	Mt. Hagen	-5.79419	143.99600	AMNH	705343*
		PNG: Southern Highlands Province				
BO1	*P. c. atricapilla*	Mt. Bosavi	-6.62206	142.82021	PNGNM	25443*
		PNG: West Sepik Province				
ST1	*P. c. atricapilla*	Mt. Stolle	-4.81331	141.65293	KUNHM	97213
ST2	*P. c. atricapilla*	Mt. Stolle	-4.81331	141.65293	KUNHM	97635
ST3	*P. c. atricapilla*	Mt. Stolle	-4.81331	141.65293	KUNHM	113305
ST4	*P. c. atricapilla*	Mt. Stolle	-4.81331	141.65293	KUNHM	113306
ST5	*P. c. atricapilla*	Mt. Stolle	-4.81331	141.65293	KUNHM	114182

Topology Code	Taxon	Locality	Latitude	Longitude	Source	Voucher Number
ST6	*P. c. atricapilla*	Mt. Stolle	-4.81331	141.65293	KUNHM	114183
ST7	*P. c. atricapilla*	Mt. Stolle	-4.81331	141.65293	KUNHM	114185
ST8	*P. c. atricapilla*	Mt. Stolle	-4.81331	141.65293	KUNHM	114186
ST9	*P. c. atricapilla*	Mt. Stolle	-4.81331	141.65293	KUNHM	114187
ST10	*P. c. atricapilla*	Mt. Stolle	-4.81331	141.65293	KUNHM	114188
ST11	*P. c. atricapilla*	Mt. Stolle	-4.81331	141.65293	KUNHM	114189
ST12	*P. c. atricapilla*	Mt. Stolle	-4.81331	141.65293	KUNHM	114928
ST13	*P. c. atricapilla*	Mt. Stolle	-4.81331	141.65293	KUNHM	114938
ST14	*P. c. atricapilla*	Mt. Stolle	-4.81331	141.65293	KUNHM	114951
		PNG: West Sepik Province				
BW1	*P. c. atricapilla*	Bewani Mts., Mt. Menawa	-3.30373	141.72652	AMNH	829660*
BW2	*P. c. atricapilla*	Bewani Mts., Mt. Menawa	-3.30373	141.72652	AMNH	829658*
BW3	*P. c. atricapilla*	Bewani Mts., Mt. Menawa	-3.30373	141.72652	AMNH	829662*
BW4	*P. c. atricapilla*	Bewani Mts., Mt. Menawa	-3.30373	141.72652	AMNH	829659*
TO1	*P. c. atricapilla*	Torricelli Mts., Mt. Nibo	-3.41243	142.16337	AMNH	829661*
TO2	*P. c. atricapilla*	Torricelli Mts., Mt. Somoro	-3.40879	142.18570	AMNH	829642*
TO3	*P. c. atricapilla*	Torricelli Mts., Mt. Somoro	-3.40879	142.18570	AMNH	829643*
TO4	*P. c. atricapilla*	Torricelli Mts., Mt. Nibo	-3.41243	142.16337	AMNH	829652*
TO5	*P. c. atricapilla*	Torricelli Mts., Mt. Nibo	-3.41243	142.16337	AMNH	829651*
TO6	*P. c. atricapilla*	Torricelli Mts., Mt. Nibo	-3.41243	142.16337	AMNH	829657*
		Indonesia: Papua Province				
CY1	*P. c. atricapilla*	Cyclops Mts.	-2.5077	140.52608	AMNH	608172*
CY2	*P. c. atricapilla*	Cyclops Mts.	-2.5077	140.52608	AMNH	608173*
CY3	*P. c. atricapilla*	Cyclops Mts.	-2.5077	140.52608	AMNH	608175*
CY4	*P. c. atricapilla*	Cyclops Mts.	-2.5077	140.52608	AMNH	608174*
CY5	*P. c. atricapilla*	Cyclops Mts.	-2.5077	140.52608	AMNH	294086*
CY6	*P. c. atricapilla*	Cyclops Mts.	-2.5077	140.52608	AMNH	294082*
CY7	*P. c. atricapilla*	Cyclops Mts.	-2.5077	140.52608	AMNH	608176*
CY8	*P. c. atricapilla*	Cyclops Mts.	-2.5077	140.52608	AMNH	294084*
CY9	*P. c. atricapilla*	Cyclops Mts.	-2.5077	140.52608	AMNH	294083*
CY10	*P. c. atricapilla*	Cyclops Mts.	-2.5077	140.52608	AMNH	294081*
IL1	*P. c. atricapilla*	Nassau Range: Ilaga	-3.98963	137.54045	YPBM	76024*
IL2	*P. c. atricapilla*	Nassau Range: Ilaga	-3.98963	137.54045	YPBM	76026*
IL3	*P. c. atricapilla*	Nassau Range: Ilaga	-3.98963	137.54045	YPBM	76027*
IL4	*P. c. atricapilla*	Nassau Range: Ilaga	-3.98963	137.54045	YPBM	76028*
IL5	*P. c. atricapilla*	Nassau Range: Ilaga	-3.98963	137.54045	YPBM	76029*
GO1	*P. c. atricapilla*	Oranje Mts: Mt. Goliath	-3.98963	137.54045	AMNH	608183*
GO2	*P. c. atricapilla*	Oranje Mts: Mt. Goliath	-3.98963	137.54045	AMNH	608182*
GO3	*P. c. atricapilla*	Oranje Mts: Mt. Goliath	-3.98963	137.54045	AMNH	608181*
GO4	*P. c. atricapilla*	Oranje Mts: Mt. Goliath	-3.98963	137.54045	AMNH	608187*
GO5	*P. c. atricapilla*	Oranje Mts: Mt. Goliath	-3.98963	137.54045	AMNH	608185*
WE1	*P. c. atricapilla*	Weyland Mts.	-3.89137	135.4664	AMNH	302887*
WE2	*P. c. atricapilla*	Weyland Mts.	-3.89137	135.4664	AMNH	302888*
WE3	*P. c. atricapilla*	Weyland Mts.	-3.89137	135.4664	AMNH	302082*
WE4	*P. c. atricapilla*	Weyland Mts.	-3.89137	135.4664	AMNH	302080*
WE5	*P. c. atricapilla*	Weyland Mts.	-3.89137	135.4664	AMNH	302079*
WE6	*P. c. atricapilla*	Weyland Mts.	-3.89137	135.4664	AMNH	302085*
WE7	*P. c. atricapilla*	Weyland Mts.	-3.89137	135.4664	AMNH	302086*
WE8	*P. c. atricapilla*	Weyland Mts.	-3.89137	135.4664	AMNH	302087*
WE9	*P. c. atricapilla*	Weyland Mts.	-3.89137	135.4664	AMNH	302088*
WE10	*P. c. atricapilla*	Weyland Mts.	-3.89137	135.4664	AMNH	302089*
		Indonesia: West Papua Province				
WA1	*P. c. atricapilla*	Wandamen Mts.	-2.75584	134.58458	AMNH	608167*
WA2	*P. c. atricapilla*	Wandamen Mts.	-2.75584	134.58458	AMNH	294088*

Topology Code	Taxon	Locality	Latitude	Longitude	Source	Voucher Number
WA3	*P. c. atricapilla*	Wandamen Mts.	-2.75584	134.58458	AMNH	294087*
WA4	*P. c. atricapilla*	Wandamen Mts.	-2.75584	134.58458	AMNH	608169*
WA5	*P. c. atricapilla*	Wandamen Mts.	-2.75584	134.58458	AMNH	608166*
AR1	*P. c. cyanus*	Arfak Mts.	-1.09181	133.9073	AMNH	608164*
AR2	*P. c. cyanus*	Arfak Mts.	-1.09181	133.9073	AMNH	608163*
AR3	*P. c. cyanus*	Arfak Mts.	-1.09181	133.9073	AMNH	294089*
AR4	*P. c. cyanus*	Arfak Mts.	-1.09181	133.9073	AMNH	294090*
AR5	*P. c. cyanus*	Arfak Mts.	-1.09181	133.9073	AMNH	608162*
TA1	*P. c. cyanus*	Tamrau Mts., Bonkouragen	-0.54878	132.73	ANSP	132303*
TA2	*P. c. cyanus*	Tamrau Mts., Bonkouragen	-0.54878	132.73	ANSP	132299*
TA3	*P. c. cyanus*	Tamrau Mts., Bonkouragen	-0.54878	132.73	ANSP	132297*
TA4	*P. c. cyanus*	Tamrau Mts., Bonkouragen	-0.54878	132.73	ANSP	132302*
TA5	*P. c. cyanus*	Tamrau Mts., Bonkouragen	-0.54878	132.73	ANSP	132298*
TA6	*P. c. cyanus*	Tamrau Mts., Mt. Bantjiet	-0.71553	132.96645	AMNH	793006*
TA7	*P. c. cyanus*	Tamrau Mts., Mt. Bantjiet	-0.71553	132.96645	AMNH	793005*
TA8	*P. c. cyanus*	Tamrau Mts., Mt. Bantjiet	-0.71553	132.96645	AMNH	793004*
Outgroup						
	Peneothello bimaculata	PNG: EHP	-6.78849	145.03674	KUNHM	T12898
	Peneothello sigillata	PNG: Morobe Province	-6.08165	146.57224	KUNHM	T4599
	Peneothello cryptoleuca	Indonesia: West Papua Province	-0.71553	132.96645	AMNH	793000*
	Peneoenanthe pulverulenta	Australia: Northern Territory	-14.7442	135.33437	KUNHM	T22867
	Melanodryas cucullata	Australia:	-26.4667	114.48333	KUNHM	T6207
	Poecilodryas placens	PNG: EHP	-6.7885	145.70341	KUNHM	T5177
	Poecilodryas albispecularis	PNG: Morobe Province	-6.08165	146.57224	KUNHM	95822
	Poecilodryas hypoleuca	PNG: Western Province	-4.61525	142.71338	KUNHM	93150
	Poecilodryas albonotata	PNG: Morobe	-6.08165	146.57224	KUNHM	93564

Institutional Sources: American Museum of Natural History (AMNH), Yale Peabody Museum (YPM), Harvard Museum of Comparative Zoology (MCZ), Philadelphia Academy of Natural Sciences (ANSP), Australian National Wildlife Collection (ANWC), University of Kansas Natural History Museum (KUNHM); Papua New Guinea National Museum (PNGNM).

Appendix 1.2. Summary of primers used for *Peneothello cyanus* samples.

Gene	Primer name	Sequence 5'– 3'
NADH dehydrogenase subunit–2	L5216[a]	GGCCCATACCCCGRAAATG
	H6313[a]	CTCTTATTTAAGGCTTTGAAGGC
	PC–ND2–1H[b]	GGA GGT GCC TTG TAR GAC TTC TGG
	PC–ND2–2L[b]	GAC ATT ACA CAA CTA ACA CAT CCC A
	PC–ND2–2H[b]	TGA GTT GAG AGT TAG GAA TAC AGC
	PC–ND2–3L[b]	TAG CCT TCT CCT CCA TCT CTC AC
	PC–ND2–3H[b]	CAG TAT GCG AGT CGG AGG TAG AAG AAT AG
NADH dehydrogenase subunit–3	L10755[d]	GACTTCCAATCTTTAAAATCTGG
	H11151[d]	GATTTGTTGAGCCGAAATCAAC
ATP synthase subunits–6 and 8	tRNA–Lys–L[c]	CAGCACTAGCCTTTTAAGCT
	COIII–RH[c]	ATTATTCCGTATCGNAGNCCYTTTTG
	PC–ATP–1H[b]	ATTAGGGATGTGAGGATGAGGGC
	PC–ATP–2L[b]	TAGACAACCGATGAATCACCAACCG
	PC–ATP–2H[b]	AGGGCTAGTGGACGGATTAGGAG
	PC–ATP–3L[b]	CCTCAGCATCCCTAAGTCACCTCC
	PC–ATP–3H[b]	TGGGTCATGGGCTTGGATCTACTATGT

[a] Johnson and Sorenson (1998)
[b] Designed by B.W. Benz for this study
[c] Sorenson et al. (1999)
[d] Chesser (1999)

Appendix 1.3. Uncorrected ND2 sequence divergence (%) among populations of *P. cyanus*, with intra-population divergences given on the diagonal. Pairwise F_{ST} values are indicated in bold below the diagonal.

	Vogelkop Penin.	Wandamen Range	Weyland Range	Ilaga Goliath	Cyclops Range	Torricelli Range	Mt. Stolle	Eastern Highlands	Huon Penin.	Adelbert Range	Owen Stanley	Mt. Simpson
	P1	P2	P3	P4	P5	P6	P7	P8	P9	P10	P11	P12
P1	0.0-0.8	3.5-3.8	2.9-3.6	2.5-3.3	2.7-3.4	2.9-3.7	3.1-4.0	2.7-3.8	3.1-3.8	3.0-3.7	2.9-3.9	3.3-4.0
P2	**0.940**	0.0-0.1	0.5-0.8	1.2-1.6	1.4-1.6	1.6-2.0	2.1-2.7	2.0-2.4	2.1-2.4	2.2-2.4	2.0-2.8	2.4-2.7
P3	**0.914**	**0.749**	0.0-0.6	0.7-1.5	0.9-1.6	1.3-1.9	1.8-2.7	1.8-2.4	2.0-2.3	2.1-2.4	2.0-2.7	2.2-2.5
P4	**0.893**	**0.892**	**0.840**	0.0-0.5	0.2-0.8	0.6-1.0	1.2-2.1	1.3-2.0	1.5-2.2	1.5-2.1	1.4-2.3	1.5-2.0
P5	**0.934**	**0.947**	**0.902**	**0.775**	0.0-0.3	0.7-1.3	1.4-2.3	1.4-2.1	1.7-2.3	1.7-2.2	1.6-2.4	1.7-2.1
P6	**0.927**	**0.936**	**0.893**	**0.764**	**0.874**	0.0-0.3	1.7-2.5	1.6-2.3	2.7-2.7	2.0-2.5	2.0-2.8	2.1-2.4
P7	**0.894**	**0.910**	**0.887**	**0.849**	**0.902**	**0.896**	0.0-0.7	0.0-0.8	0.2-0.9	0.2-0.7	0.3-1.3	0.3-0.9
P8	**0.890**	**0.911**	**0.887**	**0.852**	**0.903**	**0.896**	**0.482**	0.0-0.7	0.2-0.8	0.5-0.7	0.1-1.2	0.5-0.8
P9	**0.900**	**0.915**	**0.888**	**0.862**	**0.914**	**0.907**	**0.502**	**0.504**	0.0-0.5	0.1-0.7	0.3-1.3	0.4-0.9
P10	**0.899**	**0.914**	**0.889**	**0.845**	**0.903**	**0.894**	**0.597**	**0.602**	**0.528**	0.0-0.6	0.3-1.2	0.6-0.7
P11	**0.916**	**0.942**	**0.915**	**0.886**	**0.937**	**0.929**	**0.624**	**0.315**	**0.628**	**0.699**	0.0-0.7	0.5-1.3
P12	**0.932**	**0.954**	**0.93**	**0.901**	**0.95**	**0.942**	**0.743**	**0.755**	**0.749**	**0.734**	**0.838**	0.0-0.2

Appendix 1.4. Paleoecological niche reconstruction based on the CCSM general circulation model, depicting the potential distribution of *P. cyanus* under LGM climatic conditions.

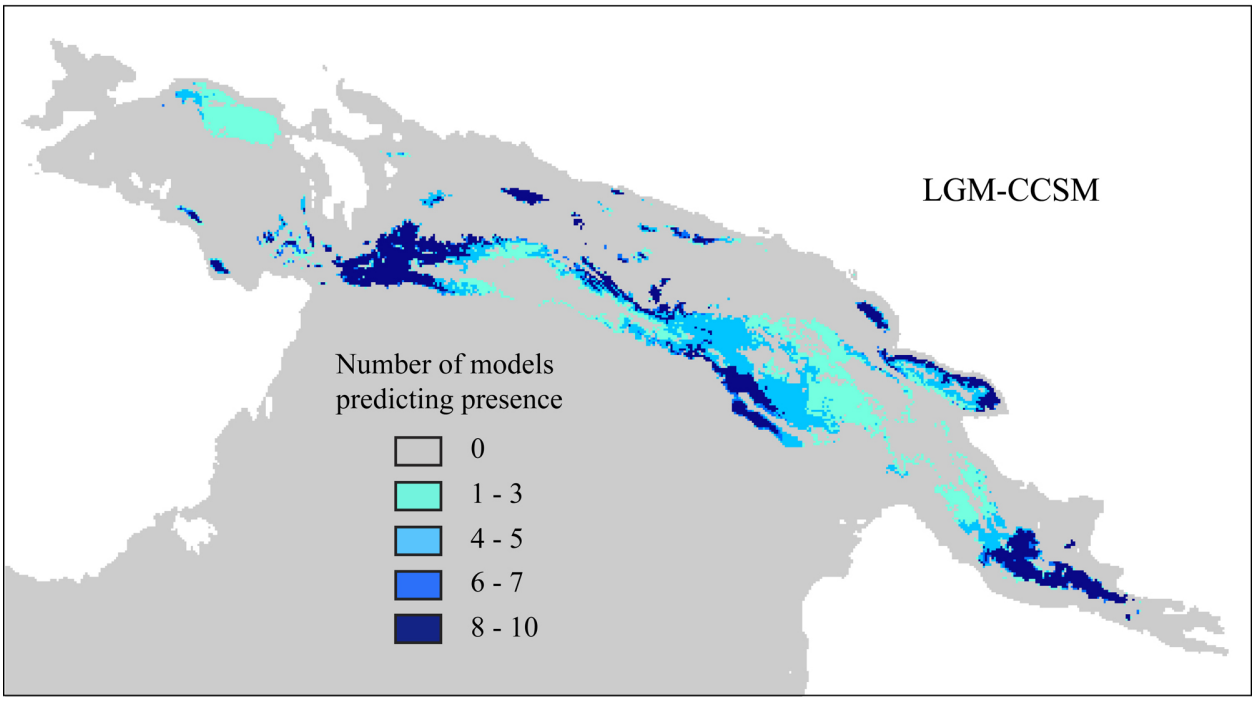

Appendix 1.5. Results of niche identity tests depicting Hellinger's *I* a nd Schoener's *D* similarity statistics for comparisons among primary geographic lineages within *P. cyanus*.

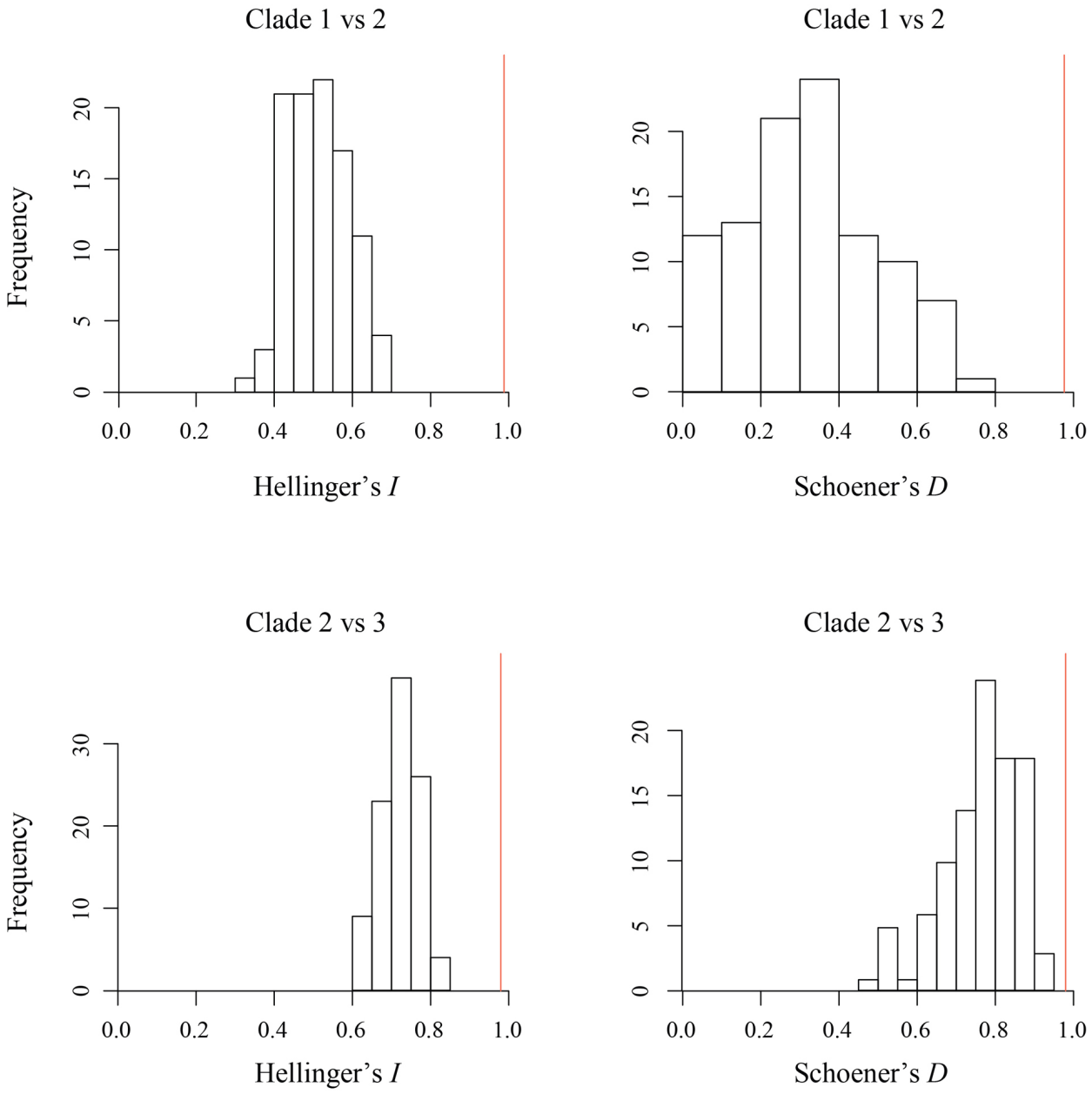

Appendix 1.6. Results of background similarity tests depicting Hellinger's I statistic for comparisons among three primary clades of *P. cyanus*.

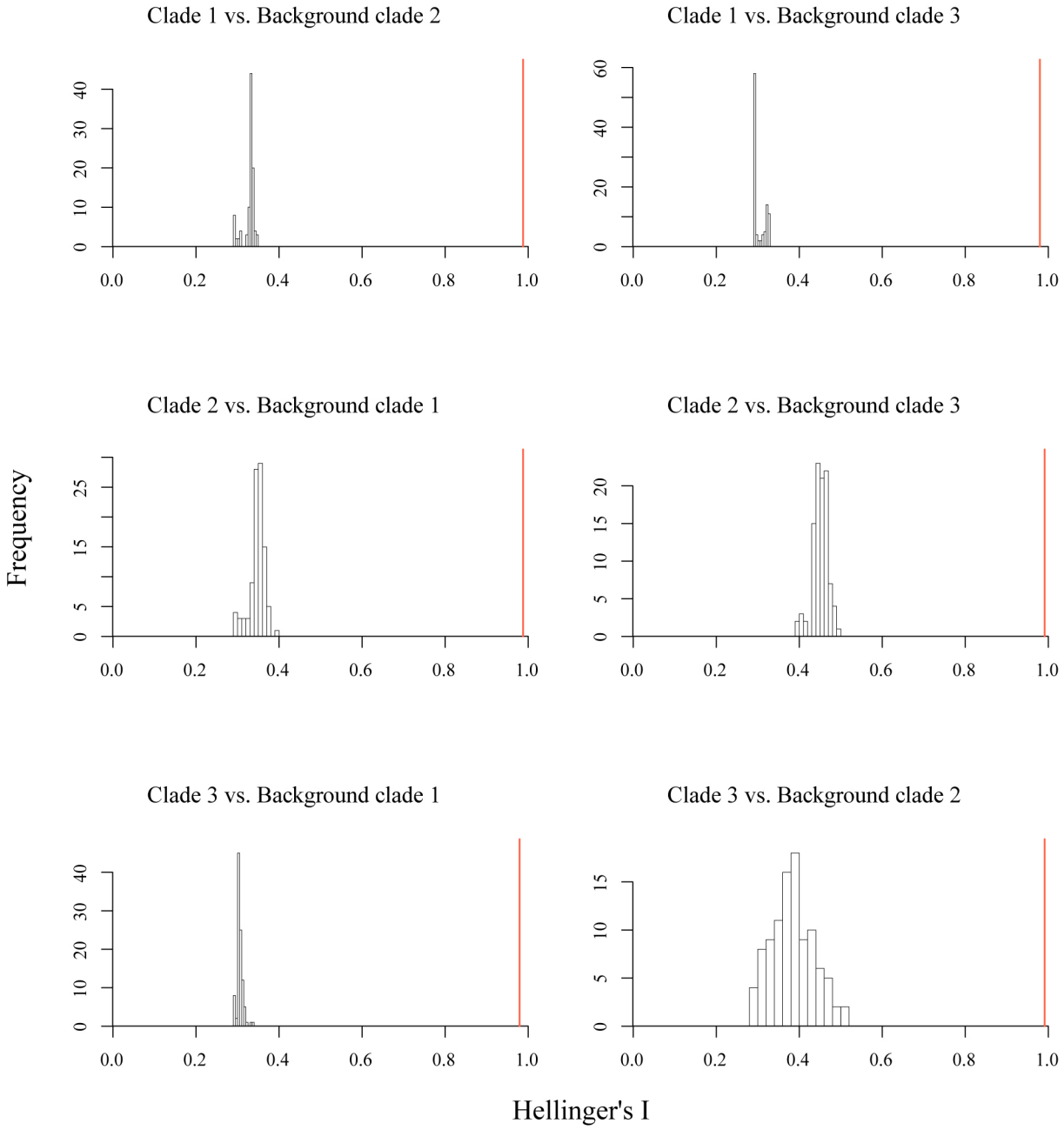

CHAPTER TWO

PHYLOGEOGRAPHY, DEMOGRAPHIC HISTORY, AND EVOLUTIONARY ORIGIN OF 'LEAPFROG' DISTRIBUTION PATTERNS IN THE MOUNTAIN MOUSE-WARBLER COMPLEX (*CRATEROSCELIS ROBUSTA*)

ABSTRACT

Leapfrog patterns of geographic variation in phenotype have been reported within several avian genera across New Guinea's montane landscape; however, the historical mechanisms responsible for these distributions remain obscure given the lack of robust phylogenetic hypotheses for much of the regional avifauna. Herein, I use mitochondrial sequence data (ND2, ATP6-8) to reconstruct the phylogeographic history of the Mountain Mouse-Warbler complex (*Crateroscelis robusta*) and examine the evolutionary basis of its leapfrog distribution in the New Guinea highlands. Broad geographic sampling (n=127) was employed to evaluate phylogenetic relationships among all currently recognized subspecies, and assess the influence of putative environmental barriers in governing spatial distributions of genetic and morphological diversity. Phylogenetic analyses recovered two primary phylogroups within *C. robusta*, which exhibit a deep genetic break across the Strickland River Valley. Coalescent estimates of divergence times indicate that these lineages arose in the middle to late Pliocene, with ND2 pairwise sequence divergences ranging from 7.95–8.97% between phylogroups. The absence of contemporary gene flow or ancestral polymorphism across this boundary suggest these lineages merit species status given the maintenance of independent evolutionary trajectories through recurrent periods of extensive environmental connectivity in the Pleistocene. Ancestral character state reconstructions revealed a pattern of labile plumage evolution as inferred by multiple

independent gains of brown throat and abdominal coloration among western populations; however, *K* statistics and CI/RI values indicate low-level phylogenetic signal in both traits. These phylogeographic results disprove common ancestry and long distance dispersal hypotheses in explaining the origin of leapfrog variation, and suggest that stochastic or selective mechanisms among disjunct populations have differentially shaped the evolution of plumage coloration in the *C. robusta* complex. By contrast, shallow genetic structure and evidence of admixture among populations in the Eastern Highlands, Huon Peninsula, and Owen Stanley Ranges corroborate enhanced environmental connectivity associated with Pleistocene climate cycles, which may account for the broad distribution of uniform plumage traits in eastern New Guinea.

INTRODUCTION

New Guinea's striking ecological diversity and rugged topographic relief have fostered the evolution of a rich endemic avifauna exhibiting diverse patterns of geographic variation across the Central Dividing Ranges (CDRs) and outlying coastal sky-islands (Pratt, 1982; Keast, 1996; Frith & Beehler, 1998). Among the least understood and perhaps most intriguing of these geographic patterns are "leapfrog" distributions (Remsen, 1984), in which phenotypically similar populations are geographically isolated from one another by intervening populations of a distinct phenotype. The prevalence of this counterclinal phenomenon has yet to be thoroughly examined in New Guinea's highland avifauna, given a lack of comparative voucher collections from key montane sites; however, biogeographic assessments of phenotypic variation have reported multiple instances of leapfrog distributions from diverse taxonomic groups (*Amalocichla*, *Crateroscelis*, *Drepanornis*, *Malurus*, *Meliphaga*, *Parotia*), suggesting that this pattern is potentially more common than presently recognized (Diamond, 1972; Heads 2001a; 2002).

Several evolutionary mechanisms have been proposed to explain the origin of leapfrog distributions, each of which carry distinct phylogeographic predictions (Remsen, 1984; Norman et al., 2002; Cadena et al., 2011). Hypotheses that attribute patterns of phenotypic similarity to differential rates of morphological diversification between terminal and central populations have been embraced by several authors, particularly in the Andean avifauna, which exhibits a high incidence of leapfrog variation at disparate geographic scales (Chapman, 1923; Remsen, 1984). Under the unequal rates hypothesis, convergent or parallel evolution among terminal populations may arise either through stochastic processes such as genetic drift, or via environmentally influenced selective pressures that differ from those within intervening populations. Alternatively, stochastic or selective forces may drive morphological diversification exclusively within intervening populations, producing a similar pattern of phenotypic variation in which terminal lineages retain ancestral character states as apposed to the former case where phenotypic similarity is independently derived.

In contrast to unequal rates mechanisms, common ancestry hypotheses predict sister relationships among phenotypically similar terminal taxa, and thus typically invoke long-distance dispersal processes to explain leapfrog distributions that by-pass central populations. Diamond (1973) surmised that competitive exclusion interactions potentially contribute to such patterns in New Guinea, by limiting dispersal between adjacent populations and thereby promoting colonization of disjunct communities. Phenotypic similarity due to common ancestry may also arise from vicariant events, in which environmental corridors that formerly joined terminal populations are reduced or lost altogether due to shifts of ecological suitability associated with Pleistocene climate cycling or deeper geological events such as orogenic uplift and river drainage formation. Vicariant scenarios generally predict strong congruence in the

geographic distribution of intervening populations, whereas leapfrog variation produced by long-distance dispersal processes would likely show discordance in these distributional breaks across codistributed taxa, with patterns of geographic variation reflecting taxonomic composition of adjacent communities (i.e. competitive exclusion interactions), dispersal capacity, and regional topographic complexity.

Despite considerable advances in understanding the genetic and developmental basis of avian plumage coloration over the past decade (Mundy, 2005; Prum, 2006; Uy et al., 2009; Driskell et al., 2010), the evolutionary processes promoting and maintaining leapfrog distributions remain obscure, as few studies have addressed their origin within a molecular phylogenetic framework (Norman et al., 2002; Cadena et al., 2010). Herein, I use mitochondrial sequence data to reconstruct the phylogenetic relationships within the Mountain Mouse-Warbler complex (*Crateroscelis robusta*) and evaluate the evolutionary mechanisms that have shaped its historical diversification and leapfrog variation in phenotype across the New Guinea's highlands.

Study system

The Acanthizidae encompasses a diverse assemblage of small-bodied largely insectivorous oscine passerines comprised of ~ 60 species in 13 genera, which are endemic to the Australo-Papuan realm (Christidis & Boles, 2008; Gardner et al.; 2010). Among these, the *Crateroscelis* mouse-warblers include 3 species broadly distributed throughout New Guinea's lowland and montane rainforest environments. Although each taxon exhibits similar foraging strategies specialized on insect gleaning amid understory vegetation, allopatry is maintained through sharp elevational breaks that are likely a consequence of competitive exclusion processes, as these distributional limits do not correspond with abrupt ecological transitions (Diamond, 1972; 1973).

Moreover, elevational contact zones may vary by several hundred meters from site to site depending on the taxonomic composition of the community and regional topographic setting.

Primary hill forest and lower montane closed canopy environments are inhabited by *C. murina*, which ranges from ~ 400–1500 m on mainland New Guinea and has established populations on most Pleistocene land-bridge islands including Aru, Salawati, Yapen, Misol, Waigeo, and Batanta. The distribution of *C. nigrorufa* remains poorly understood, but it appears to occupy a narrow elevational band from 1250–2200 m, and is generally uncommon throughout its patchy distribution spanning the Central Highlands, Huon Peninsula, and Owen Stanley Ranges. This species is replaced at higher elevations by *C. robusta*, whose elevational distribution ranges from 1400 m to near tree line (3700 m), with peak densities in primary and mature-secondary montane rainforest environments between 1600–2400 m (Coates, 1990; Gregory, 2008). Excluding the Adelbert Range, *C. robusta* has colonized all of New Guinea's coastal sky-island communities and is ubiquitous in appropriate habitats throughout the CDRs and Papuan Peninsula.

Six subspecies are currently recognized within the Mountain Mouse-warbler complex (Fig. 2.1), which Diamond (1985) arranged in three groups based on coloration of throat and ventral plumage, presence of dark pectoral band, and prominence of sexual dimorphism (Diamond, 1969; Gregory, 2007). Nominate *C. r. robusta* ranges throughout the Papuan and Huon Peninsulas west to the Strickland River valley, with all populations showing strong sexual dimorphism. Both sexes are dark grey-brown dorsally with bright white to ivory throat and abdominal plumage, whereas males are overall darker than females and have a wide grey-brown pectoral band and dark grey-brown flanks. Sky-island populations of the Foya Mountains and

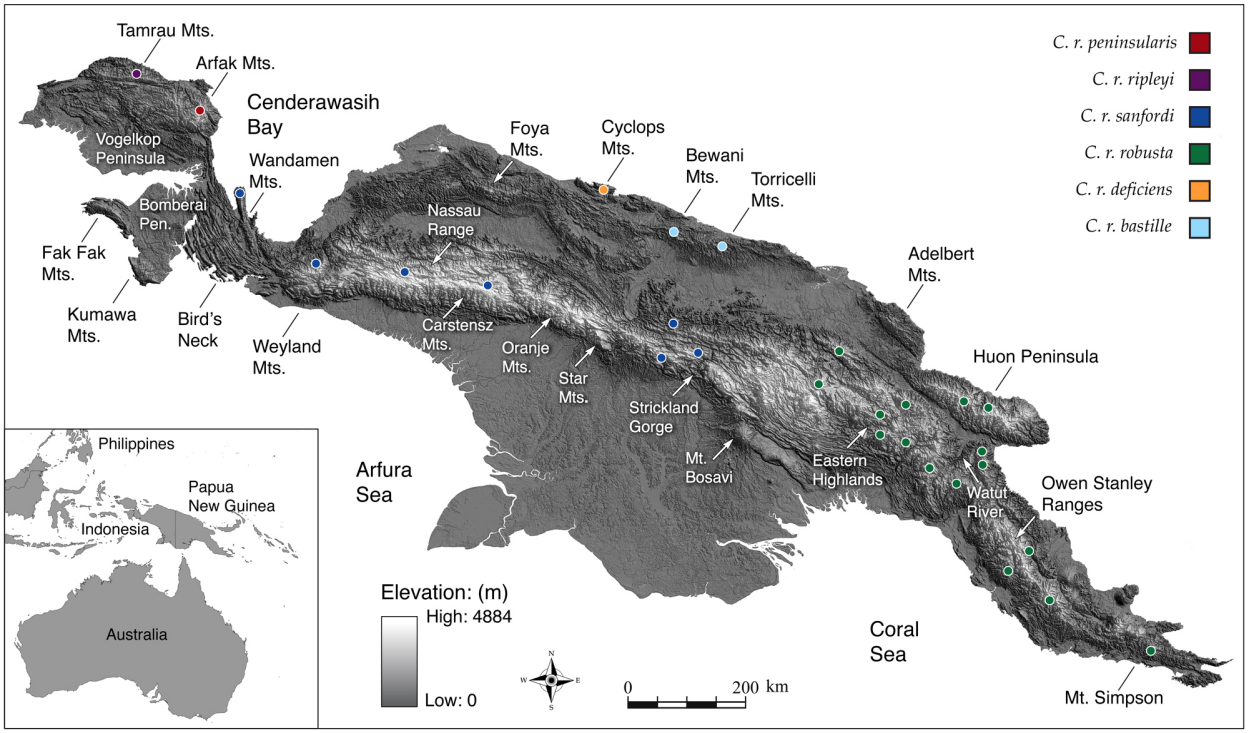

Figure 2.1. Digital elevation model of New Guinea depicting the prominent Central Highlands and outlying coastal sky-islands. Collection localities of *Crateroscelis robusta* specimens genetically sampled for this study are color coded to indicate the approximate distribution of currently recognized subspecies within the complex.

Bomberai Peninsula (Fak Fak & Kumawa ranges) share this nominate phenotype; however, these lineages have yet to be formally described due to a lack of specimen material (Diamond, 1985). The distinctive *C. r. sanfordi*, which ranges from the Strickland Gorge west to the Wandamen Mountains, and *C. r. bastille* of the Bewani, Torricelli, and Prince Alexander ranges, are both uniform dark brown to olive brown dorsally, transitioning to russet brown on the lower abdomen and tawny hues on the upper chest and throat. Sexes of both taxa are monomorphic and lack pectoral banding. Sky-island populations of the Cyclops (*C. r. deficiens*), Arfak (*C. r. peninsularis*) and Tamrau Mountains (*C. r. ripleyi*) share similar plumage attributes, with both sexes resembling the female phenotype of nominate *C. r. robusta*. The dorsum is uniform grey brown, with brown flanks that transition to ivory or buffy abdominal plumage and a bright white

throat, but with no evidence of pectoral banding (Fig. 2.3). Rand (1942) synonymized *C. r. steini* of the Weyland Mountains with the broadly distributed *C. r. sanfordi* as the paler olive-brown plumage characteristic of *steini* is also present in some *sanfordi* specimens from the Snow Mountains. The proposed *C. r. pratti* of Mt. Dayman has been retained within nominate *robusta* given the subtle phenotypic variation exhibited in the latter taxon throughout its broad distribution (Gregory, 2007).

Hypotheses that infer long-distance dispersal to explain the origin of this 450 to 1275 km disjunction between eastern populations of *C. r. robusta* and the phenotypically similar sky-island populations of the Bomberai, Vogelkop, Foya, and Cyclops ranges are difficult to reconcile with the species' largely terrestrial habits, strong association with montane closed-canopy environments, and ostensibly weak dispersal capacity. Nonetheless, common ancestry mechanisms cannot be discounted outright, as *C. robusta* has successfully colonized the full extent of New Guinea's montane landscape and recent biogeographic investigation of codistributed avian taxa has implicated west-lateral rifting of accreted terranes to explain purported sister relationships between the Vogelkop and montane communities far to the east (Heads, 2001a; 2001b; 2002), thereby providing a potential but unlikely vicariant mechanism to explain such disjunctions.

In this investigation, I test the evolutionary predictions associated with common ancestry and unequal rates hypotheses using molecular phylogenetic methods to shed light on the origin of leapfrog variation in the Mountain Mouse-warbler complex and explore the environmental factors that have shaped its diversification in a topographically fragmented montane landscape. Specifically, I examine spatial distributions of genetic diversity, coalescent estimates of lineage formation, demographic summary statistics, contemporary and Last Glacial Maximum (LGM)

ecological niche reconstructions, and ancestral character state reconstructions of plumage coloration to address the following questions: (1) Are patterns of population genetic structure concordant with the geographic distribution of contemporary sky-islands and putative biogeographic boundaries in the CDRs, or is the distribution of genetic diversity better explained by spatial patterns of environmental connectivity inferred by Pleistocene climatic shifts? (2) Does phenotypic variation in plumage coloration reflect phylogenetic relationships among geographic lineages, suggesting a history of long-distance dispersal, or is phenotypic similarity between "terminal" populations a consequence of labile plumage evolution, with genetic distances among populations reflecting an isolation by distance effect? (3) Are coalescent estimates of divergence times consistent with patterns of environmental connectivity associated with Pleistocene climate cycles, or are genetic splits indicative of deeper geological processes including uplift of the CDRs and terrane accretion events? (4) Do signatures of historical demography corroborate shifts of environmental suitability predicted by contemporary and LGM ecological niche reconstructions, and how have these processes influenced genetic diversity within the CDRs versus outlying sky-island communities?

METHODS

Genetic sampling

Populations of *C. robusta* were sampled throughout the species' geographic range (save the Foya Mountains and Bomberai Peninsula), including all currently recognized subspecies: *C. r. robusta* (n=63), *C. r. bastille* (n=9), *C. r. deficiens* (n=10), *C. r. sanfordi* (n=31), *C. r. peninsularis* (n=9), and *C. r. ripleyi* (n=5). I collected fresh tissue samples (muscle) from multiple sites across Papua New Guinea (Fig. 2.1), which were stored in 99% ethanol while in the field and later

transferred to -70ºC storage at the University of Kansas Natural History Museum (KUNHM). Ancient DNA tissues (toepad clippings) were sampled from historical collections (1928–1973) to include populations from Papua and West Papua, Indonesia, and to refine phylogeographic resolution near the Tauri and Strickland river drainages. Selection of appropriate outgroups was based on a recent molecular phylogenetic hypothesis of the Meliphagoidea (Gardner et al., 2010) and included the two remaining congeners *C. nigrorufa* and *C. murina*, as well as closely related representatives of the Acanthizidae (*Sericornis nouhuysi*; *Sericornis papuensis*) and Meliphagidae (*Myzomela rosenbergi*; *Phylidonyris novaehollandiae*). Detailed specimen data including collection locality, latitude/longitude, institutional source, and topology code used in BI results are given in Appendix 2.1.

DNA extraction and sequencing

Standard proteinase K digestion and ethanol precipitation protocols were used to extract whole genomic DNA from fresh tissue samples according to the manufacturer's protocols (DNeasy Tissue Kit, QIAGEN). Three mtDNA genes including NADH dehydrogenase subunit-2 (ND2, 1041 bp) and ATP synthase subunits-6 and 8 (ATP6, 684bp; ATP8, 168 bp) were amplified via 12µl polymerase chain reactions (PCR) using PureTaq RTG PCR beads (GE Healthcare). Thermocycle parameters for each external primer pair (Appendix 2.2) consisted of an initial 3 min denaturation at 94 ºC, followed by 35 cycles of 20 s at 94 ºC, 15 s at 53 ºC, and 60 s at 72 ºC, followed by a 7 min final extension at 72 ºC and 4 ºC soak. All PCR products were cleaned of unincorporated DNTPs and primers with ExoSaP-IT purification (USB Corp.), visualized on a 1% agarose gel stained with ethidium bromide to assess amplification quality, and cycle-sequenced with ABI Prism BigDye v3.1 terminator chemistry under manufacture's

thermocycling protocols using the same external PCR primer pairs. Cycle-sequencing products were desalted and cleaned of excess terminator dyes with Sephadex G-50 (medium) purification columns, and subsequently analyzed on an ABI 3730 Genetic Analyzer (Applied Biosystems).

Extractions of ancient DNA samples were carried out in a lab free of avian PCR and genomic procedures, and workstations were cleaned with a 10% bleach solution prior to each set of extractions to protect against contamination. Filtered pipette tips and multiple negative controls were also used in all extraction and sequencing procedures involved with ancient DNA samples to further guard against contamination. Samples were extracted using a DNeasy Tissue Kit (QIAGEN), with the duration of tissue lysis extended overnight and 10 μl of 1M Dithiothreitol added to ensure complete digestion of the toepad sample. Negative controls were tested for contaminant DNA using a NanoDrop spectrophotometer (Thermo Scientific). I designed a suite of internal primers to sequence 834 bp of the ND2 gene via 3 overlapping amplicons ~350 bp in length with a minimal 15 bp overlap between fragments excluding primer sequences (Appendix 2.2). The same approach was used to sequence the entire ATP6–8 subunits (852 bp). Thermocycling protocols for all ancient DNA PCRs were modified to incorporate an annealing touch down of 10 cycles at 60 ºC, 10 cycles at 56 ºC, and 25 cycles at 52 ºC, followed by a 10 min extension at 72 ºC and 4 ºC soak. An additional 15 cycles were added to ABI's standard thermocycling protocols to maximize signal strength of chromatograms. All other sequencing procedures followed standard protocols detailed above for fresh DNA samples.

Phylogenetic analysis

Sequence alignment was straightforward and conducted by eye in MESQUITE v. 2.72 (Maddison & Maddison, 2009) followed by amino acid translation for comparison with *Gallus gallus*

sequences (Dejardins & Morias, 1990) to confirm reading frames. The combined sequence alignment was partitioned by codon position and the Bayesian Information Criterion (BIC) applied in JMODELTEST v. 0.1.1 (Guindon & Gascuel, 2003; Posada, 2008) to determine the best-fit nucleotide substitution model for each data partition.

Estimates of phylogenetic relationships were determined via Bayesian inference (BI) implemented in MRBAYES v. 3.1.2 (Ronquist & Huelsenbeck, 2003; Altekar et al., 2004) with a flat prior specified for parameter estimation, and default heating conditions applied to four Markov chains run for $2x10^7$ generations sampled every 1000 generations, resulting in 15,000 trees after a conservative 25% burnin. Multiple analyses were conducted to guard against convergence on local optima, and stationarity of each run was assessed by monitoring average standard deviation of split frequencies, plotting –lnL against generation time, assessing model parameter posterior probability densities in TRACER v. 1.5 (Rambaut & Drummond, 2007), and examining clade posterior probabilities across runs using the compare and slide functions in AWTY (Nylander et al., 2008).

Phylogenetic relationships were also examined in a maximum likelihood framework (ML) using GARLI v. 0.95 (Zwickl, 2006), with fifty independent runs conducted on the combined sequence alignment using default parameters. Topologies were selected after 50,000 generations with no significant improvement in –lnL (improvement values set at 0.01 with a total improvement of < 0.05 compared to the last topology recovered). Node support was assessed using 1000 non-parametric bootstrap replicates using a reduced run termination criterion of 10,000 generations.

Population structure and demographic history

Geographic patterns of genetic variation were examined using median-joining networks constructed in NETWORK v. 4.5 (fluxus-engineering.com) under default parameters with the MP algorithm implemented to reduce superfluous median vectors (Polzin & Daneschmand, 2003). Population genetic structure was examined further using pairwise F_{ST} statistics calculated in DNASP v. 5.0 (Librado & Rozas, 2009), which combined with topographic relief and ecological niche models were used to define population limits among the 28 sampling localities. Population genetic summary statistics including number of unique haplotypes (h), number of segregating sites (S), haplotype diversity (Hd), and the nucleotide diversity parameter π along with its standard deviation were also calculated in DNASP v. 5.0 (Table 2.2). I conducted analyses of molecular variance (AMOVA) in ARLEQUIN v. 3.5 (Excoffier & Lischer, 2010) to examine the impact of Pleistocene climatic oscillations in shaping the distribution of genetic diversity within *C. robusta*. Sequences were partitioned by taxonomy, contemporary sky-island populations, and Pleistocene sky-islands inferred from LGM ecological niche reconstructions (see below for ENM methods). Mantel tests were conducted in IBDWS v. 3.16 (Isolation By Distance Web Service: http://ibdws.sdsu.edu/; Jensen et al., 2005) using 10,000 permutations to test for correlations between genetic and geographic distances within regional phylogroups and the species as a whole. Geographic straight-line distances (km) between the center points of populations were estimated from geo-referenced collecting localities using ArcGIS (ESRI, Redlands, CA). Genetic distances were computed as $F_{ST}/1-F_{ST}$ as recommended in Rousset (1997) and were not log-transformed given the stepping stone mode of dispersal.

I examined patterns of population demography using a variety of standard summary statistics including Tajima's *D*, Fu & Li's *D* (Fu & Li, 1993), Fu's *Fs* (Fu, 1997), and R_2

(Ramos-Onsins & Rozas, 2002), with statistical significance determined using 10,000 coalescent simulations conducted in DNASP v. 5.0. The distribution of pairwise differences was used to infer demographic history of individual populations with the fit of the observed data assessed using the raggedness statistic (*r*) calculated in DNASP v. 5.0, and significance determined using 10,000 coalescent simulations (Harpending, 1994). All population genetic summary statistics were derived from the full sequence alignment, whereas mismatch distributions were based solely on ND2 sequences.

Gene flow and divergence times

I conducted coalescent analyses in IMA2 (Hey, 2010) to assess gene flow within *C. r. robusta* including pairwise analyses between populations from the Eastern Highlands and Owen Stanley Range, and between the Huon Peninsula and Eastern Highlands. Each analysis was run for 1 x 10^7 steps with 20 geometrically heated chains and an initial burnin period of 2 x 10^6 steps. Multiple runs were performed to determine whether convergence was reached, whereas effective sample size values and parameter plots were inspected to ensure adequate mixing among chains was achieved.

Coalescent estimates of divergence times between primary east-west phylogroups and secondary regional clades were conducted in IMA2 with a broad range of mutation scalars applied (2–5% per million years). Each run was conducted with 20 geometrically heated chains for 3 x10^7 steps and a 1 x 10^7 burnin. The migration parameter was set to zero, given the reciprocal monophyly among these lineages. Divergence times between populations were also estimated by calculating the net nucleotide diversity between adjacent population pairs and applying a conservative range of divergence rates as above (2–5%) to account for uncertainty in

ND2 mutation rate estimates (Lovette, 2004; Arbrogast et al., 2006). Net nucleotide diversity was determined from the equation $d = d_{xy} – 0.5 (d_x + d_y)$ where d_x and d_y represent average pairwise divergences within populations x and y, and d_{xy} is the average divergence among populations. The latter statistic was calculated in DNASP V. 5.0, whereas average pairwise divergences were calculated in PAUP V. 4.0b10 (Swofford, 2002).

Analysis of plumage evolution

Considering the absence of genetic sampling from Bomberai Peninsula and Foya Mountain populations (i.e. sexually dimorphic phenotypes with strong pectoral banding), analyses of plumage evolution focus herein on variation of throat and abdominal coloration, traits that exhibit leapfrog patterns across the Papuan Peninsula, CDRs, and Vogelkop. These plumage characters are conserved within regional clades and show little to no variation at the population level. As such, I constructed a simplified sequence alignment for analysis of ancestral character state reconstructions, with single representatives chosen randomly from each regional lineage identified by the full BI analysis. The resulting data matrix included 10 *C. robusta* samples, with *C. murina* designated as the outgroup to polarize character states. I employed a relaxed clock approach implemented in BEAST v1.5 (Drummond & Rambaut, 2006; 2007) to infer relationships among lineages, using a Yule tree prior and the HKY+Γ model of sequence evolution based on BIC values acquired in JMODELTEST V. 0.1.1 (Guindon & Gascuel, 2003; Posada, 2008). Analyses were run for $2x10^7$ generations sampled every 1000 generations, resulting in 15,000 trees after a conservative 25% burnin. Stationarity of each run was assessed using the same convergence metrics as above in the full BI analysis.

Character states were scored as white or brown for each population by examining series of museum specimens at the American Museum of Natural History (AMNH), Philadelphia Academy of Sciences (ANSP), Papua New Guinea National Museum (PNGNM) and the University of Kansas Natural History Museum (KUNHM). Based on the maximum clade credibility topology acquired from the BEAST analysis, I employed parsimony and likelihood ancestral character state reconstructions in MESQUITE v. 2.72 (Maddison & Maddison, 2009) with the Markov k-state 1 parameter model implemented for the latter approach. I used the PICANTE software package (Kimbel et al., 2010) in R as an alternative means to explore phylogenetic signal and evolutionary history of plumage traits in *C. robusta* by estimating *K* statistics (Blomberg et al., 2003) for throat and abdominal coloration based on relationships recovered in the full and reduced BI topologies. The *K* statistic provides a measure of phylogenetic signal for a given trait by comparing the observed signal to that under a Brownian motion model of character evolution. Values which approach 1 indicate the trait is evolving under a Brownian motion process, suggesting a moderate level of trait conservatism, whereas values greater than 1 indicate strong phylogenetic signal and values less than 1 signify lability.

Ecological niche reconstructions

I generated contemporary and Last Glacial Maximum (LGM) ecological niche models (ENMs) for *C. robusta* using GARP (Genetic Algorithm for Rule-Set Prediction; Stockwell & Peters 1999) and MAXENT v 3.3 (Phillips et al., 2006) software applications. Occurrence data were compiled from GPS coordinates (spatial resolution ~5 m) recorded during PNG collecting expeditions, whereas distributional data from Papua and West Papua, Indonesia, were assembled from museum-specimen locality information and first-hand sightings by BWB, with locality

names georeferenced from published and online gazetteers when locality descriptions were sufficiently detailed and reliable. A subset of the 19 bioclimatic coverages from the WorldClim dataset (1960-1990; Hijmans et al., 2005a) was used as the basis for ENMs, with dimensions including annual mean temperature, mean diurnal range, maximum temperature of the warmest month, minimum temperature of the coldest month, total annual precipitation, and precipitation of the wettest and driest months. Last Glacial Maximum climates were analyzed at 2.5' spatial resolution based on a downscaling developed by R. Hijmans of general circulation model simulation results from CCSM and MIROC climate models (Waltari et al., 2007). See Chapter 1 methods for further details on this process as well as modeling parameters and "best subset" procedures used in GARP and Maxent analyses. All models were reclassified using the lowest presence thresholding approach described in Pearson et. al., (2007). Given that MAXENT results consistently over predicted suitability in alpine grassland environments well above tree line, discussion and interpretation of ENM results are strictly based on GARP analyses herein.

RESULTS

Sequence attributes

The concatenated 3-gene sequence alignment contained 1676 base pairs [ND2 (834 bp), ATP6 (684 bp) and ATP8 (168 bp)] for 127 ingroup samples and 6 outgroup taxa, resulting in 348 variable sites among *C. robusta* samples, of which 262 (15.6%) were parsimony informative. An absence of stop codons in open reading frames coupled with base frequencies characteristic of avian mtDNA and expected patterns of codon-specific nucleotide evolution confirmed sequences were of mitochondrial origin rather than nuclear copies. Strong extractions from ancient DNA samples combined with clade-specific primers produced clean PCR's that resulted in high-

Table 2.1. Sequence attributes and parameter estimates for ND2, ATP6-8, and codon partitions used in this study.

	ND2	ATP6-8	mtDNA 1st	mtDNA 2nd	mtDNA 3rd
Length	834	842	558	558	558
Variable sites	167 (20.0%)	181 (21.5%)	68 (12.2%)	30 (5.37%)	257 (46.0%)
Informative sites	131 (15.7%)	131 (15.5%)	47 (8.42%)	16 (2.86%)	201 (36.0%)
BIC model	TIM2+I+Γ	TrN+Γ	HKY+Γ	TrN+I	HKY+Γ
BIC model weight	0.8198	0.7478	0.8108	0.7056	0.4184
Frequency A	0.3096	0.3023	0.3127	0.1618	0.4185
Frequency C	0.3696	0.3844	0.3321	0.3353	0.3720
Frequency G	0.1162	0.1000	0.1734	0.0954	0.0922
Frequency T	0.2046	0.2133	0.1818	0.4075	0.1174
TS/TV	NA	NA	7.3646	NA	21.1764

quality chromatograms with no evidence of degradation from deamination phenomena (Hofreiter et al., 2001; Sefc et al., 2006). Lastly, overlapping gene fragments exhibited no discrepancies among amplicons and patterns of sequence variation were consistent with expected codon substitution rates across sites sampled by fresh and ancient DNA tissues.

Phylogenetic relationships and divergence times

Bayes factors strongly favored partitioning the combined sequence alignment by codon position as opposed to less complex partitioning strategies (i.e. by gene or treating the sequence alignment as a single partition); thus, BIC selected substitution models were applied to each codon partition for the 3-gene concatenated sequence alignment. BIC values determined in JMODELTEST v. 0.1.1 (Posada, 2008) indicated the HKY+Γ model was most appropriate for 1st and 3rd position partitions whereas the TrN+ I model was selected for 2nd position codons. Although BIC model weights were below 95% confidence intervals for each partition, the uncertainty in model selection was limited to variants of the same model class (Table 2.1). Both

Figure 2.2. Bayesian inference topology of 127 *C. robusta* samples based on analysis of 1676 bp of mitochondrial sequence data. Nodes with significant posterior probability support (≥ 0.95) are indicated by blacked circles. Color coded terminals correspond to populations depicted in Figure 2.3. Relationships among *Crateroscelis* congenerics and outgroup taxa are indicated in the inset.

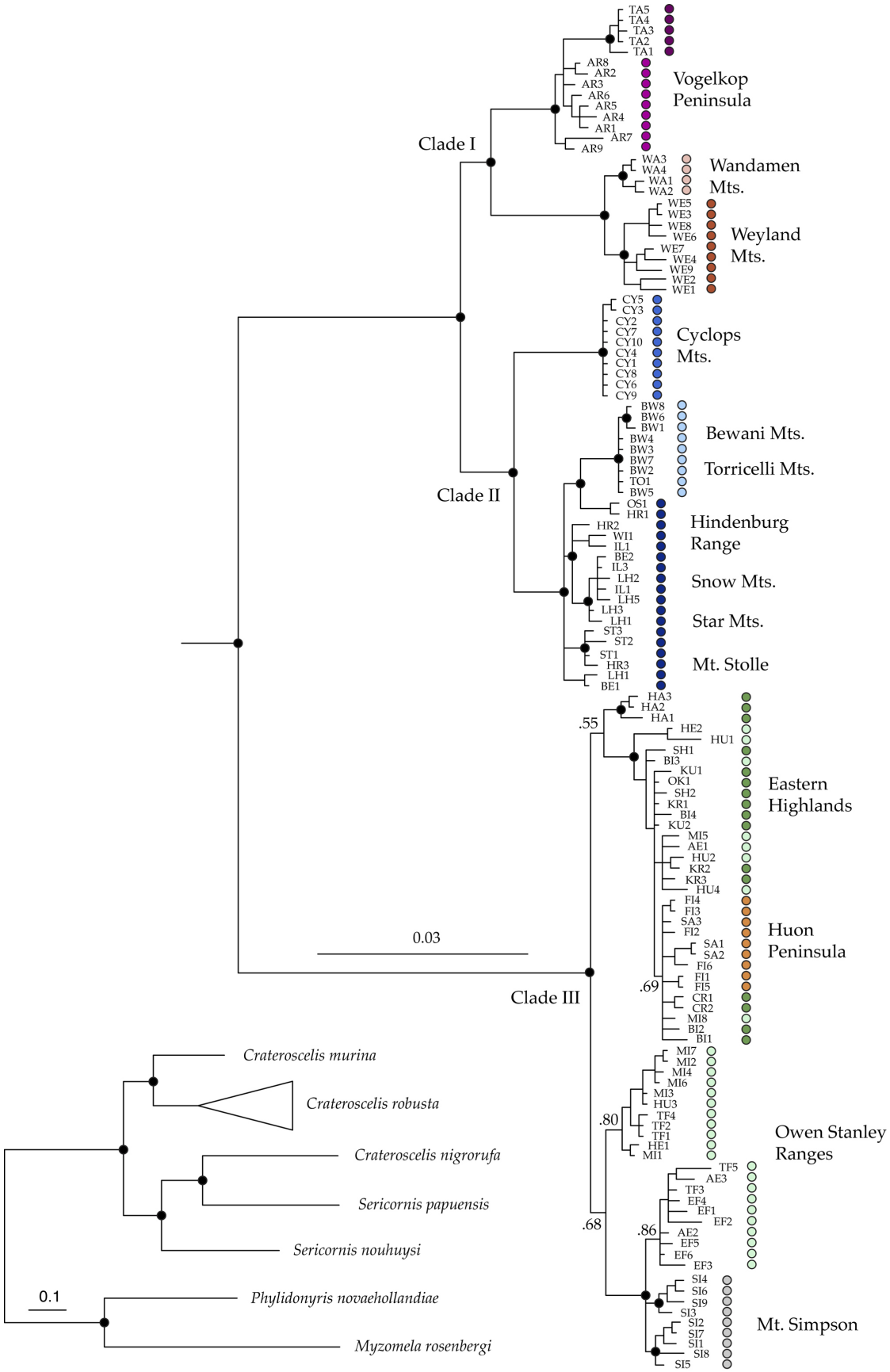
Clade I
Clade II
Clade III
Vogelkop Peninsula
Wandamen Mts.
Weyland Mts.
Cyclops Mts.
Bewani Mts.
Torricelli Mts.
Hindenburg Range
Snow Mts.
Star Mts.
Mt. Stolle
Eastern Highlands
Huon Peninsula
Owen Stanley Ranges
Mt. Simpson
0.03
0.1
.55
.69
.80
.68
.86
Crateroscelis murina
Crateroscelis robusta
Crateroscelis nigrorufa
Sericornis papuensis
Sericornis nouhuysi
Phylidonyris novaehollandiae
Myzomela rosenbergi

Table 2.2. Summary of genetic diversity among twelve populations of *Crateroscelis robusta* based on 500 bp of the ND2 sequence alignment.

Population	*n*	Unique Haplotypes	Segregating Sites	Θ (site)	*k*	Haplotype Diversity	Nucleotide Diversity (π)	π stdev
Tamrau Mountains	5	2	1	0.00096	0.4000	0.40000	0.00080	0.0004
Arfak Mountains	9	3	4	0.00294	1.2222	0.66667	0.00244	0.0009
Wandamen Range	4	1	0	NA	NA	NA	NA	NA
Weyland Range	9	4	6	0.00442	1.3333	0.58333	0.00267	0.0011
Western CDRs	18	9	11	0.00640	1.7124	0.80392	0.00342	0.0007
Cyclops Range	10	2	1	0.00071	0.3555	0.35556	0.00071	0.0003
Torricelli Range	9	2	1	0.00074	0.2222	0.22222	0.00044	0.0003
Eastern Highlands	17	12	13	0.00769	2.1176	0.94118	0.00424	0.0006
Huon Peninsula	9	4	3	0.00221	1.0000	0.77778	0.00200	0.0004
Owen Stanley Ranges	28	14	15	0.00771	2.0343	0.88360	0.00407	0.0005
Mt. Simpson	9	4	3	0.00222	0.9444	0.75000	0.00189	0.0004
Crateroscelis robusta	127	53	89	0.03286	24.670	0.96863	0.04934	0.0009

BI and ML phylogenetic analyses converged on near-identical topologies with no significant differences in node support; therefore, the BI results are presented herein for simplicity.

Paraphyly was recovered within *Crateroscelis* as inferred by an unexpected sister relationship between *C. nigrorufa* and *S. papuensis*, which combined with *S. nouhuysi* form a mid-montane clade that is sister to a *C. robusta* + *C. murina* lineage (Fig. 2.2). Although these relationships received significant posterior probability support, the morphological and behavioral similarity between *C. nigrorufa* and it congenerics suggest that this mtDNA-based topology may not reflect the true speciation history within *Crateroscelis*. Additional nuclear loci will be required to clarify the phylogenetic relationships between New Guinea's mouse-warblers, the monotypic *Origama solitaria* of Australia, and the closely related Australo-Papuan *Sericornis* scrub-wrens. The potential for paraphyly among these taxa introduces some uncertainty in establishing ancestral character states for analysis of plumage evolution in *Crateroscelis*; however, such species-level relationships have little bearing on phylogeographic analyses within *C. robusta*, and are beyond the focus of this study.

Significant posterior probability support confirmed the monophyly of *C. robusta*, which is comprised of two highly divergent phylogroups geographically isolated by the Strickland River Valley and headwater drainages (Fig. 2.1). Coalescent estimates of divergence times indicate that these lineages arose in the Pliocene from 1,933,000–4,830,000 ybp (using mutation scalars of 2–5% per million years; 95% HPD 836,000–2,478,000 to 2,090,000–6,195,000 ybp), with average ND2 sequence divergences ranging from 7.95–8.97% among phylogroups (Appendix 2.3). Two secondary clades were recovered west of the Strickland River Valley, including a Vogelkop + Wandamen/Weyland clade (I) that is sister to a CDRs/Bewani + Cyclops clade (II), each of which are reciprocally monophyletic and supported by significant posterior probabilities. Coalescent analyses in IMa2 suggest these lineages diverged in the early-to-mid Pleistocene from 695,00–1,738,000 ybp (95% HPD 352,000–954,000 to 880,000–2,385,000 ybp), with average sequence variation ranging from 2.24–4.60% among clades. Two distinct lineages were recovered within nominate *C. r. robusta* (Clade III), including a weakly resolved Eastern Highlands + Huon Peninsula lineage that is sister to a Papuan Peninsula lineage ranging from Mt. Missim (Watut–Tauri drainages) southeast to Mt Simpson. Coalescent estimates of divergence times indicate these lineages split in the Pleistocene 103,000–510,000 ybp (95% HPD 14,000–226,000 to 180,000–1,001,000 ybp), with average sequence divergences of 0.32–0.54%.

Population structure, demography, and gene flow

Given the high sequence divergence recovered among eastern and western phylogroups, haplotype networks were analyzed separately for each phylogroup, with analyses limited to ND2 sequences (500 bp) for consistency with demographic analyses conducted in DnaSP. The median-joining network recovered 53 unique haplotypes among 127 *C. robusta* samples, of

Figure 2.3. Minimum spanning network of ND2 haplotype relationships among 10 populations of *C. robusta*. The number of individuals sharing a given haplotype are indicated within each ellipse, while values along network branches denote the number of mutational steps between haplotypes. Populations are color-coded and linked with collection localities depicted on the ecological niche model projection (dark grey shading) of *C. robusta* inferred under contemporary climatic conditions.

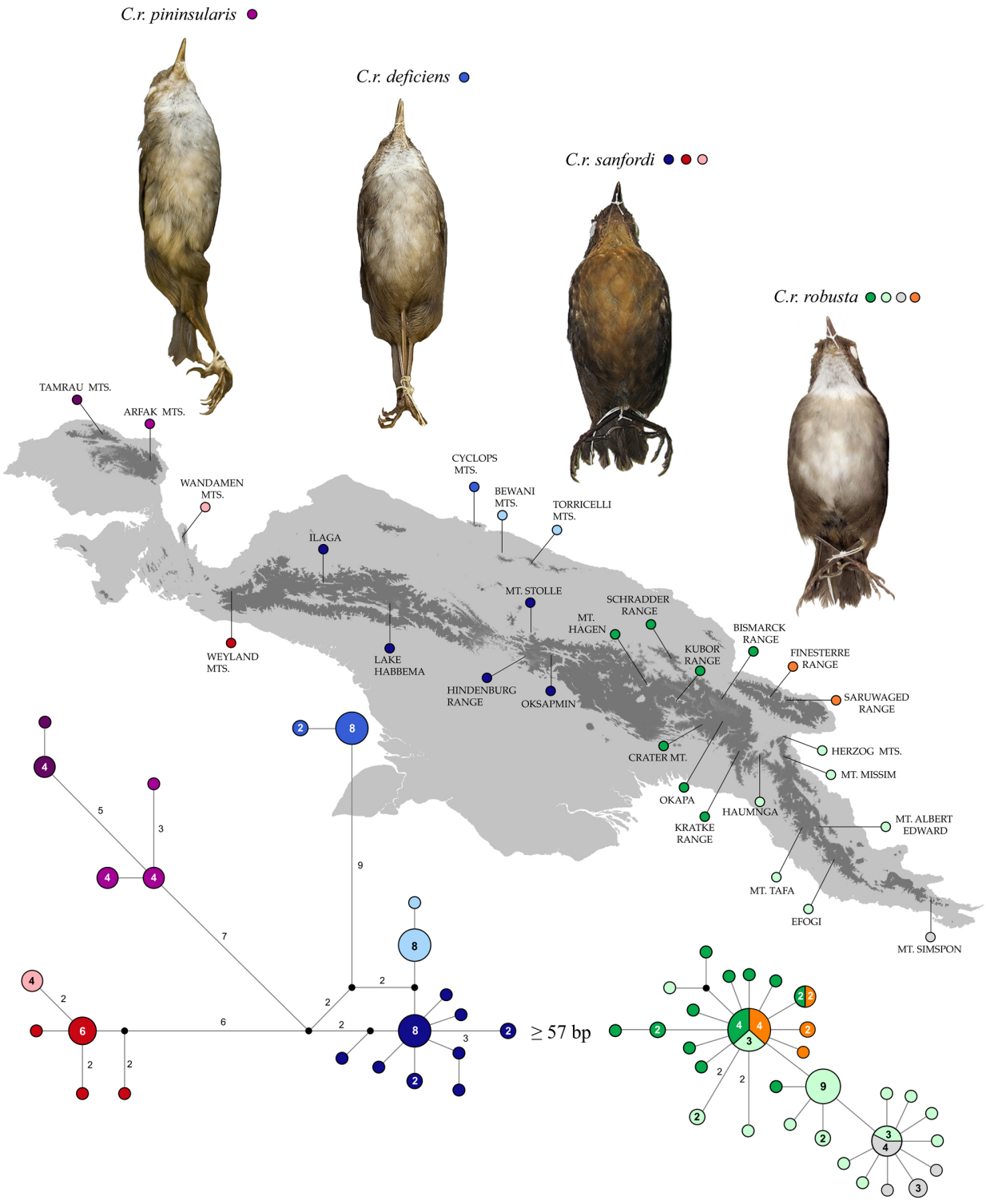
C.r. pininsularis
C.r. deficiens
C.r. sanfordi
C.r. robusta
TAMRAU MTS.
ARFAK MTS.
WANDAMEN MTS.
CYCLOPS MTS.
BEWANI MTS.
TORRICELLI MTS.
ILAGA
WEYLAND MTS.
LAKE HABBEMA
MT. STOLLE
MT. HAGEN
SCHRADDER RANGE
BISMARCK RANGE
KUBOR RANGE
FINESTERRE RANGE
SARUWAGED RANGE
HINDENBURG RANGE
OKSAPMIN
CRATER MT.
HERZOG MTS.
MT. MISSIM
OKAPA
HAUMNGA
KRATKE RANGE
MT. ALBERT EDWARD
MT. TAFA
EFOGI
MT. SIMSPON
≥ 57 bp

Figure 2.4. Mismatch distributions depicting observed frequencies of pairwise nucleotide differences within 11 populations of *C. robusta* (gray bar graph). The distribution of expected frequencies under a model of demographic expansion are indicated by the black line graph.

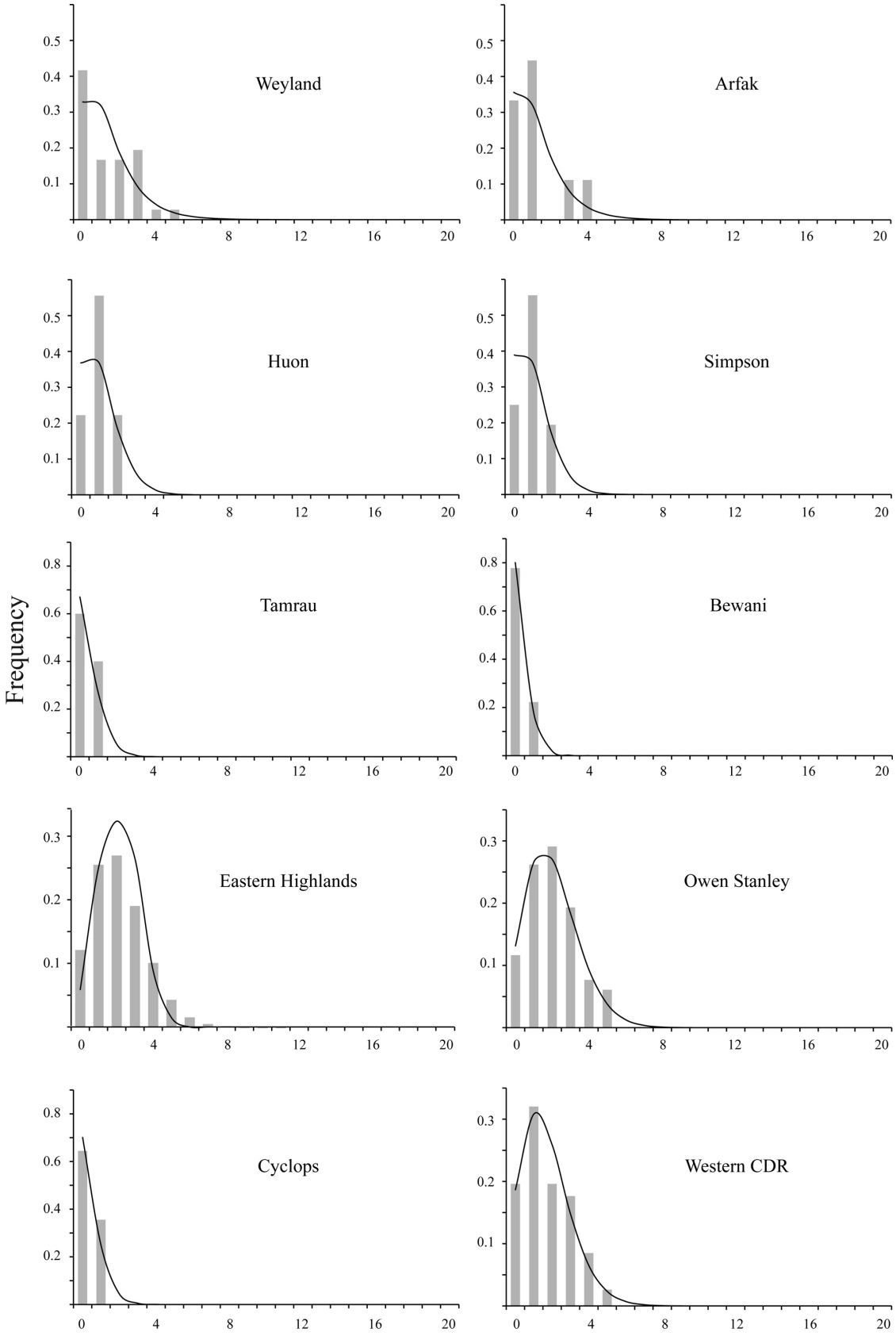
Weyland
Arfak
Huon
Simpson
Tamrau
Bewani
Eastern Highlands
Owen Stanley
Cyclops
Western CDR
Frequency
Pairwise differences

Table 2.3. Demographic summary statistics derived from the haplotype distribution, frequency spectrum of mutation, and distribution of pairwise sequence differences. All analyses were conducted on the full ND2 data set and statistically significant results (p-value ≤ 0.05) are indicated in bold.

Population	*n*	Tajima's *D*	Fu & Li 's *D*	Ramos-Onsin & Rozas R_2	FU's *Fs*	Raggedness Index (*r*)
Tamrau Mountains	5	-0.5089	-0.97256	0.4000	1.040	0.6800
Arfak Mountains	9	-0.76457	-0.80052	0.1635	-0.877	0.0741
Wandamen Mountains	4	-0.61237	-0.61237	0.4330	0.172	0.2500
Weyland Mountains	9	-1.15164	-1.45487	**0.1072**	**-4.279**	0.0563
Western CDRs	18	-1.19159	-0.88447	**0.0818**	**-6.571**	0.0295
Cyclops Mountains	10	0.01499	0.80424	0.1778	0.417	0.2099
Bewani Mountains	9	-0.06382	0.22104	0.2008	-0.239	0.0802
Eastern Highlands	17	-1.1497	-0.93610	**0.0863**	**-4.070**	0.0313
Huon Peninsula	9	-1.14917	-0.04974	0.1525	-1.776	0.0980
Owen Stanley Ranges	28	-0.83212	-1.31268	**0.0853**	**-7.618**	0.0160
Mt. Simpson	9	-0.50521	-0.61519	**0.1254**	**-3.427**	0.2014

which 33 were private haplotypes and 7 were shared by 5 or more individuals (Fig. 2.3). These results are highly consistent with the BI analysis, identifying three closely related haplotype clusters within nominate *C. robusta*, each separated by a single mutation whereas more substantial divergences were evident within the western phylogroup, with six haplotype groups recovered among the CDRs and outlying sky-island populations. Samples from the Arfak (*C. r. peninsularis*) and Tamrau Mountains (*C. r. ripleyi*) were linked to western CDRs haplotypes (*C. r. sanfordi*) by a minimum of 10 and 15 mutational steps respectively, with *C. r. sanfordi* samples from the Weyland and Wandamen Mountains comprising a distinct haplotype cluster separated from western CDRs populations by 10 or more substitutions. Specimens from the Bewani and Torricelli ranges (*C. r. bastille*) were linked to western CDRs haplotypes by just two mutational steps despite the substantial geographic and environmental isolation of these ranges, whereas samples from the Cyclops Mountains were separated from CDRs and Bewani haplotypes by a minimum of 12 substitutions. The "star" haplotype patterns observed in the Eastern Highlands, Papuan Peninsula, and western CDRs are indicative of recent demographic

expansion and corroborate results from mismatch distributions and population genetic summary statistics (Fig. 2.4, Table 2.3).

Analysis of pairwise F_{st} values recovered evidence of strong population genetic structure within the CDRs and outlying coastal sky-islands, identifying 11 distinct populations among the 28 sampling localities (Table 2.2). Estimates of haplotype diversity (h), mean pairwise nucleotide differences (k), and nucleotide diversity (π) were highest among populations in the central highlands including the Western CDRs (h = 0.804, k = 1.712, π = 0.00342), Eastern Highlands (h = 0.941, k = 2.117, π = 0.00424), and Owen Stanley ranges (h = 0.883, k = 2.034, π = 0.00407); however, indices of genetic variation within the latter two sites may be elevated due to low-level migration among populations. Coastal sky-island populations of the Tamrau (h = 0.400, k = 0.400, π = 0.0008), Cyclops (h = 0.355, k = 0.355, π = 0.0007), Torricelli (h = 0.222, k = 0.222, π = 0.0004), and Wandamen ranges (h = 0, k = 0, π = 0) exhibited the lowest levels of genetic variation, which is consistent with their smaller size, geographic isolation, and absence of apparent gene flow.

Hierarchical three-way analyses of molecular variance revealed that the distribution of genetic diversity within *C. robusta* is best explained by current taxonomy (Fig. 2.5), with 80% of the genetic variation partitioned by subspecies, 13% among populations, and 7% within populations (Φ_{ct} = 0.79, P<0.001; Φ_{st} = 0.92, P<0.001; Φ_{sc} = 0.64, P<0.001). By comparison, sequences partitioned by contemporary sky-islands accounted for 55% of the genetic variation among geographic groups, 37% among populations, and 8% within populations (Φ_{ct} = 0.54, P= 0.19; Φ_{st} = 0.91, P<0.001; Φ_{sc} = 0.81, P<0.001), whereas the distribution of Pleistocene sky-islands explained just 16% among groups, 76% among populations, and 8% within populations (Φ_{ct} = 0.15, P = 0.17; Φ_{st} = 0.91, P<0.001; Φ_{sc} = 0.90, P<0.001). A Mantel test conducted on the

full data set recovered a positive correlation (r= .41, P=0.001) between genetic and geographic distances among population indicating that isolation-by-distance effects contributed to the distribution of genetic diversity within *C. robusta*. Mantel tests on regional phylogroups recovered a significant positive correlation among eastern populations (r=0.68, P=0.001) whereas results among western populations were non-significant, reflecting the substantial genetic divergences among adjacent sky-island populations along the north coast and Bird's Neck region (Fig. 2.6).

Analyses of mismatch distributions and population genetic summary statistics indicate a complex demographic history within *C. robusta*, including wide spread geographic expansion throughout the central highlands and potential population bottlenecks among coastal sky-islands. Ramos-Onsin & Rozas R_2 and Fu's F_s statistics rejected the null hypothesis of population stability, revealing significant support ($P \leq 0.05$) for demographic expansion in the Weyland Mountains, Western CDRs, Eastern Highlands, Owen Stanley Ranges, and Mt. Simpson (Table 2.3). Tajima's D and Fu & Li's D statistics were also negative for these populations indicating potential expansion, yet these results were non-significant, reflecting the greater sensitivity of the R_2 and F_s statistics. Mismatch distributions from the Western CDRs, Eastern Highlands, Huon Peninsula, Owen Stanley Ranges, and Mt. Simpson closely resembled simulated distributions of demographic expansion (Fig. 2.4), whereas sequences from the Tamrau, Arfak, Weyland, Cyclops, and Bewani/Torricelli Ranges exhibited peak frequencies of 0 to 1 pairwise differences, suggesting a history of demographic contraction (Marjoram & Donnelly, 1994; Bertorelle & Slatkin, 1995). These results are consistent with higher R_2 and F_s values observed among the smaller coastal sky-island populations, although neither statistic recovered significant

evidence of contraction. Strong signatures of demographic expansion within the Eastern Highlands, Huon Peninsula, and Owen Stanley ranges may be the consequence of admixture between populations, as coalescent estimates of the migration parameter (*m*) in IMa2 revealed evidence of low-level gene flow from the Owen Stanley Ranges to the Eastern Highlands, with a non-zero posterior probability peak of 4.52 females per generation (95% HPD 0.1968–20.3). Estimates of migration in the opposite direction were extremely low at 0.028 females per generation (95% HPD 0.0–8.79). Coalescent estimates of gene flow between the Huon and Central Highlands populations consistently produced unreliable results, and not presented given the limitations associated with small sample sizes the single locus data set.

Evolution of plumage traits

Results of the reduced taxon sampling BI analysis were congruent with phylogenetic relationships recovered among primary geographic lineages in the full BI topology, yielding significant posterior probability support for all but two nodes (Fig. 2.7). Parsimony-based ancestral character state reconstructions of throat and abdominal coloration confirmed that phenotypic similarities between *C. r. robusta* and sky-island populations from the Cyclops (*C. r. deficiens*), Arfak (*C. r. peninsularis*), and Tamrau Mountains (*C. r. ripleyi*) are not due to close phylogenetic affinity (i.e. long-distance dispersal or vicariance), but rather retention of ancestral character states among terminal populations (Fig. 2.7). Two independent evolutionary origins of brown throat and abdominal coloration were recovered in the parsimony analysis (CI = 0.5; RI = 0.66), indicating either random genetic drift processes or differential selective pressures between terminal and intervening populations (*C. r. sanfordi*) are responsible for the leapfrog distribution of phenotypic variation in the Mountain Mouse-warbler complex.

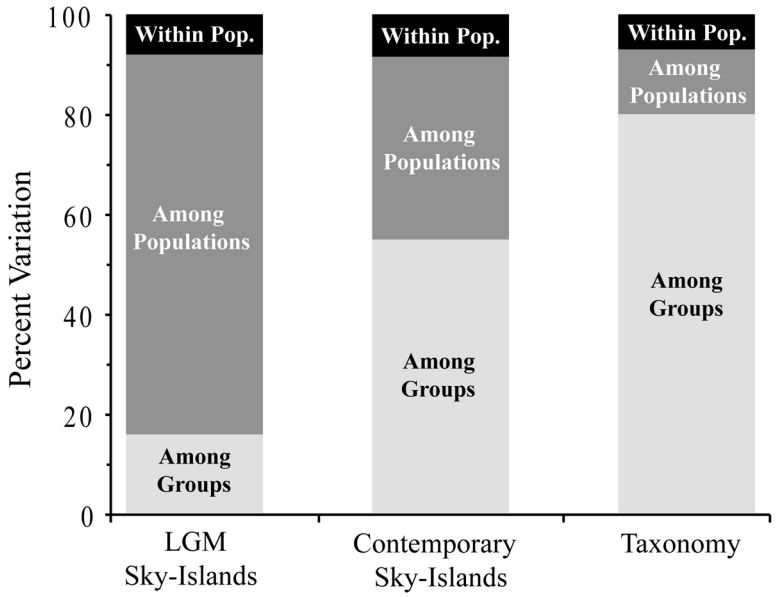

Figure 2.5. Results of hierarchical three-way analyses of molecular variance in which genetic diversity was partitioned by Last Glacial Maximum sky-islands, contemporary sky-islands, and taxonomy (i.e. by the 6 morphologically defined subspecies identified in Fig. 2.1). Each analysis was statistically significant at the $P < 0.001$ level.

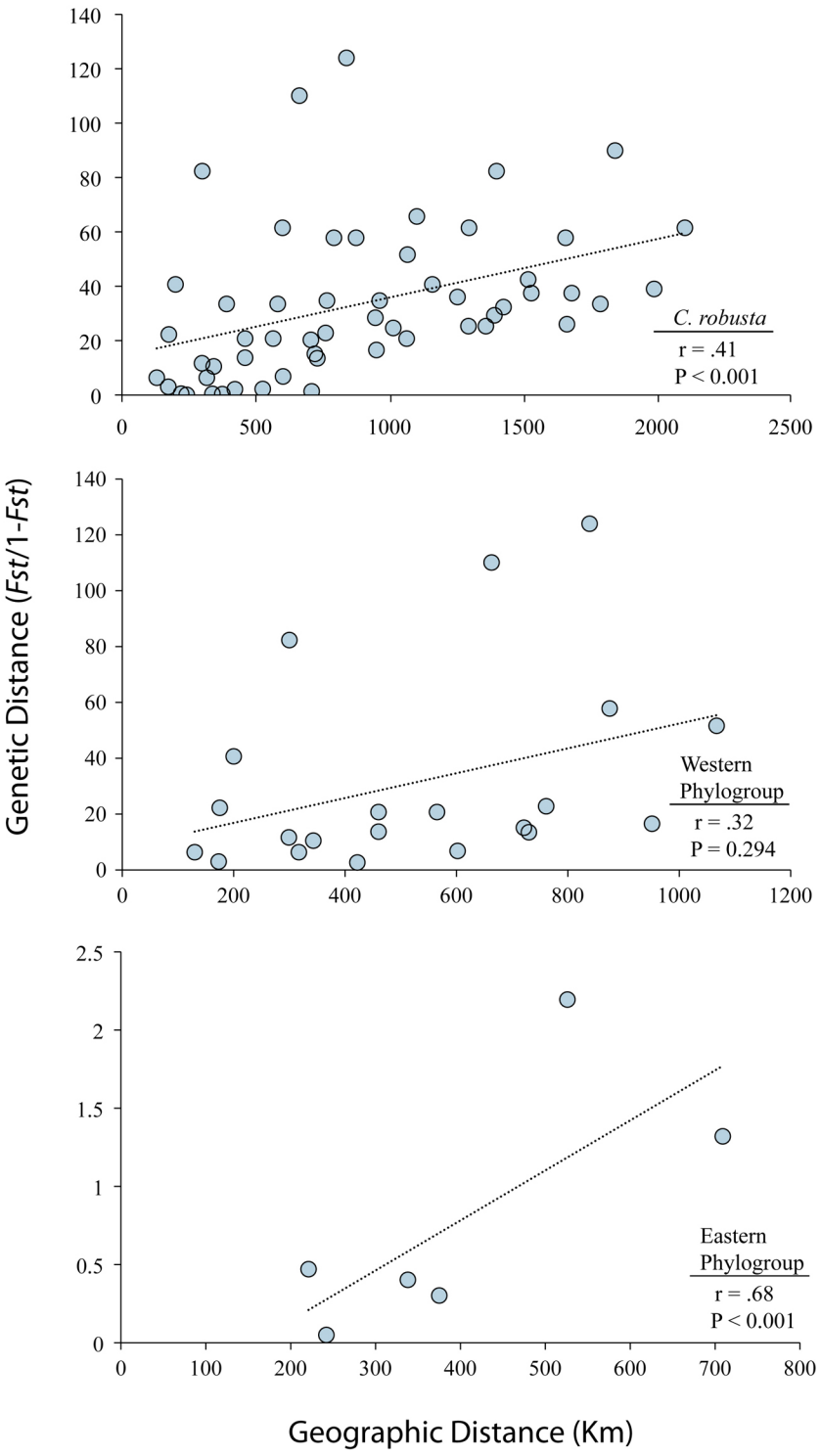

Figure 2.6. Results of Mantel tests conducted within regional phylogroups and the full data set. Positive correlations and moderate to high *r* values suggest an isolation-by-distance effect within the species complex as a whole, and the eastern phylogroup, whereas deep genetic divergences among adjacent sky-island populations in the western phylogroup suggest that other factors are involved.

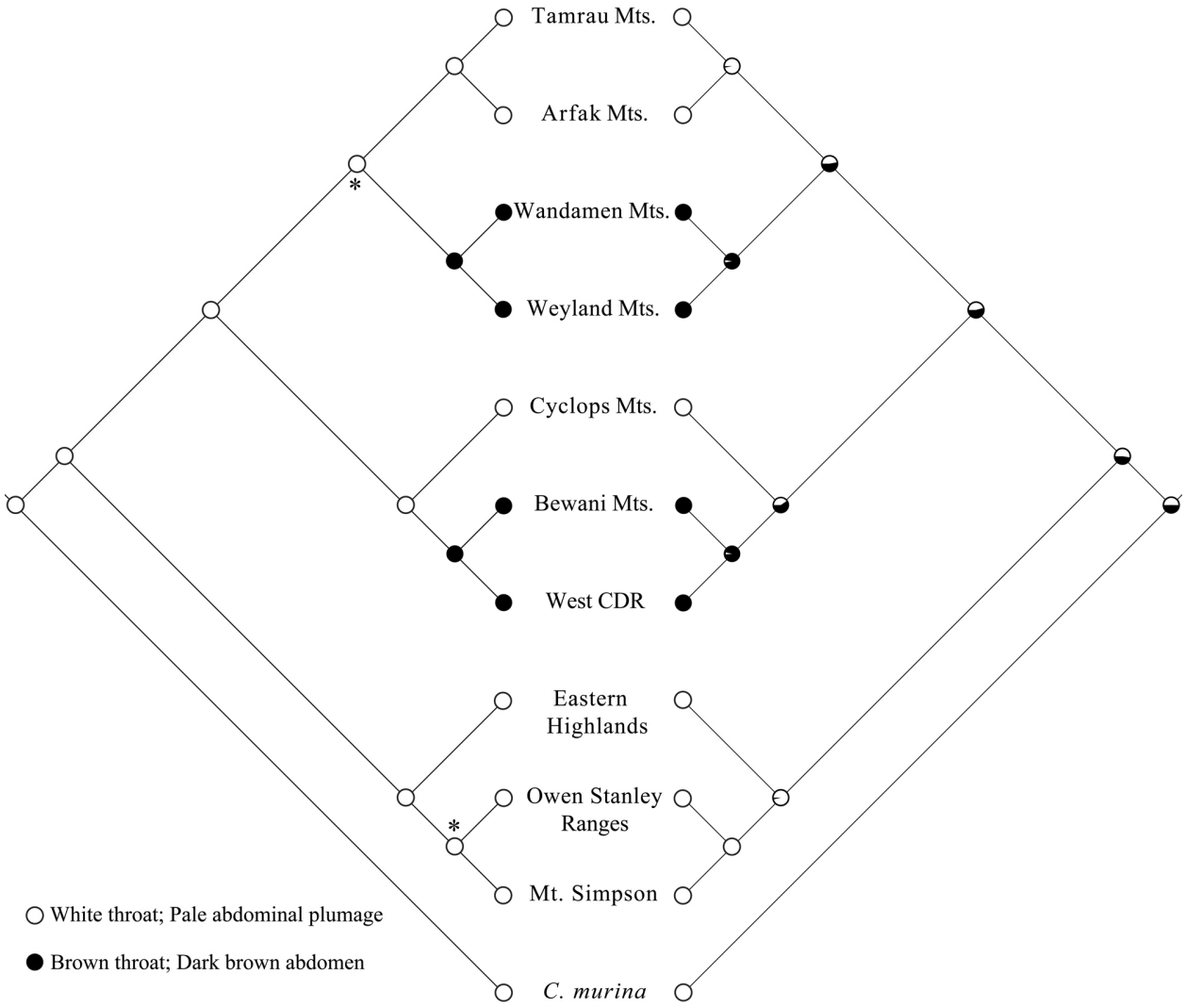

Figure 2.7. Bayesian inference topology depicting relationships among primary geographic lineage in *C. robusta*, with *C. murina* designated as the outgroup to polarize character states. Parsimony-based ancestral reconstructions are given on the left and likelihood analyses on the right, with area of circle shading indicating the proportional likelihood of alternative character states in the latter analysis. Nodes that received non-significant posterior probability values (<0.95) are indicated by an asterisk.

Likelihood-based reconstructions were less conclusive, as most ancestral nodes received proportional likelihoods of 0.5 or higher for each character, leaving open the possibility that melanic ventral coloration may have evolved once in the western phylogroup ancestor, with two subsequent gains of white throat coloration and pale abdominal plumage in the Cyclops and Vogelkop lineages.

Considering the shallow genetic divergences between *C. r. sanfordi* specimens from the western CDRs and *C. r. bastille* of the Bewani and Torricelli ranges, the phenotypic similarity among these populations is likely attributed to recent long-distance dispersal from the northern slopes of the Star Mountains or Mt. Stolle region, and subsequent population expansion throughout the Bewani, Torricelli, and Prince Alexander ranges. Assessments of phylogenetic signal in throat and abdominal coloration using Picante in R revealed both traits are moderately conserved as inferred by *K* statistics for the full ($K = 6.65$) and reduced taxon sampling ($K = 1.24$) BI topologies; although the addition of Foya Mountain and Bomberai Peninsula samples may have significant impacts on these estimates.

Ecological niche modeling

GARP-based ecological niche distributions generated under contemporary climatic conditions predict high suitability throughout New Guinea's montane rainforest environments, and are consistent with the known distribution of *C. robusta*, to the exclusion of predictivity in the Adelbert Mountains (Fig. 2.8). Several prominent breaks in environmental suitability were observed across the Central Highlands corresponding with the Strickland River Valley, Watut/Tauri River valleys, and Adau River drainage, with the latter barrier separating the Keveri Hills from the Dayman terrane to the east. The Ramu–Markham River Valley comprises an

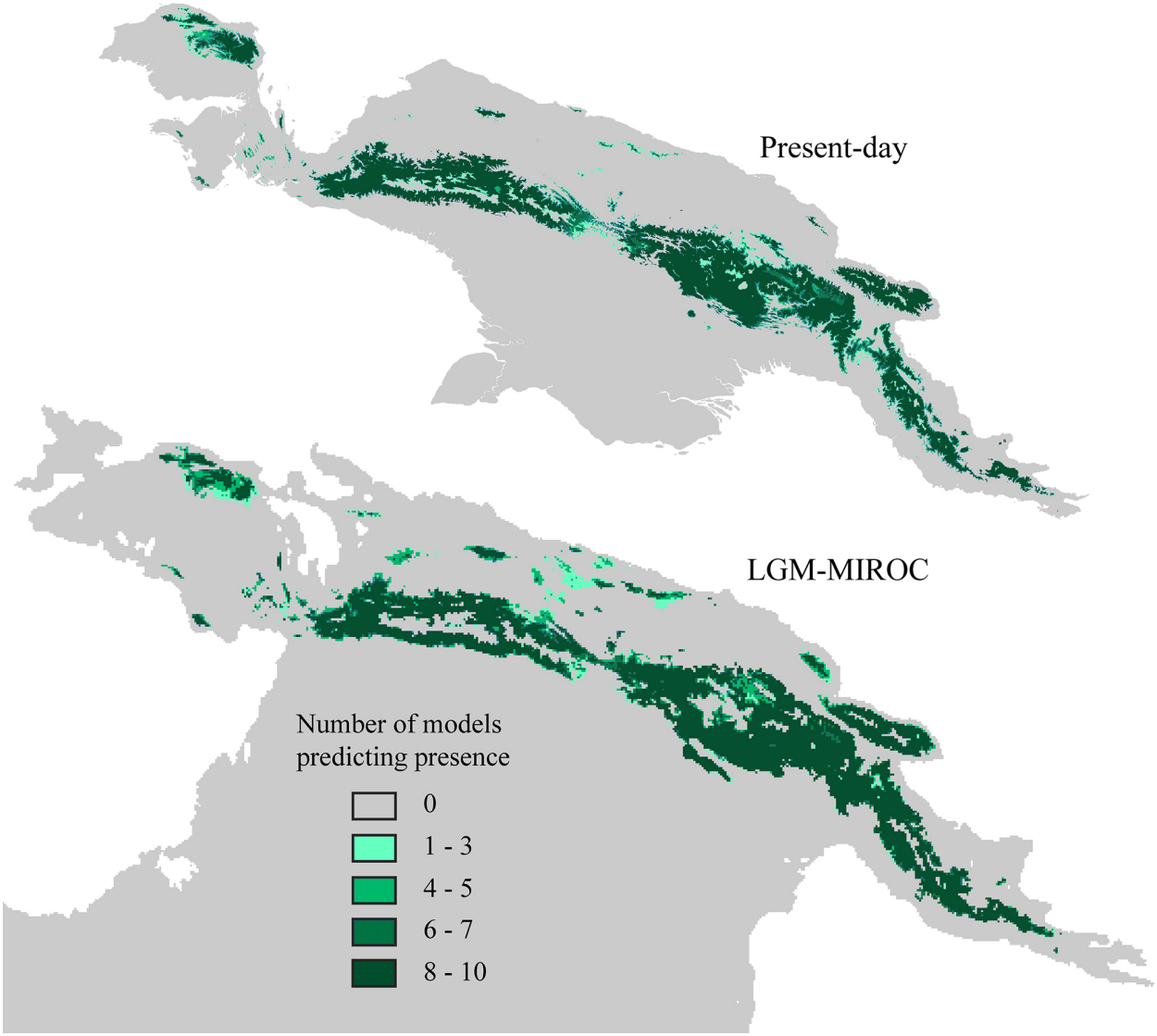

Figure 2.8. Ecological niche modeling projections depicting the potential distribution of *C. robusta* under contemporary and Last Glacial Maximum climatic conditions. The LGM ecological niche projection is based on the MIROC (Model for Interdisciplinary Research on Climate) general circulation model.

extensive break in the projected ecological niche distribution of nominate *C. robusta*, isolating Huon Peninsula populations from the Eastern Highlands and Owen Stanley Ranges. North coast sky-island populations are separated from the CDRs by the Sepik and Idenburg River drainages that form large tracts of unsuitable environmental conditions. Vogelkop and Bomberai Peninsula populations are isolated from the Weyland Mountains by low suitability values corresponding with foothill and lowland rainforest across the "Bird's Neck" region.

Strong evidence of elevational compression in the species' potential distribution was recovered from LGM paleoecological niche reconstructions derived from the MIROC and CCSM general circulation models. As the latter model produced several distributional anomalies inferred by low suitability scores across regions of the CDRs (Appendix 2.5), I present the MIROC results herein (Fig. 2.8). Elevational shifts in ecological suitability resulted in enhanced population connectivity within the CDRs and Papuan Peninsula, including fully contiguous habitat corridors across the Strickland, Watut/Tauri, and Adau River drainages. With exception of the Vogelkop, each population exhibited substantial geographic expansion under a LGM climatic scenario; particularly in range-restricted north coast populations.

DISCUSSION

This investigation provides the first detailed picture of phylogenetic relationships within the Mountain Mouse-Warbler complex, revealing high levels of genetic diversity and strong geographic structure across New Guinea's highland landscape. Previous taxonomic arrangements recognized 6 subspecies within *C. robusta* based on subtle size differences and marked variation in plumage coloration; however, BI analyses of ND2 and ATP6–8 sequence data (Fig. 2.2, 2.7) indicate that reliance upon these phenotypic traits has confounded several

aspects of phylogeographic history among geographic forms. These results are discussed in context of New Guinea's geological history and paleoecology to examine how environmental factors have shaped population genetic structure and demographic history within the *C. robusta* complex, shedding new light on the evolutionary origin of its leapfrog variation in plumage traits.

Species limits and population genetic structure

Median-joining networks and model-based phylogenetic analyses recovered two primary phylogroups within *C. robusta*, the distributions of which are consistent with a genetic break along the Strickland River Valley (Fig. 2.2, 2.3). Although additional sampling is required from the eastern banks of the Strickland Gorge and Ok Om headwater drainages to determine the precise location of this genetic break, an absence of contemporary gene flow or ancestral polymorphism across the region confirms these lineages are maintaining independent evolutionary trajectories despite recurrent periods of extensive environmental connectivity in the Pleistocene (Fig. 2.8). Moreover, the deep genetic divergences (7.95–8.97%) revealed among these lineages are characteristic of levels typically seen between species and some avian genera (Herbert et al., 2004; Moyle et al., 2009; Gardner, 2010), indicating that post speciation isolating mechanisms are likely in place. Consequently, I advocate elevating the western phylogroup to species status. Given that *Crateroscelis sanfordi* has priority over other conspecific taxa (Hartert, 1930), I suggest Sanford's Mouse-Warbler as an appropriate English name. The general ecology and behavior of these taxa remain little known across much of their distribution and merit closer examination to establish whether subtle variation in vocalizations or other life history attributes may have played a role in shaping the evolution of this species complex.

Based on coalescent estimates of divergence times, these genealogical lineages arose during the late Pliocene ~1.9–4.8 Mya, which broadly corresponds with the primary orogenic uplift of New Guinea's CDRs (Pigram & Davies, 1987; Hall, 2002). Nonetheless, the impact of these tectonic events on montane avian diversification across the region remain unclear, as considerable uncertainty surrounds the local orogenic history and rate of uplift among the constituent terranes (e.g. Dimaie, Landslip, Sepik, and Australian Craton) that comprise this composite geological landscape (Dow, 1977; Audley-Charles, 1991; Pigram & Davies, 1987). Furthermore, the wide range of genetic divergences observed across the Strickland River Valley (BWB unpub. data) suggest that this biogeographic boundary may be acting as a secondary contact zone rather than a primary source of vicariant diversification (Irestedt, et al., 2009). Additional comparative data sets, coupled with multi-locus coalescent analyses and a refined understanding of the region's orogenic history, will be essential to advancing understanding of how this extensive ecological barrier has governed avian diversification within New Guinea's Central Highlands.

Broad geographic sampling among outlying sky-island populations revealed substantial genetic divergences (2.2–4.6%) within *C. sanfordi*, which is composed of two reciprocally monophyletic clades (I, II)—a Vogelkop + Bird's Neck lineage in the west that is sister to a CDRs/Bewani + Cyclops lineage to the east (Fig. 2.2). Patterns of population genetic structure within these clades are largely consistent with the distribution of contemporary and LGM sky-island networks inferred from ecological niche reconstructions (Fig. 2.3, 2.8), yet several exceptions to this trend merit discussion. Despite their close geographic proximity, Arfak (*C. s. peninsularis*) and Tamrau Mountain (*C. s. ripleyi*) populations have likely remained isolated under LGM climatic conditions, and show no evidence of gene flow across the narrow Sorong

Fault zone. The presence of moderate genetic divergences (~1.2%) between these lineages suggest that they have persisted through multiple climate cycles during the latter half of the Pleistocene, which likely reflects the limited dispersal capacity that is characteristic of this species complex as a whole. Alternatively, the Sorong Fault zone may have represented a more substantial environmental barrier to dispersal throughout much of the Pleistocene given the recent accretion history of the Tamrau terrane, which began to dock with the Vogelkop Peninsula in the late Pliocene approximately 2 to 3 Mya (Pigram & Davies, 1987; Audley-Charles, 1991; Hall, 2002). Although *C. s. peninsularis* and *C. s. ripleyi* exhibit few diagnostic morphological traits based on the limited specimen material available at the time of this study, I defer taxonomic recommendations pending further sampling along the Sorong Fault and eastern limits of Tamrau Mountains, as no modern collecting expeditions have been conducted within the Vogelkop Peninsula.

Bayesian inference analyses recovered strong evidence of paraphyly within *C. s. sanfordi* as the taxon is presently defined (Gregory, 2007), revealing surprisingly deep genetic divergences between Weyland Mountain and Ilaga Valley samples. This phylogenetic arrangement is difficult to reconcile with present-day and LGM ecological niche reconstructions considering the broad corridor of suitable habitat predicted between these localities (Fig. 2.8), suggesting that geological factors may be responsible for this unexpected genetic break. Divergence time estimates indicate coalescence among clades I & II ~0.7–1.7 Mya, which is congruent with the hypothesis that montane rainforest habitats of the Weyland terrane only recently came into contact with the western limits of the CDRs, either through east lateral rifting along the Tarera Aiduna Fault or by uplift of the intervening Australian Miogeocline. Few landscapes within New Guinea approach the geological complexity of that exhibited by the

Bird's Neck region, which is comprised of four principal terranes juxtaposed (Weyland, Mangguar, Wandamen, and Lengguru) east to west along the Tarera Aiduna Fault (Dow, 1977; Pigram & Davies 1987). The accretion histories of these terranes remain poorly understood with respect to the timing of docking, extent of lateral rifting along the Australian Craton, and subsequent rate of uplift. In light of the deep genetic split and strong node support for reciprocal monophyly among clades I & II, I suggest restoring *C. s. steini* to recognize the distinct genealogical lineages present in the Weyland and Wandamen Mountains, thereby restricting *C. s. sanfordi* to populations of the western CDRs east to the Strickland River Valley. The lack of significant genetic structure among *C. s. sanfordi* samples from the Nassau, Snow, Star, Hindenburg, and Victor Emmanuel ranges is consistent with wide-spread environmental connectivity predicted by ecological niche models throughout the western CDRs; however, further sampling is needed among each of these regions to assess rates of gene flow and potential low-level genetic structure between north and south slope populations.

Results of the median-joining network were ambiguous with respect to the phylogeographic relationships between *C. s. deficiens* (Cyclops Mts.), *C. s. bastille* (Bewani/Torricelli Ranges) and *C. s. sanfordi* (CDRs), whereas the BI topology recovered clear evidence that *C. s. deficiens* and *C. s. bastille* originated via two independent colonization events, most likely from the northern slopes of the CDRs (Fig. 2.2). A close sister relationship supported by shallow genetic divergences between *C. s. bastille* and *C. s. sanfordi* indicate a recent dispersal history from the Victor Emmanuel Ranges that may have been facilitated by patchy networks of montane rainforest across the Border and Nimboran Ranges during LGM climatic conditions. By contrast, deep genetic divergences between *C. s. deficiens* and *C. s. sanfordi* + *C. s. bastille* suggest that the former has persisted across multiple climate cycles

despite a highly limited distribution of suitable environmental conditions across the Cyclops Mountains during interglacial climates (Fig. 2.8). It remains unclear whether the Border and Nimboran Ranges support intermediate populations, as these ranges have yet to be thoroughly surveyed, which combined with a lack of genetic sampling from the Foya Mountains leaves a critical gap in understanding the phylogeographic relationships and colonization history among New Guinea's north coast sky-island populations.

A pattern of shallow genetic structure and low-level gene flow throughout the Eastern Highlands and Owen Stanley Ranges revealed a recent evolutionary history among *C. r. robusta* populations, which is congruent with the extensive environmental connectivity revealed across much of the eastern Central Highland by contemporary and LGM ecological niche reconstructions (Fig. 2.8). The distribution of haplotype diversity between the Eastern Highlands and Owen Stanley Ranges reflects a shallow genetic break along the Watut/Tauri River valleys, which together comprise a narrow ecological barrier during interglacial climates. However, the impact of this barrier on dispersal during interglacial climates appears to be limited, as coalescent analyses in IMa2 recovered a significant non-zero rate of gene flow (4.5 females per generation) from the Owen Stanley Ranges to the Eastern Highlands. Moreover, these regions are fully contiguous during cooler LGM climatic conditions, likely preventing the accumulation of strongly divergent lineages among these distinct biogeographic regions. A third haplotype cluster was recovered within the southeastern tip of the Papuan Peninsula (Fig. 2.3), supporting a pattern of reduced gene flow across the Keveri Hills and Adau River drainage during interglacial climatic conditions (Fig. 2.8); nonetheless, coalescent estimates of gene flow to test the influence of this putative ecological barrier were not feasible given the limited genetic sampling from these sites. The presence of shared haplotypes between Mt. Simpson and the Owen Stanley Ranges

suggest that the Adau River drainage may be acting more as a filter, limiting dispersal during interglacial periods, while forming as contiguous corridor for dispersal between these regions during LGM conditions. Finally, results of the median-joining network and BI analyses indicate a recent colonization history within the Huon Peninsula as evidenced by shared haplotypes between the Eastern Highlands, Owen Stanley Ranges, and Finisterre/Saruwaged Ranges of the Huon. This result was most unexpected, as the Ramu/Markham River valley forms a broad ecological barrier between these highland communities that is thought to have promoted the evolution of high endemicity within the Huon avifauna as well as other taxonomic groups.

Pleistocene climatic oscillations have clearly played an important role in governing distributions of genetic diversity within the *robusta–sanfordi* species complex; however, the deep genetic divergences among these taxa coupled with minor discord in patterns of ecological suitability and population genetic structure suggest that other environmental factors such as geographic distance and local orogenic history cannot be discounted in explaining the evolutionary history of these taxa. Hierarchical three-way analyses of molecular variance indicate that 80% of the genetic diversity within the complex is distributed among traditionally recognized subspecies, which closely correspond with the linear distribution of New Guinea's CDRs and contemporary sky-island networks. Moreover, Mantel tests revealed significant positive correlations between genetic and geographic distances in *C. robusta* and the species complex as a whole. These results are consistent with the hypothesis that both geological and climatic processes have contributed to the complex phylogeographic history revealed in this study, which has important implications for understanding regional patterns of biodiversity and guiding further phylogeographic investigation in the New Guinea highlands.

Demographic history and Pleistocene climate change

Based on projections of contemporary and paleoecological niche reconstructions, the *robusta–sanfordi* species complex underwent substantial elevational shifts during colder LGM climatic conditions, with populations descending by 1000 m or more at sites within the Central Highlands (Fig. 2.8). These results corroborate palynological spectra sampled across the CDRs, which indicate widespread depression of montane rainforest environments by as much as 1800 m during the height of the last ice age ~18,000-21,000 ybp (Hope, 1996). Coastal sky-island populations also experienced elevational shifts during LGM climates; however, the limited pollen data from these sites suggest that vegetational shifts were far more moderate, most likely due to regional climatic phenomena associated with oceanic currents and patterns of cloud formation.

Demographic analyses within the Central Highlands recovered clear signatures of population expansion in response to these elevational shifts in distribution, as evidenced by unimodal mismatch distributions that closely approximate simulated distributions of population growth in the Eastern Highlands, Owen Stanley Ranges, Huon Peninsula, Mt. Simpson and Western CDRs (Fig. 2.4). Ramos-Onsin & Rozas R_2 and Fu's F_s statistics also rejected the null hypothesis of stability in each of the above populations, with the exception of the Huon Peninsula, in which values were small and negative but non-significant (Table 2.3). By contrast, mismatch distributions recovered evidence of demographic bottlenecks in each of the coastal sky-island populations, which exhibited peak frequencies of 0 to 1 pairwise differences; a pattern consistent with that of demographic contraction rather than expansion (Marjoram & Donnelly, 1994; Bertorelle & Slatkin, 1995). Although R_2 and F_s values were higher from each of these sky-island populations, stability could not be rejected with statistical significance (Table 2.3).

This disparity in demographic response among the CDRs and coastal sky-island populations is on the one hand surprising considering coastal populations experienced the greatest relative expansion in distribution during LGM climatic conditions. However, these range-restricted sky-island lineages are undoubtedly more susceptible to rapid and dramatic reductions in genetic diversity (i.e. fixation) during interglacial climates due to their inherently small effective population size, whereas the much larger and geographically complex populations of the Central Highlands may be somewhat insulated to these effects in the short term and slower to respond. Montane rainforest habitats within the Wandamen, Cyclops, and Bewani/Torricelli ranges are restricted the highest peaks under present-day climatic conditions, with some lineages likely approaching their minimum viable population size. Consequently, if recent climate change projections across the New Guinea region are realized (1.4–5.8 ºC increase over current conditions by 2100) several of these sky-island taxa may well be pushed to extinction by the end of this century, and perhaps much sooner given the expanding influence of agricultural practices and general lack of natural resource management across much the island. The absence of *C. robusta* in the Adelbert Mountains may be evidence that montane extinctions are already underway among New Guinea's sky-island populations, as extensive surveys of this range by the author during 2007 confirmed that both *C. robusta* and *C. murina* are absent from the Adelbert's restricted lower-montane rainforest habitats—a curious gap in this species' distribution given *robusta–sanfordi* lineages have otherwise colonized the full extent of the New Guinea highlands.

Plumage evolution and leapfrog distributions

Leapfrog distributions of phenotypic variation occur across a wide variety of landscapes and geographic scales, yet this phenomenon appears to be most prevalent in linear, topographically

complex environments, as evidenced by the high frequency of leapfrog patterns within the Andean avifauna (Remsen, 1984; Graves, 1988). This investigation provides the first phylogenetic perspective on the evolutionary mechanisms underlying leapfrog variation in a montane-endemic New Guinea passerine. Ancestral character state reconstructions based on BI analyses disprove phylogenetic affinity and long-distance dispersal hypotheses (e.g. Diamond, 1972; 1973), indicating that patterns of phenotypic similarity between *C. robusta* populations in the east and *C. sanfordi* lineages of the Vogelkop and Cyclops ranges are attributable to parallel or convergent evolution, with two independent origins of brown throat and abdominal coloration among intervening populations (Fig, 2.2, 2.3, 2.7). Reliance upon linked mitochondrial markers in the present study precludes distinguishing among genetic drift and natural selection processes; however, a sister relationship between *C. murina* and the *robusta–sanfordi* complex suggests that retention of ancestral character states has contributed to these patterns of phenotypic variation.

Few instances of avian leapfrog distributions have been examined explicitly within a phylogenetic framework. Nonetheless, recent molecular-based phylogeographic studies in several unrelated Australo-Papuan avian genera revealed that convergent evolution or retention of ancestral character states best explain phenotypic similarity among lineages geographically isolated by intervening taxa of a distinct phenotype (Dumbacher & Fleischer, 2001; Norman et al., 2002). Likewise, phylogeographic analyses within Andean *Arremon* brush-finches have also rejected common ancestry hypotheses, and suggest that genetic drift or differential selection processes among intervening populations have contributed to multiple instances of leapfrog variation in plumage traits across the species complex (Cadena et al., 2010).

Given the remarkable acuity of the avian visual system, variation in plumage traits is thought to play a fundamental role in sexual selection processes, species recognition, and

genealogical lineage formation (Hill & McGraw, 2006). Although substantial progress has been made in understanding the developmental and genetic basis of avian plumage coloration in model study systems, the microevolutionary mechanisms that drive patterns of geographic variation in coloration remain little known within wild populations (Hoekstra, 2006; Prum, 2006; Uy et al., 2009; Driskell et al., 2010; Hubbard, 2010). Several microevolutionary mechanisms may potentially explain the origin of leapfrog variation in the *robusta–sanfordi* species complex, including developmental processes (e.g. heterochrony), stochastic processes (e.g. genetic drift), and sexual selection, each of which may be acting alone or in concert. Sky-island populations within *C. sanfordi* are highly restricted in distribution with small effective population sizes that enhance their susceptibility to random genetic drift processes. Alternatively, the presence of sexual dimorphism in multiple unrelated populations may be attributed to sex-linked mutations associated with melanin regulation that is either differentially selected for via geographic variation in female preferences or through developmental processes such as heterochrony. The latter mechanism may explain the independent origins of brown ventral coloration in *C. sanfordi*, as juveniles within *C. robusta* populations typically exhibit rusty brown flanks and abdominal plumage which is later lost the following year. Additional nuclear loci will be key to distinguish among stochastic and selective processes, as will sampling from the distinctive Foya Mountain and Bomberai Peninsula populations to examine the evolution sexual dimorphism. Investigation of sequence variation in loci associated with melanin regulation such as the MC1R and Agouti genes may also provide further insight into the processes underlying leapfrog variation among *robusta–sanfordi* phylogroups.

APPENDIX

Appendix 2.1. Summary of specimens included in this study.

Topology Code	Taxon	Locality	Latitude	Longitude	Source	Voucher Number
Ingroup	*Crateroscelis robusta*	PNG: Central Province				
SI1	*C. r. robusta*	Mt. Simpson	-9.99982	149.50718	KUNHM	T14598
SI2	*C. r. robusta*	Mt. Simpson	-9.99982	149.50718	KUNHM	114829
SI3	*C. r. robusta*	Mt. Simpson	-9.99982	149.50718	KUNHM	114832
SI4	*C. r. robusta*	Mt. Simpson	-9.99982	149.50718	KUNHM	114143
SI5	*C. r. robusta*	Mt. Simpson	-9.99982	149.50718	KUNHM	114142
SI6	*C. r. robusta*	Mt. Simpson	-9.99982	149.50718	KUNHM	114144
SI7	*C. r. robusta*	Mt. Simpson	-9.99982	149.50718	KUNHM	114145
SI8	*C. r. robusta*	Mt. Simpson	-9.99982	149.50718	KUNHM	114146
SI9	*C. r. robusta*	Mt. Simpson	-9.99982	149.50718	KUNHM	114108
EF1	*C. r. robusta*	Owen Stanley Range: Efogi	-9.15	147.66667	ANWC	24439
EF2	*C. r. robusta*	Owen Stanley Range: Efogi	-9.15	147.66667	ANWC	24444
EF3	*C. r. robusta*	Owen Stanley Range: Efogi	-9.15	147.66667	ANWC	26560
EF4	*C. r. robusta*	Owen Stanley Range: Efogi	-9.15	147.66667	ANWC	26574
EF5	*C. r. robusta*	Owen Stanley Range: Efogi	-9.15	147.66667	ANWC	26496
EF6	*C. r. robusta*	Owen Stanley Range: Efogi	-9.15	147.66667	ANWC	24440
AE1	*C. r. robusta*	Mt. Albert Edward	-8.45962	147.4001	AMNH	420054
AE2	*C. r. robusta*	Mt. Albert Edward	-8.45962	147.4001	AMNH	420030
AE3	*C. r. robusta*	Mt. Albert Edward	-8.45962	147.4001	AMNH	420053
TF1	*C. r. robusta*	Mt. Tafa	-8.63351	147.18387	AMNH	420027
TF2	*C. r. robusta*	Mt. Tafa	-8.63351	147.18387	AMNH	420028
TF3	*C. r. robusta*	Mt. Tafa	-8.63351	147.18387	AMNH	420039
TF4	*C. r. robusta*	Mt. Tafa	-8.63351	147.18387	AMNH	420042
TF5	*C. r. robusta*	Mt. Tafa	-8.63351	147.18387	AMNH	420055
		PNG: Morobe Province				
HE1	*C. r. robusta*	Herzog Mts: Wagu	-6.8	146.8	ANWC	25568
HE2	*C. r. robusta*	Herzog Mts: Wagu	-6.8	146.8	ANWC	25630
MI1	*C. r. robusta*	Owen Stanley Range: Mt. Missim	-7.21991	146.81598	MCZ	330571
MI2	*C. r. robusta*	Owen Stanley Range: Mt. Missim	-7.21991	146.81598	MCZ	167702
MI3	*C. r. robusta*	Owen Stanley Range: Mt. Missim	-7.21991	146.81598	MCZ	167703
MI4	*C. r. robusta*	Owen Stanley Range: Mt. Missim	-7.21991	146.81598	MCZ	167701
MI5	*C. r. robusta*	Owen Stanley Range: Mt. Missim	-7.21991	146.81598	MCZ	167700
MI6	*C. r. robusta*	Owen Stanley Range: Mt. Missim	-7.21991	146.81598	MCZ	167699
MI7	*C. r. robusta*	Owen Stanley Range: Mt. Missim	-7.21991	146.81598	MCZ	167698
MI8	*C. r. robusta*	Owen Stanley Range: Mt. Missim	-7.21991	146.81598	MCZ	167697
MI9	*C. r. robusta*	Owen Stanley Range: Mt. Missim	-7.21991	146.81598	MCZ	167696
HU1	*C. r. robusta*	Haumnga	-7.33416	146.4680	ANWC	4184
HU2	*C. r. robusta*	Haumnga	-7.33416	146.4680	ANWC	4213
HU3	*C. r. robusta*	Haumnga	-7.33416	146.4680	ANWC	4257
HU4	*C. r. robusta*	Haumnga	-7.33416	146.4680	ANWC	4295
FI1	*C. r. robusta*	Huon Peninsula: Finisterre Range	-6.08165	146.57224	KUNHM	95791
FI2	*C. r. robusta*	Huon Peninsula: Finisterre Range	-6.08165	146.57224	KUNHM	92357
FI3	*C. r. robusta*	Huon Peninsula: Finisterre Range	-6.08165	146.57224	KUNHM	92361
FI4	*C. r. robusta*	Huon Peninsula: Finisterre Range	-6.08165	146.57224	KUNHM	93568
FI5	*C. r. robusta*	Huon Peninsula: Finisterre Range	-6.08165	146.57224	KUNHM	95289
FI6	*C. r. robusta*	Huon Peninsula: Finisterre Range	-6.08165	146.57224	KUNHM	T4576
SA1	*C. r. robusta*	Huon Peninsula: Saruwaged Mts	-6.11056	146.89576	KUNHM	111622
SA2	*C. r. robusta*	Huon Peninsula: Saruwaged Mts	-6.11056	146.89576	KUNHM	111623
SA3	*C. r. robusta*	Huon Peninsula: Saruwaged Mts	-6.11056	146.89576	KUNHM	111624
		PNG: Madang Province				
SH1	*C. r. robusta*	Schradder Range	-5.22057	144.48821	KUNHM	111629

Topology Code	Taxon	Locality	Latitude	Longitude	Source	Voucher Number
SH2	*C. r. robusta*	Schradder Range	-5.22057	144.48821	KUNHM	114756
		PNG: Eastern Highlands Province				
KR1	*C. r. robusta*	Kratke Range	-7.061	145.82433	KUNHM	113275
KR2	*C. r. robusta*	Kratke Range	-7.061	145.82433	KUNHM	114282
KR3	*C. r. robusta*	Kratke Range	-7.061	145.82433	KUNHM	114281
OK1	*C. r. robusta*	Okapa District: Kimigomo	-6.42718	145.58016	KUNHM	114886
BI1	*C. r. robusta*	Bismarck Range	-5.95166	145.4	KUNHM	114233
BI2	*C. r. robusta*	Bismarck Range	-5.95166	145.4	KUNHM	114232
BI3	*C. r. robusta*	Bismarck Range	-5.95166	145.4	KUNHM	114234
BI4	*C. r. robusta*	Bismarck Range	-5.95166	145.4	KUNHM	114896
CR1	*C. r. robusta*	Crater Mountain	-6.69444	145.10666	KUNHM	91987
CR2	*C. r. robusta*	Crater Mountain	-6.69444	145.10666	KUNHM	T5260
KU1	*C. r. robusta*	Kubor Range	-6.04883	144.52266	AMNH	705065
KU2	*C. r. robusta*	Kubor Range	-6.04883	144.52266	AMNH	705067
		PNG: Western Highlands Province				
HA1	*C. r. robusta*	Mt. Hagen	-5.79419	143.99600	AMNH	705075
HA2	*C. r. robusta*	Mt. Hagen	-5.79419	143.99600	AMNH	705074
HA3	*C. r. robusta*	Mt. Hagen	-5.79419	143.99600	AMNH	705405
		PNG: West Sepik Province				
ST1	*C. r. sanfordi*	Mt. Stolle	-4.81331	141.65293	KUNHM	97650
ST2	*C. r. sanfordi*	Mt. Stolle	-4.81331	141.65293	KUNHM	114287
ST3	*C. r. sanfordi*	Mt. Stolle	-4.81331	141.65293	KUNHM	114286
OS1	*C. r. sanfordi*	Oksapmin	-5.21812	142.24981	PNGNM	23462
HR1	*C. r. sanfordi*	Hindenburg Range: Ilkivip	-5.25066	141.38472	AMNH	765679
HR2	*C. r. sanfordi*	Hindenburg Range: Ilkivip	-5.25066	141.38472	AMNH	765680
HR3	*C. r. sanfordi*	Hindenburg Range: Ilkivip	-5.25066	141.38472	AMNH	765681
BW1	*C. r. bastille*	Bewani Mts., Mt. Menawa	-3.30373	141.72652	AMNH	829331
BW2	*C. r. bastille*	Bewani Mts., Mt. Menawa	-3.30373	141.72652	AMNH	829328
BW3	*C. r. bastille*	Bewani Mts., Mt. Menawa	-3.30373	141.72652	AMNH	829329
BW4	*C. r. bastille*	Bewani Mts., Mt. Menawa	-3.30373	141.72652	AMNH	829330
BW5	*C. r. bastille*	Bewani Mts., Mt. Menawa	-3.30373	141.72652	AMNH	829327
BW6	*C. r. bastille*	Bewani Mts., Mt. Menawa	-3.30373	141.72652	AMNH	829326
BW7	*C. r. bastille*	Bewani Mts., Mt. Menawa	-3.30373	141.72652	AMNH	829332
BW8	*C. r. bastille*	Bewani Mts., Mt. Menawa	-3.30373	141.72652	AMNH	829333
TO1	*C. r. bastille*	Torricelli Mts., Mt. Nibo	-3.40879	142.18570	AMNH	829325
		Indonesia: Papua Province				
LH1	*C. r. sanfordi*	Bele River: Lake Habbema	-4.08416	138.7391	AMNH	340449
LH2	*C. r. sanfordi*	Bele River: Lake Habbema	-4.08416	138.7391	AMNH	340443
LH3	*C. r. sanfordi*	Bele River: Lake Habbema	-4.08416	138.7391	AMNH	340469
LH4	*C. r. sanfordi*	Bele River: Lake Habbema	-4.08416	138.7391	AMNH	340461
LH5	*C. r. sanfordi*	Bele River: Lake Habbema	-4.08416	138.7391	AMNH	340487
BE1	*C. r. sanfordi*	Bernhard Camp	--	--	AMNH	340439
BE2	*C. r. sanfordi*	Bernhard Camp	--	--	AMNH	340435
WI1	*C. r. sanfordi*	Mt. Wilhemina	-4.24376	138.6212	AMNH	340491
IL1	*C. r. sanfordi*	Nassau Range: Ilaga	-3.98963	137.54045	YPBM	75553
IL2	*C. r. sanfordi*	Nassau Range: Ilaga	-3.98963	137.54045	YPBM	75554
IL3	*C. r. sanfordi*	Nassau Range: Ilaga	-3.98963	137.54045	YPBM	75556
CY1	*C. r. deficiens*	Cyclops Mts	-2.5077	140.52608	AMNH	293887
CY2	*C. r. deficiens*	Cyclops Mts	-2.5077	140.52608	AMNH	589357
CY3	*C. r. deficiens*	Cyclops Mts	-2.5077	140.52608	AMNH	293889
CY4	*C. r. deficiens*	Cyclops Mts	-2.5077	140.52608	AMNH	293888
CY5	*C. r. deficiens*	Cyclops Mts	-2.5077	140.52608	AMNH	589360
CY6	*C. r. deficiens*	Cyclops Mts	-2.5077	140.52608	AMNH	293891
CY7	*C. r. deficiens*	Cyclops Mts	-2.5077	140.52608	AMNH	293886

Topology Code	Taxon	Locality	Latitude	Longitude	Source	Voucher Number
CY8	*C. r. deficiens*	Cyclops Mts	-2.5077	140.52608	AMNH	589359
CY9	*C. r. deficiens*	Cyclops Mts	-2.5077	140.52608	AMNH	293890
CY10	*C. r. deficiens*	Cyclops Mts	-2.5077	140.52608	AMNH	589358
WE1	*C. r. sanfordi*	Weyland Mts.	-3.89137	135.4664	AMNH	301921
WE2	*C. r. sanfordi*	Weyland Mts.	-3.89137	135.4664	AMNH	301986
WE3	*C. r. sanfordi*	Weyland Mts.	-3.89137	135.4664	AMNH	301922
WE4	*C. r. sanfordi*	Weyland Mts.	-3.89137	135.4664	AMNH	301925
WE5	*C. r. sanfordi*	Weyland Mts.	-3.89137	135.4664	AMNH	301926
WE6	*C. r. sanfordi*	Weyland Mts.	-3.89137	135.4664	AMNH	301924
WE7	*C. r. sanfordi*	Weyland Mts.	-3.89137	135.4664	AMNH	301923
WE8	*C. r. sanfordi*	Weyland Mts.	-3.89137	135.4664	AMNH	301977
WE9	*C. r. sanfordi*	Weyland Mts.	-3.89137	135.4664	AMNH	301918
		Indonesia: West Papua Province				
WA1	*C. r. sanfordi*	Wandamen Mts.	-2.75584	134.58458	AMNH	589365
WA2	*C. r. sanfordi*	Wandamen Mts.	-2.75584	134.58458	AMNH	589366
WA3	*C. r. sanfordi*	Wandamen Mts.	-2.75584	134.58458	AMNH	589367
WA4	*C. r. sanfordi*	Wandamen Mts.	-2.75584	134.58458	AMNH	293892
WA5	*C. r. sanfordi*	Wandamen Mts.	-2.75584	134.58458	AMNH	293894
TA1	*C. r. ripleyi*	Tamrau Mts., Mt. Bantjiet	-0.71553	132.96645	AMNH	792948
TA2	*C. r. ripleyi*	Tamrau Mts., Mt. Bantjiet	-0.71553	132.96645	AMNH	792949
TA3	*C. r. ripleyi*	Tamrau Mts., Mt. Bantjiet	-0.71553	132.96645	AMNH	792950
TA4	*C. r. ripleyi*	Tamrau Mts., Mt. Bantjiet	-0.71553	132.96645	AMNH	792951
TA5	*C. r. ripleyi*	Tamrau Mts., Mt. Bantjiet	-0.71553	132.96645	AMNH	792952
AR1	*C. r. peninsularis*	Arfak Mts.	-1.09181	133.9073	AMNH	589364
AR2	*C. r. peninsularis*	Arfak Mts.	-1.09181	133.9073	AMNH	589361
AR3	*C. r. peninsularis*	Arfak Mts.	-1.09181	133.9073	AMNH	293884
AR4	*C. r. peninsularis*	Arfak Mts.	-1.09181	133.9073	AMNH	293881
AR5	*C. r. peninsularis*	Arfak Mts.	-1.09181	133.9073	AMNH	589362
AR6	*C. r. peninsularis*	Arfak Mts.	-1.09181	133.9073	AMNH	293880
AR7	*C. r. peninsularis*	Arfak Mts.	-1.09181	133.9073	AMNH	589363
AR8	*C. r. peninsularis*	Arfak Mts.	-1.09181	133.9073	AMNH	293885
AR9	*C. r. peninsularis*	Arfak Mts.	-1.09181	133.9073	AMNH	293882
Outgroup						
1	*Crateroscelis murina*	PNG: Madang Province	-4.71727	145.27482	KUNHM	111639
2	*Crateroscelis murina*	PNG: Madang Province:	-4.4825	145.0316	KUNHM	97904
3	*Crateroscelis murina*	PNG: East Sepik Province	-4.61525	142.7133	KUNHM	T9167
1	*Crateroscelis nigrorufa*	PNG: Eastern Highlands Province	-6.6545	145.1714	KUNHM	91986
2	*Crateroscelis nigrorufa*	PNG: Eastern Highlands Province	-7.061	145.82433	KUNHM	114280
3	*Crateroscelis nigrorufa*	PNG: Eastern Highlands Province	-7.061	145.82433	KUNHM	113274
	Sericornis nouhuysi	PNG: Central Province	9.98955	149.4866	KUNHM	T14587
	Sericornis papuenis	PNG: Central Province	-9.99982	149.50718	KUNHM	114153
	Myzomela rosenbergi	PNG: Madang Province	-4.71727	145.27482	KUNHM	111482
	P. novaehollandiae	Australia: NSW, Clarence	-33.4767	150.2232	KUNHM	98269

Institutional Sources: American Museum of Natural History (AMNH), Yale Peabody Museum (YPM), Harvard Museum of Comparative Zoology (MCZ), Philadelphia Academy of Natural Sciences (ANSP), Australian National Wildlife Collection (ANWC), University of Kansas Natural History Museum (KUNHM); Papua New Guinea National Museum (PNGNM).

Appendix 2.2. Summary of primers used in this study.

Gene	Primer name	Sequence 5'– 3'
NADH dehydrogenase subunit–2	L5216[a]	GGCCCATACCCCGRAAATG
	H6313[a]	CTCTTATTTAAGGCTTTGAAGGC
	CR–ND2–1H[b]	GGAATCAGAARTGRAATGGGACTA
	CR–ND2–2L[b]	CGGACAATGRGACATCACCC
	CR–ND2–2H[b]	GTGGGAGATGGAGGAGAAGGC
	CR–ND2–3L[b]	CTGACCTCACCATCCYTAAACCC
	CR–ND2–3H[b]	GGAGAGGAGGGAGATGATTATTGC
ATP synthase subunits–6 and 8	tRNA–Lys–L[c]	CAGCACTAGCCTTTTAAGCT
	COIII–RH[c]	ATTATTCCGTATCGNAGNCCYTTTTG
	CR–ATP–1H[b]	GCTCATTTGTGGCCYTTCTTGTCTA
	CR–ATP–2L[b]	ACCGACTATCAACCCTACAACTCTGA
	CR–ATP–2H[b]	AGAGATTAGTTGGATGAGAAGGTGGC
	CR–ATP–3L[b]	AGCCTTCTCATCCGCCCTYTA
	CR–ATP–3H[b]	GGCTGCTCCGAAGATGGGTCA

[a] Johnson and Sorenson (1998)
[b] Designed by B.W. Benz for this study
[c] Sorenson et al. (1999)

Appendix 2.3. Average ND2 sequence divergence (%) among populations of *C. robusta*. Pairwise F_{ST} values are indicated in bold below the diagonal.

	Tamrau Mts.	Arfak Mts.	Wandamen Range	Weyland Range	Western CDRs	Cyclops Range	Bewani Range	Eastern Highlands	Huon Penin	Owen Stanley	Mt. Simpson
	P1	P2	P3	P4	P5	P6	P7	P8	P9	P10	P11
P1	--	1.20	3.36	3.85	3.09	4.60	3.38	8.49	8.34	8.47	8.42
P2	**0.864**	--	2.86	2.95	2.30	3.80	2.58	8.80	8.64	8.78	8.73
P3	**0.988**	**0.957**	--	0.53	2.55	4.04	2.82	8.92	8.77	8.92	8.86
P4	**0.954**	**0.913**	**0.750**	--	2.24	3.68	2.51	8.97	8.82	8.97	8.91
P5	**0.931**	**0.872**	**0.932**	**0.864**	--	2.61	0.60	8.18	8.00	8.15	8.10
P6	**0.983**	**0.958**	**0.991**	**0.954**	**0.921**	--	2.46	8.59	8.42	8.54	8.37
P7	**0.981**	**0.943**	**0.992**	**0.938**	**0.677**	**0.976**	--	8.13	7.95	8.34	8.04
P8	**0.970**	**0.962**	**0.976**	**0.961**	**0.953**	**0.971**	**0.971**	--	0.32	0.54	0.40
P9	**0.983**	**0.974**	**0.988**	**0.973**	**0.966**	**0.983**	**0.984**	**0.038**	--	0.40	0.60
P10	**0.971**	**0.963**	**0.977**	**0.962**	**0.954**	**0.972**	**0.972**	**0.232**	**0.320**	--	0.40
P11	**0.984**	**0.975**	**0.989**	**0.974**	**0.967**	**0.984**	**0.985**	**0.569**	**0.687**	**0.287**	--

Appendix 2.4. Estimates of population divergence times based on corrected genetic distances of ND2 sequences.

Population	Time (5%/Myr)	Time (2%/Myr)
Arfak–Tamrau	207,600	519,00
Arfak –Weyland	538,900	1,347,250
Arfak –Western CDR	401.400	1,003,500
Western CDR – Bewani	81.400	203,500
Western CDR – Cyclops	480,700	1,201,750
Western CDR – Eastern Highlands	1,559,400	3,898,500
Eastern Highlands – Huon	16,000	40,000
Eastern Highlands – Owen Stanley Ranges	24,900	62,250
Owen Stanley Ranges – Huon	19,300	48,250
Owen Stanley Range – Mt Simpson	20,400	51,000

Appendix 2.5. Ecological niche reconstruction of *C. robusta* projected to LGM climatic conditions based on. the CCSM general circulation model.

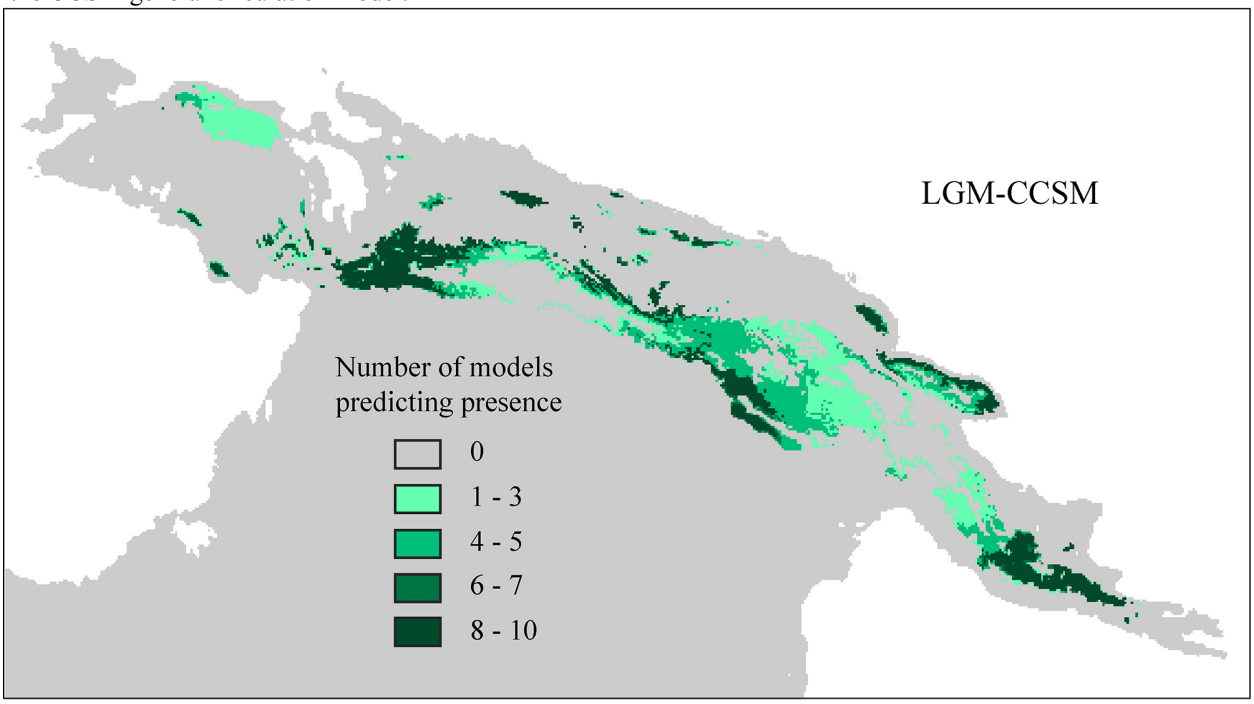

CHAPTER THREE

COMPARATIVE PHYLOGEOGRAPHY REVEALS DISPARATE PATTERNS OF AVIAN DIVERSIFICATION ACROSS THE NEW GUINEA HIGHLANDS

ABSTRACT

New Guinea's montane rainforest environments are endowed with remarkable avian diversity, yet the origin and evolutionary history of this endemic avifauna remains poorly understood, owing to an absence of modern genetic sampling throughout much of the island's rugged highland topography. Herein, I reconcile contemporary and paleoecological niche reconstructions with spatial analyses of genetic diversity in four co-distributed montane New Guinea passerines to investigate how Pleistocene climate fluctuations and putative biogeographic barriers influenced avian diversification across the New Guinea highlands. Phylogeographic analyses revealed substantial disparity in the distribution of genetic diversity, with *Peneothello cyanus* and *Crateroscelis robusta* exhibiting deep divergences along the Strickland River Valley, whereas *Rhipidura atra* and *Amblyornis macgregoriae* displayed evidence of ongoing gene flow and shallow genetic structure across this biogeographic boundary. Patterns of population genetic structure in *P. cyanus* and *C. robusta* largely reflect the distribution of contemporary sky-islands and patterns of population connectivity inferred from Last Glacial Maximum ecological niche reconstructions; however, instances of discord among genetic and ecological data sets are evident across the Strickland, Watut, and Tauri river drainages. By contrast, *R. atra* and *A. macgregoriae* exhibit relatively weak geographic structure throughout much of the Central Highlands, and show indications of admixture or ancestral polymorphism among multiple sky-island populations while maintaining highly divergent reciprocally monophyletic lineages in the

Vogelkop and Huon Peninsula, respectively. Bayesian skyline analyses revealed signatures of demographic expansion in all 4 species, followed by slight contractions in all but *R. atra*, corroborating elevational shifts and range expansion/contraction predicted by LGM and contemporary ecological niche models. This investigation provides novel insight into the complex evolutionary dynamics underlying patterns of avian diversification across the New Guinea highlands—knowledge requisite to developing effective conservation measures for a key component of the Melanesian biodiversity hotpot.

INTRODUCTION

Since Darwin's (1859) seminal work on adaptive radiation and evolutionary mechanisms of lineage formation, insular landscapes and their biotas have featured prominently in the development of speciation theory and biogeographic understanding (Wallace, 1876; 1880; Mayr, 1942; MacArthur & Wilson, 1967; Grant & Grant 2002; Lovette *et al*., 2002; Mayr & Diamond, 2001; Filardi & Moyle; 2005). Such island systems are particularly appealing as natural laboratories in evolutionary biology in part owing to their reduced species richness and sharply delineated geographic boundaries, attributes that typically provide enhanced clarity in hypothesis testing compared to more complex continental systems. The Melanesian avifauna has attracted considerable attention in this regard, advancing basic understanding of speciation processes and historical biogeography throughout the region (Diamond, 1973; Mayr & Diamond, 2001; Filardi & Smith, 2005; 2007; Steadman, 2006; Uy et al., 2009; Jønsson et al., 2010). Despite New Guinea's influential role in shaping the evolutionary history of Melanesian birds, few molecular studies have examined how population dynamics and environmental factors have impacted patterns of intraspecific variation and speciation within the island (Norman et al., 2002; Norman

et al., 2006; Murphy et al., 2007; Joseph et al., 2001). Consequently, species limits and phylogeographic relationships remain obscure for much of the New Guinea avifauna, as current taxonomic frameworks are based primarily on traditional arrangements (Mayr, 1941; Rand & Gillard, 1967; Pratt, 1982; Mayr & Diamond, 2001; Joseph & Omland, 2009).

New Guinea's montane bird communities bear resemblance to island archipelago model study systems, in that they are effectively isolated from one another by expanses of unsuitable environmental conditions (lowland rainforest and anthropogenic grasslands) and generally exhibit sharp distributional limits. Accordingly, the origin and phylogeographic relationships of these sky-island populations have long intrigued evolutionary biologists, with traditional dogma centering on hypotheses of long-distance dispersal to explain distribution patterns both within the Central Highlands and among coastal sky-island populations (Diamond, 1973; Pratt, 1982). The distribution of avian species richness throughout New Guinea's highland terranes is generally consistent with "downstream" colonization of coastal sky-island populations from the CDRs; however, several instances of potential peripatric diversification (i.e. "upstream" colonization of the CDRs from coastal populations) merit investigation within a modern phylogenetic framework (Pratt, 1982; Diamond, 1985; Keast, 1996).

Diamond (1973) suggested that competitive exclusion processes among adjacent populations may promote colonization of distantly isolated sky-island populations, whereas patterns of diversification within the largely continuous Central Highlands were accounted for by a "drop-out" hypothesis based on vicariant processes within the Eastern Highlands (Diamond, 1972). In the later hypothesis, Diamond (1972) surmised that continuous populations differentiate across an east-west cline within the CDRs and subsequently undergo localized extinctions that further limit admixture among terminal populations, thereby permitting allopatric

divergence processes and eventually the evolution of discrete lineages. As two sister lineages reinvade their former distribution, Diamond again invokes competitive exclusion mechanisms to promote elevational sorting that leads to the evolution of sharply delineated elevational sister taxa. Although Diamond's dropout hypothesis is vague as to what initiates these localized extinctions, he suggests that climatic fluctuations and the associated elevational compression of montane vegetation zones may have been a predominant force, acting to restrict population connectivity during cooler periods (Diamond 1972; 1973). However, analyses of palynological spectra examined from multiple coring sites throughout the Central Highlands have shown that Pleistocene climate oscillations likely had the opposite effect, linking montane rainforest communities within the CDRs rather than isolating them (Nix & Kalma, 1972; Hope & Peterson, 1976; Walker & Hope 1982; Haberle et al., 1990; Hope & Tulip, 1994; Hope, 1996). Summaries of pollen spectra from these independent study sites indicate a depression of present-day tree line from 3700 m (6ºC annual isotherm) to 2200 m during the Last Glacial Maximum (LGM), spanning 23,000–15,000 years before present (ybp), with ~2000 km^2 of glacial cover above 3500 m during this period. The elevational compression of montane floral communities differed among montane habitats, with alpine grasslands experiencing a significant down-slope expansion from the 3500 m snow line to 2200 m, whereas subalpine moss forests were constrained to a narrow elevational band limited to 200 m down-slope from the alpine grassland ecotone, or were lost altogether, depending on local topography (Hope, 1996). Upper to mid-montane *Nothofagus* forests experienced more moderate elevational displacement, ranging from 900–2000 m, roughly a 1000 m drop from present-day distributions, while lower montane habitats were compressed to just 300 m down-slope of their present distribution before giving way to foothill and lowland forest environments. By contrast, New Guinea's coastal montane rainforest communities were

affected less by cooler LGM climatic conditions, with floral distributions descending only a few hundred meters, as the biota of these terranes already exhibit considerable elevational compression given their costal proximity and limited high altitude topography (Paijmans, 1976; Hope, 1996).

More recently, advances in deciphering the complex geological history of Melanesia has led several researchers to invoke New Guinea's tectonic history in explaining patterns of species richness and historical diversification of the island's avifauna (Michaux, 1994; Heads, 2001b; 2002; Jønsson, 2009). In a series of studies examining geographic distributions of the Paradisaeidae and other co-distributed avian groups, Heads (2001a; 2001b; 2002) proposed that New Guinea's terrane accretion history and rapid orogenic formation has uplifted elements of the island's lowland avifauna, providing opportunities for vicariant diversification across elevational gradients within the interior highlands. Heads (2001b; 2002) further surmised that west lateral rifting of these accreted terranes may explain broad-scale disjunctions among closely related avian lineages distributed across New Guinea's composite montane landscape (e.g. *Parotia*, *Paradisaea*, and *Astrapia*). Although similar biogeographic hypotheses have been suggested to explain the evolutionary history of other floral and faunal groups across the New Guinea orogen (Flanery 1995; Polhemus & Polhemus, 1996; van Welzen, 1997), researchers have yet to test explicitly the spatiotemporal predictions of these tectonic-based hypotheses of diversification using modern phylogenetic techniques with robust geological and molecular calibrations (Heads, 2001a; 2001b; 2002; Norman, 2007; Irestedt, 2009).

In the present study, I use mitochondrial sequence data and ecological niche reconstructions to compare phylogeographic patterns of diversification among 4 montane New Guinea passerines and assess the underlying environmental factors that have shaped population

genetic structure and lineage formation across the island's complex montane landscape. Broad geographic sampling was employed for each target species to address the following questions: (1) Is phylogeographic structure congruent with the distribution of contemporary sky-islands and traditionally recognized biogeographic boundaries within the Central Highlands, or are spatial patterns of genetic diversity better explained by the distribution of LGM rainforest sky-islands and environmental connectivity inferred from paleoecological niche reconstructions? (2) Do coastal sky-island populations represent independent colonization events from the Central Highlands, and has "upstream" dispersal influenced population genetic structure within the CDRs? (3) To what extent do morphologically defined taxonomic units and traditionally recognized areas of endemism reflect the distribution of genetic diversity? (4) Are trends of demographic expansion/contraction predicted by contemporary and paleoecological niche reconstructions congruent with genetic signatures of population demography, and how have isolated coastal populations responded to climate change in comparison to larger communities of the Central Highlands?

METHODS

Taxon sampling

I sampled a total of 542 ingroup specimens from 4 focal taxa, including *Peneothello cyanus* (n=163), *Crateroscelis robusta* (n=127), *Rhipidura atra* (n=150), and *Amblyornis macgregoriae* (n=104). Fresh tissue samples were collected from key biogeographic regions across Papua New Guinea (Fig. 3.1) and stored in 99% ethanol prior to archival storage (-70ºC) at the University of Kansas Natural History Museum (KUNHM). Ancient DNA tissues (toepad clippings) sampled from historical collections spanning 1928–1973 were utilized to include populations from Papua

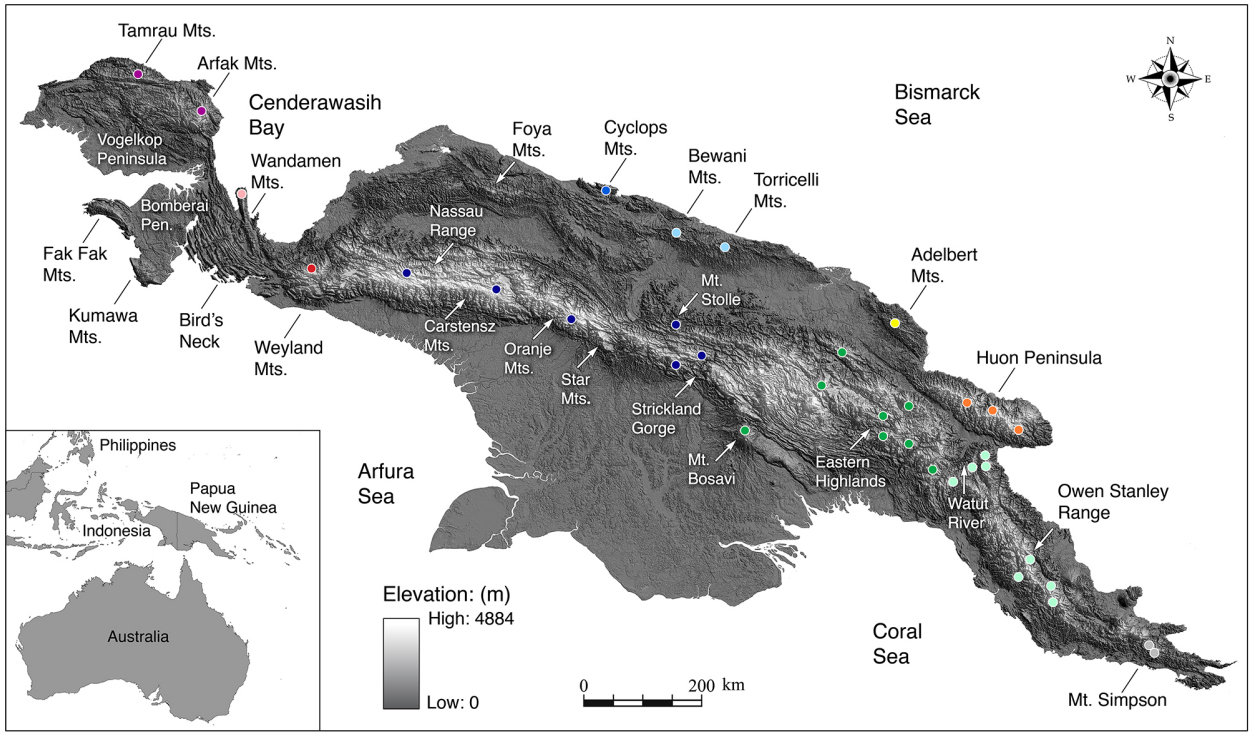

Figure. 1.1. Digital elevation model of New Guinea depicting the principal montane topographic features addressed in the present study. Collection localities are color coded by population and correspond to colors shown on Bayesian inference topologies and haplotype networks for each of the focal taxa.

and West Papua, Indonesia, and to refine sampling resolution near suspected geographic breaks. I employed extensive outgroup sampling for each species complex based on recent higher-level phylogenetic analyses to assess monophyly and species limits within focal taxa (Loynes et al., 2009; Nyari et al., 2009; Gardner et al., 2010). Specimen data including collection locality, latitude and longitude, institutional source, voucher number, and tissue type are detailed in Appendix 3.1.

Sequencing protocols

Genomic DNA was extracted from frozen or ethanol-preserved tissue samples using standard Qiagen DNeasy™ extraction protocols (Qiagen, Valencia, CA). I amplified a suite of four

mitochondrial genes including NADH dehydrogenase subunit-2 (ND2, 867 to 1041 bp), ATP synthase subunits-6 and 8 (ATP6, 684bp; ATP8, 171bp), and NADH dehydrogenase subunit-3 (ND3, 351 bp) via 12µl polymerase chain reactions (PCR) using PureTaq RTG PCR beads (GE Healthcare). Thermocycle parameters for each external primer pair (Appendix 1.2, 2.2, 3.2, 3.3) consisted of an initial 3 min denaturation at 94 ºC, followed by 35 cycles of 20 s at 94 ºC, 15 s at 53 ºC, and 60 s at 72 ºC, followed by a 7 min final extension at 72 ºC and 4 ºC soak. All PCR products were cleaned of unincorporated DNTPs and primers with ExoSaP-IT purification (USB Corp.), visualized on a 1% agarose gel stained with ethidium bromide to assess amplification quality, and cycle-sequenced with ABI Prism BigDye v3.1 terminator chemistry under manufacture's thermocycling protocols using the same external PCR primer pairs. Cycle-sequencing products were desalted and cleaned of excess terminator dyes with Sephadex G-50 (medium) purification columns, and subsequently analyzed on an ABI 3730 Genetic Analyzer (Applied Biosystems).

Genomic extractions of ancient DNA samples were conducted outside of the main KUNHM molecular facility in a laboratory that is free of PCR products. Workstations and all equipment were cleaned with a 10% bleach solution prior to performing each set of extractions; to protect further against downstream contamination, filtered pipette tips were used throughout all ancient DNA sequencing procedures, as were multiple negative controls during extraction and amplification to enhance detection of potential contamination. Samples were extracted using a DNeasy^{TM} Tissue Kit (QIAGEN), extending the tissue lysis step overnight with the addition of 10 µl of 1M Dithiothreitol to facilitate complete digestion of the toepad sample, and all negative controls were tested for contamination using a NanoDrop spectrophotometer (Thermo Scientific). Complete ND3 sequences were obtained via the same external primer pair used for

fresh tissues (Chesser, 1999), whereas a suite of internal primers was designed to sequence the entire ATP6–8 subunits using three ~350 bp amplicons with a minimal 15 bp overlap between fragments excluding primer sequences. The same approach was used to obtain 834 – 1041 bp from the ND2 gene. Thermocycling protocols for all ancient DNA PCRs were modified to incorporate an annealing touch down of 10 cycles at 60 ºC, 10 cycles at 56 ºC, and 25 cycles at 52 ºC, followed by a 10 min extension at 72 ºC and 4 ºC soak. An additional 15 cycles were added to ABI's standard thermocycling protocols to maximize signal strength of chromatograms. All other sequencing procedures followed standard protocols detailed above for fresh DNA samples.

Phylogenetic analysis

Chromatograms of complimentary strands were reconciled in SEQUENCHER v. 4.1 (Gencodes) and an initial sequence alignment was performed in CLUSTAL X (Thompson et al., 1997) under default settings. Subsequent gap adjustments were conducted by eye in MESQUITE v. 2.72 (Maddison & Maddison, 2009), followed by amino acid translation for comparison with *Gallus gallus* sequences (Dejardins & Morias, 1990) to confirm reading frames. Best-fit models of sequence evolution were determined in JMODELTEST v. 0.1.1 (Guindon & Gascuel, 2003; Posada, 2008) using the Bayesian Information Criterion.

I estimated phylogenetic relationships within each species complex using the concatenated mtDNA data and Bayesian inference (BI) analyses implemented in MRBAYES v. 3.1.2 (Ronquist & Huelsenbeck, 2003; Altekar et al., 2004), with taxon specific BIC selected models of nucleotide substitution applied to each taxonomic data set. Analyses were conducted with a flat prior specified for parameter estimation, and modified heating conditions of 0.15 were

applied to four Markov chains run for $2x10^7$ generations sampled every 1000 generations resulting in 15,000 total trees after a conservative 25% initial burnin. Two or more analyses were conducted per partitioning scheme to guard against convergence on local optima, and stationarity of each run was assessed by monitoring average standard deviation of split frequencies, plotting –lnL against generation time, assessing model parameter posterior probability densities in TRACER v. 1.5 (Rambaut & Drummond, 2007), and examining clade posterior probabilities across runs using the compare and slide functions in AWTY (Nylander et al., 2008).

Phylogenetic relationships were also inferred via maximum likelihood (ML) analyses conducted in GARLI v. 2.0 (Zwickl, 2006), which implements a genetic algorithm and jointly estimates topology, branch lengths, and model parameters, yielding significant advances in computational efficacy for large data sets. Twenty independent runs were conducted under default parameters for the combined nine-partition data set to ensure that the optimal –lnL solution had been reached. Topologies were selected after 50,000 generations with no significant improvement in –lnL (improvement values set at 0.01 with a total improvement of < 0.05 compared to the last topology recovered). Node support was assessed using 1000 non-parametric bootstrap replicates using a reduced run termination criterion of 10,000 generations.

Coalescent estimates of divergence times between primary phylogroups were conducted in IMA2 with samples grouped by clade and a conservative range of mutation scalars (2–5%) applied to account for uncertainty in ND2 mutation rate estimates (Lovette, 2004; Arbrogast et al., 2006). Each run was conducted with 20 geometrically heated chains for 3×10^7 steps and a 1×10^7 burnin. The migration parameter was set to zero, given the reciprocal monophyly among regional lineages.

Population structure and demography

Minimum spanning networks of haplotype relationships were constructed for each gene using the Bandelt et al. (1999) algorithm implemented in NETWORK v. 4.5 (fluxus-engineering.com) to visualize spatial patterns of genetic variation. Analyses were performed using default parameters, with the MP optimization algorithm applied to minimize extraneous median vectors (Polzin & Daneschmand, 2003). Results of haplotype networks presented herein are limited to ND2 sequences, as this gene was representative of the other markers, which are part of the same mtDNA linkage group.

Genetic variation within populations was characterized using DNASP v. 5.0 (Librado & Rozas, 2009) to calculate summary statistics, including number of unique haplotypes (h), number of segregating sites (S), haplotype diversity (Hd), and the nucleotide diversity parameter π along with its 95% confidence interval. Pairwise F_{ST} statistics were used to estimate geographic structure of genetic diversity among sites and define population limits across the 35 collection localities. Three-way analyses of molecular variance (AMOVA) were conducted in ARLEQUIN v. 3.5 (Excoffier & Lischer, 2010) to examine further the distribution of genetic diversity among populations and test the role of Pleistocene climate change in shaping geographic structure across New Guinea's Central Highlands and outlying costal sky-islands. Samples were grouped by contemporary populations (Table 2), Pleistocene sky-islands inferred from LGM ecological niche reconstructions (Fig. 8), and current taxonomy. Pleistocene sky-islands include the same suite of coastal populations defined in contemporary groupings, whereas populations of the CDRs and Papuan Peninsula were grouped into a single contiguous population based on extensive habitat connectivity. Mantel tests were implemented in IBDWS v. 3.16 (Isolation By Distance Web Service: http://ibdws.sdsu.edu/; Jensen et al., 2005) using 10,000 permutations to

test for correlations between genetic and geographic distances within regional lineages and the species as a whole. Geographic straight-line distances (km) between populations were estimated from geo-referenced collecting localities using ArcGIS (ESRI, Redlands, CA). Genetic distances were computed as $F_{ST}/(1-F_{ST})$ as recommended in Rousset (1997), and geographic distances were not log-transformed given the stepping-stone dispersal pattern expected in these taxa.

I evaluated the historical demography of populations in DNASP v. 5.0 using a suite of summary statistics based on the frequency spectrum of mutations including Tajima's *D*, Fu & Li's *D* (Fu & Li, 1993), and the R_2 statistic (Ramos-Onsins & Rozas, 2002). Fu's *Fs* statistic (Fu, 1997), which is based on the haplotype distribution, was also calculated, as this statistic is among the most sensitive to recent population contractions (Ramos-Onsins & Rozas, 2002). The significance of each test statistic was assessed using 10,000 coalescent simulations conducted in DNASP v. 5.0. Lastly, the distribution of pairwise differences was used to infer demographic history by plotting mismatch distributions for each population and compared to a null hypothesis of demographic expansion, which exhibits a smooth, unimodal Poisson distribution (Harpending, 1994). The fit of observed data was assessed using the raggedness statistic (*r*) calculated in DNASP v. 5.0, with significance determined using 10,000 coalescent simulations.

Bayesian skyline analyses were conducted using BEAST v1.6.1 (Drummond & Rambaut, 2006; 2007) to explore the demographic history within focal taxa, as this approach incorporates the full compliment of historical phylogeographic information inherent to sequence variation, thereby offering advantages over traditional summary statistics that rely on the frequency spectrum of mutation or haplotype distribution (Drummond et al., 2005). Models of sequence evolution were determined for each taxon using the BIC in JMODELTEST v. 0.1.1, and analyses were run for 1×10^7 generations under default parameters with sampling every 1000 generations.

Multiple analyses were conducted per lineage to ensure that the run achieved stationarity as determined from posterior probability densities of model parameters examined in TRACER v. 1.5; a conservative 25% burnin was implemented for final analyses.

Ecological niche modeling

I used the Genetic Algorithm for Rule-Set Prediction (GARP v 1.1.3; Stockwell & Peters, 1999) and Maxent v. 3.3 (Phillips et al., 2006) software applications to generate ecological niche models for each taxon under contemporary conditions, which in turn were projected to LGM climate surfaces to reconstruct the species potential distribtuion18,000–25,000 ybp. Both software applications are evolutionary-computing approaches that use known occurrence points and raster GIS data layers summarizing relevant environmental dimensions to build ENMs based on relationships between the two data sets. The result of each approach is a map summarizing suitability of environmental conditions for the species' in question. Optimization of model accuracy in GARP analyses is achieved via a genetic algorithm, with rule 'fitness' evaluated from independent subsets of available occurrence data (Stockwell & Peters, 1999). Predictive accuracy is further refined by developing 100 replicate models and identifying a 'best subset' based on omission and commission error statistics to produce a final consensus result (Anderson et al., 2003). I used a soft omission threshold of 20% and commission threshold of 50%, with all other parameters left at default settings. This procedure produced a best subset comprised of 10 models that were in turn compiled to generate an estimate of the species' potential distribution.

Maxent represents an alternative methodology based on the principle of maximum entropy, in which probabilities assigned to each pixel in the landscape are spread out maximally between 0 and 1, subject to the constraint of matching the environmental attributes of known

occurrences as closely as possible. As in GARP analyses, independent subsets of available occurrence data are used for model generation and training. All Maxent runs were conducted under default settings as recommended in Phillips et al. (2006).

Occurrence data for each species were drawn from GPS coordinates (spatial resolution ~10 m) recorded during PNG collecting expeditions, whereas distributional data from Papua and West Papua, Indonesia, were assembled from museum-specimen locality information and first-hand sightings by BWB, with locality names georeferenced from published and online gazetteers when locality descriptors were sufficiently detailed and reliable. Because the focal taxa co-occur broadly, presence/absence data sets were nearly identical for each species, and hence the contemporary and paleoecological ENMs were also identical. Consequently, I present a single set of models for the combined analyses.

Of the 19 WorldClim bioclimatic coverages (1960-1990; Hijmans et al., 2005a), annual mean temperature, mean diurnal range, maximum temperature of the warmest month, minimum temperature of the coldest month, total annual precipitation, and precipitation of the wettest and driest months were used to develop the ENMs, as these variables show reduced correlation. Last Glacial Maximum climates were analyzed at 2.5' spatial resolution based on a downscaling recently developed by R. Hijmans (Waltari et al., 2007). To achieve this downscaling, general circulation model simulation results from two climate models (Community Climate System Model, CCSM, http://www.ccsm.ucar.edu/, Kiehl & Gent 2004; Model for Interdisciplinary Research on Climate (MIROC), ver. 3.2; http://www.ccsr.utokyo.ac.jp/) were downloaded from the PMIP2 website (http://www.pmip2.cnrs-gif.fr/) at a 2.8° spatial resolution (~300 x ~300 km). The 2.5' spatial resolution surfaces were created by calculating the difference between LGM and contemporary conditions, and interpolating the differences to a 2.5' resolution grid using the

spline function in ArcInfo (ESRI, Redlands, CA). Interpolated differences were then added to high-resolution WorldClim present-day climate data sets (Hijmans et al., 2005b) to create LGM bioclimatic coverages at resolutions relevant to the spatial scale of analysis while calibrating the simulated climate change data to the actual observed climate data. For spatial analyses of population expansion and contraction across climatic scenarios, GARP models were reclassified using the lowest presence thresholding approach described in Pearson et al. (2007), and area estimates calculated in ArcMap.

RESULTS

Sequence attributes

Sequence data were obtained from a combination of 4 mitochondrial genes for a total of 542 ingroup samples, with the concatenated data matrix varying in length from 1233 to 2063 base pairs depending on amplicon length and locus combination, as detailed in Table 3.1. Sequence alignment was straightforward for each taxon, and all samples appeared to be of mitochondrial origin rather than numts, as no stop codons were present within open reading frames, base composition was homogenous across samples, and codon-specific substitution rates were consistent with known biases (Sorenson & Quinn, 1998). Parsimony-informative sequence variation differed substantially among taxa, with *P. cyanus* containing the lowest percentage of informative sites at 7.9% (ND2); *C. robusta* sequences contained nearly twice the informative variation at 15.7%, while *R. atra* and *A. macgregoriae* exhibited more moderate levels at 11.1% and 9.5%, respectively (Table 3.1).

Ancient DNA sequencing resulted in clean chromatograms with no discrepancies among light and heavy strands due to degradation phenomena (e.g. deamination), as has been reported

Table 3.1. Attributes of sequence variation and best-fit substitution models for 3 mitochondrial markers across the 4 montane New Guinea birds examined in this study.

Taxon	Gene	Total sites	Informative sites (%)	Variable sites (%)	Nucleotide frequencies %A	%C	%G	%T	Best-fit model (BIC)
Amblyornis macgregoriae	ND2	1041	99 (9.5)	159 (15.3)	32.2	32.8	12.0	23.0	GTR+Γ
	ND3	351	25 (7.1)	35 (10.0)	30.5	33.2	13.0	23.3	TPM1uf+Γ
	mtDNA	1392	124 (8.9)	194 (13.9)	33.1	34.4	10.6	21.9	GTR+I+Γ
Rhipidura atra	ND2	882	98 (11.1)	119 (13.5)	31.4	30.4	12.1	26.2	HKY+I
	ND3	351	33 (9.4)	47 (13.4)	32.8	31.8	11.3	24.1	TPM2uf+I+Γ
	mtDNA	1233	131 (10.6)	119 (13.4)	30.1	30.7	13.0	26.2	TrN+I
Peneothello cyanus	ND2	867	69 (7.9)	95 (11.3)	30.3	34.3	11.9	23.5	TrN+I
	ND3	351	39 (11.1)	48 (13.7)	27.0	34.3	13.4	25.3	HKY+I
	ATP6-8	845	64 (9.3)	113 (13.3)	28.1	36.5	10.5	24.9	TrN+I
	mtDNA	2063	190 (9.2)	256 (12.4)	30.0	34.9	10.4	24.7	TrN+I+Γ
Crateroscelis robusta	ND2	834	131 (15.7)	167 (20.0)	31.0	37.0	11.6	20.4	TIM2+I+Γ
	ATP6-8	842	131 (15.5)	181 (21.5)	30.2	38.4	10.0	21.3	TrN+Γ
	mtDNA	1676	262 (15.6)	348 (20.7)	30.9	38.1	10.6	20.4	TrN+I+Γ

in previous studies that examined numerous ancient DNA samples of similar age (Hofreiter et al., 2001; Sefc et al., 2006). Furthermore, overlapping amplicons aligned without conflict, and patterns of genetic variation were congruent across fresh and ancient DNA samples.

Phylogenetic analyses and divergence times

Bayesian inference and maximum likelihood analyses produced near-identical topologies, differing only in terminal rearrangements within clusters of genetically similar individuals. As such, I present the BI phylogenetic results herein to maintain simplicity and clarity among topological comparisons (Figs. 3.2–3.5).

Monophyly was recovered for each focal taxon with significant posterior probability support; however, the presence of substantial genetic divergences within each taxon suggests that multiple species may be involved, and will require in depth analysis of regional variation in behavior, morphology, and ecology to address these issues thoroughly. Topological resolution and node support varied among taxa, with 2–3 primary phylogroups recovered in each species

complex. Deep genetic splits were revealed along the Strickland River Valley in *P. cyanus* and *C. robusta*, both of which consist of two reciprocally monophyletic phylogroups in western New Guinea that are sister to a Central Highlands + Papuan Peninsula phylogroup in the east (Figs. 3.2–3.3). By contrast, *R. atra* exhibited little genetic differentiation across the Strickland River Valley, and is composed of 3 geographically structured phylogroups including a highly divergent Vogelkop lineage that is sister to a Papuan Peninsula lineage in the east and a broadly distributed lineage that extends from the Watut/Tauri River valley west to the Wandamen Mountains, including outlying sky-island populations along the north coast (Fig. 3.4). Perhaps most surprising given its polygynous breeding system, *A. macgregoriae* exhibited the least genetic variation of any taxon throughout the CDRs and Papuan Peninsula, with populations forming a weakly structured Central Highlands, Papuan Peninsula, and Adelbert Mountains phylogroup that is sister to a highly divergent Huon Peninsula lineage (Fig. 3.5). Intraspecific ND2 pairwise sequence divergences also varied considerably among focal taxa with *P. cyanus* and *A. macgregoriae* showing the least genetic divergence among primary phylogroups at 1.15%–4.08% and 4.2%–4.7% respectively, whereas *R. atra* and *C. robusta* and contained more substantial divergences among phylogroups at 1.8%–7.7% and 2.3%–8.97%, respectively. As such, coalescent estimates of divergence times were more recent among *P. cyanus* and *A. macgregoriae* ranging from 515,500–1,242,000 ybp (95% HPD 279,000 –742,500 to 691,000 – 1,844,000 ybp) to 682,000–1,522,500 ybp (95% HPD 254,500–871,000 to 653,200–2,050,000) respectively, assuming mutation scalars of 2–5%. By contrast, coalescence of *R. atra* and *C. robusta* primary phylogroups appear to have taken place in the mid Pliocene, ranging from 1,698,000–4,275,500 (95% HPD 705,500–2,291,000 to 1,889,500–5,684,000) to 1,933,000–4,830,000 ybp (95% HPD 836,000–2,478,000 to 2,090,000–6,195,000 ybp), respectively.

Population structure and demography

Pairwise F_{ST} values and median-joining networks revealed evidence of strong geographic structure consistent with ML and BI results (Fig. 3.6). Population genetic analyses identified 78 (*P. cyanus*), 58 (*C. robusta*), 62 (*R. atra*), and 54 (*A. macgregoriae*) unique ND2 haplotypes among focal taxa, of which 49, 53, 48, and 49 were private haplotypes respectively (Table 3.2, Fig. 3.6). The average pairwise number of nucleotide differences among taxa (*k*) ranged from 6.48 in *A. macgregoriae* to 24.67 in *C. robusta*, a pattern also evident in estimates of nucleotide diversity (π), which ranged from 1.29% to 4.93% respectively. Estimates of haplotype diversity were high in each species complex, ranging from 0.934 in *R. atra* to 0.968 in *C. robusta*. As expected, indices of intraspecific genetic diversity were highest among populations of the Central Highlands and Papuan Peninsula, whereas smaller sky-island populations along the northern coast exhibited lower levels of genetic diversity (Table 3.2). Populations in the Vogelkop and Huon Peninsula represent exceptions to this trend, with levels of genetic diversity comparable to populations of the CDRs, likely reflecting their larger size and perhaps weak regional genetic structure associated with rugged local topography.

Hierarchical three-way analyses of molecular variance revealed that much of the genetic variation within *P. cyanus* (63.2%) and *C. robusta* (80.0%) is partitioned by subspecific taxonomic arrangements, which largely coincide with the distribution of contemporary sky-islands (Table 3.3). The distribution of LGM sky-island populations accounted for the least genetic diversity among the 3 partitioning schemes, and relatively little variation was distributed within populations for either taxa. By comparison, taxonomy had no explanatory power within *R. atra*, in which 81% of the genetic diversity is distributed among contemporary sky-islands. These results are in contrast with *A. macgregoriae*, in which 76% of the variation among groups

Figure 3.2–3.5. Bayesian inference topologies of 4 montane New Guinea passerines including *Amblyornis macgregoriae* (3.2), *Rhipidura atra* (3.3), *Peneothello cyanus* (3.4), and *Crateroscelis robusta* (3.5). Significant posterior probability node support (≥ 0.95) is indicated by blacked circles, whereas nodes that received < 0.50 posterior probability support were collapsed. Phylogenetic relationship among outgroup taxa are depicted within the insets.

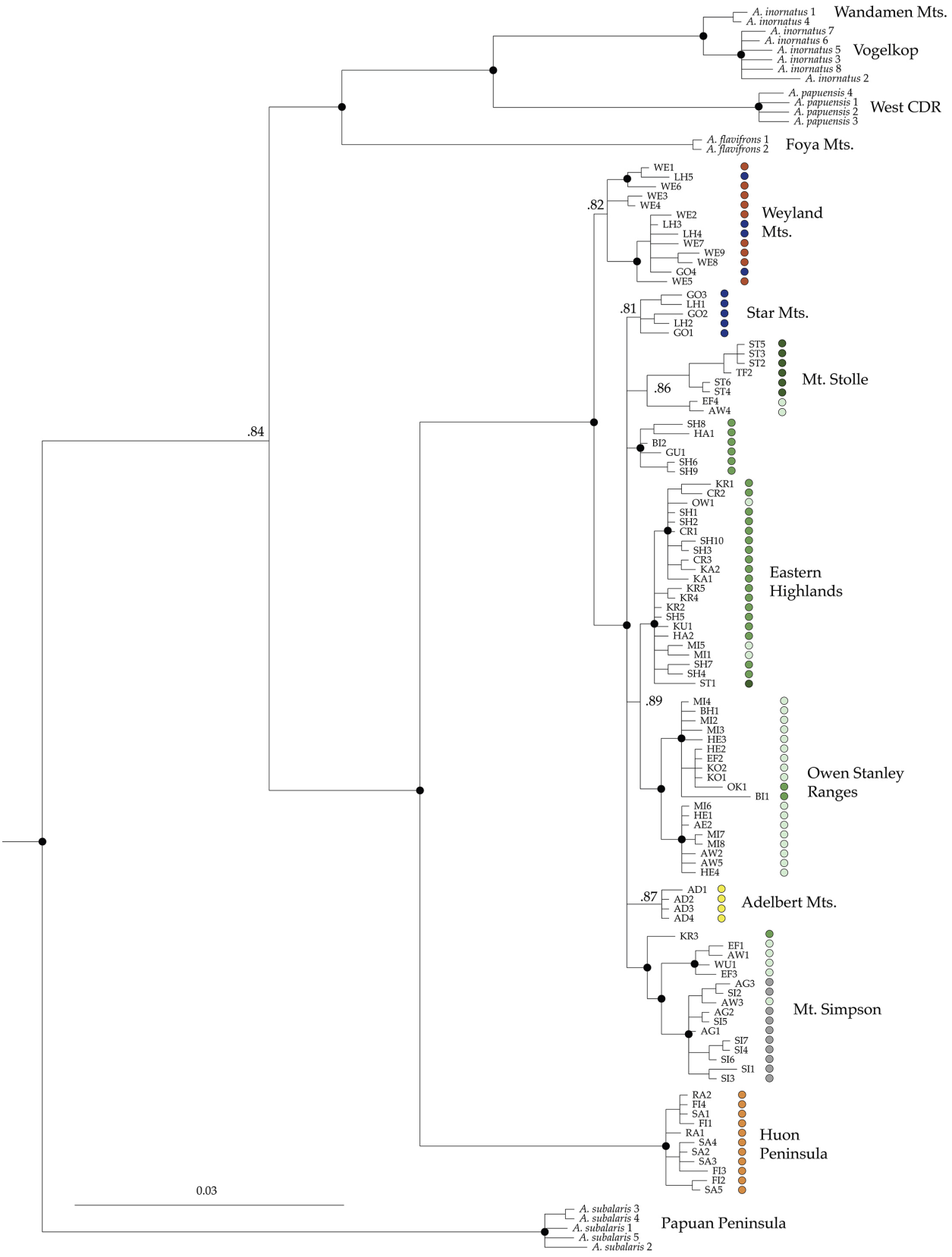
A. inornatus 1
A. inornatus 4
Wandamen Mts.
A. inornatus 7
A. inornatus 6
A. inornatus 5
A. inornatus 3
A. inornatus 8
A. inornatus 2
Vogelkop
A. papuensis 4
A. papuensis 1
A. papuensis 2
A. papuensis 3
West CDR
A. flavifrons 1
A. flavifrons 2
Foya Mts.
WE1
LH5
WE6
WE3
WE4
WE2
LH3
LH4
WE7
WE9
WE8
GO4
WE5
.82
Weyland Mts.
GO3
LH1
GO2
LH2
GO1
.81
Star Mts.
ST5
ST3
ST2
TF2
ST6
ST4
.86
EF4
AW4
Mt. Stolle
.84
SH8
HA1
BI2
GU1
SH6
SH9
KR1
CR2
OW1
SH1
SH2
CR1
SH10
SH3
CR3
KA2
KA1
KR5
KR4
KR2
SH5
KU1
HA2
MI5
MI1
SH7
SH4
ST1
Eastern Highlands
.89
MI4
BH1
MI2
MI3
HE3
HE2
EF2
KO2
KO1
OK1
BI1
MI6
HE1
AE2
MI7
MI8
AW2
AW5
HE4
Owen Stanley Ranges
AD1
AD2
AD3
AD4
.87
Adelbert Mts.
KR3
EF1
AW1
WU1
EF3
AG3
SI2
AW3
AG2
SI5
AG1
SI7
SI4
SI6
SI1
SI3
Mt. Simpson
RA2
FI4
SA1
FI1
RA1
SA4
SA2
SA3
FI3
FI2
SA5
Huon Peninsula
0.03
A. subalaris 3
A. subalaris 4
A. subalaris 1
A. subalaris 5
A. subalaris 2
Papuan Peninsula

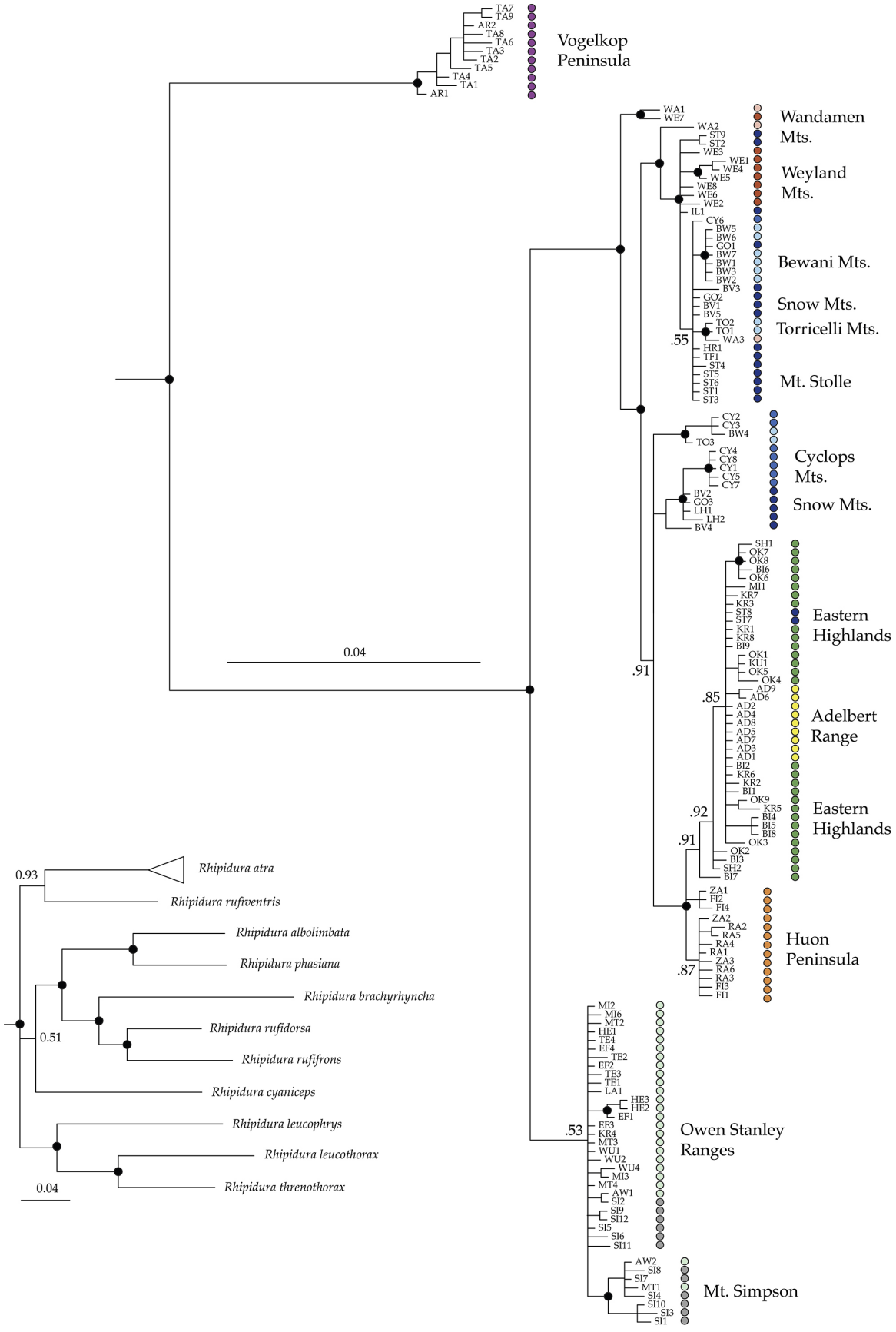
Vogelkop Peninsula
Wandamen Mts.
Weyland Mts.
Bewani Mts.
Snow Mts.
Torricelli Mts.
Mt. Stolle
Cyclops Mts.
Snow Mts.
Eastern Highlands
Adelbert Range
Eastern Highlands
Huon Peninsula
Owen Stanley Ranges
Mt. Simpson
0.04
.91
.85
.92
.91
.87
.55
.53
0.93
0.51
0.04
Rhipidura atra
Rhipidura rufiventris
Rhipidura albolimbata
Rhipidura phasiana
Rhipidura brachyrhyncha
Rhipidura rufidorsa
Rhipidura rufifrons
Rhipidura cyaniceps
Rhipidura leucophrys
Rhipidura leucothorax
Rhipidura threnothorax

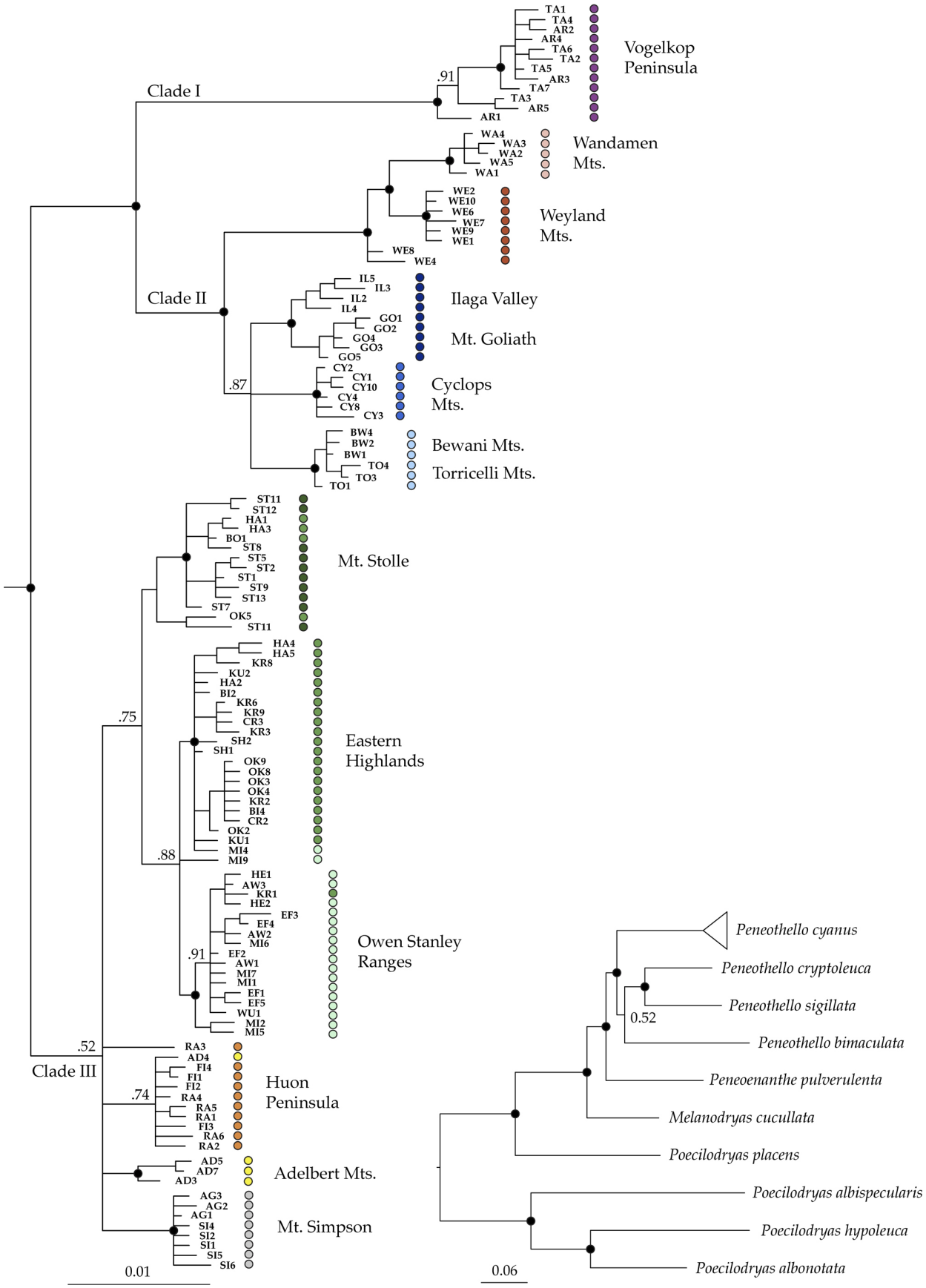
Clade I
Clade II
Clade III
.91
.87
.75
.88
.52
.74
.91
TA1
TA4
AR2
AR4
TA6
TA2
TA5
AR3
TA7
TA3
AR5
AR1
Vogelkop Peninsula
WA4
WA3
WA2
WA5
WA1
Wandamen Mts.
WE2
WE10
WE6
WE7
WE9
WE1
WE8
WE4
Weyland Mts.
IL5
IL3
IL2
IL4
GO1
GO2
GO4
GO3
GO5
Ilaga Valley
Mt. Goliath
CY2
CY1
CY10
CY4
CY8
CY3
Cyclops Mts.
BW4
BW2
BW1
TO4
TO3
TO1
Bewani Mts.
Torricelli Mts.
ST11
ST12
HA1
HA3
BO1
ST8
ST5
ST2
ST1
ST9
ST13
ST7
OK5
ST11
Mt. Stolle
HA4
HA5
KR8
KU2
HA2
BI2
KR6
KR9
CR3
KR3
SH2
SH1
OK9
OK8
OK3
OK4
KR2
BI4
CR2
OK2
KU1
MI4
MI9
Eastern Highlands
HE1
AW3
KR1
HE2
EF3
EF4
AW2
MI6
EF2
AW1
MI7
MI1
EF1
EF5
WU1
MI2
MI5
Owen Stanley Ranges
RA3
AD4
FI4
FI1
FI2
RA4
RA5
RA1
FI3
RA6
RA2
Huon Peninsula
AD5
AD7
AD3
Adelbert Mts.
AG3
AG2
AG1
SI4
SI2
SI1
SI5
SI6
Mt. Simpson
0.01
Peneothello cyanus
Peneothello cryptoleuca
Peneothello sigillata
0.52
Peneothello bimaculata
Peneoenanthe pulverulenta
Melanodryas cucullata
Poecilodryas placens
Poecilodryas albispecularis
Poecilodryas hypoleuca
Poecilodryas albonotata
0.06

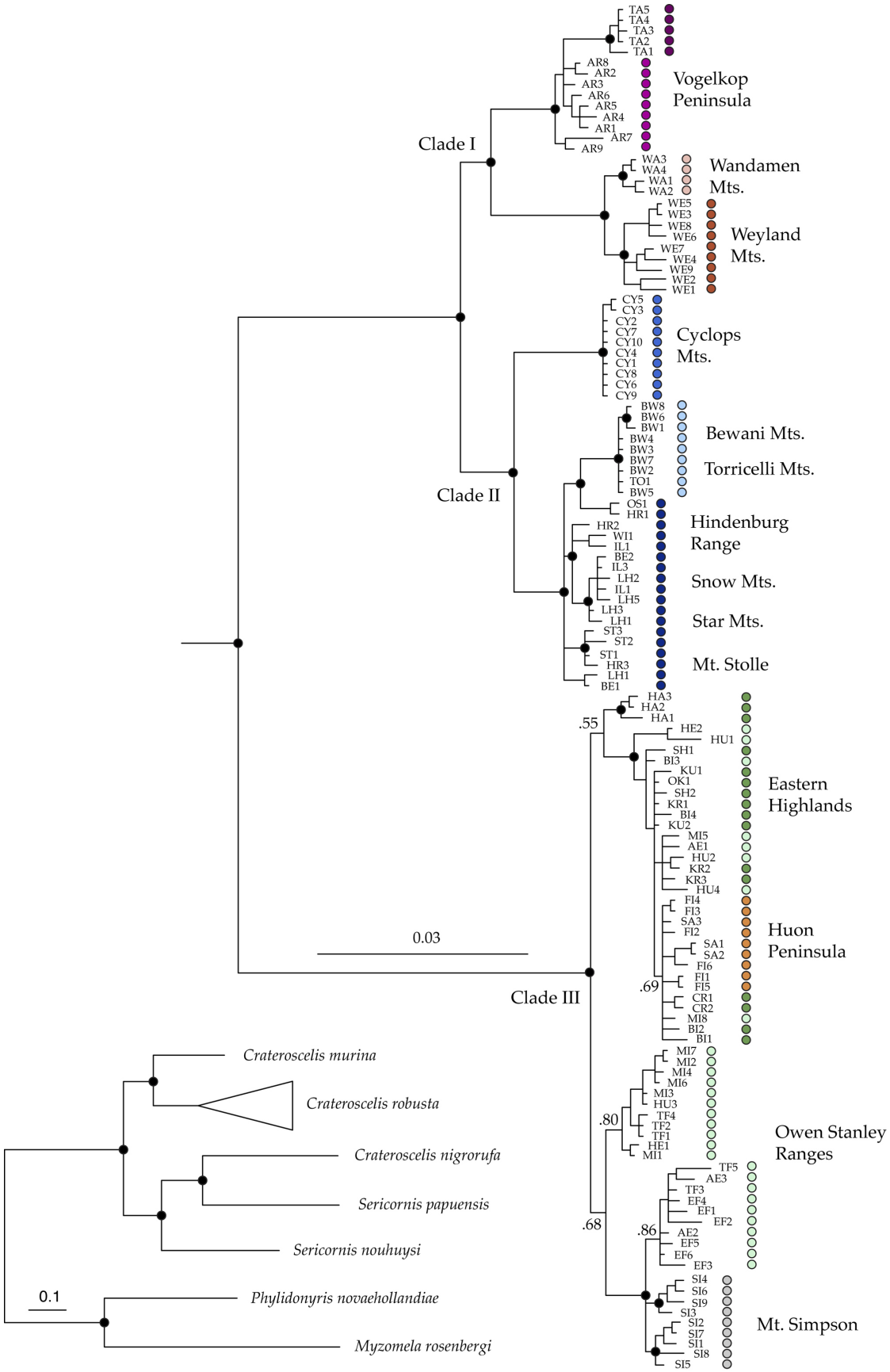
Clade I
Clade II
Clade III
Vogelkop Peninsula
Wandamen Mts.
Weyland Mts.
Cyclops Mts.
Bewani Mts.
Torricelli Mts.
Hindenburg Range
Snow Mts.
Star Mts.
Mt. Stolle
Eastern Highlands
Huon Peninsula
Owen Stanley Ranges
Mt. Simpson
0.03
0.1
.55
.69
.80
.68
.86
Crateroscelis murina
Crateroscelis robusta
Crateroscelis nigrorufa
Sericornis papuensis
Sericornis nouhuysi
Phylidonyris novaehollandiae
Myzomela rosenbergi

Table 3.2. Summary of population-level genetic diversity among 4 avian taxa based on ND2 sequences (500bp).

Taxon	Population	*n*	Unique Haplotypes	Segregating Sites	Θ (site)	*k*	Haplotype Diversity	Nucleotide Diversity (π)
Peneothello cyanus	Vogelkop	13	5	5	0.00322	1.000	0.628	0.00200
	Wandamen	5	2	1	0.00096	0.600	0.600	0.00120
	Weyland	10	5	4	0.00263	1.311	0.756	0.00282
	Ilaga /Goliath	10	5	5	0.00354	1.511	0.756	0.00302
	Cyclops	10	2	2	0.00141	0.400	0.200	0.00080
	Torricelli	10	3	2	0.00141	0.667	0.600	0.00133
	Mt. Stolle	14	5	4	0.00251	1.088	0.725	0.00217
	E. Highlands	39	8	8	0.00378	1.371	0.781	0.00274
	Huon	10	4	3	0.00212	0.600	0.533	0.00120
	Adelbert	8	3	2	0.00154	0.821	0.679	0.00164
	Owen Stanley	22	8	8	0.00438	1.186	0.602	0.00237
	Mt. Simpson	10	3	2	0.00141	0.400	0.37.8	0.00080
	Total	161	49	54	0.01941	7.604	0.953	0.01518
Crateroscelis robusta	Tamrau	5	2	1	0.00096	0.400	0.400	0.00080
	Arfak	9	3	4	0.00294	1.222	0.666	0.00244
	Wandamen	4	1	0	NA	NA	NA	NA
	Weyland	9	4	6	0.00442	1.333	0.583	0.00267
	Western CDR s	18	9	11	0.00640	1.712	0.803	0.00342
	Cyclops	10	2	1	0.00071	0.355	0.355	0.00071
	Torricelli	9	2	1	0.00074	0.222	0.222	0.00044
	E. Highlands	17	12	13	0.00769	2.117	0.941	0.00424
	Huon	9	4	3	0.00221	1.000	0.777	0.00200
	Owen Stanley	28	14	15	0.00771	2.034	0.883	0.00407
	Mt. Simpson	9	4	3	0.00222	0.944	0.750	0.00189
	Total	127	53	89	0.03286	24.67	0.968	0.04934
Rhipidura atra	Vogelkop	11	6	6	0.00365	1.818	0.873	0.00364
	Wandamen	3	3	6	0.00809	4.000	1.0	0.00800
	Weyland	8	5	8	0.00402	2.000	0.786	0.00400
	Western CDRs	22	8	12	0.00549	2.723	0.740	0.00545
	Cyclops	8	3	12	0.01021	5.036	0.607	0.01007
	Torricelli	10	4	9	0.00618	3.067	0.644	0.00613
	E. Highlands	29	8	14	0.00330	1.640	0.707	0.00328
	Huon	13	6	4	0.00195	0.974	0.718	0.00195
	Adelbert	9	3	2	0.00122	0.611	0.417	0.00122
	Owen Stanley	25	8	19	0.00435	2.160	0.637	0.00432
	Mt. Simpson	12	8	9	0.00577	2.864	0.924	0.00573
	Total	150	48	75	0.02297	11.145	0.93.4	0.02098
Amblyornis macgregoriae	Weyland	9	7	7	0.00514	2.389	0.917	0.00477
	Western CDRs	9	8	11	0.00808	3.667	0.972	0.00732
	Mt. Stolle	7	4	7	0.00570	2.571	0.810	0.00513
	E. Highlands	27	12	20	0.01036	2.142	0.769	0.00428
	Huon	11	6	5	0.00341	1.564	0.873	0.00312
	Adelbert	4	2	1	0.00109	0.500	0.500	0.00100
	Owen Stanley	27	12	14	0.00777	3.157	0.855	0.00630
	Mt. Simpson	10	3	2	0.00141	0.711	0.622	0.00142
	Total	104	49	58	0.0291	6.480	0.962	0.01293

Figure 3.6. Minimum spanning networks of ND2 haplotype relationships among 4 montane New Guinea passerines. The number of individuals sharing a given haplotype are indicated within each ellipse, while values along network branches denote the number of mutational steps between haplotypes. Populations are color-coded and linked with collection localities depicted in the DEM featured in Figure 3.1.

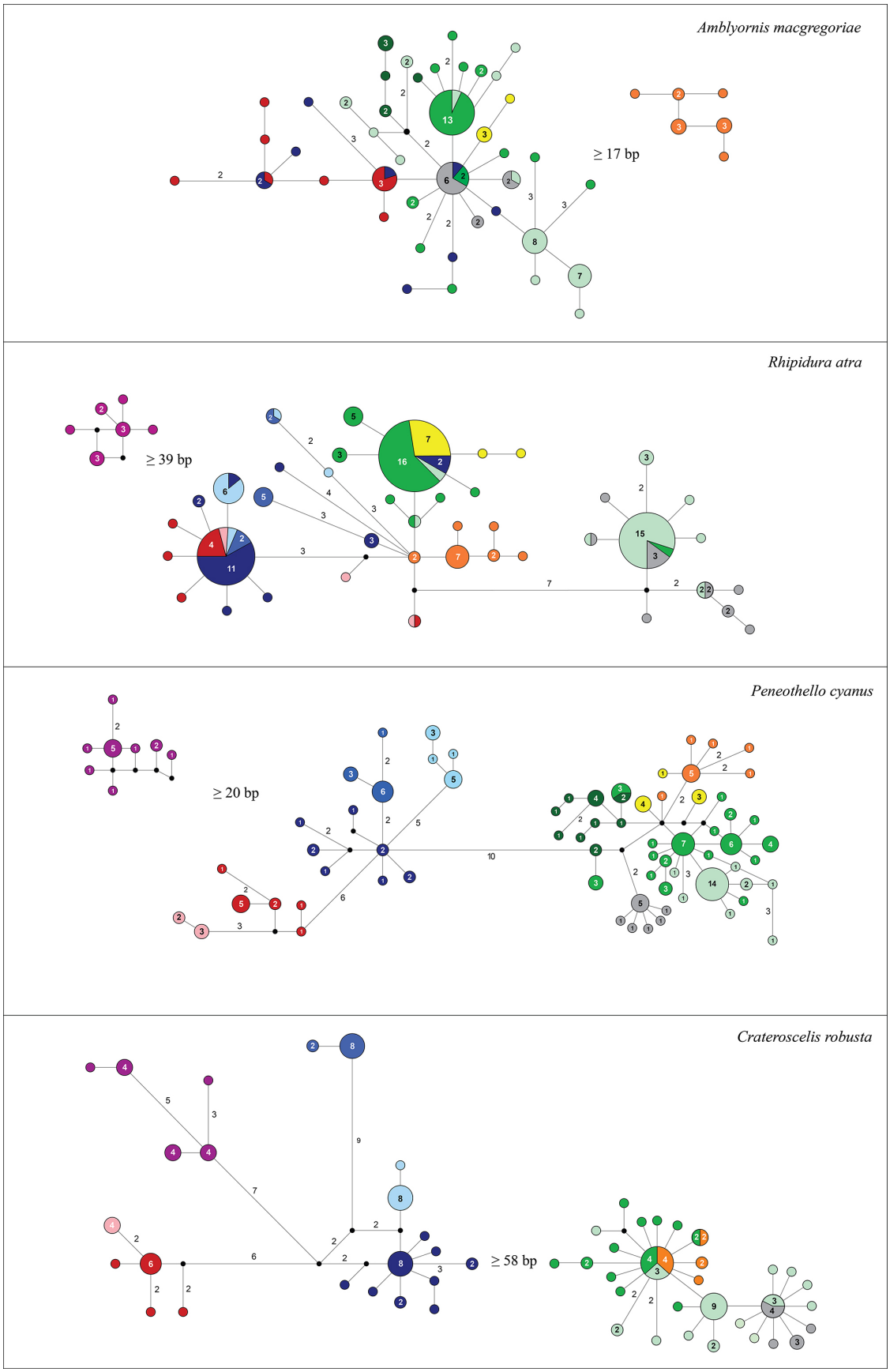
Amblyornis macgregoriae
≥ 17 bp
Rhipidura atra
≥ 39 bp
Peneothello cyanus
≥ 20 bp
Crateroscelis robusta
≥ 58 bp

Table 3.3 Results of hierarchical three-way analyses of molecular variance partitioned by contemporary sky-islands, LGM sky-islands, and taxonomy. Statistical significance at the P=0.001 level is indicated by **, whereas significance at the $P \leq 0.05$ in denoted by *.

		Percent Variation					
Taxon	Partitioning Scheme	Among Groups	Among Populations	Within Populations	Φ_{ct}	Φ_{st}	Φ_{sc}
Peneothello cyanus	Present	50	36	14	0.56**	0.86**	0.67*
	LGM	34	53	13	0.80**	0.87**	0.34
	Taxonomy	63	26	11	0.71**	0.89**	0.63**
Crateroscelis robusta	Present	55	37	8	0.54	0.91**	0.81**
	LGM	16	76	8	0.15	0.91**	0.90**
	Taxonomy	80	13	7	0.79**	0.92**	0.64**
Rhipidura atra	Present	81	2	17	0.09**	0.82	0.81*
	LGM	44	41	15	0.74**	0.85**	0.44
	Taxonomy	0	76	24	0.83**	0.75**	0.47
Amblyornis macgregoriae	Present	53	19	28	0.41**	0.72**	0.52
	LGM	76	10	14	0.42**	0.86**	0.76*
	Taxonomy	50	22	28	0.44**	0.71**	0.49

was explained by the distribution of LGM sky-island populations, whereas contemporary sky-island populations accounted for 53% of the variation among groups. Mantel tests recovered significant evidence of an isolation-by-distance effect in *P. cyanus* (r=0.57, P=0.0002), *C. robusta* (r=0.41, P<0.0001), and *R. atra* (r=0.32, P=0.001), with each analysis indicating positive correlations between genetic and geographic distances; however, moderate to low r values suggest other factors are at play as well. A weak but significant negative correlation was revealed in *A. macgregoriae*, which reflects its shallow genetic structure throughout the CDRs and Papuan Peninsula coupled with the presence of a highly divergent lineage in the Huon.

Bayesian skyline analyses recovered clear signatures of population growth in each taxon, followed by slight contractions in effective population size in all but *R. atra* (Fig. 3.7). Analyses of population genetic summary statistics revealed evidence of non-neutrality in each species complex, with negative Fu's *Fs* and Tajima's *D* values indicating demographic expansion among populations of the CDRs and Papuan Peninsula. Evidence of population growth was also recovered from Vogelkop and Huon Peninsula populations in *P. cyanus*, *R. atra* and *A.*

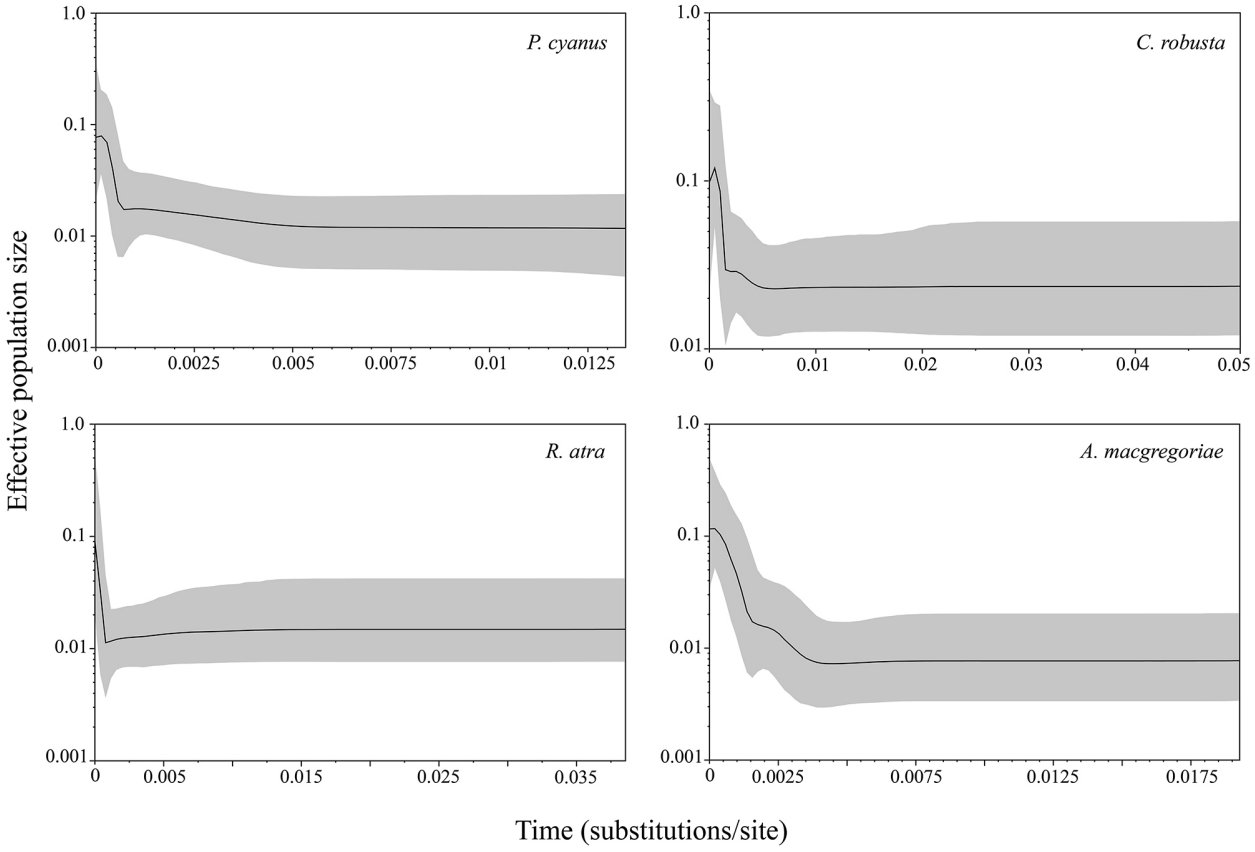

Figure 3.7. Bayesian skyline plots depicting the demographic history of 4 montane New Guinea passerines. The central black line represents the median effective population size as a function of time, N_e*t ($\log_{10}$) and the grey shaded interval depicts the 95% highest posterior probability density.

Table 3.4. Demographic summary statistics derived from the haplotype distribution, frequency spectrum of mutation, and distribution of pairwise sequence differences. Statistically significant results (p-value ≤ 0.05) are indicated in bold. FU's *Fs* statistics are significant at the $p \leq 0.02$ level.

Taxon	Population	*n*	Tajima's *D*	Ramos-Onsin & Rozas R_2	FU's *Fs*	Raggedness Index (*r*)
Peneothello cyanus	Vogelkop	13	-0.9823	**0.0957**	**-5.304**	0.064
	Wandamen	5	-0.5619	**0.1612**	**-2.862**	0.140
	Weyland	10	-0.7637	0.1189	-1.976	0.034
	Ilaga /Goliath	10	-0.1275	0.1400	-3.087	0.023
	Cyclops	10	-1.1163	0.1818	-2.082	0.161
	Torricelli	10	0.5193	0.1792	-1.002	0.227
	Mt. Stolle	14	-0.6752	0.1155	-2.247	**0.013**
	E. Highlands	39	-1.4008	**0.0641**	**-11.106**	**0.010**
	Huon	10	**-1.8528**	**0.1019**	**-5.147**	0.043
	Adelbert	8	-0.3030	0.2278	2.913	0.146
	Owen Stanley	22	**-1.9335**	**0.0533**	**-13.134**	0.031
	Mt. Simpson	10	-1.4628	**0.1110**	**-3.713**	0.112
	Total	161	-0.8008	0.0655	**-34.055**	**0.0010**
Craterosceli s robusta	Tamrau	5	-0.5089	0.4000	1.040	0.6800
	Arfak	9	-0.76457	0.1635	-0.877	0.0741
	Wandamen	4	-0.61237	0.4330	0.172	0.2500
	Weyland	9	-1.15164	**0.1072**	**-4.279**	0.0563
	Western CDR s	18	-1.19159	**0.0818**	**-6.571**	0.0295
	Cyclops	10	0.01499	0.1778	0.417	0.2099
	Torricelli	9	-0.06382	0.2008	-0.239	0.0802
	E. Highlands	17	-1.1497	**0.0863**	**-4.070**	0.0313
	Huon	9	-1.14917	0.1525	-1.776	0.0980
	Owen Stanley	28	-0.83212	**0.0853**	**-7.618**	0.0160
	Mt. Simpson	9	-0.50521	**0.1254**	**-3.427**	0.2014
	Total	127	0.88366	0.1183	-12.998	0.0013
Rhipidura atra	Vogelkop	11	-1.25910	**0.0874**	**-4.781**	0.0417
	Wandamen	3	NA	0.1000	NA	0.4444
	Weyland	8	-1.32527	0.1575	**-3.514**	0.0510
	Western CDRs	22	-0.79279	0.1020	0.013	0.0493
	Cyclops	8	0.12850	0.1933	4.356	0.6620
	Torricelli	10	-0.33667	0.1578	3.142	0.3960
	E. Highlands	29	**-2.22164**	0.0910	**-8.163**	0.0276
	Huon	13	-0.99041	**0.0999**	**-4.370**	0.0764
	Adelbert	9	-0.58325	0.1848	-0.532	0.1690
	Owen Stanley	25	**-2.06203**	0.1220	**-8.176**	**0.0194**
	Mt. Simpson	12	-0.56834	0.1056	**-4.490**	0.0944
	Total	150	-0.53302	0.0765	**-20.447**	0.0074
Amblyornis macgregoriae	Weyland	9	-0.46795	**0.0510**	**-3.286**	**0.0028**
	Western CDRs	9	-0.69828	**0.1056**	-2.778	**0.0293**
	Mt. Stolle	7	-0.57081	0.2587	2.627	0.1995
	E. Highlands	27	**-2.11889**	**0.0464**	**-14.404**	**0.0053**
	Huon	11	-0.97023	**0.1016**	**-4.090**	**0.0360**
	Adelbert	4	-0.70990	0.4330	1.099	0.7500
	Owen Stanley	27	-1.12609	0.0795	**-7.643**	0.0328
	Mt. Simpson	10	-0.33947	0.1489	-2.732	0.0444
	Total	104	-1.48544	0.0532	-30.176	0.0129

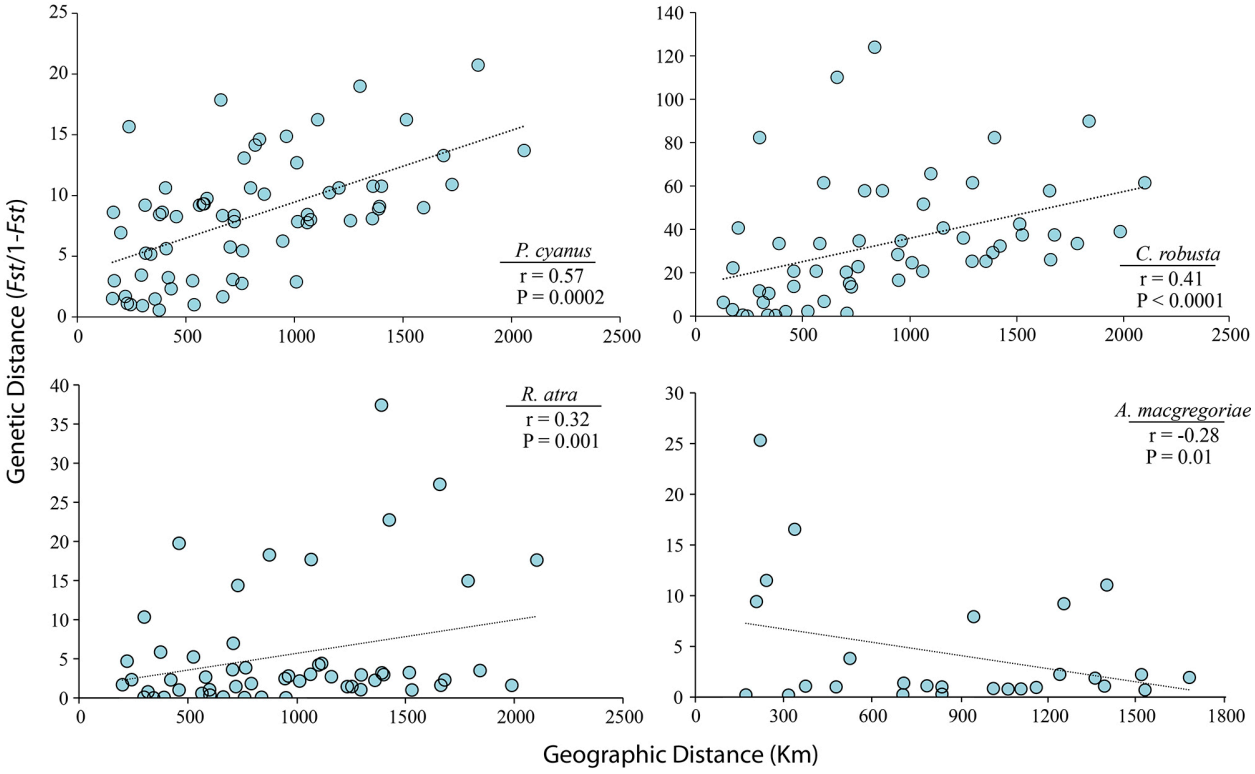

Figure 3.8. Results of Mantel tests conducted on 4 montane New Guinea passerines indicating significant positive relationships among geographic and genetic distances in all but *Amblyornis macgregoriae*.

macgregoriae (Table 3.4). Ramos-Onsin & Rozas R_2 statistics were consistent with Fu's *Fs* and Tajima's *D* values, indicating demographic expansion in the same populations, whereas raggedness indices failed to reject stability in most populations (Table 3.4).

Ecological niche modeling

As expected, ecological niche reconstructions were nearly identical across all focal taxa, reflecting the high degree of co-distribution and shared sampling localities among analyses. Although each species complex exhibits subtle differences in local ecological niche preferences (e.g. forest age, floristic composition, and level of disturbance), the environmental data layers used in the present study are incapable of resolving these dimensions of ecological variation. Consequently, I present a single set of contemporary and LGM distribution models generated in desktop GARP to form the basis of discussion on climate change and historical diversification within the island's montane avifauna. Because co-distributed species exhibit individual and potentially distinct responses to shared climatic fluctuations (Graham, et al., 1999; Mousalli, et al., 2009; Lawson, 2010), the use of representative ecological niche models in this comparative investigation requires cautious interpretation and constitutes a critical methodological limitation.

Contemporary ENMs recovered strong environmental suitability throughout the New Guinea highlands with sharp elevational boundaries that correspond to lower and upper montane rainforest distributional limits. These models are largely consistent with known distributions of each focal species; however, *A. macgregoriae* has yet to colonize suitable habitats predicted in the Torricelli/Bewani Ranges, whereas favorable conditions in the Foya, Wandamen, Bomberai, and Vogelkop highland terranes are occupied by closely related sister taxa (Fig. 3.2). Extensive intermontane valleys associated with the Strickland, Watut, Tari, and Adau river drainages

Figure 3.9. Ecological niche reconstructions depicting the potential distribution of focal taxa under contemporary and Last Glacial Maximum climatic conditions. Insets show greater detail in the Strickland (I), Watut/Tauri (II) and Adau (III) river drainages under present-day and LGM climates.

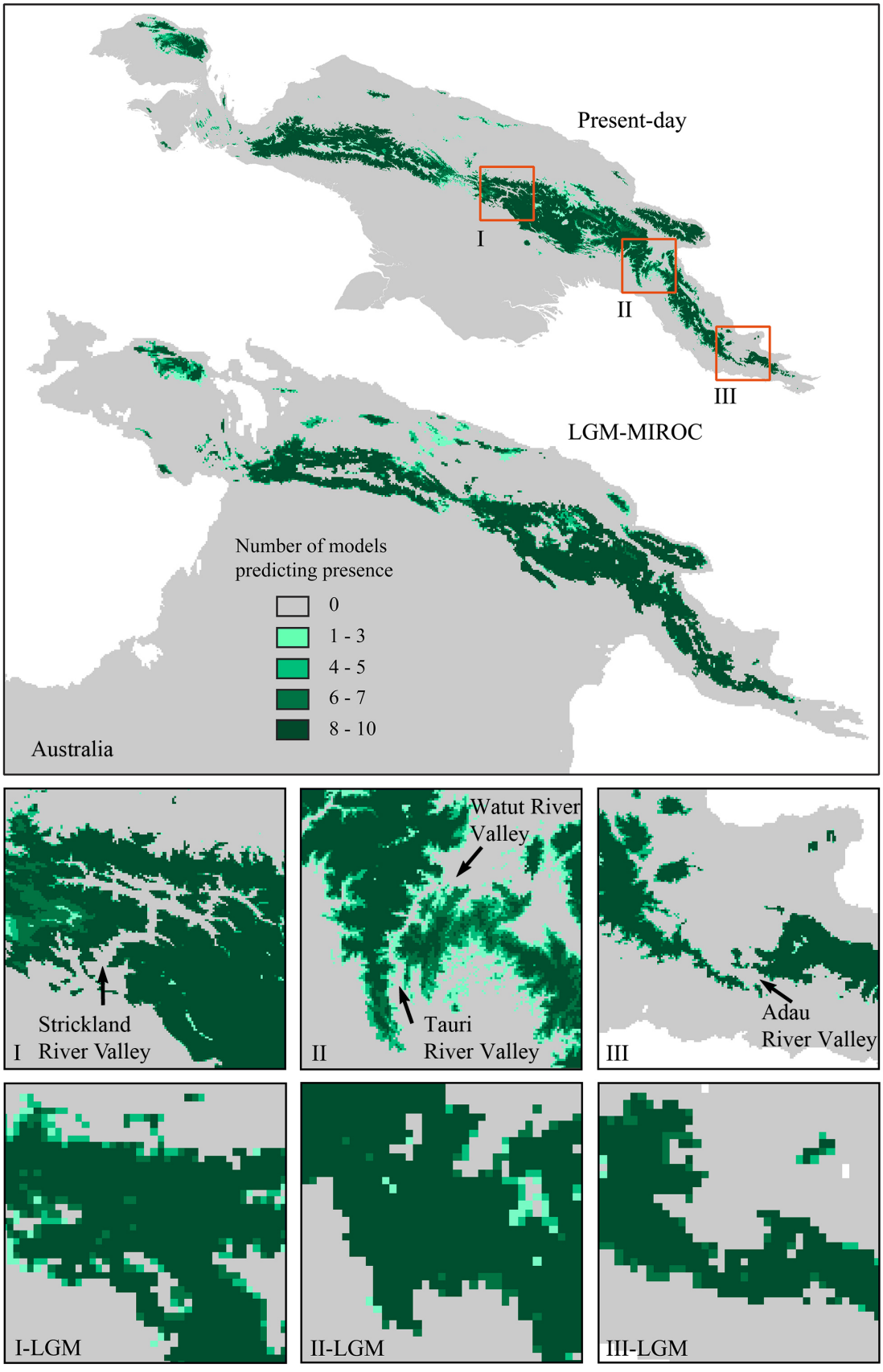
Present-day
I
II
III
LGM-MIROC
Number of models
predicting presence
0
1 - 3
4 - 5
6 - 7
8 - 10
Australia
Strickland
River Valley
I
Watut River
Valley
Tauri
River Valley
II
Adau
River Valley
III
I-LGM
II-LGM
III-LGM

correspond to narrow breaks in ecological suitability predicted across the CDRs and Papuan Peninsula; nonetheless, these potential geographic barriers seldom span more than 5 km at their widest points, and the headwater drainages of the Strickland River Valley fail to bisect fully the northern slopes of the Central Ranges (Fig. 3.9). The Ramu–Markham River Valley forms a more substantial biogeographic barrier, spanning ~35 km near the Markham Delta and effectively isolating the Huon Peninsula from adjacent Bismarck and Owen Stanley ranges. Broad lowland basins associated with the Sepik and Idenburg drainages comprise far more expansive barriers, isolating coastal sky-islands of the Torricelli/Bewani and Cyclops ranges, whereas the Bird's Neck, and Vogelkop populations are isolated by expanses of unsuitable environmental conditions associated with lowland rainforest and narrow hill forest land bridges. An unexpected break in ecological suitability was recovered in the vicinity of Oksibil, along the southern slopes of the Star Mountains; however, this feature appears to be the consequence of a localized anomaly in the BIO12 (mean annual precipitation) environmental data layer, likely owing to the lack of weather stations in the region, as contemporary Spot-4 satellite imagery indicates that narrow but continuous corridors of montane rainforest extend along the southern and northern slopes of the Star Mountains (Stibig, et al., 2003).

Although clear signatures of elevational depression were revealed among LGM ecological niche reconstructions based on MIROC and CCSM general circulation models, the distribution of environmental suitability differed substantially among these models, particularly in the Vogelkop, CDRs, and Papuan Peninsula. Niche projections generated with the MIROC data set recovered a pattern of increased population connectivity throughout the CDRs, whereas CCSM projections exhibited extensive breaks in environmental suitability across the southern slopes of the Snow Mountains and northern limits of the Owen Stanley Ranges, contradicting

what is currently known in terms of the paleoecology of the region (Appendix 2.5). As such, the MIROC paleoecological niche reconstructions were used to form the basis of discussion on LGM climate fluctuations and spatial patterns of genetic diversity. Fully contiguous corridors of environmental suitability were recovered across the Eastern Highlands and Papuan Peninsula including the Strickland, Watut, Tauri, and Adau river valleys (Fig. 3.9). Evidence of a narrow corridor linking Mt. Bosavi to the Muller Range was revealed in the Southern Highlands, whereas sky-island populations along the north coast and Bird's Neck region most likely remained isolated by substantial tracts of lowland rainforest and seasonal swamplands.

DISCUSSION

Deciphering the evolutionary mechanisms that generate geographic variation among closely related populations is fundamental to advancing understanding of speciation processes and regional patterns of biotic diversity (Darwin, 1859; Mayr, 1963; Coyne & Orr, 2002; Futuyma, 2009). The origin of New Guinea's high species richness and fine-scale endemism within broadly distributed montane lineages has frequently been attributed to the island's complex geological history, rugged topographic relief, and paleoclimatic oscillations associated with Milankovitch cycles; however, the absence of detailed phylogeographic knowledge throughout the region has hindered testing these hypotheses with rigor for most taxonomic groups (Diamond, 1972; 1973; Pratt, 1982; Heads, 2002). This investigation represents the first comparative phylogeographic analysis for any vertebrate group within the New Guinea highlands, yielding novel insight into the evolutionary history of the island's montane avian diversity. Bayesian inference analyses and haplotype networks revealed substantial discordance in the distribution of genetic diversity among focal taxa, which coupled with disparity in

estimates of divergence times between regional phylogroups and contrasting patterns of lineage sorting, indicates a complex evolutionary history within New Guinea's highland avifauna. Herein, spatial distributions of genetic diversity are discussed in context of the island's geological history and paleoecology to evaluate how environmental factors have shaped avian diversification across New Guinea's extensive montane landscape.

Phylogeny and population genetic structure

Amblyornis macgregoriae —In contrast to its range restricted congenerics, *A. macgregoriae* is broadly distributed throughout the New Guinea highlands, spanning the Papuan Peninsula and CDRs as well as north coast Finisterre terranes in the Adelbert Mountains and Huon Peninsula. Bayesian inference analysis recovered two primary phylogroups within *A. macgregoriae*, including a highly divergent Huon Peninsula lineage that is sister to a weakly structured cluster of populations from the CDRs, Papuan Peninsula, and Adelbert Mountains (Fig. 3.2). Estimates of divergence times indicate coalescence among these lineages in the mid to early Pleistocene (682,000–1,522,500 ybp), which is consistent with the recent accretion history and rapid orogenic uplift of the Huon Peninsula (Pigram & Davies, 1987; Abbott et al., 1994; 1997). Although genetic divergences among phylogroups (4.2%–4.7%) are comparable to species-level splits among other *Amblyornis* bowerbirds, I defer taxonomic recommendations pending in-depth analysis of courtship phenotype and morphological variation throughout the complex (in prep). Analysis of pairwise F_{st} values and median-joining networks revealed 8 distinct populations within *A. macgregoriae*, yet with the exception of Adelbert Mountain and Huon Peninsula samples; all populations exhibited evidence of gene flow or ancestral polymorphism as inferred by shared haplotypes throughout the CDRs and Papuan Peninsula (Fig. 3.6). The

absence of substantial genetic structure across prominent biogeographic boundaries such as the Strickland Gorge and Watut/Tauri River Valley is surprising, which, combined with the lack of lineage sorting among adjacent and distantly isolated populations, casts doubt on the validity of four currently recognized subspecies in the Central Highlands (Schodde & McKean, 1973). This pattern of shallow genetic structure may reflect the extended maturation period characteristic of *Amblyornis* bowerbirds in which young males typically spend 4–5 years attaining the skills to successfully construct and defend their own courtship bowers (Frith & Frith, 2004). During this time, young males often inhabit substandard environments at lower elevations because prime ridge-top habitats are occupied by dominant adult males. Consequently, these immature individuals are thought to be prone to wandering, which may facilitate admixture among adjacent populations during climatic conditions associated with glacial maxima (Fig. 3.9). Despite the shared geological history of the Huon Peninsula and Adelbert Mountains, samples from the latter population clearly represent a recent colonization event from the CDRs, most likely from the northern slopes of the Schrader or Bismarck Ranges. Although the distinctive Mt. Bosavi population has yet to be examined within in a molecular framework, its inclusion will likely have little impact on resolving the key facets of phylogeographic history in the *A. macgregoriae* complex.

Rhipidura atra —The fantails (Rhipiduridae) comprise a diverse radiation of small insectivorous passerines ubiquitous throughout much of the South Pacific with a center of diversity in New Guinea's lowland and montane rainforest environments (Boles, 2006). Recent molecular analyses of fantail systematics failed to resolve unambiguously the phylogenetic position of *R. atra* (Nyari et al., 2009); however, this species appears to occupy a basal position in the family with no closely related sister taxa (Benz, unpub. data). These results are consistent

with the phylogeographic patterns revealed herein, which indicate a long independent evolutionary history in *R. atra* as evidenced by highly divergent lineages from the Vogelkop and Papuan Peninsula (Fig. 3.3). Three primary phylogroups were recovered in the BI topology, with the distribution of genetic diversity corresponding to geographic breaks in the Bird's Neck region and Watut/Tauri River Valley. Coalescent estimates of divergence times indicate the Vogelkop lineage arose in the late Pliocene to early Pleistocene ~1,698,000–4,275,500 ybp, broadly corresponding with the accretion history and orogenic uplift of the Vogelkop. Coalescence between western New Guinea and Papuan Peninsula lineages was more recent, in the mid-to-early Pleistocene ~744,000–1,524,00 ybp, indicating retention of genetic diversity across multiple climate cycles. Given the strong dispersal capacity characteristic of this species and the family as a whole, a substantial genetic break across the Watut/Tauri River Valley was unexpected, and suggests this geological suture zone may have represented a more substantial geographic barrier in the past (Dow, 1977; Pigram & Davies, 1987; Hall, 2002). Alternatively, the Watut/Tauri break may represent a secondary contact zone, with the Papuan lineage originating from the Dayman terrane southeast of the Adau River drainage. Extensive geographic sampling revealed 11 distinct populations within *R. atra*, the distributions of which largely correspond to contemporary sky-island communities (Table 3.2; Fig. 3.6). Shallow genetic divergences among populations of the Central Highlands and distantly isolated coastal communities indicates a pattern of recent colonization, with shared haplotypes among the Torricelli/Bewani and Cyclops ranges suggesting potential lateral dispersal among these sky-island populations. The latter population represents the only described subspecies within the complex (Mayr, 1941; Boles, 2006); however, the lack of lineage sorting, substantial phylogeographic structure, and diagnosable morphological variation suggests that subspecific

recognition is not warranted. Conversely, the deep genetic divergence and reciprocal monophyly recovered within the Vogelkop, indicates that post speciation isolating mechanisms may be in place, and presents a strong case for modern biodiversity surveys within the Arfak and Tamrau Mountains to assess the prevalence of cryptic avian diversity throughout the Bird's Head Region. Additional sampling from the Bomberai Peninsula and Foya Mountains will be imperative to fully resolving the evolutionary history of *R. atra* across New Guinea's western sky-islands.

Peneothello cyanus—Broadly distributed throughout New Guinea's foothill and montane rainforest ecosystems, *Peneothello* (Petroicidae) comprises 4 species of small-bodied passerine exhibiting strong elevational segregation with little to no sympatry among taxa (Boles, 2007). Phylogenetic relationships within *Peneothello* remain uncertain, as does the taxonomic status of the enigmatic *Peneoenanthe pulverulenta*, raising questions of monophyly within the clade (Fig. 3.4). Phylogeographic analyses recovered three reciprocally monophyletic phylogroups in *P. cyanus*, the distributions of which are consistent with morphologically defined subspecies and correspond to geographic breaks in ecological suitability across the Bird's Neck region and Strickland River Valley. Although it remains unclear whether the latter barrier played an active role in the origin of geographic structure within the CDRs or simply represents a secondary contact zone, the lack of gene flow across this region indicates reproductive isolating mechanisms may be contributing to the retention of genetic diversity. Coalescent estimates of divergence times indicate these lineages emerged in the mid Pleistocene ~ 343,000–924,00 to 515,500–1,242,000 YBP, respectively, which coincides with the orogenic uplift of the CDRs and outlying coastal terranes; however, uncertainty in the local geological history of these regions as well as large confidence intervals associated mtDNA linked markers precludes linking these genetic breaks with explicit geological events. The ND2 haplotype network and pairwise F_{st}

values recovered 12 distinct populations among these geographic lineages that primarily reflect the distribution of contemporary sky-islands and ecological barriers in the CDRs (Fig. 3.4, 3.9). With exception of the Eastern Highlands – Owen Stanley Ranges split, all adjacent populations show genetic divergences that predate LGM habitat corridors revealed by ecological niche models across the Central Highlands, suggesting Pleistocene climate cycles have played a limited role in shaping this species' phylogeographic history. Moreover, the presence of substantial genetic structure between fully contiguous populations in the Weyland Mountains and western CDRs lends further support to the hypothesis that New Guinea's recent orogenic history has influenced patterns of population genetic structure across this composite montane landscape.

Crateroscelis robusta—The *Crateroscelis* mouse-warblers (Acanthizidae) include 3 species of insectivorous passerine endemic to New Guinea's lowland and montane rainforest environments (Gregory, 2007). Although paraphyly of this clade remains in question based on outgroup sampling and marker selection employed herein, the BI topology revealed strong support for monophyly of *C. robusta*, which is comprised of 3 primary phylogroups corresponding to deep genetic splits across the Bird's Neck region and Strickland River Valley. Genetic divergences across the latter barrier (7.95–8.97%) are comparable to species-level splits within the Acanthizidae (Gardner, et al., 2010), and correspond to strong phenotypic variation in plumage coloration. Estimates of divergence times indicate coalescence in the late Pliocene from 1,933,000–4,830,000 ybp. Although the initial point of origin among this east west split remains unclear, these lineages are clearly maintaining unique evolutionary trajectories that originated during the primary orogenic uplift of the CDRs. Maintenance of genetic diversity within Wandamen and Weyland populations, as well as the distantly isolated Cyclops Range,

indicates a long evolutionary history within these populations extending to the mid-Pleistocene (Appendix 2.3), whereas shallow genetic divergences among populations of the Bewani/Torricelli ranges and CDRs suggests a recent colonization event most likely from the northern slopes of the Victor Emmanuel or Central Ranges. In contrast to reciprocal monophyly and deep genetic structure among western populations, a pattern of incomplete lineage sorting and shallow genetic structure indicates active or recent gene flow among the Eastern Highlands and Papuan Peninsula that are consistent with LGM environmental corridors assuming a ND2 mutation scalar of 5% (Appendix 2.3). Shared haplotypes between the Eastern Highlands, Papuan Peninsula, and Huon Peninsula indicate a recent colonization event across the Markham River valley perhaps during the LGM when dispersal distances were substantially reduced among elevationally depressed montane rainforest communities.

Biogeographic barriers and comparative phylogeography

Comparisons of branching patterns and spatial distributions of genetic diversity highlight the unique evolutionary histories among these montane endemic passerines, yet all 4 focal taxa share core phylogeographic features that also reflect higher-level biogeographic patterns across New Guinea's montane landscape. The Central Highlands have featured prominently in the geographic origin of these taxa, as inferred by branching patterns in *C. robusta* and *P. cyanus*, which are consistent with a simultaneous or fragmented ancestor model of diversification within the CDRs. By contrast, highly divergent basal lineages in the Vogelkop (*R. atra*) and Huon Peninsula (*A. macgregoriae*) raise the possibility of "upstream" colonization from peripherally isolated sky-islands and subsequent diversification within the Central Highlands and Papuan Peninsula. While these scenarios seem unlikely given the more recent orogenic history of these

accreted terranes, estimates of divergence times do not reject the hypothesis outright. A multi-locus approach may shed additional light on the branching patterns and geographic origin of these taxa, as the mtDNA gene trees presented herein may not represent the species' true diversification history.

Isolated from highland terranes of the Bomberai Peninsula and western CDRs by a narrow land bridge of foothill and lowland rainforest, the Vogelkop harbors a number montane endemic bird species and comprises an important center of endemism for diverse taxonomic groups (Gressitt, 1982; Pratt, 1982; Keast & Miller, 1996). Consequently, the presence of highly divergent Vogelkop lineages across each species complex suggests the Lengguru land bridge barrier has strongly limited gene flow between these montane communities across a wide variety avian taxa with diverse life history attributes. A complex suture zone comprised of multiple accreted terranes (Wandamen, Mangguar, and Weyland) lies to the west of the Lengguru land bridge along the Tarera-Aiduna Fault (Pigram & Davies, 1987; Hall, 1998; 2002). Although a pattern of strong population genetic structure associated with the Wandamen sky-island was not unexpected given its geographic isolation, the close relationship among Wandamen and Weyland terranes in *C. robusta* and *P. cyanus* was surprising given that the latter montane community is fully contiguous with populations in the western CDRs. The presence of reciprocal monophyly within Weyland populations suggests that the contemporary topographic configuration along the Tarera-Aiduna Fault may be a recent development, reflecting the dynamic accretion and orogenic history of the region (Hall, 1998; 2002). Likewise, strong geographic structure associated with the Strickland River Valley and Watut/Tauri suture zone illustrates the recent and ongoing orogenic uplift of the Central Highlands and Papuan Peninsula, as the extensive habitat corridors projected across these barriers by LGM ecological niche reconstructions are

difficult to reconcile with the presence of deeply divergent and fully sorted lineages. Hierarchical three-way analyses of molecular variance confirmed that much this genetic diversity is congruent with the distribution of contemporary sky-islands rather than LGM sky-islands (Fig. 3.3). This pattern is largely attributed to the highly linear configuration of sky-islands within the CDRs, which fosters an isolation-by-distance effect as revealed by Mantel tests indicating positive correlations between genetic and geographic distances in 3 of the 4 taxa. Low to moderate *r* values in Mantel tests are perhaps a consequence of variation in dispersal capacity among taxa, disparity in colonization histories, or stochastic processes between population. Lastly, substantial discord in the distribution of genetic diversity among north coast sky-island populations appears to reflect taxonomic differences in dispersal capacity and perhaps stochastic processes (e.g. genetic drift or selective sweeps) associated with the small effective population size of these communities.

Historical demography and Pleistocene climate change

Pleistocene climatic oscillations have clearly impacted the distribution of New Guinea's montane floral communities as inferred by pollen core data sampled from multiple sites throughout the Central Highlands (Walker & Hope, 1982; Haberle et al., 1990; Hope & Tulip, 1994; Hope, 1996). Montane rainforest habitats underwent elevational shifts of as much as 1800 m between climatic extremes, resulting in recurrent episodes of sky-island expansion and contraction as taxa tracked ecological niche requirements along elevational gradients. The contemporary and paleoecological niche reconstructions developed herein corroborate these findings, predicting dramatic elevational shifts in ecological suitability under LGM climatic conditions (Fig 3.9). Based on the contrasting phylogeographic patterns recovered across the CDRs, these recurrent

shifts in distribution have played a limited role in shaping the core aspects of phylogeographic structure among focal taxa. These results are also incompatible with Diamond's (1972) "dropout" hypothesis, which identified paleoclimatic fluctuations as a potential driver of allopatric diversification processes.

By contrast, Bayesian skyline analyses and population genetic summary statistics indicate that Pleistocene climate fluctuations have strongly influenced the demographic history of these taxa, revealing clear signatures of population growth across the Central Highlands, Vogelkop, and Huon Peninsula (Table 3.4, Fig. 3.7). Bayesian skyline analyses also recovered a slight downturn in effective population size over the most recent time interval, which is consistent with the demographic response expected under the current interglacial climate. Although Fu's *Fs* and Ramos-Onsin & Rozas R_2 statistics failed to recover evidence of population bottlenecks with statistical significance, Fu's *Fs* values were positive in a number north coast sky-island populations, which corroborates the dramatic shifts in distribution between LGM and interglacial climates among coastal sky-island populations (Fig. 1.10). Moreover, Bayesian skyline analyses take into account the full compliment of historical phylogeographic information inherent to sequence variation, thereby offering advantages over traditional summary statistics that rely on the frequency spectrum of mutation or haplotype distribution, which may explain the differences among analyses (Drummond et al., 2005).

CONCLUSIONS

New Guinea's rich endemic avifauna has long fascinated evolutionary biologists for its extraordinary morphological and behavioral diversity as well as complex higher-level biogeographic relationships and fine-scale endemism (Wallace, 1869; Gilliard, 1969; Diamond,

1972; Mayr & Diamond, 2001; Scholes, 2008; Irestedt et al., 2009). Nonetheless, progress in unraveling underlying environmental factors driving patterns of in situ avian diversification and has been limited, reflecting the dearth of modern voucher collections and associated genetic sampling from key biogeographic regions (Murphy et al., 2007; Joseph & Omland, 2009). Now, as agricultural practices, natural resource extraction, and regional climate change threatens the future of this diversity, the conservation community lacks the fundamental knowledge to identify conservation priorities and establish effective preservation measures. This contribution sheds light on the spatial distributions of genetic diversity within New Guinea's montane avifauna, highlighting the island's dynamic geological history as a key driver of phylogeographic structure, while taxonomic differences in dispersal capacity and Pleistocene climatic oscillations have clearly played important roles in shaping patterns of population genetic structure, gene flow, and historical demography. Discovery of unexpected endemism within the Weyland Range coupled with species-level genetic divergences across the Bird's Neck region, CDRs, and Markham River Valley illustrate the importance of continued ornithological collecting expeditions throughout the New Guinea highlands. Comparative analyses across a broader suite of taxonomic groups coupled with denser geographic sampling and multi-locus data sets will be imperative to understanding the overarching patterns of avian phylogeographic structure and establishing effective conservation initiatives across New Guinea's rugged montane landscape.

APPENDIX

Appendix 3.1. Summary of specimens included in this study.

Topology Code	Taxon	Locality	Latitude	Longitude	Source	Voucher Number
Ingroup	*Peneothello cyanus*	PNG: Central Province				
SI1	*P. c. subcyanea*	Mt. Simpson	-9.99982	149.50718	KUNHM	114154
SI2	*P. c. subcyanea*	Mt. Simpson	-9.99982	149.50718	KUNHM	114155
SI3	*P. c. subcyanea*	Mt. Simpson	-9.99982	149.50718	KUNHM	114156
SI4	*P. c. subcyanea*	Mt. Simpson	-9.98955	149.48674	KUNHM	114902
SI5	*P. c. subcyanea*	Mt. Simpson	-9.99982	149.50718	KUNHM	114091
SI6	*P. c. subcyanea*	Mt. Simpson	-9.99982	149.50718	KUNHM	T14586
SI7	*P. c. subcyanea*	Mt. Simpson	-9.98955	149.48674	KUNHM	T14629
EF1	*P. c. subcyanea*	Owen Stanley Range: Efogi	-9.15	147.66667	ANWC	26578
EF2	*P. c. subcyanea*	Owen Stanley Range: Efogi	-9.15	147.66667	ANWC	24506
EF3	*P. c. subcyanea*	Owen Stanley Range: Efogi	-9.15	147.66667	ANWC	24505
EF4	*P. c. subcyanea*	Owen Stanley Range: Efogi	-9.15	147.66667	ANWC	24504
EF5	*P. c. subcyanea*	Owen Stanley Range: Efogi	-9.15	147.66667	ANWC	26524
		PNG: Milne Bay Province				
AG1	*P. c. subcyanea*	Agaun	-9.92917	149.38333	ANWC	8078*
AG2	*P. c. subcyanea*	Agaun	-9.92917	149.38333	ANWC	8079*
AG3	*P. c. subcyanea*	Agaun	-9.92917	149.38333	ANWC	8111*
		PNG: Oro Province				
AW1	*P. c. subcyanea*	Owen Stanley Range: Awoma	-9.18333	148.13333	ANWC	E199
AW2	*P. c. subcyanea*	Owen Stanley Range: Awoma	-9.18333	148.13333	ANWC	E187
AW3	*P. c. subcyanea*	Owen Stanley Range: Awoma	-9.18333	148.13333	ANWC	26830
AW4	*P. c. subcyanea*	Owen Stanley Range: Awoma	-9.18333	148.13333	ANWC	26847
		PNG: Morobe Province				
HE1	*P. c. subcyanea*	Herzog Mts: Wagu	-6.8	146.8	ANWC	25196*
HE2	*P. c. subcyanea*	Herzog Mts: Wagu	-6.8	146.8	ANWC	25256*
HE3	*P. c. subcyanea*	Herzog Mts: Wagu	-6.8	146.8	ANWC	25319*
MI1	*P. c. subcyanea*	Owen Stanley Range: Mt. Missim	-7.21991	146.81598	MCZ	167492*
MI2	*P. c. subcyanea*	Owen Stanley Range: Mt. Missim	-7.21991	146.81598	MCZ	167493*
MI3	*P. c. subcyanea*	Owen Stanley Range: Mt. Missim	-7.21991	146.81598	MCZ	167494*
MI4	*P. c. subcyanea*	Owen Stanley Range: Mt. Missim	-7.21991	146.81598	MCZ	167495*
MI5	*P. c. subcyanea*	Owen Stanley Range: Mt. Missim	-7.21991	146.81598	MCZ	167496*
MI6	*P. c. subcyanea*	Owen Stanley Range: Mt. Missim	-7.21991	146.81598	MCZ	167497*
MI7	*P. c. subcyanea*	Owen Stanley Range: Mt. Missim	-7.21991	146.81598	MCZ	167498*
MI8	*P. c. subcyanea*	Owen Stanley Range: Mt. Missim	-7.21991	146.81598	MCZ	167499*
MI9	*P. c. subcyanea*	Owen Stanley Range: Mt. Missim	-7.21991	146.81598	MCZ	167500*
WU1	*P. c. subcyanea*	Owen Stanley Range: Wau	-7.34099	146.68141	PNGNM	23523*
FI1	*P. c. subcyanea*	Huon Peninsula: Finisterre Range	-6.08165	146.57224	KUNHM	95794
FI2	*P. c. subcyanea*	Huon Peninsula: Finisterre Range	-6.08165	146.57224	KUNHM	92365
FI3	*P. c. subcyanea*	Huon Peninsula: Finisterre Range	-6.08165	146.57224	KUNHM	93567
FI4	*P. c. subcyanea*	Huon Peninsula: Finisterre Range	-6.08165	146.57224	KUNHM	T4584
RA1	*P. c. subcyanea*	Huon Peninsula: Rawlinson Mts.	-6.45833	147.4333	AMNH	823638*
RA2	*P. c. subcyanea*	Huon Peninsula: Rawlinson Mts.	-6.45833	147.4333	AMNH	823635*
RA3	*P. c. subcyanea*	Huon Peninsula: Rawlinson Mts.	-6.45833	147.4333	ANWC	25690*
RA4	*P. c. subcyanea*	Huon Peninsula: Rawlinson Mts.	-6.45833	147.4333	ANWC	25691*
RA5	*P. c. subcyanea*	Huon Peninsula: Rawlinson Mts.	-6.45833	147.4333	ANWC	25761*
RA6	*P. c. subcyanea*	Huon Peninsula: Rawlinson Mts.	-6.45833	147.4333	ANWC	25762*
		PNG: Madang Province				
AD1	*P. c. subcyanea*	Adelbert Range	-4.71727	145.27482	KUNHM	111475
AD2	*P. c. subcyanea*	Adelbert Range	-4.71727	145.27482	KUNHM	114781
AD3	*P. c. subcyanea*	Adelbert Range	-4.71727	145.27482	KUNHM	114787
AD4	*P. c. subcyanea*	Adelbert Range	-4.71727	145.27482	KUNHM	111570

Topology Code	Taxon	Locality	Latitude	Longitude	Source	Voucher Number
AD5	*P. c. subcyanea*	Adelbert Range	-4.71727	145.27482	KUNHM	111571
AD6	*P. c. subcyanea*	Adelbert Range	-4.71727	145.27482	KUNHM	111572
AD7	*P. c. subcyanea*	Adelbert Range.	-4.71727	145.27482	KUNHM	111573
AD8	*P. c. subcyanea*	Adelbert Range.	-4.71727	145.27482	KUNHM	111574
SH1	*P. c. subcyanea*	Schradder Range	-5.22057	144.48821	KUNHM	114747
SH2	*P. c. subcyanea*	Schradder Range	-5.22057	144.48821	KUNHM	114809
		PNG: Eastern Highlands Province				
KR1	*P. c. subcyanea*	Kratke Range	-7.061	145.82433	KUNHM	113283
KR2	*P. c. subcyanea*	Kratke Range	-7.061	145.82433	KUNHM	113284
KR3	*P. c. subcyanea*	Kratke Range	-7.061	145.82433	KUNHM	113285
KR4	*P. c. subcyanea*	Kratke Range	-7.061	145.82433	KUNHM	113286
KR5	*P. c. subcyanea*	Kratke Range	-7.061	145.82433	KUNHM	114184
KR6	*P. c. subcyanea*	Kratke Range	-7.061	145.82433	KUNHM	114293
KR7	*P. c. subcyanea*	Kratke Range	-7.061	145.82433	KUNHM	114294
KR8	*P. c. subcyanea*	Kratke Range	-7.061	145.82433	KUNHM	T16485
KR9	*P. c. subcyanea*	Kratke Range	-7.061	145.82433	KUNHM	T16487
OK1	*P. c. subcyanea*	Okapa District: Kimigomo	-6.42718	145.58016	KUNHM	113254
OK2	*P. c. subcyanea*	Okapa District: Kimigomo	-6.42718	145.58016	KUNHM	113255
OK3	*P. c. subcyanea*	Okapa District: Kimigomo	-6.42718	145.58016	KUNHM	114828
OK4	*P. c. subcyanea*	Okapa District: Kimigomo	-6.42718	145.58016	KUNHM	111557
OK5	*P. c. subcyanea*	Okapa District: Kimigomo	-6.42718	145.58016	KUNHM	T16176
OK6	*P. c. subcyanea*	Okapa District: Kimigomo	-6.42718	145.58016	KUNHM	T16184
OK7	*P. c. subcyanea*	Okapa District: Kimigomo	-6.42718	145.58016	KUNHM	T16186
OK8	*P. c. subcyanea*	Okapa District: Kimigomo	-6.42718	145.58016	KUNHM	T16187
OK9	*P. c. subcyanea*	Okapa District: Kimigomo	-6.42718	145.58016	KUNHM	T16201
CR1	*P. c. subcyanea*	Crater Mountain	-6.69444	145.10666	KUNHM	95984
CR2	*P. c. subcyanea*	Crater Mountain	-6.69444	145.10666	KUNHM	95985
CR3	*P. c. subcyanea*	Crater Mountain	-6.65045	145.17143	KUNHM	T12291
BI1	*P. c. subcyanea*	Bismarck Range	-5.95166	145.4	KUNHM	113263
BI2	*P. c. subcyanea*	Bismarck Range	-5.95166	145.4	KUNHM	113264
BI3	*P. c. subcyanea*	Bismarck Range	-5.95166	145.4	KUNHM	114850
BI4	*P. c. subcyanea*	Bismarck Range	-5.95166	145.4	KUNHM	114863
BI5	*P. c. subcyanea*	Bismarck Range	-5.95166	145.4	KUNHM	114869
BI6	*P. c. subcyanea*	Bismarck Range	-5.95166	145.4	KUNHM	114244
BI7	*P. c. subcyanea*	Bismarck Range	-5.95166	145.4	KUNHM	114245
BI8	*P. c. subcyanea*	Bismarck Range	-5.95166	145.4	KUNHM	T16290
		PNG: Chimbu Province				
KU1	*P. c. subcyanea*	Kubor Range	-6.04883	144.52266	AMNH	705338
KU2	*P. c. subcyanea*	Kubor Range	-6.04883	144.52266	AMNH	802635
		PNG: Western Highlands Province				
HA1	*P. c. subcyanea*	Mt. Hagen	-5.79419	143.99600	AMNH	802633*
HA2	*P. c. subcyanea*	Mt. Hagen	-5.79419	143.99600	AMNH	705341*
HA3	*P. c. subcyanea*	Mt. Hagen	-5.79419	143.99600	AMNH	705344*
HA4	*P. c. subcyanea*	Mt. Hagen	-5.79419	143.99600	AMNH	705342*
HA5	*P. c. subcyanea*	Mt. Hagen	-5.79419	143.99600	AMNH	705343*
		PNG: Southern Highlands Province				
BO1	*P. c. atricapilla*	Mt. Bosavi	-6.62206	142.82021	PNGNM	25443*
		PNG: West Sepik Province				
ST1	*P. c. atricapilla*	Mt. Stolle	-4.81331	141.65293	KUNHM	97213
ST2	*P. c. atricapilla*	Mt. Stolle	-4.81331	141.65293	KUNHM	97635
ST3	*P. c. atricapilla*	Mt. Stolle	-4.81331	141.65293	KUNHM	113305
ST4	*P. c. atricapilla*	Mt. Stolle	-4.81331	141.65293	KUNHM	113306
ST5	*P. c. atricapilla*	Mt. Stolle	-4.81331	141.65293	KUNHM	114182
ST6	*P. c. atricapilla*	Mt. Stolle	-4.81331	141.65293	KUNHM	114183

Topology Code	Taxon	Locality	Latitude	Longitude	Source	Voucher Number
ST7	*P. c. atricapilla*	Mt. Stolle	-4.81331	141.65293	KUNHM	114185
ST8	*P. c. atricapilla*	Mt. Stolle	-4.81331	141.65293	KUNHM	114186
ST9	*P. c. atricapilla*	Mt. Stolle	-4.81331	141.65293	KUNHM	114187
ST10	*P. c. atricapilla*	Mt. Stolle	-4.81331	141.65293	KUNHM	114188
ST11	*P. c. atricapilla*	Mt. Stolle	-4.81331	141.65293	KUNHM	114189
ST12	*P. c. atricapilla*	Mt. Stolle	-4.81331	141.65293	KUNHM	114928
ST13	*P. c. atricapilla*	Mt. Stolle	-4.81331	141.65293	KUNHM	114938
ST14	*P. c. atricapilla*	Mt. Stolle	-4.81331	141.65293	KUNHM	114951
		PNG: West Sepik Province				
BW1	*P. c. atricapilla*	Bewani Mts., Mt. Menawa	-3.30373	141.72652	AMNH	829660*
BW2	*P. c. atricapilla*	Bewani Mts., Mt. Menawa	-3.30373	141.72652	AMNH	829658*
BW3	*P. c. atricapilla*	Bewani Mts., Mt. Menawa	-3.30373	141.72652	AMNH	829662*
BW4	*P. c. atricapilla*	Bewani Mts., Mt. Menawa	-3.30373	141.72652	AMNH	829659*
TO1	*P. c. atricapilla*	Torricelli Mts., Mt. Nibo	-3.41243	142.16337	AMNH	829661*
TO2	*P. c. atricapilla*	Torricelli Mts., Mt. Somoro	-3.40879	142.18570	AMNH	829642*
TO3	*P. c. atricapilla*	Torricelli Mts., Mt. Somoro	-3.40879	142.18570	AMNH	829643*
TO4	*P. c. atricapilla*	Torricelli Mts., Mt. Nibo	-3.41243	142.16337	AMNH	829652*
TO5	*P. c. atricapilla*	Torricelli Mts., Mt. Nibo	-3.41243	142.16337	AMNH	829651*
TO6	*P. c. atricapilla*	Torricelli Mts., Mt. Nibo	-3.41243	142.16337	AMNH	829657*
		Indonesia: Papua Province				
CY1	*P. c. atricapilla*	Cyclops Mts.	-2.5077	140.52608	AMNH	608172*
CY2	*P. c. atricapilla*	Cyclops Mts.	-2.5077	140.52608	AMNH	608173*
CY3	*P. c. atricapilla*	Cyclops Mts.	-2.5077	140.52608	AMNH	608175*
CY4	*P. c. atricapilla*	Cyclops Mts.	-2.5077	140.52608	AMNH	608174*
CY5	*P. c. atricapilla*	Cyclops Mts.	-2.5077	140.52608	AMNH	294086*
CY6	*P. c. atricapilla*	Cyclops Mts.	-2.5077	140.52608	AMNH	294082*
CY7	*P. c. atricapilla*	Cyclops Mts.	-2.5077	140.52608	AMNH	608176*
CY8	*P. c. atricapilla*	Cyclops Mts.	-2.5077	140.52608	AMNH	294084*
CY9	*P. c. atricapilla*	Cyclops Mts.	-2.5077	140.52608	AMNH	294083*
CY10	*P. c. atricapilla*	Cyclops Mts.	-2.5077	140.52608	AMNH	294081*
IL1	*P. c. atricapilla*	Nassau Range: Ilaga	-3.98963	137.54045	YPBM	76024*
IL2	*P. c. atricapilla*	Nassau Range: Ilaga	-3.98963	137.54045	YPBM	76026*
IL3	*P. c. atricapilla*	Nassau Range: Ilaga	-3.98963	137.54045	YPBM	76027*
IL4	*P. c. atricapilla*	Nassau Range: Ilaga	-3.98963	137.54045	YPBM	76028*
IL5	*P. c. atricapilla*	Nassau Range: Ilaga	-3.98963	137.54045	YPBM	76029*
GO1	*P. c. atricapilla*	Oranje Mts: Mt. Goliath	-3.98963	137.54045	AMNH	608183*
GO2	*P. c. atricapilla*	Oranje Mts: Mt. Goliath	-3.98963	137.54045	AMNH	608182*
GO3	*P. c. atricapilla*	Oranje Mts: Mt. Goliath	-3.98963	137.54045	AMNH	608181*
GO4	*P. c. atricapilla*	Oranje Mts: Mt. Goliath	-3.98963	137.54045	AMNH	608187*
GO5	*P. c. atricapilla*	Oranje Mts: Mt. Goliath	-3.98963	137.54045	AMNH	608185*
WE1	*P. c. atricapilla*	Weyland Mts.	-3.89137	135.4664	AMNH	302887*
WE2	*P. c. atricapilla*	Weyland Mts.	-3.89137	135.4664	AMNH	302888*
WE3	*P. c. atricapilla*	Weyland Mts.	-3.89137	135.4664	AMNH	302082*
WE4	*P. c. atricapilla*	Weyland Mts.	-3.89137	135.4664	AMNH	302080*
WE5	*P. c. atricapilla*	Weyland Mts.	-3.89137	135.4664	AMNH	302079*
WE6	*P. c. atricapilla*	Weyland Mts.	-3.89137	135.4664	AMNH	302085*
WE7	*P. c. atricapilla*	Weyland Mts.	-3.89137	135.4664	AMNH	302086*
WE8	*P. c. atricapilla*	Weyland Mts.	-3.89137	135.4664	AMNH	302087*
WE9	*P. c. atricapilla*	Weyland Mts.	-3.89137	135.4664	AMNH	302088*
WE10	*P. c. atricapilla*	Weyland Mts.	-3.89137	135.4664	AMNH	302089*
		Indonesia: West Papua Province				
WA1	*P. c. atricapilla*	Wandamen Mts.	-2.75584	134.58458	AMNH	608167*
WA2	*P. c. atricapilla*	Wandamen Mts.	-2.75584	134.58458	AMNH	294088*
WA3	*P. c. atricapilla*	Wandamen Mts.	-2.75584	134.58458	AMNH	294087*

Topology Code	Taxon	Locality	Latitude	Longitude	Source	Voucher Number
WA4	*P. c. atricapilla*	Wandamen Mts.	-2.75584	134.58458	AMNH	608169*
WA5	*P. c. atricapilla*	Wandamen Mts.	-2.75584	134.58458	AMNH	608166*
AR1	*P. c. cyanus*	Arfak Mts.	-1.09181	133.9073	AMNH	608164*
AR2	*P. c. cyanus*	Arfak Mts.	-1.09181	133.9073	AMNH	608163*
AR3	*P. c. cyanus*	Arfak Mts.	-1.09181	133.9073	AMNH	294089*
AR4	*P. c. cyanus*	Arfak Mts.	-1.09181	133.9073	AMNH	294090*
AR5	*P. c. cyanus*	Arfak Mts.	-1.09181	133.9073	AMNH	608162*
TA1	*P. c. cyanus*	Tamrau Mts., Bonkouragen	-0.54878	132.73	ANSP	132303*
TA2	*P. c. cyanus*	Tamrau Mts., Bonkouragen	-0.54878	132.73	ANSP	132299*
TA3	*P. c. cyanus*	Tamrau Mts., Bonkouragen	-0.54878	132.73	ANSP	132297*
TA4	*P. c. cyanus*	Tamrau Mts., Bonkouragen	-0.54878	132.73	ANSP	132302*
TA5	*P. c. cyanus*	Tamrau Mts., Bonkouragen	-0.54878	132.73	ANSP	132298*
TA6	*P. c. cyanus*	Tamrau Mts., Mt. Bantjiet	-0.71553	132.96645	AMNH	793006*
TA7	*P. c. cyanus*	Tamrau Mts., Mt. Bantjiet	-0.71553	132.96645	AMNH	793005*
TA8	*P. c. cyanus*	Tamrau Mts., Mt. Bantjiet	-0.71553	132.96645	AMNH	793004*
Outgroup						
	Peneothello bimaculata	PNG: EHP	-6.78849	145.03674	KUNHM	T12898
	Peneothello sigillata	PNG: Morobe Province	-6.08165	146.57224	KUNHM	T4599
	Peneothello cryptoleuca	Indonesia: West Papua Province	-0.71553	132.96645	AMNH	793000*
	Peneoenanthe pulverulenta	Australia: Northern Territory	-14.7442	135.33437	KUNHM	T22867
	Melanodryas cucullata	Australia:	-26.4667	114.48333	KUNHM	T6207
	Poecilodryas placens	PNG: EHP	-6.7885	145.70341	KUNHM	T5177
	Poecilodryas albispecularis	PNG: Morobe Province	-6.08165	146.57224	KUNHM	95822
	Poecilodryas hypoleuca	PNG: Western Province	-4.61525	142.71338	KUNHM	93150
	Poecilodryas albonotata	PNG: Morobe	-6.08165	146.57224	KUNHM	93564
Ingroup	*Rhipidura atra*	PNG: Central Province				
SI1	*R. a. atra*	Mt. Simpson	-9.99982	149.50718	KUNHM	T14551
SI2	*R. a. atra*	Mt. Simpson	-9.99982	149.50718	KUNHM	T14570
SI3	*R. a. atra*	Mt. Simpson	-9.99982	149.50718	KUNHM	T14575
SI4	*R. a. atra*	Mt. Simpson	-9.98955	149.48674	KUNHM	T14604
SI5	*R. a. atra*	Mt. Simpson	-9.99982	149.50718	KUNHM	114830
SI6	*R. a. atra*	Mt. Simpson	-9.99982	149.50718	KUNHM	114831
SI7	*R. a. atra*	Mt. Simpson	-9.99982	149.50718	KUNHM	114837
SI8	*R. a. atra*	Mt. Simpson	-9.99982	149.50718	KUNHM	114839
SI9	*R. a. atra*	Mt. Simpson	-9.99982	149.50718	KUNHM	114874
SI10	*R. a. atra*	Mt. Simpson	-9.99982	149.50718	KUNHM	114127
SI11	*R. a. atra*	Mt. Simpson	-9.99982	149.50718	KUNHM	114128
SI12	*R. a. atra*	Mt. Simpson	-9.99982	149.50718	KUNHM	114873
EF1	*R. a. atra*	Owen Stanley Range: Efogi	-9.92917	149.38333	ANWC	24533
EF2	*R. a. atra*	Owen Stanley Range: Efogi	-9.92917	149.38333	ANWC	24535
EF3	*R. a. atra*	Owen Stanley Range: Efogi	-9.92917	149.38333	ANWC	26528
EF4	*R. a. atra*	Owen Stanley Range: Efogi	-9.92917	149.38333	ANWC	24534
	R. a. atra	PNG: Oro Province				
AW1	*R. a. atra*	Owen Stanley Range: Awoma	-9.18333	148.13333	ANWC	26645
AW2	*R. a. atra*	Owen Stanley Range: Awoma	-9.18333	148.13333	ANWC	26831
TE1	*R. a. atra*	Owen Stanley Range: Tetebedi	-9.16667	148.08333	ANWC	26700
TE2	*R. a. atra*	Owen Stanley Range: Tetebedi	-9.16667	148.08333	ANWC	TE071
TE3	*R. a. atra*	Owen Stanley Range: Tetebedi	-9.16667	148.08333	ANWC	26753
TE4	*R. a. atra*	Owen Stanley Range: Tetebedi	-9.16667	148.08333	ANWC	26744
		PNG: Morobe Province				
HE1	*R. a. atra*	Herzog Mts: Wagu	-6.8	146.8	ANWC	25403
HE2	*R. a. atra*	Herzog Mts: Wagu	-6.8	146.8	ANWC	25495
HE3	*R. a. atra*	Herzog Mts: Wagu	-6.8	146.8	ANWC	25540
MI1	*R. a. atra*	Owen Stanley Range: Mt. Missim	-7.21991	146.81598	MCZ	167333

Topology Code	Taxon	Locality	Latitude	Longitude	Source	Voucher Number
MI2	*R. a. atra*	Owen Stanley Range: Mt. Missim	-7.21991	146.81598	MCZ	167334
MI3	*R. a. atra*	Owen Stanley Range: Mt. Missim	-7.21991	146.81598	MCZ	167335
WU1	*R. a. atra*	Owen Stanley Range: Wau	-7.34099	146.68141	MCZ	330570
WU2	*R. a. atra*	Owen Stanley Range: Wau	-7.34099	146.68141	MCZ	167330
WU3	*R. a. atra*	Owen Stanley Range: Wau	-7.34099	146.68141	MCZ	167331
WU4	*R. a. atra*	Owen Stanley Range: Wau	-7.34099	146.68141	MCZ	167332
ZA1	*R. a. atra*	Huon Peninsula: Zakaheme	-6.31827	147.6449	AMNH	267296
ZA2	*R. a. atra*	Huon Peninsula: Zakaheme	-6.31827	147.6449	AMNH	267299
ZA3	*R. a. atra*	Huon Peninsula: Zakaheme	-6.31827	147.6449	AMNH	267298
TF1	*R. a. atra*	Owen Stanley Range: Mt. Tafa	-8.63351	147.18387	AMNH	420379
TF2	*R. a. atra*	Owen Stanley Range: Mt. Tafa	-8.63351	147.18387	AMNH	420437
TF3	*R. a. atra*	Owen Stanley Range: Mt. Tafa	-8.63351	147.18387	AMNH	420381
TF4	*R. a. atra*	Owen Stanley Range: Mt. Tafa	-8.63351	147.18387	AMNH	420380
FI1	*R. a. atra*	Huon Peninsula: Finisterre Range	-6.08165	146.57224	KUNHM	95790
FI2	*R. a. atra*	Huon Peninsula: Finisterre Range	-6.08165	146.57224	KUNHM	95286
FI3	*R. a. atra*	Huon Peninsula: Finisterre Range	-6.08165	146.57224	KUNHM	95068
FI4	*R. a. atra*	Huon Peninsula: Finisterre Range	-6.08165	146.57224	KUNHM	T4602
RA1	*R. a. atra*	Huon Peninsula: Rawlinson Mts.	-6.45833	147.4333	ANWC	25773
RA2	*R. a. atra*	Huon Peninsula: Rawlinson Mts.	-6.45833	147.4333	ANWC	25774
RA3	*R. a. atra*	Huon Peninsula: Rawlinson Mts.	-6.45833	147.4333	ANWC	25790
RA4	*R. a. atra*	Huon Peninsula: Rawlinson Mts.	-6.45833	147.4333	ANWC	25791
RA5	*R. a. atra*	Huon Peninsula: Rawlinson Mts.	-6.45833	147.4333	ANWC	25795
RA6	*R. a. atra*	Huon Peninsula: Rawlinson Mts.	-6.45833	147.4333	AMNH	823619
		PNG: Gulf Province				
LA1	*R. a. atra*	Owen Stanley Range: Lakekamu	-7.73333	146.48333	KUNHM	92014
		PNG: Madang Province				
AD1	*R. a. atra*	Adelbert Range.	-4.71727	145.27482	KUNHM	111633
AD2	*R. a. atra*	Adelbert Range.	-4.71727	145.27482	KUNHM	111474
AD3	*R. a. atra*	Adelbert Range.	-4.71727	145.27482	KUNHM	T12268
AD4	*R. a. atra*	Adelbert Range.	-4.71727	145.27482	KUNHM	111635
AD5	*R. a. atra*	Adelbert Range.	-4.71727	145.27482	KUNHM	111634
AD6	*R. a. atra*	Adelbert Range.	-4.71727	145.27482	KUNHM	111485
AD7	*R. a. atra*	Adelbert Range.	-4.71727	145.27482	KUNHM	111637
AD8	*R. a. atra*	Adelbert Range.	-4.71727	145.27482	KUNHM	111636
AD9	*R. a. atra*	Adelbert Range.	-4.71727	145.27482	KUNHM	111491
SH1	*R. a. atra*	Schradder Range	-5.22057	144.48821	KUNHM	111526
SH2	*R. a. atra*	Schradder Range	-5.22057	144.48821	KUNHM	111625
		PNG: Eastern Highlands Province				
KR1	*R. a. atra*	Kratke Range	-7.061	145.82433	KUNHM	T16494
KR2	*R. a. atra*	Kratke Range	-7.061	145.82433	KUNHM	T16495
KR3	*R. a. atra*	Kratke Range	-7.061	145.82433	KUNHM	T16496
KR4	*R. a. atra*	Kratke Range	-7.061	145.82433	KUNHM	113288
KR5	*R. a. atra*	Kratke Range	-7.061	145.82433	KUNHM	113287
KR6	*R. a. atra*	Kratke Range	-7.061	145.82433	KUNHM	114268
KR7	*R. a. atra*	Kratke Range	-7.061	145.82433	KUNHM	114269
KR8	*R. a. atra*	Kratke Range	-7.061	145.82433	KUNHM	T16545
OK1	*R. a. atra*	Okapa District: Kimigomo	-6.42718	145.58016	KUNHM	T16177
OK2	*R. a. atra*	Okapa District: Kimigomo	-6.42718	145.58016	KUNHM	T16178
OK3	*R. a. atra*	Okapa District: Kimigomo	-6.42718	145.58016	KUNHM	T16189
OK4	*R. a. atra*	Okapa District: Kimigomo	-6.42718	145.58016	KUNHM	T16190
OK5	*R. a. atra*	Okapa District: Kimigomo	-6.42718	145.58016	KUNHM	T16191
OK6	*R. a. atra*	Okapa District: Kimigomo	-6.42718	145.58016	KUNHM	113249
OK7	*R. a. atra*	Okapa District: Kimigomo	-6.42718	145.58016	KUNHM	T16203
OK8	*R. a. atra*	Okapa District: Kimigomo	-6.42718	145.58016	KUNHM	113251

Topology Code	Taxon	Locality	Latitude	Longitude	Source	Voucher Number
OK9	*R. a. atra*	Okapa District: Kimigomo	-6.69444	145.10666	KUNHM	T16205
OK10	*R. a. atra*	Okapa District: Kimigomo	-6.69444	145.10666	KUNHM	T16208
BI1	*R. a. atra*	Bismarck Range	-5.95166	145.4	KUNHM	114872
BI2	*R. a. atra*	Bismarck Range	-5.95166	145.4	KUNHM	114842
BI3	*R. a. atra*	Bismarck Range	-5.95166	145.4	KUNHM	114848
BI4	*R. a. atra*	Bismarck Range	-5.95166	145.4	KUNHM	114849
BI5	*R. a. atra*	Bismarck Range	-5.95166	145.4	KUNHM	114223
BI6	*R. a. atra*	Bismarck Range	-5.95166	145.4	KUNHM	113258
BI7	*R. a. atra*	Bismarck Range	-5.95166	145.4	KUNHM	114222
BI8	*R. a. atra*	Bismarck Range	-5.95166	145.4	KUNHM	114221
BI9	*R. a. atra*	Bismarck Range	-5.95166	145.4	KUNHM	114859
		PNG: Chimbu Province				
KU1	*R. a. atra*	Kubor Range	-6.04883	144.52266	AMNH	705236
		PNG: West Sepik Province				
ST1	*R. a. atra*	Mt. Stolle	-4.81331	141.65293	KUNHM	97637
ST2	*R. a. atra*	Mt. Stolle	-4.81331	141.65293	KUNHM	114924
ST3	*R. a. atra*	Mt. Stolle	-4.81331	141.65293	KUNHM	114215
ST4	*R. a. atra*	Mt. Stolle	-4.81331	141.65293	KUNHM	114217
ST5	*R. a. atra*	Mt. Stolle	-4.81331	141.65293	KUNHM	114216
ST6	*R. a. atra*	Mt. Stolle	-4.81331	141.65293	KUNHM	113318
ST7	*R. a. atra*	Mt. Stolle	-4.81331	141.65293	KUNHM	114218
ST8	*R. a. atra*	Mt. Stolle	-4.81331	141.65293	KUNHM	114219
ST9	*R. a. atra*	Mt. Stolle	-4.81331	141.65293	KUNHM	113319
HR1	*R. a. atra*	Hindenburg Range: Ilkivip	-5.25066	141.38472	AMNH	765758
TF1	*R. a. atra*	Telefomin	-5.12561	141.63596	AMNH	765753
BW1	*R. a. atra*	Bewani Mts., Mt. Menawa	-3.30373	141.72652	AMNH	829476
BW2	*R. a. atra*	Bewani Mts., Mt. Menawa	-3.30373	141.72652	AMNH	829475
BW3	*R. a. atra*	Bewani Mts., Mt. Menawa	-3.30373	141.72652	AMNH	829482
BW4	*R. a. atra*	Bewani Mts., Mt. Menawa	-3.30373	141.72652	AMNH	829480
BW5	*R. a. atra*	Bewani Mts., Mt. Menawa	-3.30373	141.72652	AMNH	829479
BW6	*R. a. atra*	Bewani Mts., Mt. Menawa	-3.30373	141.72652	AMNH	829477
BW7	*R. a. atra*	Bewani Mts., Mt. Menawa	-3.30373	141.72652	AMNH	829481
TO1	*R. a. atra*	Torricelli Mts., Mt. Nibo	-3.40879	142.18570	AMNH	829473
TO2	*R. a. atra*	Torricelli Mts., Mt. Nibo	-3.40879	142.18570	AMNH	829471
TO3	*R. a. atra*	Torricelli Mts., Mt. Nibo	-3.40879	142.18570	AMNH	829472
CY1	*R. a. atra*	Cyclops Mts	-2.5077	140.52608	AMNH	293935
CY2	*R. a. atra*	Cyclops Mts	-2.5077	140.52608	AMNH	293933
CY3	*R. a. atra*	Cyclops Mts	-2.5077	140.52608	AMNH	293937
CY4	*R. a. atra*	Cyclops Mts	-2.5077	140.52608	AMNH	293934
CY5	*R. a. atra*	Cyclops Mts	-2.5077	140.52608	AMNH	651764
CY6	*R. a. atra*	Cyclops Mts	-2.5077	140.52608	AMNH	651766
CY7	*R. a. atra*	Cyclops Mts	-2.5077	140.52608	AMNH	651767
CY8	*R. a. atra*	Cyclops Mts	-2.5077	140.52608	AMNH	651768
		Indonesia: Papua Province				
GO1	*R. a. atra*	Oranje Mts: Mt. Goliath	-4.66857	139.84815	AMNH	651760
GO2	*R. a. atra*	Oranje Mts: Mt. Goliath	-4.66857	139.84815	AMNH	651756
GO3	*R. a. atra*	Oranje Mts: Mt. Goliath	-4.66857	139.84815	AMNH	651759
IL1	*R. a. atra*	Nassau Range: Ilaga	-3.98963	137.54045	YPBM	75814
BV1	*R. a. atra*	Baliem Valley: Wamena	-4.050	138.933	YPBM	75815
BV2	*R. a. atra*	Baliem Valley: Wamena	-4.050	138.933	YPBM	75816
BV3	*R. a. atra*	Baliem Valley: Wamena	-4.050	138.933	YPBM	75817
BV4	*R. a. atra*	Baliem Valley: Wamena	-4.050	138.933	YPBM	75818
BV5	*R. a. atra*	Baliem Valley: Wamena	-4.050	138.933	YPBM	75819
LH1	*R. a. atra*	Bele River: Lake Habbema	-4.08416	138.7391	AMNH	341058

Topology Code	Taxon	Locality	Latitude	Longitude	Source	Voucher Number
LH2	*R. a. atra*	Bele River: Lake Habbema	-4.08416	138.7391	AMNH	341059
WE1	*R. a. atra*	Weyland Mts: Kunupi	-3.89137	135.4664	AMNH	302193
WE2	*R. a. atra*	Weyland Mts: Kunupi	-3.89137	135.4664	AMNH	302195
WE3	*R. a. atra*	Weyland Mts: Kunupi	-3.89137	135.4664	AMNH	302194
WE4	*R. a. atra*	Weyland Mts: Sumuri	-3.89137	135.4664	AMNH	302192
WE5	*R. a. atra*	Weyland Mts: Kunupi	-3.89137	135.4664	AMNH	302199
WE6	*R. a. atra*	Weyland Mts: Kunupi	-3.89137	135.4664	AMNH	302197
WE7	*R. a. atra*	Weyland Mts.	-3.89137	135.4664	AMNH	302198
WE8	*R. a. atra*	Weyland Mts.	-3.89137	135.4664	AMNH	302196
		Indonesia: West Papua Province				
WA1	*R. a. atra*	Wandamen Mts.	-2.75584	134.58458	AMNH	651761
WA2	*R. a. atra*	Wandamen Mts.	-2.75584	134.58458	AMNH	293941
WA3	*R. a. atra*	Wandamen Mts.	-2.75584	134.58458	AMNH	651762
AR1	*R. a. atra*	Vogelkop: Arfak Mts.	-1.09181	133.9073	AMNH	651730
AR2	*R. a. atra*	Vogelkop: Arfak Mts.	-1.09181	133.9073	AMNH	651731
TA1	*R. a. atra*	Vogelkop: Tamrau Mts.	-0.71553	132.96645	AMNH	792975
TA2	*R. a. atra*	Vogelkop: Tamrau Mts.	-0.71553	132.96645	AMNH	792976
TA3	*R. a. atra*	Vogelkop: Tamrau Mts.	-0.71553	132.96645	AMNH	792977
TA4	*R. a. atra*	Vogelkop: Tamrau Mts.	-0.54878	132.73	ANSP	132675
TA5	*R. a. atra*	Vogelkop: Tamrau Mts.	-0.54878	132.73	ANSP	132673
TA6	*R. a. atra*	Vogelkop: Tamrau Mts.	-0.54878	132.73	ANSP	132676
TA7	*R. a. atra*	Vogelkop: Tamrau Mts.	-0.54878	132.73	ANSP	132677
TA8	*R. a. atra*	Vogelkop: Tamrau Mts.	-0.54878	132.73	ANSP	132111
TA9	*R. a. atra*	Vogelkop: Tamrau Mts.	-0.54878	132.73	ANSP	132674
Outgroup						
	Rhipidura albolimbata	PNG: Morobe Province	-6.08165	146.57224	KUNHM	93573
	Rhipidura brachyrhyncha	PNG: Morobe Province	-6.08165	146.57224	KUNHM	92363
	Rhipidura cyaniceps	Philippines: Panay Island	10.812	122.182	KUNHM	T15299
	Rhipidura leucophrys	Australia: WA, ~Wubin Station	-30.0485	116.71145	KUNHM	T6148
	Rhipidura phasiana	Australia: WA, ~Carnarvon	-25.5	113.6833	KUNHM	T6194
	Rhipidura rufifrons	Solomon Islands: Makira Island	-10.6133	161.8866	KUNHM	T12828
	Rhipidura rufidorsa	PNG: Gulf Province, Wabo	-6.90833	145.05833	KUNHM	T5083
	Rhipidura rufiventris	PNG: Oro Province, Mt. Suckling	-9.53333	149.06666	KUNHM	T6867
	Rhipidura threnothorax	PNG: Chimbu Province, Haia	-6.69583	144.97516	KUNHM	T4857
	Chaetorhynchus papuensis	PNG: Oro Province, Mt. Suckling	-9.52643	149.10465	KUNHM	T6974
	Dicrurus hottentottus	Philippines: Samar Island	11.8174	125.27788	KUNHM	T14164
Ingroup	*Amblyornis macgregoriae*	PNG: Milne Bay Province				
AG1	*A. m. nubicola*	Agaun	-9.92917	149.38333	ANWC	8030
AG2	*A. m. nubicola*	Agaun	-9.92917	149.38333	ANWC	8113
AG3	*A. m. nubicola*	Agaun	-9.92917	149.38333	ANWC	8137
		PNG: Central Province				
SI1	*A. m. nubicola*	Mt. Simpson	-9.99982	149.50718	KUNHM	114130
SI2	*A. m. nubicola*	Mt. Simpson	-9.99982	149.50718	KUNHM	114133
SI3	*A. m. nubicola*	Mt. Simpson	-9.99982	149.50718	KUNHM	114134
SI4	*A. m. nubicola*	Mt. Simpson	-9.98955	149.48674	KUNHM	114135
SI5	*A. m. nubicola*	Mt. Simpson	-9.99982	149.50718	KUNHM	114132
SI6	*A. m. nubicola*	Mt. Simpson	-9.99982	149.50718	KUNHM	114131
SI7	*A. m. nubicola*	Mt. Simpson	-9.98955	149.48674	KUNHM	NV
EF1	*A. m. macgregoriae*	Owen Stanley Range: Efogi	-9.15	147.66667	ANWC	9183
EF2	*A. m. macgregoriae*	Owen Stanley Range: Efogi	-9.15	147.66667	ANWC	9222
EF3	*A. m. macgregoriae*	Owen Stanley Range: Efogi	-9.15	147.66667	ANWC	25004
EF4	*A. m. macgregoriae*	Owen Stanley Range: Efogi	-9.15	147.66667	ANWC	25005
AE1	*A. m. macgregoriae*	Mt. Albert Edward	-8.45962	147.4001	PNGNM	19181
AE2	*A. m. macgregoriae*	Mt. Albert Edward	-8.45962	147.4001	AMNH	816488

Topology Code	Taxon	Locality	Latitude	Longitude	Source	Voucher Number
OW1	*A. m. macgregoriae*	Owagarra: Angabunga River	-8.21596	146,9096	PNGNM	679561
		PNG: Oro Province				
AW1	*A. m. macgregoriae*	Owen Stanley Range: Awoma Ridge	-9.18333	148.13333	ANWC	26832
AW2	*A. m. macgregoriae*	Owen Stanley Range: Awoma Ridge	-9.18333	148.13333	ANWC	26952
AW3	*A. m. macgregoriae*	Owen Stanley Range: Awoma Ridge	-9.18333	148.13333	ANWC	26871
AW4	*A. m. macgregoriae*	Owen Stanley Range: Awoma Ridge	-9.18333	148.13333	ANWC	E354a
AW5	*A. m. macgregoriae*	Owen Stanley Range: Awoma Ridge	-9.18333	148.13333	ANWC	E333
BH1	*A. m. mayri*	Mambare River: Bihagi	-8.73413	147.7732	AMNH	679550
		PNG: Morobe Province				
HE1	*A. m. macgregoriae*	Herzog Mts: Wagu	-6.8	146.8	ANWC	25463
HE2	*A. m. macgregoriae*	Herzog Mts: Wagu	-6.8	146.8	ANWC	25513
HE3	*A. m. macgregoriae*	Herzog Mts: Wagu	-6.8	146.8	ANWC	25514
HE4	*A. m. macgregoriae*	Herzog Mts: Wagu	-6.8	146.8	ANWC	25573
MI1	*A. m. macgregoriae*	Owen Stanley Range: Mt. Missim	-7.21991	146.81598	MCZ	168327
MI2	*A. m. macgregoriae*	Owen Stanley Range: Mt. Missim	-7.21991	146.81598	MCZ	168329
MI3	*A. m. macgregoriae*	Owen Stanley Range: Mt. Missim	-7.21991	146.81598	MCZ	168330
MI4	*A. m. macgregoriae*	Owen Stanley Range: Mt. Missim	-7.21991	146.81598	MCZ	168331
MI5	*A. m. macgregoriae*	Owen Stanley Range: Mt. Missim	-7.21991	146.81598	MCZ	168332
MI6	*A. m. macgregoriae*	Owen Stanley Range: Mt. Missim	-7.21991	146.81598	MCZ	168334
MI7	*A. m. macgregoriae*	Owen Stanley Range: Mt. Missim	-7.21991	146.81598	MCZ	168335
MI8	*A. m. macgregoriae*	Owen Stanley Range: Mt. Missim	-7.21991	146.81598	MCZ	168336
WU1	*A. m. macgregoriae*	Owen Stanley Range: Wau	-7.34099	146.68141	PNGNM	26321
KO1	*A. m. macgregoriae*	Owen Stanley Range: Mt. Kolorong	-7.4840	146.6943	PNGNM	26761
KO2	*A. m. macgregoriae*	Owen Stanley Range: Mt. Kolorong	-7.4840	146.6943	PNGNM	26763
FI1	*A. m. germanus*	Huon Peninsula: Finisterre Range	-6.08165	146.57224	KUNHM	95810
FI2	*A. m. germanus*	Huon Peninsula: Finisterre Range	-6.08165	146.57224	KUNHM	92337
FI3	*A. m. germanus*	Huon Peninsula: Finisterre Range	-6.08165	146.57224	KUNHM	93598
FI4	*A. m. germanus*	Huon Peninsula: Finisterre Range	-6.08165	146.57224	KUNHM	93599
SA1	*A. m. germanus*	Huon Peninsula: Saruwaged Mts.	-6.11056	146.89576	KUNHM	111535
SA2	*A. m. germanus*	Huon Peninsula: Saruwaged Mts	-6.11056	146.89576	KUNHM	111539
SA3	*A. m. germanus*	Huon Peninsula: Saruwaged Mts	-6.11056	146.89576	KUNHM	111536
SA4	*A. m. germanus*	Huon Peninsula: Saruwaged Mts	-6.11056	146.89576	KUNHM	111538
SA5	*A. m. germanus*	Huon Peninsula: Saruwaged Mts	-6.11056	146.89576	KUNHM	111540
RA1	*A. m. germanus*	Huon Peninsula: Rawlinson Mts.	-6.45833	147.4333	ANWC	26050
RA2	*A. m. germanus*	Huon Peninsula: Rawlinson Mts.	-6.45833	147.4333	ANWC	26076
		PNG: Madang Province				
AD1	*A. m. amati*	Adelbert Range.	-4.71727	145.27482	KUNHM	111531
AD2	*A. m. amati*	Adelbert Range.	-4.71727	145.27482	KUNHM	111532
AD3	*A. m. amati*	Adelbert Range.	-4.71727	145.27482	KUNHM	111530
AD4	*A. m. amati*	Adelbert Range.	-4.71727	145.27482	KUNHM	NV
SH1	*A. m. kombok*	Schradder Range	-5.22057	144.48821	KUNHM	111525
SH2	*A. m. kombok*	Schradder Range	-5.22057	144.48821	KUNHM	111523
SH3	*A. m. kombok*	Schradder Range	-5.22057	144.48821	KUNHM	111528
SH4	*A. m. kombok*	Schradder Range	-5.22057	144.48821	KUNHM	111529
SH5	*A. m. kombok*	Schradder Range	-5.22057	144.48821	KUNHM	114752
SH6	*A. m. kombok*	Schradder Range	-5.22057	144.48821	KUNHM	111527
SH7	*A. m. kombok*	Schradder Range	-5.22057	144.48821	KUNHM	111526
SH8	*A. m. kombok*	Schradder Range	-5.22057	144.48821	KUNHM	111524
SH9	*A. m. kombok*	Schradder Range	-5.22057	144.48821	KUNHM	114733
SH10	*A. m. kombok*	Schradder Range	-5.22057	144.48821	KUNHM	114741
		PNG: Eastern Highlands Province				
KR1	*A. m. kombok*	Kratke Range	-7.061	145.82433	KUNHM	16504
KR2	*A. m. kombok*	Kratke Range	-7.061	145.82433	KUNHM	113278
KR3	*A. m. kombok*	Kratke Range	-7.061	145.82433	KUNHM	114265

Topology Code	Taxon	Locality	Latitude	Longitude	Source	Voucher Number
KR4	*A. m. kombok*	Kratke Range	-7.061	145.82433	KUNHM	114920
KR5	*A. m. kombok*	Kratke Range	-7.061	145.82433	KUNHM	114266
OK1	*A. m. kombok*	Okapa District: Awande	-6.52085	145.60102	AMNH	809357
KA1	*A. m. kombok*	Mt. Karimui	-6.5681	144.8001	AMNH	809358
KA2	*A. m. kombok*	Mt. Karimui	-6.5681	144.8001	AMNH	809359
KU1	*A. m. kombok*	Kubor Range	-6.04883	144.52266	PNGNM	14531
BI1	*A. m. kombok*	Bismarck Range	-5.95166	145.4	KUNHM	114225
BI2	*A. m. kombok*	Bismarck Range	-5.95166	145.4	KUNHM	114224
CR1	*A. m. kombok*	Crater Mountain	-6.69444	145.10666	KUNHM	91947
CR2	*A. m. kombok*	Crater Mountain	-6.69444	145.10666	KUNHM	98038
CR3	*A. m. kombok*	Crater Mountain	-6.69444	145.10666	KUNHM	T5243
	A. m. kombok	PNG: Western Highlands Province				
HA1	*A. m. kombok*	Mt. Hagen	-5.79419	143.99600	KUNHM	111534
HA2	*A. m. kombok*	Mt. Hagen	-5.79419	143.99600	KUNHM	111533
GU1	*A. m. kombok*	Mt. Gulno	5.59764	144.80465	PNGNM	26535
		PNG: West Sepik Province				
ST1	*A. m. mayri*	Mt. Stolle	-4.81331	141.65293	KUNHM	97638
ST2	*A. m. mayri*	Mt. Stolle	-4.81331	141.65293	KUNHM	97639
ST3	*A. m. mayri*	Mt. Stolle	-4.81331	141.65293	KUNHM	97640
ST4	*A. m. mayri*	Mt. Stolle	-4.81331	141.65293	KUNHM	115537
ST5	*A. m. mayri*	Mt. Stolle	-4.81331	141.65293	KUNHM	114209
ST6	*A. m. mayri*	Mt. Stolle	-4.81331	141.65293	KUNHM	114208
TF1	*A. m. mayri*	Telefomin: Miptagin	-5.12561	141.63596	AMNH	765973
		Indonesia: Papua Province				
GO1	*A. m. mayri*	Oranje Mts: Mt. Goliath	-3.98963	137.54045	AMNH	679548
GO2	*A. m. mayri*	Oranje Mts: Mt. Goliath	-3.98963	137.54045	AMNH	679546
GO3	*A. m. mayri*	Oranje Mts: Mt. Goliath	-3.98963	137.54045	AMNH	679547
GO4	*A. m. mayri*	Oranje Mts: Mt. Goliath	-3.98963	137.54045	AMNH	679541
LH1	*A. m. mayri*	Bele River: Lake Habbema	-4.08416	138.7391	AMNH	342271
LH2	*A. m. mayri*	Bele River: Lake Habbema	-4.08416	138.7391	AMNH	342286
LH3	*A. m. mayri*	Bele River: Lake Habbema	-4.08416	138.7391	AMNH	342267
LH4	*A. m. mayri*	Bele River: Lake Habbema	-4.08416	138.7391	AMNH	342285
LH5	*A. m. mayri*	Bele River: Lake Habbema	-4.08416	138.7391	AMNH	342274
WE1	*A. m. mayri*	Weyland Mts.	-3.89137	135.4664	AMNH	303010
WE2	*A. m. mayri*	Weyland Mts.	-3.89137	135.4664	AMNH	303012
WE3	*A. m. mayri*	Weyland Mts.	-3.89137	135.4664	AMNH	303015
WE4	*A. m. mayri*	Weyland Mts.	-3.89137	135.4664	AMNH	303011
WE5	*A. m. mayri*	Weyland Mts.	-3.89137	135.4664	AMNH	303013
WE6	*A. m. mayri*	Weyland Mts.	-3.89137	135.4664	AMNH	302457
WE7	*A. m. mayri*	Weyland Mts.	-3.89137	135.4664	AMNH	303017
WE8	*A. m. mayri*	Weyland Mts.	-3.89137	135.4664	AMNH	679537
WE9	*A. m. mayri*	Weyland Mts.	-3.89137	135.4664	AMNH	303016
Outgroup						
1	*Amblyornis inornatus*	Indonesia: Wandamen Range	-2.75584	134.58458	AMNH	679522
2	*Amblyornis inornatus*	Indonesia: Tamrau Mts., Mt. Bantjiet	-0.71553	132.96645	AMNH	793055
3	*Amblyornis inornatus*	Indonesia: Arfak Mts., Siwi	-1.09181	133.9073	AMNH	679511
4	*Amblyornis inornatus*	Indonesia: Wandamen Range	-2.75584	134.58458	AMNH	303093
5	*Amblyornis inornatus*	Tamrau Mts., Bonkouragen	-0.54878	132.73	AMNH	132355
6	*Amblyornis inornatus*	Indonesia: Tamrau Mts., Mt. Bantjiet	-0.71553	132.96645	AMNH	793057
7	*Amblyornis inornatus*	Indonesia: Arfak Mts., Lahuma	-1.09181	133.9073	AMNH	679510
8	*Amblyornis inornatus*	Tamrau Mts., Bonkouragen	-0.54878	132.73	ANSP	132351
1	*Archboldia papuensis*	Indonesia: Bernhard Camp	--	--	AMNH	342255
2	*Archboldia papuensis*	Indonesia: Bele River	-4.08416	138.7391	AMNH	342259
3	*Archboldia papuensis*	PNG: Mt. Hagen	-5.8024	144.02041	AMNH	705703

Topology Code	Taxon	Locality	Latitude	Longitude	Source	Voucher Number
4	*Archboldia papuensis*	Indonesia: Ilaga	-3.98963	137.54045	YPBM	75438
1	*Amblyornis subalaris*	PNG: Mt. Simpson	9.98955	149.4866	KUNHM	114110
2	*Amblyornis subalaris*	PNG: Mt. Simpson	9.98955	149.4866	KUNHM	114111
3	*Amblyornis subalaris*	PNG: Mt. Simpson	9.98955	149.4866	KUNHM	114112
4	*Amblyornis subalaris*	PNG: Mt. Simpson	9.98955	149.4866	KUNHM	114113
5	*Amblyornis subalaris*	PNG: Mt. Simpson	9.98955	149.4866	KUNHM	114114
1	*Amblyornis flavifrons*	Indonesia: Foya Mts.	-2.5825	139.0056	AMNH	679120
2	*Amblyornis flavifrons*	Indonesia: Foya Mts	-2.5825	139.0056	AMNH	679121
	Prionodura newtonia	Australia: Mt Coleman	-17.7188	145.5353	AMNH	679492
	Sericulus bakeri	PNG: Adelbert Range	-4.70521	145.4042	KUNHM	114779
	Chlamydera maculata	Australia: Noonbah Station	-24.1074	143.1862	KUNHM	98491
	Ailuroedus buccoides	Adelbert Range	-4.70521	145.4042	KUNHM	111547
	Climacteris melanura	Australia: WA	-24.9833	114.916	KUNHM	94440
	Menura novaehollandiae	Australia: NSW	--	--	Genbank	542313
Ingroup	*Crateroscelis robusta*	PNG: Central Province				
SI1	*C. r. robusta*	Mt. Simpson	-9.99982	149.50718	KUNHM	T14598
SI2	*C. r. robusta*	Mt. Simpson	-9.99982	149.50718	KUNHM	114829
SI3	*C. r. robusta*	Mt. Simpson	-9.99982	149.50718	KUNHM	114832
SI4	*C. r. robusta*	Mt. Simpson	-9.99982	149.50718	KUNHM	114143
SI5	*C. r. robusta*	Mt. Simpson	-9.99982	149.50718	KUNHM	114142
SI6	*C. r. robusta*	Mt. Simpson	-9.99982	149.50718	KUNHM	114144
SI7	*C. r. robusta*	Mt. Simpson	-9.99982	149.50718	KUNHM	114145
SI8	*C. r. robusta*	Mt. Simpson	-9.99982	149.50718	KUNHM	114146
SI9	*C. r. robusta*	Mt. Simpson	-9.99982	149.50718	KUNHM	114108
EF1	*C. r. robusta*	Owen Stanley Range: Efogi	-9.15	147.66667	ANWC	24439
EF2	*C. r. robusta*	Owen Stanley Range: Efogi	-9.15	147.66667	ANWC	24444
EF3	*C. r. robusta*	Owen Stanley Range: Efogi	-9.15	147.66667	ANWC	26560
EF4	*C. r. robusta*	Owen Stanley Range: Efogi	-9.15	147.66667	ANWC	26574
EF5	*C. r. robusta*	Owen Stanley Range: Efogi	-9.15	147.66667	ANWC	26496
EF6	*C. r. robusta*	Owen Stanley Range: Efogi	-9.15	147.66667	ANWC	24440
AE1	*C. r. robusta*	Mt. Albert Edward	-8.45962	147.4001	AMNH	420054
AE2	*C. r. robusta*	Mt. Albert Edward	-8.45962	147.4001	AMNH	420030
AE3	*C. r. robusta*	Mt. Albert Edward	-8.45962	147.4001	AMNH	420053
TF1	*C. r. robusta*	Mt. Tafa	-8.63351	147.18387	AMNH	420027
TF2	*C. r. robusta*	Mt. Tafa	-8.63351	147.18387	AMNH	420028
TF3	*C. r. robusta*	Mt. Tafa	-8.63351	147.18387	AMNH	420039
TF4	*C. r. robusta*	Mt. Tafa	-8.63351	147.18387	AMNH	420042
TF5	*C. r. robusta*	Mt. Tafa	-8.63351	147.18387	AMNH	420055
HE1	*C. r. robusta*	PNG: Morobe Province Herzog Mts: Wagu	-6.8	146.8	ANWC	25568
HE2	*C. r. robusta*	Herzog Mts: Wagu	-6.8	146.8	ANWC	25630
MI1	*C. r. robusta*	Owen Stanley Range: Mt. Missim	-7.21991	146.81598	MCZ	330571
MI2	*C. r. robusta*	Owen Stanley Range: Mt. Missim	-7.21991	146.81598	MCZ	167702
MI3	*C. r. robusta*	Owen Stanley Range: Mt. Missim	-7.21991	146.81598	MCZ	167703
MI4	*C. r. robusta*	Owen Stanley Range: Mt. Missim	-7.21991	146.81598	MCZ	167701
MI5	*C. r. robusta*	Owen Stanley Range: Mt. Missim	-7.21991	146.81598	MCZ	167700
MI6	*C. r. robusta*	Owen Stanley Range: Mt. Missim	-7.21991	146.81598	MCZ	167699
MI7	*C. r. robusta*	Owen Stanley Range: Mt. Missim	-7.21991	146.81598	MCZ	167698
MI8	*C. r. robusta*	Owen Stanley Range: Mt. Missim	-7.21991	146.81598	MCZ	167697
MI9	*C. r. robusta*	Owen Stanley Range: Mt. Missim	-7.21991	146.81598	MCZ	167696
HU1	*C. r. robusta*	Haumnga	-7.33416	146.4680	ANWC	4184
HU2	*C. r. robusta*	Haumnga	-7.33416	146.4680	ANWC	4213
HU3	*C. r. robusta*	Haumnga	-7.33416	146.4680	ANWC	4257
HU4	*C. r. robusta*	Haumnga	-7.33416	146.4680	ANWC	4295

Topology Code	Taxon	Locality	Latitude	Longitude	Source	Voucher Number
FI1	*C. r. robusta*	Huon Peninsula: Finisterre Range	-6.08165	146.57224	KUNHM	95791
FI2	*C. r. robusta*	Huon Peninsula: Finisterre Range	-6.08165	146.57224	KUNHM	92357
FI3	*C. r. robusta*	Huon Peninsula: Finisterre Range	-6.08165	146.57224	KUNHM	92361
FI4	*C. r. robusta*	Huon Peninsula: Finisterre Range	-6.08165	146.57224	KUNHM	93568
FI5	*C. r. robusta*	Huon Peninsula: Finisterre Range	-6.08165	146.57224	KUNHM	95289
FI6	*C. r. robusta*	Huon Peninsula: Finisterre Range	-6.08165	146.57224	KUNHM	T4576
SA1	*C. r. robusta*	Huon Peninsula: Saruwaged Mts	-6.11056	146.89576	KUNHM	111622
SA2	*C. r. robusta*	Huon Peninsula: Saruwaged Mts	-6.11056	146.89576	KUNHM	111623
SA3	*C. r. robusta*	Huon Peninsula: Saruwaged Mts	-6.11056	146.89576	KUNHM	111624
		PNG: Madang Province				
SH1	*C. r. robusta*	Schradder Range	-5.22057	144.48821	KUNHM	111629
SH2	*C. r. robusta*	Schradder Range	-5.22057	144.48821	KUNHM	114756
		PNG: Eastern Highlands Province				
KR1	*C. r. robusta*	Kratke Range	-7.061	145.82433	KUNHM	113275
KR2	*C. r. robusta*	Kratke Range	-7.061	145.82433	KUNHM	114282
KR3	*C. r. robusta*	Kratke Range	-7.061	145.82433	KUNHM	114281
OK1	*C. r. robusta*	Okapa District: Kimigomo	-6.42718	145.58016	KUNHM	114886
BI1	*C. r. robusta*	Bismarck Range	-5.95166	145.4	KUNHM	114233
BI2	*C. r. robusta*	Bismarck Range	-5.95166	145.4	KUNHM	114232
BI3	*C. r. robusta*	Bismarck Range	-5.95166	145.4	KUNHM	114234
BI4	*C. r. robusta*	Bismarck Range	-5.95166	145.4	KUNHM	114896
CR1	*C. r. robusta*	Crater Mountain	-6.69444	145.10666	KUNHM	91987
CR2	*C. r. robusta*	Crater Mountain	-6.69444	145.10666	KUNHM	T5260
KU1	*C. r. robusta*	Kubor Range	-6.04883	144.52266	AMNH	705065
KU2	*C. r. robusta*	Kubor Range	-6.04883	144.52266	AMNH	705067
		PNG: Western Highlands Province				
HA1	*C. r. robusta*	Mt. Hagen	-5.79419	143.99600	AMNH	705075
HA2	*C. r. robusta*	Mt. Hagen	-5.79419	143.99600	AMNH	705074
HA3	*C. r. robusta*	Mt. Hagen	-5.79419	143.99600	AMNH	705405
		PNG: West Sepik Province				
ST1	*C. r. sanfordi*	Mt. Stolle	-4.81331	141.65293	KUNHM	97650
ST2	*C. r. sanfordi*	Mt. Stolle	-4.81331	141.65293	KUNHM	114287
ST3	*C. r. sanfordi*	Mt. Stolle	-4.81331	141.65293	KUNHM	114286
OS1	*C. r. sanfordi*	Oksapmin	-5.21812	142.24981	PNGNM	23462
HR1	*C. r. sanfordi*	Hindenburg Range: Ilkivip	-5.25066	141.38472	AMNH	765679
HR2	*C. r. sanfordi*	Hindenburg Range: Ilkivip	-5.25066	141.38472	AMNH	765680
HR3	*C. r. sanfordi*	Hindenburg Range: Ilkivip	-5.25066	141.38472	AMNH	765681
BW1	*C. r. bastille*	Bewani Mts., Mt. Menawa	-3.30373	141.72652	AMNH	829331
BW2	*C. r. bastille*	Bewani Mts., Mt. Menawa	-3.30373	141.72652	AMNH	829328
BW3	*C. r. bastille*	Bewani Mts., Mt. Menawa	-3.30373	141.72652	AMNH	829329
BW4	*C. r. bastille*	Bewani Mts., Mt. Menawa	-3.30373	141.72652	AMNH	829330
BW5	*C. r. bastille*	Bewani Mts., Mt. Menawa	-3.30373	141.72652	AMNH	829327
BW6	*C. r. bastille*	Bewani Mts., Mt. Menawa	-3.30373	141.72652	AMNH	829326
BW7	*C. r. bastille*	Bewani Mts., Mt. Menawa	-3.30373	141.72652	AMNH	829332
BW8	*C. r. bastille*	Bewani Mts., Mt. Menawa	-3.30373	141.72652	AMNH	829333
TO1	*C. r. bastille*	Torricelli Mts., Mt. Nibo	-3.40879	142.18570	AMNH	829325
		Indonesia: Papua Province				
LH1	*C. r. sanfordi*	Bele River: Lake Habbema	-4.08416	138.7391	AMNH	340449
LH2	*C. r. sanfordi*	Bele River: Lake Habbema	-4.08416	138.7391	AMNH	340443
LH3	*C. r. sanfordi*	Bele River: Lake Habbema	-4.08416	138.7391	AMNH	340469
LH4	*C. r. sanfordi*	Bele River: Lake Habbema	-4.08416	138.7391	AMNH	340461
LH5	*C. r. sanfordi*	Bele River: Lake Habbema	-4.08416	138.7391	AMNH	340487
BE1	*C. r. sanfordi*	Bernhard Camp	--	--	AMNH	340439
BE2	*C. r. sanfordi*	Bernhard Camp	--	--	AMNH	340435

Topology Code	Taxon	Locality	Latitude	Longitude	Source	Voucher Number
WI1	*C. r. sanfordi*	Mt. Wilhemina	-4.24376	138.6212	AMNH	340491
IL1	*C. r. sanfordi*	Nassau Range: Ilaga	-3.98963	137.54045	YPBM	75553
IL2	*C. r. sanfordi*	Nassau Range: Ilaga	-3.98963	137.54045	YPBM	75554
IL3	*C. r. sanfordi*	Nassau Range: Ilaga	-3.98963	137.54045	YPBM	75556
CY1	*C. r. deficiens*	Cyclops Mts	-2.5077	140.52608	AMNH	293887
CY2	*C. r. deficiens*	Cyclops Mts	-2.5077	140.52608	AMNH	589357
CY3	*C. r. deficiens*	Cyclops Mts	-2.5077	140.52608	AMNH	293889
CY4	*C. r. deficiens*	Cyclops Mts	-2.5077	140.52608	AMNH	293888
CY5	*C. r. deficiens*	Cyclops Mts	-2.5077	140.52608	AMNH	589360
CY6	*C. r. deficiens*	Cyclops Mts	-2.5077	140.52608	AMNH	293891
CY7	*C. r. deficiens*	Cyclops Mts	-2.5077	140.52608	AMNH	293886
CY8	*C. r. deficiens*	Cyclops Mts	-2.5077	140.52608	AMNH	589359
CY9	*C. r. deficiens*	Cyclops Mts	-2.5077	140.52608	AMNH	293890
CY10	*C. r. deficiens*	Cyclops Mts	-2.5077	140.52608	AMNH	589358
WE1	*C. r. sanfordi*	Weyland Mts.	-3.89137	135.4664	AMNH	301921
WE2	*C. r. sanfordi*	Weyland Mts.	-3.89137	135.4664	AMNH	301986
WE3	*C. r. sanfordi*	Weyland Mts.	-3.89137	135.4664	AMNH	301922
WE4	*C. r. sanfordi*	Weyland Mts.	-3.89137	135.4664	AMNH	301925
WE5	*C. r. sanfordi*	Weyland Mts.	-3.89137	135.4664	AMNH	301926
WE6	*C. r. sanfordi*	Weyland Mts.	-3.89137	135.4664	AMNH	301924
WE7	*C. r. sanfordi*	Weyland Mts.	-3.89137	135.4664	AMNH	301923
WE8	*C. r. sanfordi*	Weyland Mts.	-3.89137	135.4664	AMNH	301977
WE9	*C. r. sanfordi*	Weyland Mts.	-3.89137	135.4664	AMNH	301918
		Indonesia: West Papua Province				
WA1	*C. r. sanfordi*	Wandamen Mts.	-2.75584	134.58458	AMNH	589365
WA2	*C. r. sanfordi*	Wandamen Mts.	-2.75584	134.58458	AMNH	589366
WA3	*C. r. sanfordi*	Wandamen Mts.	-2.75584	134.58458	AMNH	589367
WA4	*C. r. sanfordi*	Wandamen Mts.	-2.75584	134.58458	AMNH	293892
WA5	*C. r. sanfordi*	Wandamen Mts.	-2.75584	134.58458	AMNH	293894
TA1	*C. r. ripleyi*	Tamrau Mts., Mt. Bantjiet	-0.71553	132.96645	AMNH	792948
TA2	*C. r. ripleyi*	Tamrau Mts., Mt. Bantjiet	-0.71553	132.96645	AMNH	792949
TA3	*C. r. ripleyi*	Tamrau Mts., Mt. Bantjiet	-0.71553	132.96645	AMNH	792950
TA4	*C. r. ripleyi*	Tamrau Mts., Mt. Bantjiet	-0.71553	132.96645	AMNH	792951
TA5	*C. r. ripleyi*	Tamrau Mts., Mt. Bantjiet	-0.71553	132.96645	AMNH	792952
AR1	*C. r. peninsularis*	Arfak Mts.	-1.09181	133.9073	AMNH	589364
AR2	*C. r. peninsularis*	Arfak Mts.	-1.09181	133.9073	AMNH	589361
AR3	*C. r. peninsularis*	Arfak Mts.	-1.09181	133.9073	AMNH	293884
AR4	*C. r. peninsularis*	Arfak Mts.	-1.09181	133.9073	AMNH	293881
AR5	*C. r. peninsularis*	Arfak Mts.	-1.09181	133.9073	AMNH	589362
AR6	*C. r. peninsularis*	Arfak Mts.	-1.09181	133.9073	AMNH	293880
AR7	*C. r. peninsularis*	Arfak Mts.	-1.09181	133.9073	AMNH	589363
AR8	*C. r. peninsularis*	Arfak Mts.	-1.09181	133.9073	AMNH	293885
AR9	*C. r. peninsularis*	Arfak Mts.	-1.09181	133.9073	AMNH	293882
Outgroup						
1	*Crateroscelis murina*	PNG: Madang Province	-4.71727	145.27482	KUNHM	111639
2	*Crateroscelis murina*	PNG: Madang Province:	-4.4825	145.0316	KUNHM	97904
3	*Crateroscelis murina*	PNG: East Sepik Province	-4.61525	142.7133	KUNHM	T9167
1	*Crateroscelis nigrorufa*	PNG: Eastern Highlands Province	-6.6545	145.1714	KUNHM	91986
2	*Crateroscelis nigrorufa*	PNG: Eastern Highlands Province	-7.061	145.82433	KUNHM	114280
3	*Crateroscelis nigrorufa*	PNG: Eastern Highlands Province	-7.061	145.82433	KUNHM	113274
	Sericornis nouhuysi	PNG: Central Province	9.98955	149.4866	KUNHM	T14587
	Sericornis papuenis	PNG: Central Province	-9.99982	149.50718	KUNHM	114153
	Myzomela rosenbergi	PNG: Madang Province	-4.71727	145.27482	KUNHM	111482
	P. novaehollandiae	Australia: NSW, Clarence	-33.4767	150.2232	KUNHM	98269

Appendix 3.2. Summary of primers used for Rhipidura atra samples

Gene	Primer name	Sequence 5'– 3'
NADH dehydrogenase subunit–2	L5216[a]	GGCCCATACCCCGRAAATG
	H6313[a]	CTCTTATTTAAGGCTTTGAAGGC
	RA–ND2–1H[b]	AGAACCTTGAAGAACCTCTGG
	RA–ND2–1H-vogI[b]	CTACTGTTGATAGGATGAGGCCA
	RA–ND2–1H-vogII[b]	CAGTAATTAGGGAAGAACCTTGTAGG
	RA–ND2–2L[b]	GACATTACTCAACTAACCCATCCAG
	RA–ND2–2H[b]	ATTGTGTTTAGAGTYAGGAAGA
	RA–ND2–3L[b]	ATACAGCCCTAAACTCACCCTAC
	RA–ND2–3H[b]	TGTGATGGTTGCGCAGTATGC
NADH dehydrogenase subunit–3	L10755[d]	GACTTCCAATCTTTAAAATCTGG
	H11151[d]	GATTTGTTGAGCCGAAATCAAC

[a] Johnson and Sorenson (1998)
[b] Designed by B.W. Benz for this study
[c] Chesser (1999)

Appendix 3.3. Summary of primers used for *Amblyornis macgregoriae* samples

Gene	Primer name	Sequence 5'– 3'
NADH dehydrogenase subunit–2	L5216[a]	GGCCCATACCCCGARAATG
	H6313[a]	CTCTTATTTAAGGCTTTGAAGGC
	AM–ND2–1H[b]	AATGGCTGCCGTGAATACAGTGC
	AM–ND2–1L[b]	GGCTATAGTCCTATTCTCCAGC
	AM–ND2–2H[b]	GCAGCKGATAGGATRGCCATG
	AM–ND2–2L[b]	CATGAAATTCCCACCAATCACCC
	AM–ND2–3H[b]	TTAGGAAGGCAGCGGCGG
	AM–ND2–3L[b]	GCAATCATCCTCACYTACAACCC
	AM–ND2–4H[b]	CAAAATGCTAGGCGTAGGTAG
	AM–ND2–4L[b]	GAACTCACAAAACAAAGCATAGC
NADH dehydrogenase subunit–3	L10755[d]	GACTTCCAATCTTTAAAATCTGG
	H11151[d]	GATTTGTTGAGCCGAAATCAAC

[a] Johnson and Sorenson (1998)
[b] Designed by B.W. Benz for this study
[c] Chesser (1999)

Appendix 3.4. Uncorrected ND2 sequence divergence (%) among populations of *A. macgregoriae*, with pairwise F_{ST} values given in bold below the diagonal.

	Weyland Range	West CDRs	Mt. Stolle	Eastern Highlands	Adelbert Range	Owen Stanley	Huon Penin.	Mt. Simpson
	P1	P2	P3	P4	P5	P6	P7	P8
P1	--	0.008	0.012	0.01	0.011	0.01	0.043	0.013
P2	**0.165**	--	0.011	0.007	0.009	0.007	0.043	0.01
P3	**0.533**	**0.413**	--	0.01	0.011	0.01	0.047	0.013
P4	**0.458**	**0.191**	**0.501**	--	0.007	0.006	0.045	0.009
P5	**0.445**	**0.22**	**0.487**	**0.179**	--	0.007	0.046	0.009
P6	**0.651**	**0.44**	**0.691**	**0.518**	**0.501**	--	0.042	0.008
P7	**0.902**	**0.888**	**0.917**	**0.92**	**0.904**	**0.962**	--	0.046
P8	**0.659**	**0.519**	**0.689**	**0.579**	**0.526**	**0.792**	**0.943**	--

Appendix 3.5. Uncorrected ND2 sequence divergence (%) among populations of *A. atra*, with pairwise F_{ST} values indicated in bold below the diagonal.

	Vogelkop Penin.	Wandamen Range	Weyland Range	Cyclops Range	Torricelli Range	West CDRs	Eastern Highlands	Adelbert Range	Huon Penin.	Mt. Simpson	Owen Stanley
	P1	P2	P3	P4	P5	P6	P7	P8	P9	P10	P11
P1	-	0.074	0.076	0.074	0.077	0.076	0.076	0.077	0.073	0.073	0.072
P2	**0.912**	-	0.007	0.011	0.008	0.007	0.013	0.013	0.012	0.021	0.019
P3	**0.952**	**0.004**	-	0.010	0.005	0.005	0.013	0.013	0.012	0.021	0.019
P4	**0.935**	**0.262**	**0.503**	-	0.010	0.009	0.011	0.011	0.010	0.020	0.018
P5	**0.948**	**0.040**	**0.103**	**0.436**	-	0.005	0.013	0.012	0.011	0.021	0.019
P6	**0.946**	**0.014**	**0.073**	**0.365**	**0.077**	-	0.011	0.010	0.010	0.020	0.018
P7	**0.958**	**0.512**	**0.730**	**0.591**	**0.697**	**0.628**	-	0.002	0.005	0.022	0.020
P8	**0.974**	**0.591**	**0.815**	**0.683**	**0.783**	**0.727**	**0.062**	-	0.004	0.023	0.020
P9	**0.965**	**0.502**	**0.748**	**0.592**	**0.712**	**0.647**	**0.511**	**0.700**	-	0.022	0.020
P10	**0.937**	**0.618**	**0.764**	**0.692**	**0.751**	**0.737**	**0.794**	**0.854**	**0.824**	-	0.006
P11	**0.946**	**0.616**	**0.778**	**0.697**	**0.762**	**0.746**	**0.808**	**0.875**	**0.840**	**0.135**	-

LITERATURE CITED

Abbott, L.D., Silver, E.A., Thompson, P.R., Filewicz, M.V., Schneider, C. & Abdoerrias (1994) Stratigraphic constraints and timing of arc-continent collision in northern Papua New Guinea. *Journal of Sedimentary Research*, **B64**, 169–183.

Abbott, L.D., Silver, E.A., Anderson, R.S., Smith, R., Ingle, J.C., Kling, S.A., Haig, D., Small, E., Galewsky, J. & Sliter, W. (1997) Measurement of tectonic surface uplift rate in a young collisional mountain belt. *Nature*, **385**, 501–507.

Altekar, G., Dwarkadas, S., Huelsenbeck, J.P. & Ronquist, F. (2004) Parallel Metropolis-coupled Markov chain Monte Carlo for Bayesian phylogenetic inference. *Bioinformatics*, **20**, 407–415.

Arbogast, B.S., Drovetskei, S.V., Curry, R.L., Boag, P., Grant, P., Grant, R., Seutin, G. & Anderson, D.J. (2006) Origin and diversification of Galapagos mockingbirds. *Evolution*, **60**, 370–382.

Audley-Charles, M.G. (1991) Tectonics of the New Guinea area. *Annual Review of Earth and Planetary Sciences*, **19**, 17– 41.

Avise, J.C., Walker, D. & Johns, G.C. (1998) Speciation durations and Pleistocene effects in vertebrate phylogeography. *Proceedings of the Royal Society of London B: Biological Sciences*, **265**, 1707–1712.

Avise, J.C. (2000) *Phylogeography: the history and formation of species*. Harvard University Press, Cambridge, MA.

Bandelt, H.J., Forster, P. & Rohl, A. (1999) Median-joining networks for inferring intraspecific phylogenies. *Molecular Biology and Evolution*, **16**, 37–48.

Barker, F.K., Cibois, A., Schikler, P., Feinstein, J. & Cracraft, J. (2004) Phylogeny and

diversification of the largest avian radiation. *Proceeding of the National Academy of Sciences USA*, **101**, 11040–11045.

Barve, N., Barve, V., Jiménez-Valverde, A., Lira-Noriega, A., Maher, S.P., Peterson, A.T., Soberón, J. & Villalobos, F. (2011) The crucial role of the accessible area in ecological niche modeling and species distribution modeling. *Ecological Modeling*, **222**, 1810–1819.

Beehler, B.M., Pratt, T.K. & Zimmerman, D.A. (1986) *Birds of New Guinea*. Princeton University Press, New Jersey.

Bell, R.C., Parra, J.L., Tonione, M., Hoskin, C. J., Mackenzie, J.B., Williams, S.E. & Moritz, C. (2010) Patterns of persistence and isolation indicate resilience to climate change in montane rainforest lizards. *Molecular Ecology*, **19**, 2531–2544.

Bertorelle, G., & Slatkin, M. (1995) The number of segregating sites in expanding human populations, with implications for estimates of demographic parameters. *Molecular Biology and Evolution*, **12**, 887–892.

Blomberg, S.P., Garland, T. & Ives, A.R. (2003) Testing for phylogenetic signal in comparative data: behavioral traits are more labile. *Evolution*, **57**, 717–745.

Boles, W.E. (2006) Family Rhipiduridae. *Handbook of the Birds of the World*, Vol. 11 (ed. by J. del Hoyo, A. Elliott and D.A. Christie), pp. 200–243). Lynx Edicions, Barcelona.

Boles, W.E. (2007) Family Petroicidae (Australasian Robins). *Handbook of the birds of the world*, Vol. 12 (ed. by J. del Hoyo, A. Elliott and D.A. Christie), pp. 374–437. Lynx Edicions, Barcelona.

Brito, P.H. & Edwards, S.V. (2008) Multilocus phylogeography and phylogenetics using sequence-based markers. *Genetica*, **135**, 439–455.

Cadena, C.D., Cheviron, Z.A. & Funk, W.C. (2011) Testing the molecular and evolutionary causes of a "leapfrog" pattern of geographical variation in coloration. *Journal of Evolutionary Biology*, **24**, 402–414.

Carnaval, A.C., Hickerson, M.J., Haddad, C.F.B., Rodrigues, M.T. & Moritz, C. (2009) Stability predicts genetic diversity in the Brazilian Atlantic Forest Hotspot. *Science*, **323**, 785–789.

Carstens, B.C. & Richards, C.L. (2007) Integrating coalescent and ecological niche modeling in comparative phylogeography. *Evolution*, **61**, 1439–1454.

Chapman, F.M. (1923) Mutation among birds in the genus *Buarremon*. *Bulletin of the American Museum of Natural History*, **48**, 243–278.

Chesser, R.T. (1999) Molecular systematics of the rhinocryptid genus *Pteroptochos*. *Condor*, **101**, 439–446.

Christidis, L. & Boles, W. E. (2008) *Systematics and Taxonomy of Australian Birds.* CSIRO Publishing, Melbourne.

Coates, B.J. (1990) *The Birds of Papua New Guinea*. Vol. II. Dove Publications, Alderly, Queensland Australia.

Coyne, J.A., & Orr H.A. (2004) *Speciation*. Harvard Univ. Press, Cambridge, MA.

Darlington, P.J. (1957) *Zoogeography: the geographic distribution of animals*. Wiley, New York.

Darlington, P.J. (1965) *Biogeography of the Southern end of the World*. Harvard University Press, Cambridge, Mass.

Diamond, J.M. (1969) Preliminary results of an ornithological exploration of the North Coastal Range, New Guinea. *American Museum Novitates*, **2362**, 1–57.

Diamond, J.M. (1972) *Avifauna of the Eastern Highlands of New Guinea*. Nuttall Ornithological

Club, Cambridge, MA.

Diamond, J.M. (1973) Distributional ecology of New Guinea birds. *Science*, **179**, 759–769.

Diamond, J.M. (1977) Continental and insular speciation in Pacific island birds. *Systematic Zoology*, **26**, 263–268.

Diamond, J.M. (1985) New distributional records and taxa from the outlying mountain Ranges of New Guinea. *The Emu*, **85**, 65–91.

Dow, D.B. (1977) A geological synthesis of Papua New Guinea. *Bulletin of the Bureau of Mineral Resources of Australia*. **201**, 1–41.

Drummond, A.J. & Rambaut, A. (2007) BEAST: Bayesian evolutionary analysis by sampling trees. *BMC Evolutionary Biology*, **7**, 214.

Drummond, A.J., Ho, S.Y.W., Phillips, M.J. & Rambaut, A. (2006) Relaxed phylogenetics and dating with confidence. *PLoS Biology*, **4**, e88.

Dumbacher, J.P. & Fleischer, R.C. (2001) Phylogenetic evidence for colour pattern convergence in toxic pitohuis: Mullerian mimicry in birds? *Proceedings of the Royal Society of London B: Biological Sciences*, **268**, 1971–1976.

Excoffier, L. & Lischer, H.E.L. (2010) Arlequin suite ver 3.5: A new series of programs to perform population genetics analyses under Linux and Windows. *Molecular Ecology Resources*, In press.

Filardi, C.E. & Moyle, R.G. (2005) Single origin of a pan-Pacific bird group and upstream colonization of Australasia. *Nature*, **438**, 216–219.

Filardi, C.E. & Smith, C.E. (2005) Molecular phylogenetics of monarch flycatchers (genus Monarcha) with emphasis on Solomon Island endemics. *Molecular Phylogenetics and Evolution*, **37**, 776–788.

Filardi, C.E. & Smith, C.E. (2007) Patterns of molecular and morphological variation in some Solomon Island land birds. *Auk*, **124**, 479–493.

Fjeldsa J. & Lovett J.C. (1997) Biodiversity and environmental stability. *Biodiversity and Conservation*, **6**, 315–323.

Flannery, T. (1995) *Mammals of New Guinea*, 2nd edn. Reed Books, New South Wales and Cornell University Press, Ithaca.

Frith C.B. & Beehler B.M. (1998) *The Birds of Paradise*. Oxford University Press, Oxford.

Frith, C.B. & Frith, D.W. (2004) *The Bowerbirds.* Oxford University Press, Oxford.

Futuyma, D.J. (2009) *Evolution*. Sinauer Associates, Sunderland, MA.

Galtier, N., Nabholz, B., Glémin, S. & Hurst, G. (2009) Mitochondrial DNA as a marker of molecular diversity: a reappraisal. *Molecular Ecology*, **18**, 4541–4550.

Gardner, J.L., Trueman, J.W., Ebert, D., Joseph, L. & Magrath, R.D. (2010) Phylogeny and evolution of the Meliphagoidea, the largest radiation of Australasian songbirds. *Molecular Phylogenetics and Evolution*, **55**, 1087–1102.

Gilliard, E.T. (1969) *Birds of Paradise and Bower Birds.* The American Museum of Natural History, Garden City, New York.

Godsoe, W. (2010) Regional variation exaggerates ecological divergence in niche models. *Systematic Biology*, **59**, 298–306.

Graham, R.W., Lundelius, Jr. E.L., Graham, M. A., *et al*. (1999) Spatial response of mammals to late Pleistocene environmental fluctuations. *Science*, **272**, 1601–1606.

Grant, P.R. (1986) *Ecology and Evolution of Darwin's Finches*. Princeton University Press, Princeton, New Jersey.

Grant, P.R. & Grant, B.R. (2002) Adaptive radiation of Darwin's finches. *American Scientist*,

90, 130–139.

Graves, G. R. (1988) Linearity of geographic range and its possible effect on the population structure of Andean birds. *Auk*, **105**, 47–52.

Gregory, P. (2007) Family Acanthizidae (Thornbills). *Handbook of the birds of the world*, Vol. 12 (ed. by J. del Hoyo, A. Elliott and D.A. Christie), pp. 580–581. Lynx Edicions, Barcelona.

Gressitt, J.L. (1982). *Biogeography and ecology in New Guinea* (ed. by Gressitt, J.L.) Junk, The Hague.

Haberle, S. (1994) Anthropogenic indicators in pollen diagrams: problems and prospects for late Pleistocene palynology in New Guinea. *Tropical Archaeobotany*. (ed. by Hather, J.), pp. 172–201. Routledge, London.

Hall, R. (1998) The plate tectonics of Cenozoic SE Asia and the distribution of land and sea. *Biogeography and geological evolution of SE Asia* (ed by Hall, R. & Holloway, J. D.), pp. 99–131. Backhuys Publishers, Leiden.

Hall, R. (2001) Cenozoic reconstructions of SE Asia and the SW Pacific: changing patterns of land and sea. *Faunal and floral migrations and evolution in SE Asia and Australia* (ed. By Metcalfe, I.), pp. 35–56. Balkema, Rotterdam.

Hall, R. (2002) Cenozoic geological and plate tectonic evolution of SE Asia and the SW Pacific: computer-based reconstructions, model and animations. *Journal of Asian Earth Sciences*, **20**, 353–431.

Harpending, H. (1994) Signature of ancient population growth in a low-resolution mitochondrial DNA mismatch distribution. *Human Biology*, **66**, 591–600.

Hartert, E.J.O. (1930) List of the birds collected by Ernst Mayr. *Novitates Zoolgicae*, **17**, 27–128.

Heads, M. (2001a) Birds of Paradise, biogeography and ecology in New Guinea: a review. *Journal of Biogeography*, **28**, 893–925.

Heads, M. (2001b) Birds of paradise and bowerbirds: regional levels of biodiversity and terrane tectonics in New Guinea. *Journal of Zoology*, **255**, 331–339.

Heads, M. (2002) Birds of Paradise, vicariance biogeography and terrane tectonics in New Guinea. *Journal of Biogeography*, **29**, 261–283.

Hebert, P., Stoeckle, M., Zemlak, T., & Francis, C. (2004) Identification of birds through DNA barcodes. *PLoS Biology*, **2**, 1657–1663.

Hewitt, G.M. (1999) Postglacial re-colonization of European biota. *Biological Journal of the Linnean Society*, **68**, 87–112.

Hewitt, G.M. (2000) The genetic legacy of the Pleistocene ice ages. *Nature*, **405**, 907–913.

Hewitt, G.M. (2004) Genetic consequences of climatic oscillations in the Pleistocene. *Philosopical Transactions of the Royal Society of London. Series B Biological Sciences*, **359**, 183–195.

Hey, J. (2010) Isolation with Migration Models for More Than Two Populations. *Molecular Biology and Evolution*, **27**, 905–920.

Hijmans, R.J., Cameron, S.E. & Parra, J.L. (2005a) WorldClim, Version 1.3, http://biogeo.-berkeley.edu/worldclim/worldclim.htm. University of California, Berkeley, CA.

Hijmans, R.J., Cameron, S.E., Parra, J.L., Jones, P.G. & Jarvis, A. (2005b) Very high resolution interpolated climate surfaces for global land areas. *International Journal of Climatology*, **25**,1965–1978.

Hill, G.E. & McGraw, K.J. (2006) Bird coloration. Vol. 2. *Function and Evolution*. (ed. By G.E Hill & K.J. McGraw) Harvard University Press, Cambridge, MA.

Hoekstra, H.E. (2006) Genetics, development and evolution of adaptive pigmentation in vertebrates. *Heredity,* **97**, 222–234.

Hofreiter, M., Jaenicke,V., Serre, D., Haeseler, A.V. & Paabo, S. (2001) DNA sequences from multiple amplifications reveal artifacts induced by cytosine deamination in ancient DNA. *Nucleic Acids Research*, **29,** 4793–4799.

Hooghiemstra, H., Wijninga, V. M. & Cleef, A. M. (2006) The paleobotanical record of Colombia: implications for biogeography and biodiversity. *Annals of the Missouri Botanical Garden*, **93**, 297–324.

Hope, G.S. (1996) Pleistocene change and the historical biogeography of Pacific islands. *The origin and evolution of Pacific Island biotas, New Guinea to Eastern Polynesia: patterns and processes*. (ed. by A. Keast & S. E. Miller). pp. 165–190. SPB Academic Publishing, Amsterdam.

Hope, G.S. & Peterson, J.A. (1976) The equatorial glaciers of New Guinea. *Palaeoenvironments*. (ed. by G.S. Hope, J.A. Peterson, U. Radok, & I. Allison), pp. 173–205. Rotterdam, A.A. Balkema.

Hope, G.S. & Tulip, J. (1994) A long vegetation history from lowland Irian Jaya, Indonesia. *Palaeogeography*, *Palaeoclimatology*, *Palaeoecology*, **109**, 385–398.

Hubbard, J.K., Uy, J.A.C., Hauber, M.E., Hoekstra, H.E. & Safran, R.J. (2010) Vertebrate pigmentation: from underlying genes to adaptive function. *Trends in Genetics*, **26**, 231–239.

Hugall, A., Moritz, C., Moussalli, A. & Stanisic, J. (2002) Reconciling paleodistribution models

and comparative phylogeography in the Wet Tropics rainforest land snail Gnarosophia bellendenkerensis (Brazier 1875). *Proceedings of the National Academy of Sciences USA*, **99**, 6112–6117.

Irestedt, M., Jønsson, K.A., Fjeldså, J. Christidis, L., & Ericson, P.G.P. (2009) An unexpectedly long history of sexual selection in birds of paradise. *BMC Evolutionary Biology*, **9**, 235.

Jansson, R. & Dynesius, M. (2002) The fate of clades in a world of recurrent climatic change: Milankovitch oscillations and evolution. *Annual Review of Ecology and Systematics*, **33**, 741–777.

Johns, R.J. (1982) Plant zonation. *Biogeography and ecology in New Guinea* (ed. by Gressitt, J.L.) pp. 309–836. Junk, The Hague.

Jønsson, K.A., Bowie, R.C.K., Moyle, R.G., Christidis, L., Norman, J.A., Benz, B.W. & Fjeldså, J. (2010) Rapid Pleistocene radiation of an Indo-Pacific passerine bird family: different colonization patterns in the Indonesian and Melanesian archipelagos. *Journal of Biogeography*, **37**, 245–257.

Joseph, L., Slikas, B., Alpers, D. & Schodde, R. (2001) Molecular systematics and phylogeography of New Guinean logrunners (Orthonychidae). *Emu*, **101**, 273–280.

Joseph, L. & Omland, K.E. (2009) Phylogeography: its development and impact in Australo-Papuan ornithology with special reference to paraphyly in Australian birds. *Emu*, **109**, 1–23.

Kass, R.E. & Rafferty, A.E. (1995) Bayes factors. *Journal of the American Statistical Association*, **90**, 773–795.

Keast, A. (1996) Pacific biogeography. *The origin and evolution of Pacific Island biotas, New*

Guinea to Eastern Polynesia: patterns and processes. (ed. by Keast, A. & Miller, S. E.). pp. 477–512. SPB Academic Publishing, Amsterdam.

Keast, A. & Miller, S.E. (1996) Pacific biogeography. *The origin and evolution of Pacific Island biotas, New Guinea to Eastern Polynesia: patterns and processes*. (ed. by Keast, A. & Miller, S. E.). SPB Academic Publishing, Amsterdam.

Kimbel, S.W., Cowan, P.D., Helmus, M.R., Cornwell, W.K., Morlon, H., Ackerly, D.D., Blomberg, S.P. & Webb, C.O. (2010) Picante: R tools for integrating phylogenies and ecology. *Bioinformatics*, **26**, 1463–1464.

Knowles, L.L., Carstens, B.C., & Keat, M.L. (2007) Coupling genetic and ecological-niche models to examine how past population distributions contribute to divergence. *Current Biology*, **17**, 940–946.

Kozak, K.H. & Wiens, J.J. (2006) Does niche conservatism promote speciation? A case study in North American salamanders. *Evolution*, **11**, 2604–2621.

Lawson, L.P. (2010) The discordance of diversification: evolution in the tropical-montane frogs of the Eastern Arc Mountains of Tanzania. *Molecular Ecology*, **18**, 4046–4060.

Lerner, H.R.L. & Fleischer, R. C. (2010) Prospects for the use of next-generation sequencing methods in ornithology. *Auk*, **127**, 4–15.

Librado, P. & Rozas, J. (2009) DnaSP v5: A software for comprehensive analysis of DNA polymorphism data. *Bioinformatics*, **25**, 1451-1452.

Löffler, E. (1977) *Geomorphology of Papua New Guinea*. CSIRO/Australian National University, Canberra.

Loynes, K., Joseph, L., & Keogh, J.S. (2009) Multi-locus phylogeny clarifies the systematics

of the Australo-Papuan robins (Family Petroicidae, Passeriformes). *Molecular Phylogenetics and Evolution*, **53**, 212–219.

Lovette I.J., Bermingham E., & Rickleffs, R.E. (2002) Clade-specific morphological diversification and adaptive radiation in Hawaiian songbirds. *Proceedings of the Royal Society of London B: Biological Sciences*, **269**, 37– 42.

Lovette, I. J. (2004) Mitochondrial dating and mixed-support for the "2% rule" in birds. *Auk* **121**, 1–6.

MacArthur, R.H., & Wilson, E.O. (1963) An equilibrium theory of insular zoogeography. *Evolution*, **17**, 373–387.

MacArthur, R.H. & Wilson, E.O. (1967) *The Theory of Island Biogeography*. Princeton University Press, Princeton, New Jersey.

Maddison, W.P. & Maddison, D.R. (2009) Mesquite: a modular system for evolutionary analysis. Version 2.72 http://mesquiteproject.org.

Mantel, N. (1967) The detection of disease clustering and generalized regression approach. *Cancer Research*, **27**, 209–220.

Marjoram, P., & Donnelly, P. (1994) Pairwise comparisons of mitochondrial DNA sequences in subdivided populations and implications for early human evolution. *Genetics*, **136**, 673–683.

Mayr, E. (1941) *List of New Guinea Birds*. American Museum of Natural History, New York.

Mayr, E. (1942) *Systematics and the Origin of Species*. Columbia University Press, New York.

Mayr, E. (1953) Fragments of Papuan ornithogeography. *Proceedings of the 6th Pacific science congress*, **4**, 11–19.

Mayr, E. (1963) *Animal Species and Evolution*. Harvard University Press, Cambridge, MA.

Mayr, E. & Diamond, J. M. (1976) Birds on islands in the sky: Origin of the montane avifauna of Northern Melanesia. *Proceedings of the National Academy of Sciences USA*, **73**, 1765–1769.

Mayr, E. & Diamond, J.M. (2001) *The Birds of Northern Melanesia*. Oxford University Press, Oxford.

Michaux, B. (1994) Land movements and animal distributions in east Wallacea (eastern Indonesia, Papua New Guinea and Melanesia). *Palaeogeography, Palaeoclimatology, Palaeoecology*, **112**, 323–343.

Mindell, D.P., Sorenson, M.D., & Dimcheff, D.E. (1998) An extra nucleotide is not translated in mitochondrial ND3 of some birds and turtles. *Molecular Biology and Evolution*, **15**, 1568–1571.

Moussalli, A., Moritz, C., Williams, S.E. & Carnaval, A.C. (2009) Variable responses of skinks to a common history of rainforest fluctuation: concordance between phylogeography and palaeo-distribution models. *Molecular Ecology*, **18**, 483–499.

Moritz, C., Hoskin, C.J., MacKenzie, J.B., Phillips, B.L., Tonione, M., Silva, N., Vanderwal, J., Williams, S.E. & Graham, C.H. (2009) Identification and dynamics of a cryptic suture zone in tropical rainforest. *Proceedings of the Royal Society B-Biological Sciences*, **276**, 1235–1244.

Moyle, R.G., Filardi, C.E., Smith, C.E. & Diamond, J. (2009) Explosive Pleistocene diversification and hemispheric expansion of a 'great speciator'. *Proceedings of the National Academy of Sciences USA*, **106**, 1863–1868.

Mundy, N.I. (2005) A window on the genetics of evolution: MC1R and plumage colouration in birds. *Proceedings of the Royal Society B: Biological Sciences*, **272**: 1633–1640.

Murphy, S.A., Double, M.C., & Legge, S.M. (2007) The phylogeography of palm cockatoos *Probosciger aterrimus*, in the dynamic Australo-Papuan region. *Journal of Biogeography*, **34**, 1534–1545.

Nei, M. (1987) *Molecular evolutionary genetics*. Columbia Univ. Press, New York.

Nix, H.A. & Kalma, J.D. (1972) Climate as a dominant control in the biogeography of northern Australia and New Guinea. *Bridge and barrier: the natural and cultural history of Torres Strait* (ed. by D. Walker), pp. 61–92. The Australian National University, Canberra.

Norman, J.A., Christidis, L., Joseph, L., Slikas, B. & Alpers, D. (2002) Unraveling a biogeographical knot: origin of the 'leapfrog' distribution pattern of Australo-Papuan sooty owls (Strigiformes) and logrunners (Passeriformes). *Proceedings of the Royal Society B: Biological Sciences*, **269**, 2127–2133.

Norman, J.A., Rheindt, F.E., Rowe, D.L., Christidis, L., 2007. Speciation dynamics in the Australo-Papuan Meliphaga honeyeaters. *Molecular Phylogenetics and Evolution*, **42**, 80–91.

Nyari, A.S., Benz, B.W., Jønsson, K.A., Fjeldså, J., & Moyle, R.G. (2009) Phylogenetic relationships of fantails (Aves: Rhipiduridae). *Zoologica Scripta*, **38**, 553–561.

Nylander, J.A.A., Wilgenbusch, J.C., Warren, D.L., Swofford, D.L., 2008. AWTY (are we there yet?): a system for graphical exploration of MCMC convergence in Bayesian phylogenetics. *Bioinformatics*, **24**, 581–583.

Paijmans, K. (1976) *New Guinea Vegetation*. A.N.U. Press, Canberra.

Pearson, R.G., Raxworthy, C.J., Nakamura, M. & Peterson, A.T. (2007) Predicting species' distributions from small numbers of occurrence records: A test case using cryptic geckos in Madagascar. *Journal of Biogeography,* **34**, 102–117.

Peterson, A.T. (2009) Phylogeography is not enough: The need for multiple lines of evidence. *Frontiers of Biogeography*, **1**, 19–25.

Peterson, A.T., Soberón, J., & Sánchez-Cordero, V. (1999) Conservatism of ecological niches in evolutionary time. *Science,* **285**, 1265–1267.

Peterson, A.T. & Nyari, A. S. (2007) Ecological niche conservatism and Pleistocene refugia in the thrush-like mourner, *Schiffornis* sp., in the Neotropics. *Evolution*, **62**, 173–183.

Phillips S.J., Anderson, R.P., & Schapire, R.E. (2006) Maximum entropy modeling of species geographic distributions. *Ecological Modeling*, **190**, 231–259.

Pigram, C.J. & Davies, P.J. (1987) Terranes and the accretion history of the New Guinea orogen. *BMR Journal of Australian Geology and Geophysics*, **10**, 193–212.

Pigram. C.J. & Symonds, P.A. (1991) A review of the timing of the major tectonic events in the New Guinea orogen. *Journal of Southeast Asian Earth Sciences*, **6,** 307–318.

Polhemus, D.A. & Polhemus, J.T. (1998) Assembling New Guinea: 40 million years of island arc accretion as indicated by the distributions of aquatic Heteroptera (Insecta). *Biogeography and geological evolution of SE Asia* (ed. by Halland, R. & Holloway, J.D.), pp. 327–340. Backbuys Publishers, Leiden, The Netherlands.

Posada D. (2008) jModelTest: Phylogenetic Model Averaging. *Molecular Biology and Evolution*, **25**, 1253–1256.

Pratt, T.K. (1982) Biogeography of birds in New Guinea. *Biogeography and ecology in New Guinea* (ed. by Gressitt, J.L.) pp. 815–836. Junk, The Hague.

Pratt, T.K. (1983) Additions to the Avifauna of the Adelbert Range, Papua New Guinea. *Emu*, **82**, 117–125.

Prum, R.O. (2006) Anatomy, physics, and evolution of structural colors. *Bird coloration: mechanisms and evolution*. (ed by Hill, G.E. & McGaw, K.J.), pp. 295–353. Harvard University Press.

Rand, A.L. (1942) Results of the Archbold expeditions. No. 43. Birds of the 1938-1939 New Guinea expedition. *Ibid*, **79**, 425–516.

Rand, A.L. & Gilliard, E.T. (1967) *Handbook of New Guinea Birds*. Weidenfeld & Nicolson. London.

Rambaut, A. & Drummond, A. J. (2007) Tracer v1.4. Available at: http://beast.bio.ed.ac.uk/Tracer.

Remsen, J.V. Jr (1984) High incidence of ‘‘leapfrog’’ pattern of geographic variation in Andean birds: implications for the speciation process. *Science*, **224**, 171–173.

Richards, C.L., Carstens, B.C., & Knowles, L.L. (2007) Distribution modeling and statistical phylogeography: an integrative framework for generating and testing alternative biogeographical hypotheses. *Journal of Biogeography*, **34**, 1833–1845.

Rogers, A.R. & Harpending, H. (1992) Population growth makes waves in the distribution of pairwise genetic divergences. *Molecular Biology and Evolution*, **9**, 552–569.

Ronquist, F., Huelsenbeck, J.P. & van der Mark, P. (2005) MrBayes 3.1 manual. Available at: http://mrbayes.csit.fsu.edu/mb3.1_manual.pdf.

Rousset, F. (1997) Genetic differentiation and estimation of gene flow from F-statistics under isolation by distance. *Genetics*, **145**, 1219–1228.

Schodde, R. & Calaby, J.H. (1972) The biogeography of the Australo-Papuan bird and

mammal faunas in relation to Torres Strait. *Bridge and barrier: the natural and cultural history of Torres Strait* (ed. by Walker, D.). pp. 257–300. Australian National University, Canberra.

Schodde, R., & McKean, J.L. (1973) Distribution, taxonomy and evolution of the gardener bowerbirds *Amblyornis* spp. In eastern New Guinea with descriptions of two new subspecies. *Emu*, **73**, 51–60.

Schodde, R. & Mason, I. J. (1999) *The Directory of Australian Birds: Passerines*. CSIRO Publishing, Melbourne.

Scholes, E. (2008) Evolution of the courtship phenotype in the Bird of Paradise genus *Parotia* (Aves: Paradisaeidae): Homology, phylogeny, and modularity. *Biological Journal of the Linnean Society*, **94**, 491–504.

Sefc, K.M., Payne, R.B. & Sorenson, M.D. (2006) Single base errors in PCR products from avian museum specimens and their effect on estimates of historical genetic diversity. *Conseration Genetics*, **8**, 879–884.

Shepard, D.B. & Burbrink, F.T. (2009) Phylogeographic and demographic effects of Pleistocene climatic fluctuations in a montane salamander, *Plethodon fourchensis*. *Molecular Ecology*, **18**, 2243–2262.

Simpson, G.G. (1977) Too many lines; the limits of the Oriental and Australian zoogeographic regions. *Proceedings of the American Philosophical Society*, **121**, 107–120.

Soberón, J., & Peterson, A.T. (2005) Interpretation of models of fundamental ecological niches and species' distributional areas. *Biodiversity Informatics*, **2**, 1–10.

Sorenson, M.D. & Quinn, T.W. (1998) Numts: a challenge for avian systematics and population biology. *Auk*, **115**, 214–221.

Stattersfield, A.J. (1998) *Endemic Bird Areas of the World: Priorities for Biodiversity Conservation.* Birdlife International, Cambridge, UK.

Steadman, D.W. (2006) *Extinction and Biogeography of Tropical Pacific Birds*. University of Chicago Press, Chicago.

Stibig, H-J., Beuchle, R. & Achard, F. (2003) Mapping of the tropical forest cover of insular Southeast Asia from SPOT4-Vegetation images. *International Journal of Remote Sensing*, **24**, 3651–3662.

Stockwell D.R.B. & Peters, D.P. (1999) The GARP modeling system: problems and solutions to automated spatial prediction. *International Journal of Geographical Information Systems,* **13**, 143–158.

Swofford, D.S. (2002) PAUP*. Phylogenetic analysis using parsimony (* and other methods). Version 4.0b10. Sinauer Associates, Sunderland, Massachusetts.

Thompson, J.D., Gibson, T.J., Plewniak, F., Jeanmougin, F. & Higgins, D.G. (1997) The CLUSTAL_X windows interface: flexible strategies for multiple sequence alignment aided by quality analysis tools. *Nucleic Acids Research*, **25**, 4876–4882.

Walker, D. (1972) *Bridge and barrier: the natural and cultural history of Torres Strait* (ed. by Walker, D.). Australian National University, Canberra.

Walker, D. & Flenley, J. (1979) Late Pleistocene vegetation history of the Enga Province of upland Papua New Guinea. *Philosophical Transactions of the Royal Society of London. Series B, Biological Sciences*, **286**, 265-344.

Walker, D. & Hope, G.S. (1982) Late Pleistocene vegetation history. *Biogeography & Ecology of New Guinea* (ed. By J. Gressit) pp. 263–287 Den Haag, Junk.

Wallace, A.R. (1869) *The Malay Archipelago*. Dover Publication, New York.

Wallace, A.R. (1876) *The Geographical Distribution of Animals*. Macmillan Press, London.

Wallace, A.R. (1880) *Island Life, or the Phenomena and Causes of Insular Faunas and Floras, Including a Revision and Attempted Solution of the Problem of Geological Climates*. Macmillan Press, London.

Waltari, E., Hijmans, R. J., Peterson, A. T., Nyári, Á.S., Perkins, S.L., & Guralnick, R.P. (2007) Locating Pleistocene Refugia: Comparing Phylogeographic and Ecological Niche Model Predictions. *PLoS ONE*, **2(7)**, e563.

Warren, D.L., Glor, R.E. & Turelli, M. (2008) Environmental niche equivalency versus conservatism: quantitative approaches to niche evolution. *Evolution*, **62**, 2868–2883.

Warren, D.L., Glor, R.E. & Turelli, M. (2010) ENMTools: a toolbox for comparative studies of environmental niche models. *Ecography*, **33**, 607–611.

Weir, J.T. (2009) Implications of genetic differentiation in Neotropical montane forest birds. *Annals of the Missouri Botanical Garden*, **96**, 410–433.

Wiens, J.J. & Graham, H. G. (2005) Niche conservatism: integrating evolution, ecology and conservation biology. *Annual Review in Ecology and Systematics*, **36**, 519–539.

Uy, J.A.C., Moyle, R.G., Filardi, C.E. & Cheviron, Z.A. (2009) Difference in plumage color used in species recognition between incipient species is linked to a single amino acid substitution in the melanocortin-1 receptor. *American Naturalist*, **174**, 244–254.

van Welzen, P. (1997) Increased speciation in New Guinea: tectonic causes? *Plant diversity in Malesia III* (eds. J. Dransfield, M. J. E. Coode and D. A. Simpson), pp. 363–387. Royal Botanic Gardens, Kew.

Zink, R.M. & Remsen, J.V. Jr. (1986) Evolutionary processes and patterns of geographic variation in birds. *Current Ornithology*, **4**, 1–69.

Zink, R.M., Blackwell-Rago, R.C. & Ronquist, F. (2000) The shifting roles of dispersal and vicariance in biogeography. *Proceedings of the Royal Society B: Biological Sciences*, **267**, 497–503.